

Land snail fauna in Gunung Kuang Limestone Hill, Perak, Malaysia and its conservation implications (Mollusca, Gastropoda)

Chee-Chean Phung¹, Yuen-Zhao Yong^{1,2},
Mohamad Afandi Mat Said², Thor-Seng Liew^{1,3}

1 Institute for Tropical Biology and Conservation, Universiti Malaysia Sabah, Jalan UMS, 88400 Kota Kinabalu, Sabah, Malaysia **2** Lafarge Cement Sdn Bhd, Batu 13 1/2 Miles, Jalan Kuala Kangsar, 31200 Chemor, Perak, Malaysia **3** Rimba, 22-3A, Casa Kiara 2, Jalan Kiara 5, 50480 Kuala Lumpur, Malaysia

Corresponding author: Thor-Seng Liew (thorseng@ums.edu.my)

Academic editor: F. Köhler | Received 6 April 2018 | Accepted 17 May 2018 | Published 26 June 2018

<http://zoobank.org/86C327B5-45FF-439D-8E9F-601CAEFB69E6>

Citation: Phung C-C, Yong Y-Z, Said MAM, Liew T-S (2018) Land snail fauna in Gunung Kuang Limestone Hill, Perak, Malaysia and its conservation implications (Mollusca, Gastropoda). ZooKeys 769: 1–11. <https://doi.org/10.3897/zookeys.769.25571>

Abstract

This paper presents the first land snail species checklist for Gunung Kuang (Kuang Hill), a limestone hill located next to Gunung Kanthan that is recognised as one of the most important limestone hills for its diverse land snail fauna in Kinta Valley. Samplings were carried out at five plots in Gunung Kuang. This survey documented 47 land snail species, in which six species were identified as unique to Gunung Kuang. Approximately half of the land snails from Gunung Kanthan were found in Gunung Kuang. In addition, one of six unique species from Gunung Kanthan was also found in Gunung Kuang. These rich land snail species in Gunung Kuang are similar to other hills in Kinta Valley, but it is relatively lesser than the adjacent Gunung Kanthan. In view of Gunung Kuang's unique land snail species, and its location closest to disturbed Gunung Kanthan, Gunung Kuang should be considered in the conservation management plan for Gunung Kanthan.

Keywords

Gunung Kanthan, karst conservation, Kinta Valley, Peninsular Malaysia

Introduction

Limestone hills are known for their rich biodiversity and endemism (Clements et al. 2006; Schilthuizen 2004). In particular, land snails are the most distinctive organism inhabiting the limestone hills (Clements et al. 2008; Foon et al. 2017; Liew et al. 2014; Schilthuizen et al. 2003). The state of Perak is one of the areas with a large number of limestone hills and a long history of land snail studies in Malaysia. This area has the highest recorded number of land snail species in Malaysia at present; ironically, it also has the largest number of operating quarries (Foon et al. 2017, Liew et al. 2016). Thus, a conservation plan is needed to mitigate the impact of the ongoing quarry on the land snail biodiversity in the limestone hills in Perak.

Among the limestone hills in Perak, Foon et al. (2017) found that Gunung Kanthan, a limestone hill gazetted for quarrying, has the highest number of land snail species and half a dozen of unique species. While a large part of Gunung Kanthan is being quarried away, the entire Gunung Kuang that is located 2 km away from Gunung Kanthan remains intact. Hence, documenting the land snails in Gunung Kuang is necessary to determine whether their species, especially the unique ones, can also be found in Gunung Kanthan. This information is important for planning and managing conservation efforts, such as making Gunung Kuang a possible alternative site for the conservation and rehabilitation of land snail species in Gunung Kanthan, if both hills share significant proportion of species diversity and composition.

In view of the above reasons, we surveyed the land snails in Gunung Kuang by using the same sampling technique applied by Foon et al. (2017). We reported a checklist of land snails that were found in Gunung Kuang and compared it with Gunung Kanthan and other limestone hills in Kinta Valley, Perak. Based on the results of the comparison, we discussed the implication on future conservation strategy for land snail fauna in the region.

Materials and methods

Study site

Gunung Kuang (N4.7467°, E101.1326°) is located within Kinta Valley and the south of Gunung Kanthan. Gunung Kuang is an intermediate-sized limestone outcrop measuring 0.3155 km² (Liew et al. 2016) and is given a standardized national code of Prk 46 G. Kuang by Liew et al. (2016).

Land snail sampling, processing, and identification

Five sampling plots measuring 2 × 4 m were selected to conduct sampling in Gunung Kuang (Clements et al. 2008; Liew et al. 2008; Foon et al. 2017). The locations of the sampling plots were: Plot 1: 4.742371°N, 101.132588°E; Plot 2: 4.742500°N,

101.133611°E; Plot 3: 4.742275°N, 101.133677°E; Plot 4: 4.742222°N, 101.133889°E; Plot 5: 4.74790944°N, 101.135°E. The sampling was conducted on 7th October 2017 and 14th February 2018. In each plot, living macro-snails and empty shells were searched and collected. In addition, five litres of top soil and leaf litters were collected, dried in an oven, and subjected through a series of sieves to extract micro-snails under a dissecting microscope in the laboratory.

Morphology-based species-level identifications were carried out by referring to the checklist of limestone land snails in Perak that was prepared by Foon et al. (2017) and comparison with specimens deposited in the BORNEENSIS Mollusca collection at the Institute for Tropical Biology and Conservation, located at Universiti Malaysia Sabah. Morphospecies that could not be assigned to an existing taxonomic name was given a provisional species name (e.g., *Microcystina* 'Kuang 1'). For each of the newly recorded morphospecies recorded in this survey, photographs were taken using ZEISS EVO MA 10 scanning electron microscope. Photographs for previously recorded species are available in Foon et al. (2017). Species was listed as 'unique' if the species can only be found in one of the total limestone hills surveyed in Foon et al. (2017) and in this study. Every sample was given a collection number and catalogued into the BORNEENSIS database. In addition, all of the sampling materials were deposited into the BORNEENSIS collection at the Institute for Tropical Biology and Conservation.

Results

This survey recorded a total of 47 land snail species belonging to 29 genera and 20 families from Gunung Kuang (Table 1). Among these species, six were unique to Gunung Kuang.

Table 1. Land snail species checklist found from Gunung Kuang and remarks.

| Species | Remarks | Plot 1 | Plot 2 | Plot 3 | Plot 4 | Plot 5 |
|---|--|--------|--------|--------|--------|--------|
| Achatinidae | | | | | | |
| <i>Achatina fulica</i> (Bowdich, 1822) | | / | | | | |
| Ariophantidae | | | | | | |
| <i>Macrochlamys</i> 'Bercham 1' | Foon et al. (2017) | | | / | / | / |
| <i>Macrochlamys</i> 'Kuang 1' *# | Medium-sized shell. Whorls and size similar to <i>Macrochlamys</i> 'Batu Kebelah 1' (Foon et al. 2017) but flatter spire without undulations of radial growth lines along the suture (Figure 5). | | / | | / | |
| <i>Microcystina clarkae</i> Maassen, 2000 | | | | / | / | / |
| <i>Microcystina</i> 'Kuang 1' *# | Small yellowish shell. Whorl, shape and size similar to <i>Microcystina</i> 'kanthan 1' (Foon et al. 2017) but shell surface glossy and apical whorls with spiral grooves (Figure 1). | / | | | | |

| Species | Remarks | Plot 1 | Plot 2 | Plot 3 | Plot 4 | Plot 5 |
|--|--|--------|--------|--------|--------|--------|
| Ariophantidae | | | | | | |
| <i>Microcystina</i> 'Kuang 2' *# | Small shell. Whorl, shape and size similar to <i>Microcystina</i> 'tempurung 3' (Foon et al. 2017) but shell surface with dense spiral grooves (Figure 2). | / | | | | |
| <i>Microcystina</i> 'Kuang 3' *# | Small brown shell. Whorl, shape and size similar to <i>Microcystina</i> 'tempurung 2' (Foon et al. 2017) but with strong undulations of radial growth lines along the suture (Figure 3). | / | | | | |
| <i>Microcystina sinica</i> Von Moellendorff, 1885 | | / | | | | / |
| <i>Microcystina townsendiana</i> Godwin Austen & Nevill, 1879 | | | | / | | |
| Assimineidae | | | | | | |
| <i>Acmeila</i> 'Kanthan 1' | Foon et al. (2017) | / | | | | |
| Bradybaenidae | | | | | | |
| <i>Bradybaena similaris</i> (Férussac, 1821) * | | | | | / | |
| Camaenidae | | | | | | |
| <i>Chloritis breviseta</i> (Pfeiffer, 1862) | | / | | | | |
| Charopidae | | | | | | |
| <i>Charopa lafargei</i> Vermeulen & Marzuki, 2014 | | | | / | | |
| <i>Charopa</i> 'Kanthan 1' | Foon et al. (2017) | / | | | | |
| Clausiliidae | | | | | | |
| <i>Phaedusa filicostata kapayanensis</i> (deMorgan, 1885)* | | | | | / | |
| Cyclophoridae | | | | | | |
| <i>Alycaeus kapayanesis</i> (De Morgan, 1885) | | / | / | | | |
| <i>Chamalycaeus diplochilus</i> (von Moellendorff, 1886) | | / | | / | | / |
| <i>Cyclophorus malayanus</i> (Benson, 1852) | | / | | | | |
| <i>Cyclophorus semisulcatus</i> (Sowerby, 1843) | | / | | | | |
| <i>Platyraphe lowi</i> (De Morgan, 1885) | | / | / | | | / |
| <i>Rhiostoma jouseaumei</i> de Morgan, 1885 | | / | / | / | / | |
| Diapheridae | | | | | | |
| <i>Sinoennea subcylindrica</i> (von Moellendorff, 1891) | | / | | | | / |
| Diplommatinidae | | | | | | |
| <i>Diplommatina cf diminuta</i> | Foon et al. (2017) | | / | / | | |
| <i>Diplommatina crosseana</i> Godwin-Austen & Nevill, 1879 | | / | / | | | |
| <i>Diplommatina nevillei</i> Crosse, 1879 | | / | / | / | | / |
| <i>Diplommatina superba superba</i> Godwin Austen & Nevill, 1879 | | | / | / | | |

| Species | Remarks | Plot 1 | Plot 2 | Plot 3 | Plot 4 | Plot 5 |
|--|--|--------|--------|--------|--------|--------|
| Diplommatinidae | | | | | | |
| <i>Diplommatina ventriculus</i> (V.Moellendorff, 1891) | | | | / | | |
| <i>Opisthostoma paulucciae</i> (Crosse&Nevill, 1879) | | | | | | / |
| Dyakiidae | | | | | | |
| <i>Pseudoplecta bijuga</i> (Stoliczka, 1873) | | / | | | | |
| <i>Quantula striata</i> (Gray, 1834) | | | / | | | |
| Endodontidae | | | | | | |
| <i>Philalanka pusilla</i> Maassen, 2000 | | / | | | | |
| Euconulidae | | | | | | |
| <i>Kaliella 'Kuang 1'*</i> # | Small shell. Whorl, shape and size similar to <i>Kaliella barrakporensis</i> but shell surface without regular radial growth line. | | | / | | |
| <i>Kaliella barrakporensis</i> (Pfeiffer, 1852) | | / | | | | / |
| <i>Kaliella doliolum</i> (Pfeiffer, 1846) *# | | | | / | / | |
| <i>Kaliella microconus</i> (Mousson, 1865) * | | / | / | | / | / |
| <i>Kaliella scandens</i> (Cox, 1872) | | / | | | / | |
| Ferussaciidae | | | | | | |
| <i>Ceciloides caledonica</i> (Crosse, 1867) * | | / | | / | / | |
| Hydrocenidae | | | | | | |
| <i>Georissa monerosatiana</i> Godwin Austen & Nevill, 1879 | | / | / | / | / | |
| <i>Georissa semisculpta</i> Godwin Austen & Nevill, 1879 | | / | / | | | |
| Pupinidae | | | | | | |
| <i>Pupina tchehelensis</i> de Morgan, 1885 | | | / | / | / | / |
| Streptaxidae | | | | | | |
| <i>Discartemon plussensis</i> (de Morgan, 1885) | | | / | | / | |
| <i>Gulella bicolor</i> (Hutton, 1834) | | | / | / | | |
| Subulinidae | | | | | | |
| <i>Allopeas clavulinum</i> (Potiez & Michaud, 1838) | | | / | | | / |
| <i>Allopeas gracile</i> (Hutton, 1834) | | | / | | | |
| <i>Prosopeas tchehelense</i> (De Morgan, 1885) | | / | | | | |
| Vertiginidae | | | | | | |
| <i>Gyliotrachela hungerfordiana</i> (V.Moellendorff, 1886) | | / | / | | | |
| <i>Ptychopatula orcula</i> (Benson, 1850) | | / | | / | | / |

Species unique to Gunung Kuang.

* Species not found in Gunung Kanthan

Discussion

The richness of the land snail species in Gunung Kuang is much lesser than the adjacent Gunung Kanthan (47 vs 63 species). However, it is similar to other hills in Perak (47 ± 3 species, see Foon et al. 2017). Gunung Kuang is the closest hill to Gunung Kanthan, and these two hills are more than five kilometres away from other hills in this region. In view of this, we expected the two hills to share high percentage of species composition. However, only 37 out of the 63 land snail species of Gunung Kanthan were recorded in Gunung Kuang. Ten species including six unique species were found in Gunung Kuang but not in Gunung Kanthan.

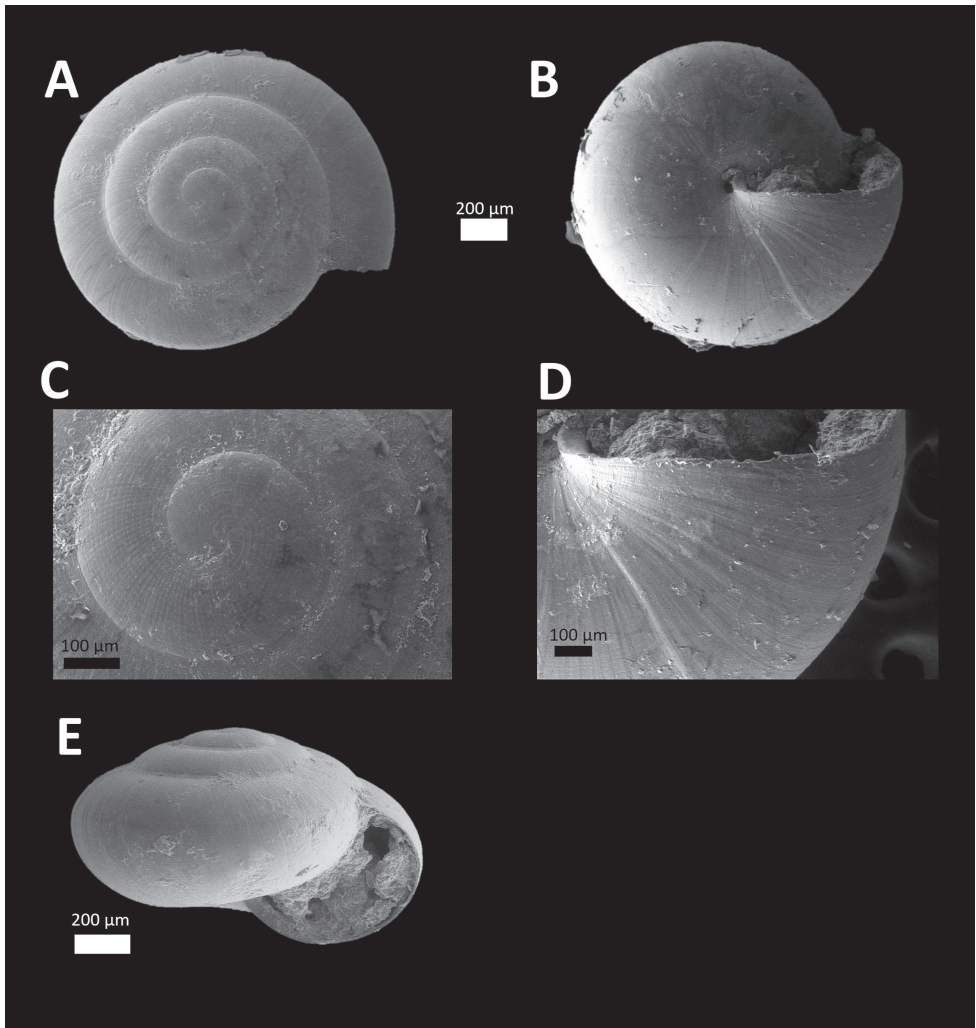


Figure 1. *Microcystina 'kuang 1'* (BORMOL 13768).

In addition, we found six new record of species that were neither listed in Foon et al. (2017) nor matched any known species descriptions in the literatures. The species that are unique to Gunung Kuang are *Macrochlamys* 'Kuang 1' (Figure 5), *Microcystina* 'Kuang 1' (Figure 1), *Microcystina* 'Kuang 2' (Figure 2), *Microcystina* 'Kuang 3' (Figure 3), *Kaliella* 'Kuang 1' (Figure 4) and *Kaliella doliolum*. Note that *Kaliella doliolum* is a widespread species, but it was not recorded from other hills surveyed in Foon et al. (2017). *Diplommatina* cf. *diminuta*, a previously known unique species in Gunung Kanthan, was found in Gunung Kuang. This species was also recorded from Bukit Pondok (pers. Comm. Jaap Vermeulen, collection no. V 13281). The number of

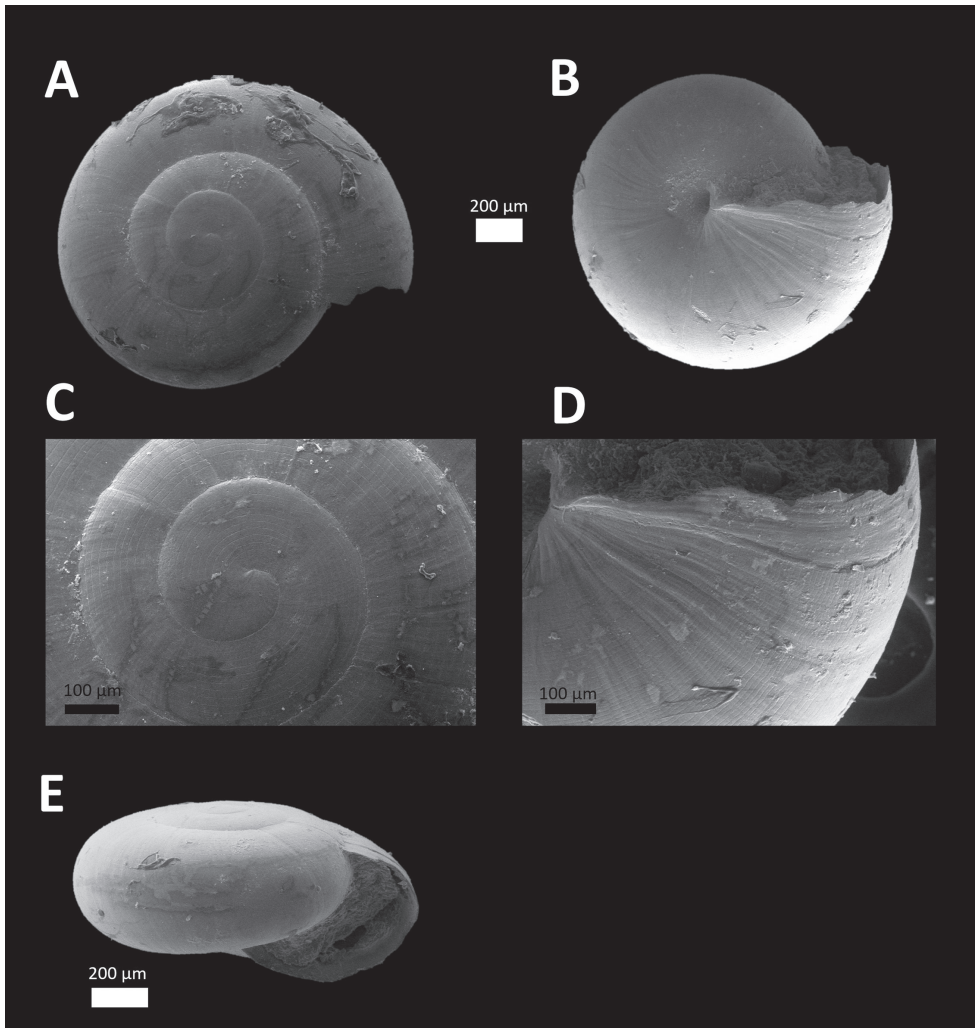


Figure 2. *Microcystina* 'kuang 2' (BORMOL 13769).

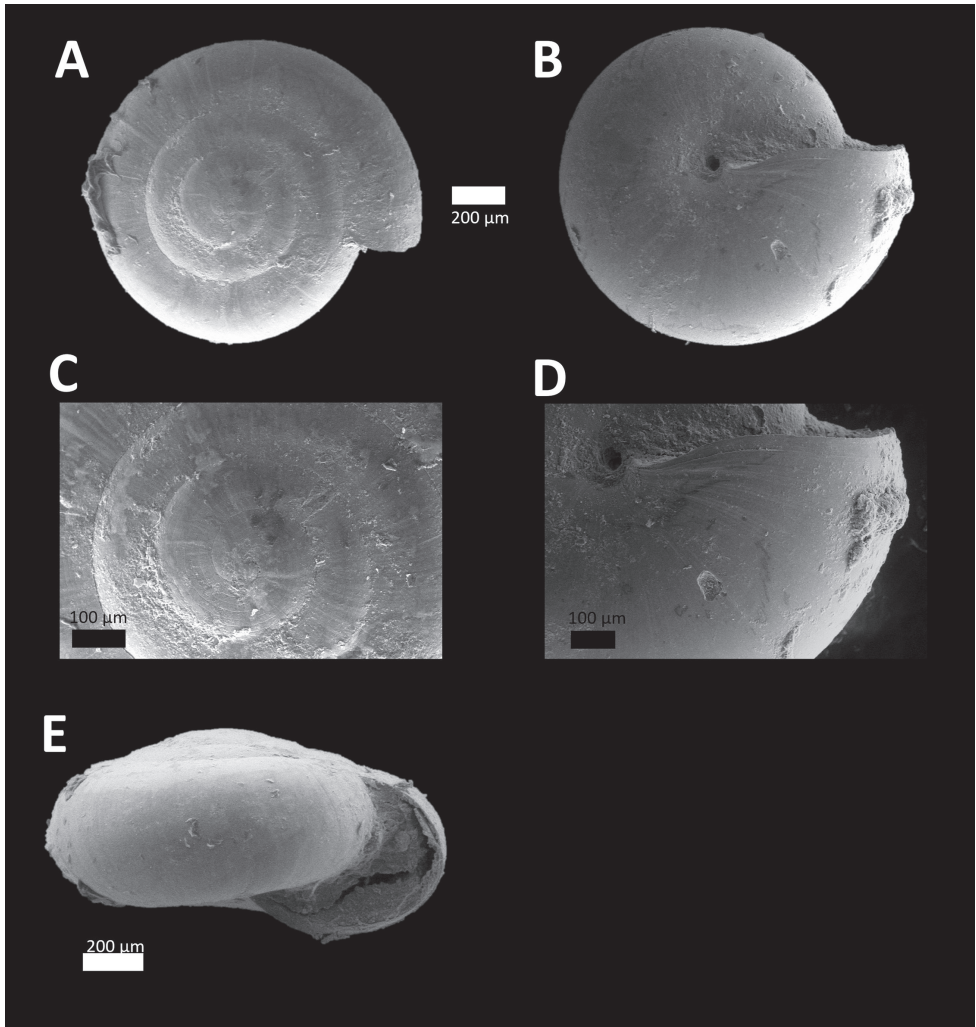


Figure 3. *Microcystina 'kuang 3'* (BORMOL 13767).

unique species found in Gunung Kuang is among the highest after Prk 1 G. Tempurung and Prk 64 Bt Kepala Gajah (Foon et al. 2017).

Our survey provides additional knowledge to the land snail fauna in Kinta Valley limestone hills. Gunung Kuang is home to a high number of land snail species and also unique species. Our result shows that Gunung Kuang shares a certain degree of species composition similarity with Gunung Kanthan. This provides possible alternatives for conservation planning and the rehabilitation of certain species, particularly land snail species that are unique to the region. Nevertheless, Gunung Kanthan still requires conservation attention, as Gunung Kuang does not fully represents its species composition.

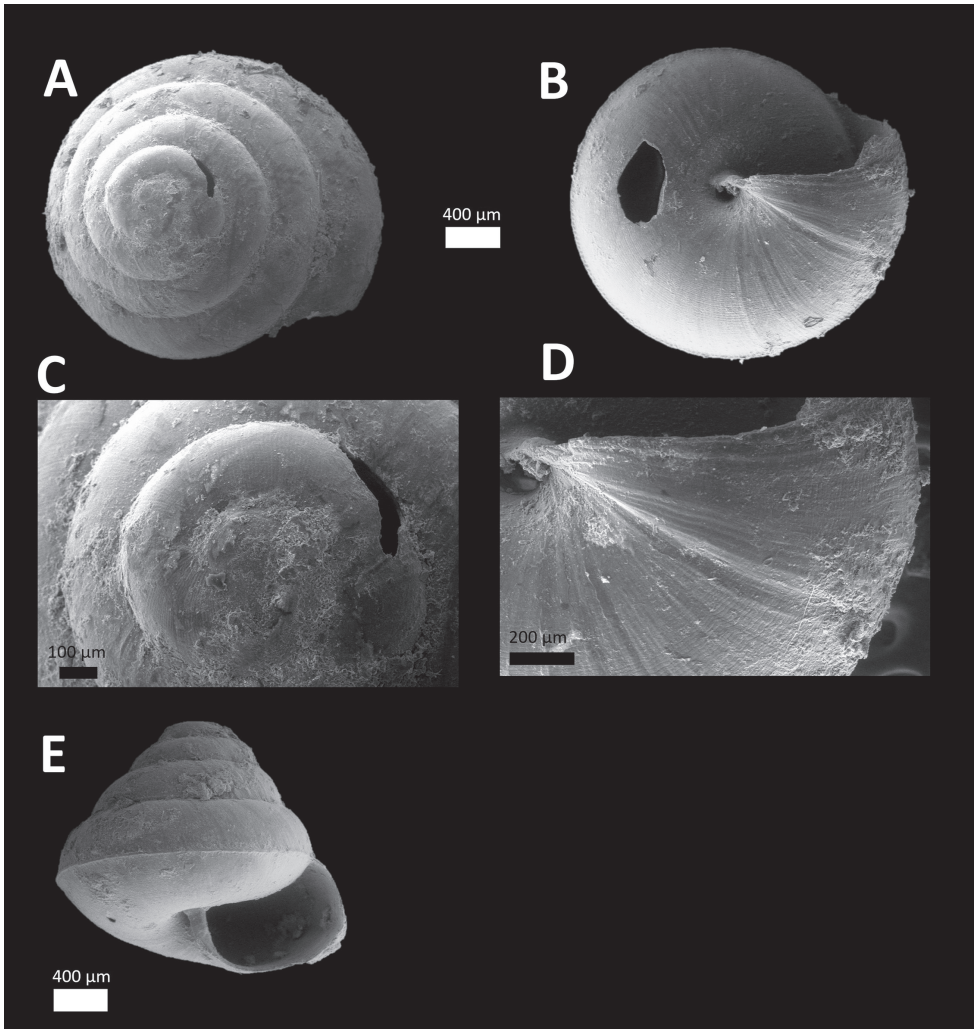


Figure 4. *Kaliella* 'kuang 1' (BORMOL 13787).

Acknowledgements

This project was financially supported by research grant from Lafarge Malaysia Sdn. Bhd, to Universiti Malaysia Sabah (GLS0006). We thank the reviewers Ta-Wei Hsiung and Jaap. J. Vermeulen for their constructive comments.

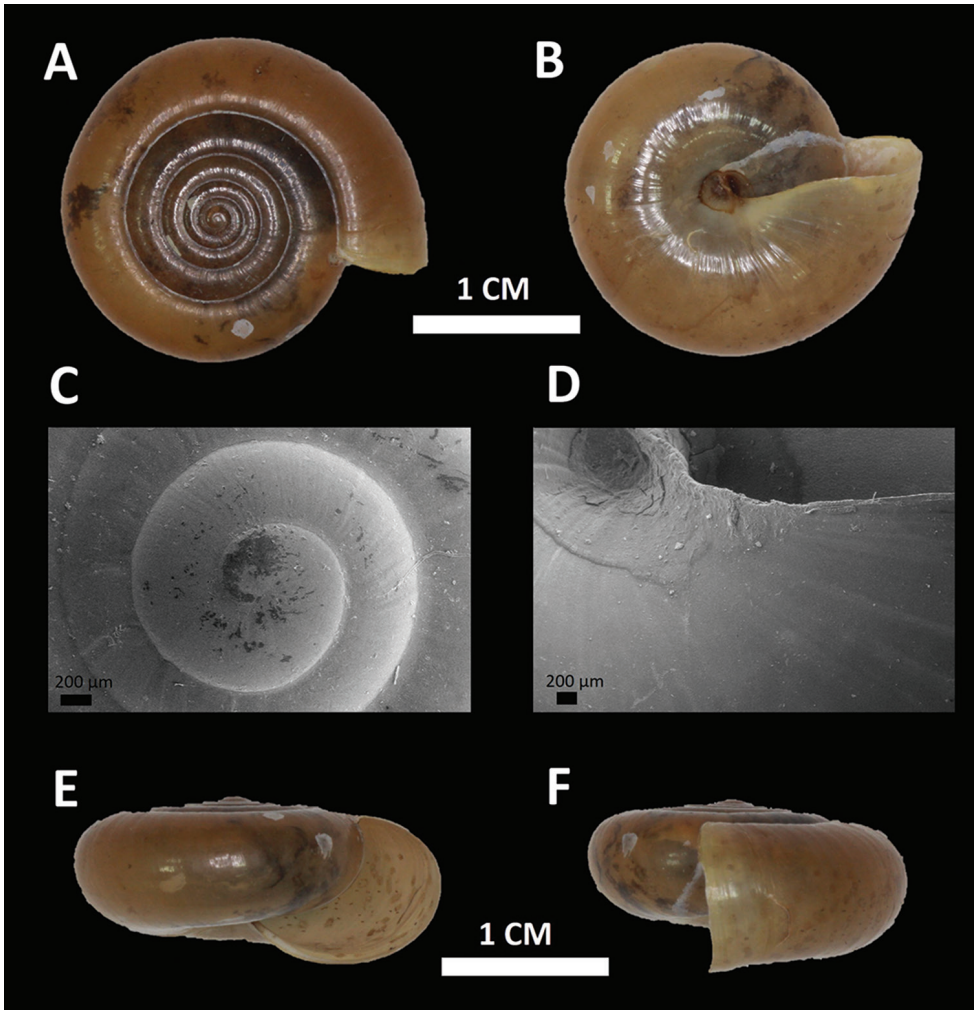


Figure 5. *Macrochlamys* 'kuang 1' (BORMOL 13784).

References

- Clements R, Sodhi NS, Schilthuizen M, Ng PK (2006) Limestone karsts of Southeast Asia: imperiled arks of biodiversity. *Bioscience* 56(9): 733–742. [https://doi.org/10.1641/0006-3568\(2006\)56\[733:LKOSAI\]2.0.CO;2](https://doi.org/10.1641/0006-3568(2006)56[733:LKOSAI]2.0.CO;2)
- Clements R, Ng PK, Lu XX, Ambu S, Schilthuizen M, Bradshaw CJ (2008) Using biogeographical patterns of endemic land snails to improve conservation planning for limestone karsts. *Biological conservation* 141(11): 2751–2764. <https://doi.org/10.1016/j.biocon.2008.08.011>
- Foon JK, Clements GR, Liew T-S (2017) Diversity and biogeography of land snails (Mollusca, Gastropoda) in the limestone hills of Perak, Peninsular Malaysia. *ZooKeys* 682: 1–94. <https://doi.org/10.3897/zookeys.682.12999>

- Liew T-S, Clements R, Schilthuizen M (2008) Sampling micromolluscs in tropical forests: one size does not fit all. *Zoosymposia* 1: 271–280.
- Liew T-S, Vermeulen JJ, Marzuki ME, Schilthuizen M (2014) A cybertaxonomic revision of the micro-landsnail genus *Plectostoma* Adam (Mollusca, Caenogastropoda, Diplommatinidae), from Peninsular Malaysia, Sumatra and Indochina. *Zookeys* 393: 1–109. <https://doi.org/10.3897/zookeys.393.6717>
- Liew T-S, Price L, Clements GR (2016) Using Google Earth to improve the management of threatened limestone karst ecosystems in Peninsular Malaysia. *Tropical Conservation Science* 9(2): 903–920.
- Schilthuizen M, Chai HN, Kimsin TE, Vermeulen JJ (2003) Abundance and diversity of land-snails (Mollusca: Gastropoda) on limestone hills in Borneo. *Raffles Bulletin of Zoology* 51(1): 35–42.
- Schilthuizen M (2004) Land snail conservation in Borneo: limestone outcrops act as arks. *Journal of Conchology Special Publication* 3: 149–154.

Supplementary material I

Species list and occurrences

Authors: Chee-Chean Phung, Yuen-Zhao Yong, Mohamad Afandi Mat Said, Thor-Seng Liew

Data type: (occurrence)

Explanation note: A CSV file which provided a list of species and occurrences of each species at each plot in Gunung Kuang Limestone Hill.

Copyright notice: This dataset is made available under the Open Database License (<http://opendatacommons.org/licenses/odbl/1.0/>). The Open Database License (ODbL) is a license agreement intended to allow users to freely share, modify, and use this Dataset while maintaining this same freedom for others, provided that the original source and author(s) are credited.

Link: <https://doi.org/10.3897/zookeys.769.25571.suppl1>

Revision of the subterranean genus *Spelaeodiscus* Brusina, 1886 (Gastropoda, Pulmonata, Spelaeodiscidae)

Barna Páll-Gergely¹, Tamás Deli², Zoltán Péter Eröss³, Peter L. Reischütz⁴,
Alexander Reischütz⁴, Zoltán Fehér⁵

1 Centre for Agricultural Research, Hungarian Academy of Sciences (MTA), Herman Ottó út 15, Budapest, H-1022, Hungary **2** Móricz Zsigmond u. 2, Gyomaendrőd, H-5500, Hungary **3** Bem u. 36., Budapest, H-1151, Hungary **4** Puechhaimg. 52, A-3580, Horn, Austria **5** Department of Zoology, Hungarian Natural History Museum, Baross u. 13, H-1088, Hungary

Corresponding author: Barna Páll-Gergely (pall-gergely.barna@agrar.mta.hu)

Academic editor: Martin Haase | Received 25 March 2018 | Accepted 16 May 2018 | Published 26 June 2018

<http://zoobank.org/C31B0F6B-D3C2-42CD-BAED-8CE9D5769E8A>

Citation: Páll-Gergely B, Deli T, Eröss ZP, Reischütz PL, Reischütz A, Fehér Z (2018) Revision of the subterranean genus *Spelaeodiscus* Brusina, 1886 (Gastropoda, Pulmonata, Spelaeodiscidae). ZooKeys 769: 13–48. <https://doi.org/10.3897/zookeys.769.25258>

Abstract

The Balkan genus *Spelaeodiscus* Brusina, 1886 is revised based on museum collections and newly collected samples from Montenegro and Albania. The following species and subspecies are introduced as new to science: *Spelaeodiscus albanicus edentatus* Páll-Gergely & P. L. Reischütz, **ssp. n.** (southern Montenegro and northern Albania), *Spelaeodiscus densecostatus* Páll-Gergely & A. Reischütz, **sp. n.**, *Spelaeodiscus hunyadii* Páll-Gergely & Deli, **sp. n.**, *Spelaeodiscus latecostatus* Páll-Gergely & Eröss, **sp. n.** (all three from southern Montenegro), *Spelaeodiscus unidentatus acutus* Páll-Gergely & Fehér, **ssp. n.**, and *Spelaeodiscus virpazarioides* Páll-Gergely & Fehér, **sp. n.** (both from northern Albania). For all species and subspecies diagnoses and suggestions for conservation status assessments according to IUCN criteria are provided. An overview is given regarding the habitat preference of *Spelaeodiscus* species, and the “scratch and flotate” method to collect subterranean gastropods.

Keywords

Aspasita, Balkans, “Milieu Souterrain Superficiel”, “scratch and flotate”, shell morphology, taxonomy

Introduction

Spelaeodiscus was described by Brusina (1886) as a subgenus of *Patula* Held, 1838. At that time, the only species in this group was *P. (S.) hauffeni* (Schmidt, 1855). This group (and the only species belonging to it) was known to inhabit Krain (Slovenia) only. The second species of *Spelaeodiscus* was *Spelaeodiscus albanicus* (A. J. Wagner, 1914), which was described from northern Albania, based on shells collected in the debris of the Kir River. *Spelaeodiscus* was first used at the genus level by Pilsbry (1926). In the 1960's Bole (1961, 1965) and Gittenberger (1969) introduced three additional species as follows: *S. unidentatus* Bole, 1961, *S. obodensis* Bole, 1965 and *S. dejongi* Gittenberger, 1969. The former two were described from present day Montenegro, whereas *S. dejongi* was originally reported from Slovenia. Later it turned out that the Slovenian specimens of *S. dejongi* were probably the result of mislabeling, and that this species is endemic to Montenegro (Gittenberger 1975). Thus, *Spelaeodiscus* is currently known from the Western Balkans (Slovenia, Montenegro, and northern Albania).

Aspasita Westerlund, 1889 was established as a “Gruppe” under *Helix* (*Gonostoma*), and originally included the three species: *Helix triaria* Rossmässler, 1839 (with its subspecies *tatrica* Hazay, 1883), *Helix trinodis* (Kimakowicz, 1884), and *H. triadis* (Kimakowicz, 1884). Gittenberger (1969) recognized a single species, *Spelaeodiscus (Aspasita) triaria*, and treated the other taxa as its subspecies (*trinodis*, *triadis*, *tatricus*). Another *Aspasita* species, *A. bulgarica* Subai & Dedov, 2008, has been described recently from Bulgaria. Currently, *Aspasita* is known from the Northern Carpathians (Tatra Mts in Slovakia, Bükk Mts in Hungary), the Apuseni Mts and the Southern Carpathians (Romania), and the Stara Planina Mts (Bulgaria and northeastern Serbia).

Aspasita and *Spelaeodiscus* have been distinguished by Schileyko (1998) and Subai and Dedov (2008) on the genus, by Gittenberger (1969, 1975) on the subgenus level. However, Welter-Schultes (2012) treated them as a single genus. In this paper we treat the two genera separately.

The conchologically similar genus *Virpazaria* Gittenberger, 1969, which is also an endemic of the West Balkans, is distinguished from *Spelaeodiscus* and *Aspasita* on the basis of the continuous peristome and the crescent-shaped aperture (Gittenberger 1969, 1975, Reischütz and Reischütz 2009).

So far, *Spelaeodiscus* species have mainly been reported from caves, and thus, they belong to the rarest genera in mollusc collections. Intensive field surveys in Montenegro and Albania, and using special collecting methods (sieving and flotating the granular rocky substrate collected from rock crevices) significantly increased the number of known populations and the amount of the available shell material of *Spelaeodiscus*. In the present revision we present the outcome of the examination of all available historical and newly collected material.

Materials and methods

The new samples were collected between 2010 and 2017 during 13 collecting trips. Sampling was done scratching out fine granulate material from the superficial fissures of rocks applying long and narrow hand rakes and separated the shells either by sieving (“scratch and sieve” method) or by flotating (“scratch and flotate” method).

Shell whorls (± 0.25) were counted according to Kerney and Cameron (1979: 13). Most shells were measured in mm to one significant digit using Zeiss Stemi 305 microscope with Zeiss Labscope software. The measured parameters are compiled on Figure 1. Ribs on the body whorl were counted using photographs of 3–5 shells per population. Differences in size are indicated in the diagnoses using the following terms: small (1.9–2.5 mm), medium sized (2.6–3.5 mm), large (3.6–4.3 mm).

Abbreviations used

| | |
|-------------|---|
| HNHM | Hungarian Natural History Museum (Budapest, Hungary) |
| DT | Collection Tamás Deli (Gyomaendrőd, Hungary) |
| EZP | Collection Zoltán Péter Eröss (Budapest, Hungary) |
| HA | Collection András Hunyadi (Budapest, Hungary) |
| JG | Collection Jozef Grego (Banská Bystrica, Slovakia) |
| MZBI | Jovan Hadži Institute of Biology, Research Centre of the Slovenian Academy of Sciences and Arts (Ljubljana, Slovenia) |
| NHMW | Naturhistorisches Museum Wien (Vienna, Austria) |
| NMBE | Natural History Museum of Bern (Bern, Switzerland) |
| PGB | Collection Barna Páll-Gergely (Mosonmagyaróvár, Hungary) |
| REI | Collection Reischütz (Horn, Austria) |
| SMF | Senckenberg Forschungsinstitut und Naturmuseum (Frankfurt am Main, Germany) |

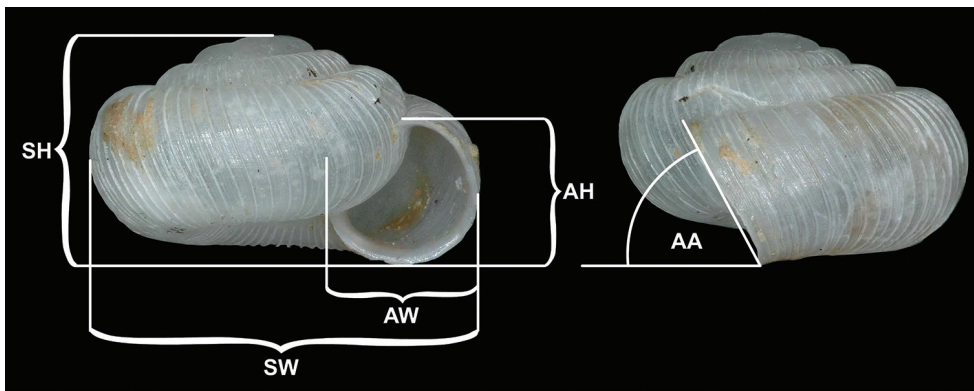


Figure 1. The following variables were measured: angle of aperture (AA); aperture height (AH); aperture width (AW); shell height (SH); shell width (SW).

Systematics

Family Spelaeodiscidae Steenberg, 1925

Remarks. Schileyko (1998) classified *Spelaeodiscus* into the family Spelaeodiscidae Steenberg, 1925, which has independently been introduced by Hudec (1970) as well. This taxon was also recognized as a separate family of the infraorder Orthurethra (and its only superfamily, Pupilloidea) by Bouchet et al. (2017). Although the genital anatomy of some species belonging to this family is known, its systematic position within Orthurethra is uncertain, because no molecular phylogenetic information is known (Harl et al. 2017).

Genus *Spelaeodiscus* Brusina, 1886

Patula (*Spelaeodiscus*) Brusina, 1886: 37.

Type species. *Helix Hauffeni* Schmidt, 1855.

Distribution. The genus *Spelaeodiscus* has a disjunct distribution. One species (*S. hauffeni*) is only known from Slovenia, whereas the rest of the genus is distributed in the vicinity of the Skadar Lake Basin (also known as Shkodër Lake or Skutari Lake) in Montenegro and northern Albania (Figure 2).

Included taxa. *Spelaeodiscus albanicus albanicus* (A. J. Wagner, 1914), *S. albanicus edentatus* Páll-Gergely & P. L. Reischütz, ssp. n., *S. dejongi* Gittenberger, 1969, *S. densecostatus* Páll-Gergely & A. Reischütz, sp. n., *S. hauffeni* (Schmidt, 1855) *S. hunyadii* Páll-Gergely & Deli, sp. n., *S. latecostatus* Páll-Gergely & Eröss, sp. n., *S. obodensis* Bole, 1965. *S. unidentatus unidentatus* Bole, 1961, *S. unidentatus acutus* Páll-Gergely & Fehér, ssp. n., *S. virpazarioides* Páll-Gergely & Fehér, sp. n. For key traits see Table 1.

Delimitation of this genus. The reproductive anatomy of *Spelaeodiscus* and *Aspasita* is characterized by a short penial caecum, a well-developed penial appendix, sometimes an epiphallic caecum, and a bursa copulatrix without a diverticulum. The retractor muscle is divided into two bounds, one inserting on the penial appendix, whereas the other at the base of the penial caecum. Examining the anatomical descriptions and drawings of *Spelaeodiscus* (Bole 1965) and *Aspasita* (Hudec 1965, Gittenberger 1975, Schileyko 1998, Subai and Dedov 2008), we were unable to find characters that would constantly differ between the two groups. For example, the penial caecum was long and slender in *A. tatratica* (see Hudec 1965) and *S. hauffeni* (see Bole 1965), but was short and conical in *A. triaria* (see Subai and Dedov 2008) and *S. unidentatus* (see Bole 1965). Also, the shape of the bursa and the position of the starting point of the penial appendix was greatly variable across genera. Clear epiphallic caecum was only found in *S. hauffeni*, but some thickening was visible in *S. unidentatus* and *A. triaria*.

As for shell characters, *Spelaeodiscus* is characterized by a mostly colourless shell that is smaller than 4.3 mm (majority of species are even smaller than 3.5 mm), the spire is relatively low (height of body whorl at least two third of the height of the en-

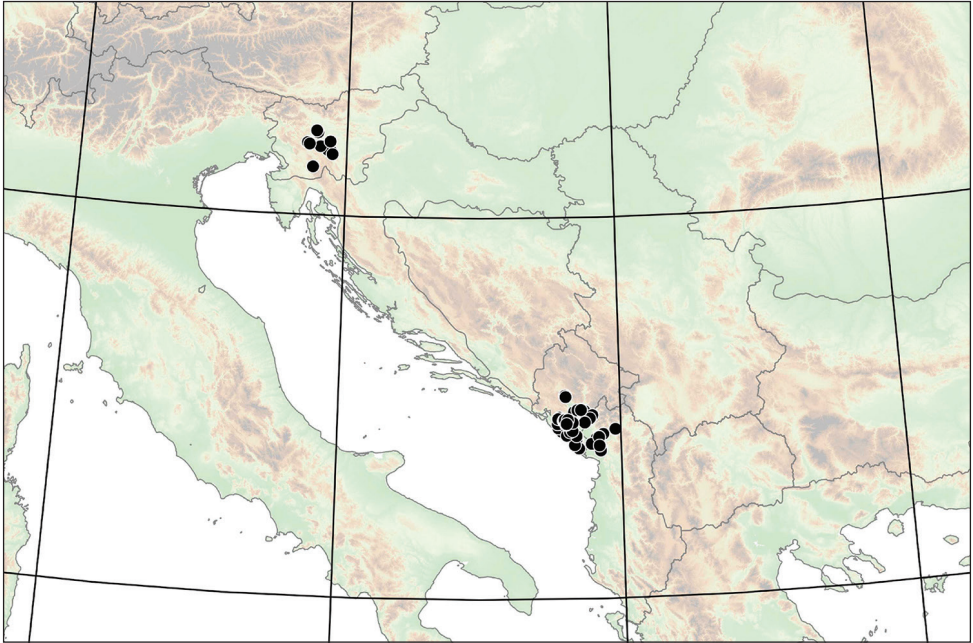


Figure 2. Distribution of the genus *Spelaodiscus* Brusina, 1886.

Table 1. Number of ribs on the body whorl, shell size, and key traits of *Spelaodiscus* species.

| (Sub)species | No. of ribs | Shell diameter (in mm) | Key traits |
|---|-------------|------------------------|---|
| <i>albanicus albanicus</i> | 43–93 | 3.6–4.3 | matte protoconch, weak palatal and two weak basal teeth |
| <i>albanicus edentatus</i> ssp. n. | 35–54 | 3.6–4.2 | widely-spaced ribs, glossy protoconch glossy, toothless aperture |
| <i>dejongi</i> | 57–112 | 1.9–3.4 | dense, low ribs, smooth protoconch, toothless aperture |
| <i>densecostatus</i> sp. n. | 116 | 3.7 | very low and dense ribs, toothless aperture |
| <i>hauffeni</i> | 41–52 | 2.8–3.5 | widely spaced, strong ribs, rounded, toothless aperture, finely granular protoconch |
| <i>latecostatus</i> sp. n. | 42 | 2.2 | strong, very widely spaced ribs, glossy protoconch, toothless aperture |
| cf. <i>latecostatus</i> sp. n. (2017/005) | 47–54 | 1.9 | strong, widely spaced ribs, glossy protoconch, toothless aperture |
| <i>hunyadii</i> sp. n. | 42–48 | 2.1–2.2 | widely spaced, strong ribs, glossy protoconch, strongly oblique, toothless aperture |
| <i>obodensis</i> | 43–76 | 2.6–3.0 | elevated spire, roughly sculptured protoconch, strong ribs, toothless aperture |
| <i>unidentatus unidentatus</i> | 74–118 | 2.4–3.2 | low basal tooth; palatal part of peristome with strong incision |
| <i>unidentatus acutus</i> ssp. n. | 64–91 | 2.9–3.5 | pointed basal tooth; palatal part of peristome with shallow incision |
| <i>virpazarioides</i> sp. n. | 40–70 | 3.3–3.6 | spiral sculpture, thickened callus |

tire shell), the body whorl is evenly rounded, the edge of the parietal callus is straight, and the peristome is only slightly expanded. In contrast, *Aspasita* shells are brownish, larger than 4.3 mm, they have higher spire (height of body whorl is approximately half of the height of the entire shell), the shell is shape reverse trapezoid from standard apertural view, the callus is heart-shaped, and the basal part of the peristome is strongly expanded.

The habitat was the only “trait” mentioned by Gittenberger (1969) as difference between the two groups. Namely, *Spelaeodiscus* is subterranean, whereas *Aspasita* can be found on rock surfaces and among leaf litter at the base of limestone rocks. In the lack of sound molecular data it is difficult to infer their relationship, but based only on ecological, conchological, and biogeographical differences it seems reasonable to keep *Aspasita* and *Spelaeodiscus* as distinct genera.

***Spelaeodiscus albanicus* (A. J. Wagner, 1914)**

Diagnosis. A large species with usually widely spaced, strong ribs, and no or weak apertural teeth.

Differential diagnosis. The most similar species in terms of shell size and shape is *Spelaeodiscus densecostatus* sp. n., for differences see under that species. *Spelaeodiscus unidentatus* is usually smaller, usually possesses denser ribs, and has stronger teeth and narrower aperture.

Conservation status. Reischütz and Fehér (2017) assessed this species as Least Concern (LC). They claimed that there are at least three known locations and is likely that further field work reveals a larger range and more locations. Although that assessment was based partly on incorrect distribution records (Peuta Cave population is currently treated as *S. unidentatus*, whereas Raps-Starjë population as *S. virpazarioides* sp. n.), together with our new distribution records there are more than five locations. As we have no reason to suppose that the habitat quality, habitat extent, or population are deteriorating or extremely fluctuating, Least Concern (LC) seems to be a correct assessment.

***Spelaeodiscus albanicus albanicus* (A. J. Wagner, 1914)**

Figure 3

Aspasita albanica A. J. Wagner, 1914 in Sturany & Wagner 1914: 67, plate 2, figs 10a–c.

Spelaeodiscus albanicus — Bole 1965: 354, Plate 76, fig. B.

Spelaeodiscus (Spelaeodiscus) albanicus — Gittenberger 1969: 294, fig. 2.

Spelaeodiscus albanicus — Pilsbry 1926: 184, plate 22, figs 12–14.

Spelaeodiscus albanicus — Welter-Schultes 2012: 213 (partim: locality data from Montenegro are of unknown origin).

Spelaeodiscus albanicus — Reischütz et al. 2013: 62, fig. 3.

Type material. Kiri-Brücke nächst Mesi b. Skutari, Albanien (im Genist), leg. Sturany, 27.04.1905, NHMW 43385 (lectotype, hereby selected, SW: 3.7 mm, SH: 2 mm, Fig. 3A–F); Drinasca-Ufer b. Skutari (angeschwemmt), leg. Sturany, 03.05.1905, NHMW 112351 (1 corroded, juvenile paralectotype).

Other material. Vrelo Pronisicut (or Pronifkut), coll. Edlauer ex coll. Kuščer, NHMW 48236/1 shell (“photo”); Pronisicut, coll. Edlauer ex coll. Kuščer, NHMW 48336/2 shells; Albania, Shkodër district, Drisht, right bank of Kir river opposite to the fortress hill, 90 m a.s.l. (roadside limestone rocks), 42°7.824'N, 19°36.540'E, (site code: 2016/32), leg. Z.P. Eröss, Z. Fehér, J. Grego & M. Szekeres, 28.06.2016, HNHM 103195/1 (photographed shell, Fig. 3G–L), NHMW 112356/1 adult + 5 juvenile shells; Albania, Shkodër district, 1 km NE of Ura e Shtrenjtë, 160 m a.s.l., (roadside limestone rocks), 42°9.180'N, 19°40.000'E (site code: 2016/33), leg. Z.P. Eröss, Z. Fehér, J. Grego & M. Szekeres, 28.06.2016, HNHM 103196/1 (photographed shell, Fig. 3M–R), NHMW 112357/9 juvenile/broken shells; Albania, Shkodër district, 4 km SW of Prekal, 170 m a.s.l., (roadside limestone rocks), 42°9.936'N, 19°41.334'E (site code: 2016/35), leg. Z.P. Eröss, Z. Fehér, J. Grego & M. Szekeres, 28.06.2016, JG/1 adult + 1 juvenile shell; Albania, Ura e Mesit, debris of the Kir river, 50 m a.s.l., 42°6.870'N, 19°34.498'E, leg. A. Reischütz, N. Reischütz & P. L. Reischütz, Apr. 2012, REI/1; Albania, rocks southwest of Zusi, southwest of Skoder, 13 m a.s.l., 42°2.316'N, 19°28.866'E, leg. A. Reischütz, N. Reischütz & P. L. Reischütz, May 2015, NHMW 112358/1 (photographed shell, Fig. 3S–X), REI/5; Albania, Felsspalten above Drisht at Mes, 115 m a.s.l., 42°7.735'N, 19°36.823'E, leg. A. Reischütz, N. Reischütz & P. L. Reischütz, Jul. 2010, REI/2 juvenile shells; Albania, ruins 3 km above Drisht at Mes, 195 m a.s.l., 42°7.468'N, 19°36.846'E, leg. A. Reischütz, N. Reischütz & P. L. Reischütz, Jul. 2010, REI/3; Albania, Periferi Shkodër, ca. 18 km upstream from dam at Koman, a left side-valley of Liqeni i Komanit, 170 m a.s.l., limestone rocks, debris, 42°13.613'N, 19°54.300'E, leg. Z.P. Eröss, Z. Fehér, A. Hunyadi & D. Murányi, 15 Apr. 2006, HNHM 102244/1.

Diagnosis. Protoconch matte; aperture with a rather weak palatal and two weak basal teeth.

Description. Shell rarely flat, usually spire somewhat elevated; protoconch consists of 1.5–1.75 whorls, very finely granulated, rather matte, not glossy; teleoconch with strong, equidistant ribs that are supported by fine periostracal filaments in fresh shells; rib density variable (43–93 ribs on body whorl), usually widely spaced; between main ribs some fine wrinkles discernible; entire shell with 4.25–4.5 whorls; aperture semilunar or due to the straight basal part triangular; peristome expanded and slightly reflected, especially on the palatal, basal and umbilical areas; palatal tooth of variable strength, usually weak, although present in all adult shells, palatal region of peristome without outer incision; basal portion of peristome usually straight, slightly thickened, with two low denticles that are visible in all adult shells; umbilicus funnel-shaped, wide (although width depends on spire height).

Measurements. SW: 3.6–4.3 mm (median = 4.0 mm), SH: 1.9–2.2 mm (median = 2.0 mm), AW: 1.3–1.7 mm (median = 1.5 mm), AH: 1.3–1.6 mm (median = 1.5 mm), (n = 6; largest and smallest specimens of multiple populations measured).

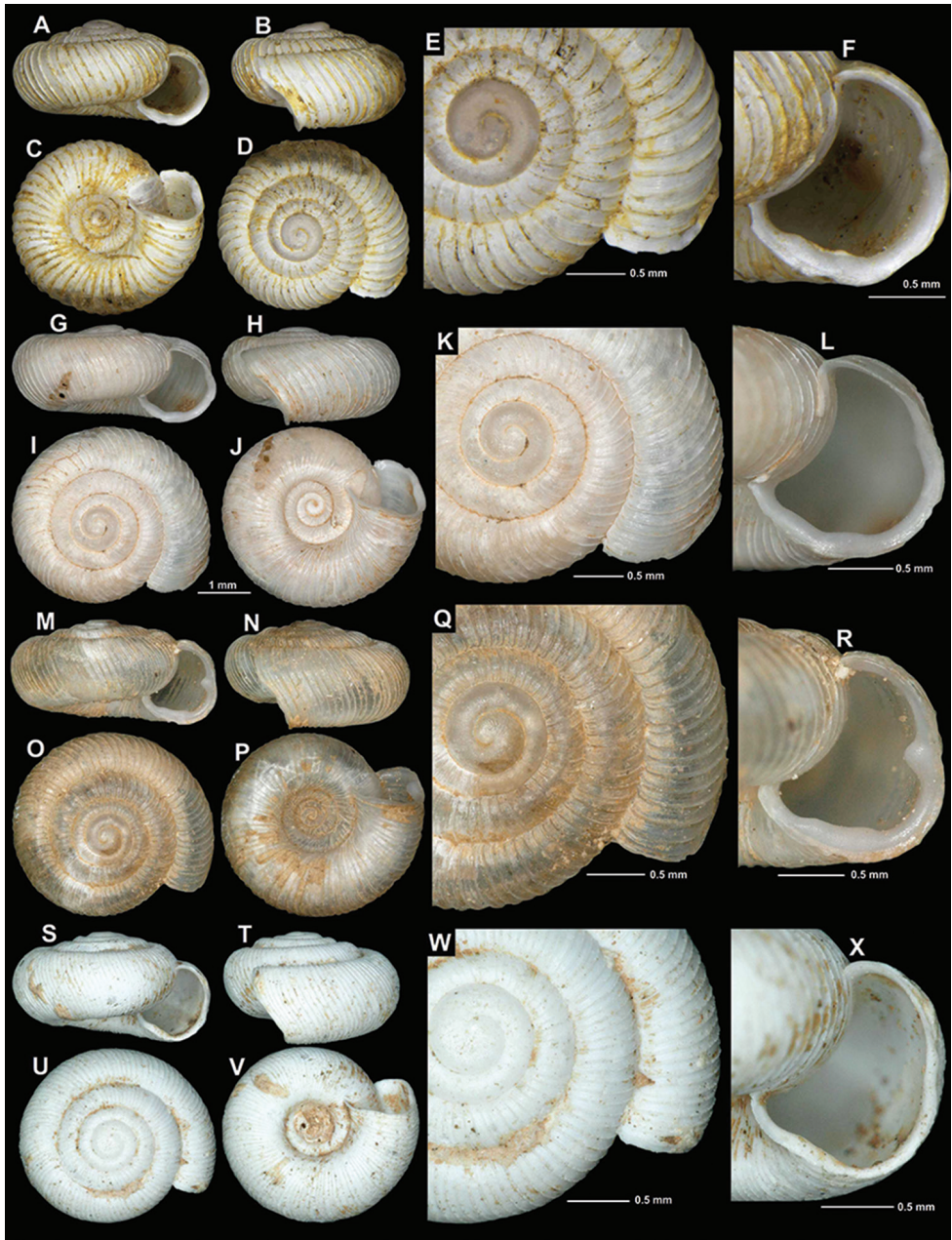


Figure 3. Shells of *Spelaediscus albanicus albanicus* (A. J. Wagner, 1914). **A–F** lectotype (NHMW 43385) **G–L** Albania, Drisht, right bank of Kir river opposite to the fortress hill (HNHM 103195) **M–R** Albania, Shkodër district, 1 km NE of Ura e Shtrenjtë (HNHM 103196) **S–X** Albania, rocks southwest of Zusi (NHMW 112358).

Differential diagnosis. See under *S. albanicus edentatus* ssp. n. Densely ribbed specimens of this subspecies might resemble large specimens of *S. unidentatus*. The latter species, however, usually has stronger teeth, and narrower aperture.

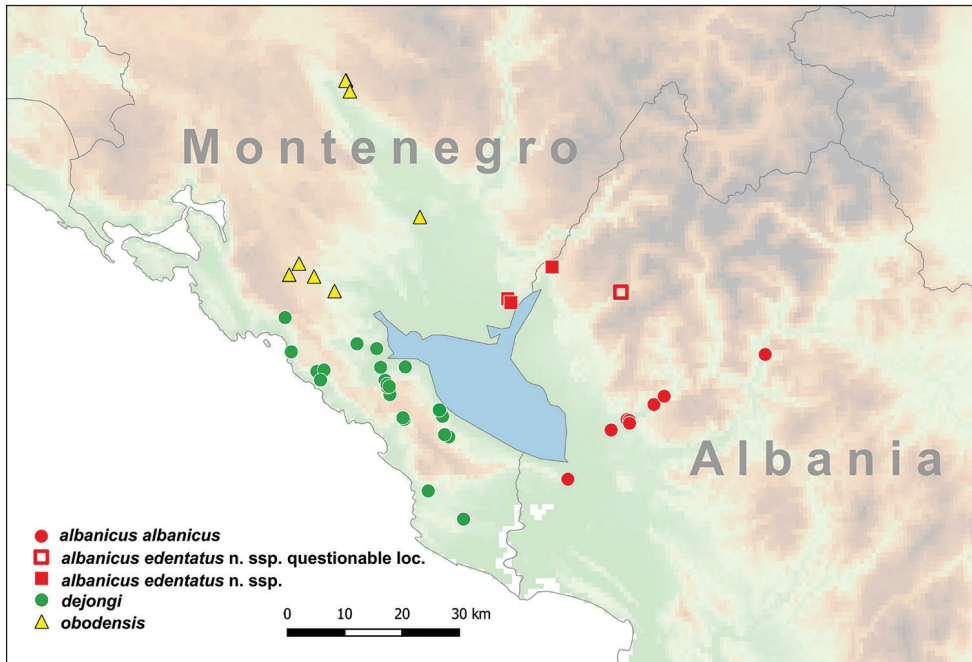


Figure 4. Distribution of *Spelaeodiscus* Brusina, 1886 species.

Variation among specimens. Some variability was found between populations in terms of rib density, spire height, and strength of apertural teeth.

Distribution. This subspecies is distributed in northwestern Albania. Most of the known distribution records are from the Kir River Valley. One shell found in the fluvial debris of the Drin River above the Koman Dam extends the range farther eastwards (Figure 4). Welter-Schultes (2012) erroneously reports this taxon from Montenegro.

Conservation status. See under *Spelaeodiscus albanicus*.

***Spelaeodiscus albanicus edentatus* Páll-Gergely & P. L. Reischütz, ssp. n.**

<http://zoobank.org/D00AA0E9-7121-451A-91C0-25655AAAED3C>

Figure 5A–L

Spelaeodiscus sp. (aff. *obodensis*) — Reischütz et al. 2013: 62.

Type material. Albania, rocks along the road Hani i Hotit to Vermosh, 7.2–7.8 km north of the junction, 370 m a.s.l., 42°22.451'N, 19°27.507'E, leg. A. Reischütz, N. Reischütz & P. L. Reischütz, Apr. 2014, NHMW 112360/1 (holotype, SW: 4.2 mm, SH: 2.2 mm, Fig. 5A–F), REI/4 paratypes; rocks above Hani i Hotit, leg. A. Reischütz, N. Reischütz & P. L. Reischütz, Apr. 2012, REI/1 paratypes; Montenegro, Podgorica Municipality, Izvor Vitoja S 1 km, near Shkodra Lake, 30 m, limestone rocks, 42°19.176'N, 19°22.158'E (site code: 2015/105), leg. Z.P. Eröss, Z. Fehér, J. Grego, 05



Figure 5. Shells of *Spelaodiscus* Brusina, 1886 species. **A–F** *Spelaodiscus albanicus edentatus* ssp. n., holotype (NHMW 112360) **G–L** *Spelaodiscus albanicus edentatus* ssp. n., Montenegro, rocks across the road at Vitoja, Skadarsko Jezero (NHMW 112361) **M–R** *Spelaodiscus densecostatus* sp. n., holotype (NHMW 112364).

Jul. 2015, HNHM 103197/4 paratypes, JG/4 paratypes, NHMW 112359/4 paratypes; Montenegro, rocks across the road at Vitoja, Skadarsko Jezero, 16 m a.s.l., 42°19.554'N, 19°21.776'E, leg. A. Reischütz, N. Reischütz & P. L. Reischütz, Apr. 2012, NHMW 112361/1 (photographed paratype, Fig. 5G–L), REI/4 paratypes.

Additional material. Albania, Malesia district, Xhajë NE 0.5 km, 650 m a.s.l., 42°19.838'N, 19°36.341'E (site code: 2015/103), rocks, leg. Z.P. Eröss, Z. Fehér & J. Grego, 04.07.2015, HNHM 103493/5 juvenile shells (not paratypes); NHMW 110430/MN/0985/5 juvenile shells (not paratypes), JG/6 juvenile shells (not paratypes).

Type locality. Albania, rocks along the road Hani i Hotit to Vermosh, 7.2–7.8 km north of the junction, 370 m a.s.l., 42°22.451'N, 19°27.507'E.

Diagnosis. Protoconch glossy; aperture without teeth.

Measurements. SW: 3.6–4.2 mm (median = 4.0 mm), SH: 1.9–2.2 mm (median = 2.1 mm), AW: 1.5–1.7 mm (median = 1.6 mm), AH: 1.3–1.6 mm (median = 1.4 mm), (n = 6; largest and smallest specimens of multiple populations measured).

Differential diagnosis. This new subspecies differs from the nominotypical subspecies in the following traits: aperture relatively larger, and its basal area not straight; apertural barriers (teeth) absent; protoconch smooth, glossy; ribs somewhat less dense (rib density on body whorl: 35–54).

Variation among specimens. This subspecies shows some variability in terms of shell size and rib density.

Etymology. This new subspecies is named after its toothless aperture, which distinguishes it from the nominotypical subspecies.

Distribution. This taxon is found in the northeastern part of the Lake Shkodër Basin (Figure 4).

Conservation status. See under *Spelaeodiscus albanicus*.

Spelaeodiscus dejongi Gittenberger, 1969

Figure 6

Spelaeodiscus (Spelaeodiscus) dejongi Gittenberger, 1969: 295–296, fig. 3.

Spelaeodiscus dejongi — Welter-Schultes 2012: 213.

Type material. Jama Nadjama bei Gnezdu (Izitovice), Krain, leg. Kuščer, coll. Edlauer, NHMW 49517a (holotype, SW: 2.8 mm, SH: 1.6 mm, Fig. 6A–E); Same data, NHMW 49517b/17 paratypes. See remarks concerning the type locality.

Other material. Vetajama bei Sokol, coll. Edlauer, NHMW 48071/2, (det. Gittenberger, 1974); Radetina pećina, Itijino brdo, 1300 m, leg. Dabović, NHMW 48312/11 (large shells, similar to the type); Pećina Marka Vuksanovića, 1400 m, leg. Dabović, coll. Edlauer ex coll. Kuščer 666/10, NHMW 49321/1 (det. Gittenberger, 1974); Montenegro, S of Virpazar, 1 km (in a straight line) ESE of Limljani, near the small road, 323 m a.s.l., 42°11.414'N, 19°06.277'E (site code: 20171019B), leg. T. Deli, Z.P. Eröss, A. Hunyadi & B. Páll-Gergely, 19.10.2017, DT/2, HA/1, HNHM 103198/2, PGB/1; Montenegro, S of Virpazar, 0.8 km (in a straight line) NE of Limljani, near the small road, 350 m a.s.l., 42°12.068'N, 19°05.969'E (site code: 20171019C), leg. T. Deli, Z.P. Eröss, A. Hunyadi & B. Páll-Gergely, 19.10.2017, DT/2, HA/2. HNHM 103199/2, PGB/1; Montenegro, 1.9 km (in a straight line) S of Virpazar, near the road, 160 m a.s.l., 42°13.312'N, 19°05.440'E (site code: 20171019E), leg. T. Deli, Z.P. Eröss, A. Hunyadi & B. Páll-Gergely, 19.10.2017, DT/24, EZP/24, HA/24, HNHM 103200/24 + 1 photographed shell (Fig. 6K–O), PGB/24; Montenegro, SE of Virpazar, 4.3 km (in a straight line) SSE of Đuravci, near Besa/Bes near Krone i Besit, 330 m a.s.l., 42°08.548'N, 19°13.165'E (site code: 20171019G), leg. T. Deli, Z.P. Eröss, A. Hunyadi & B. Páll-Gergely, 19.10.2017,

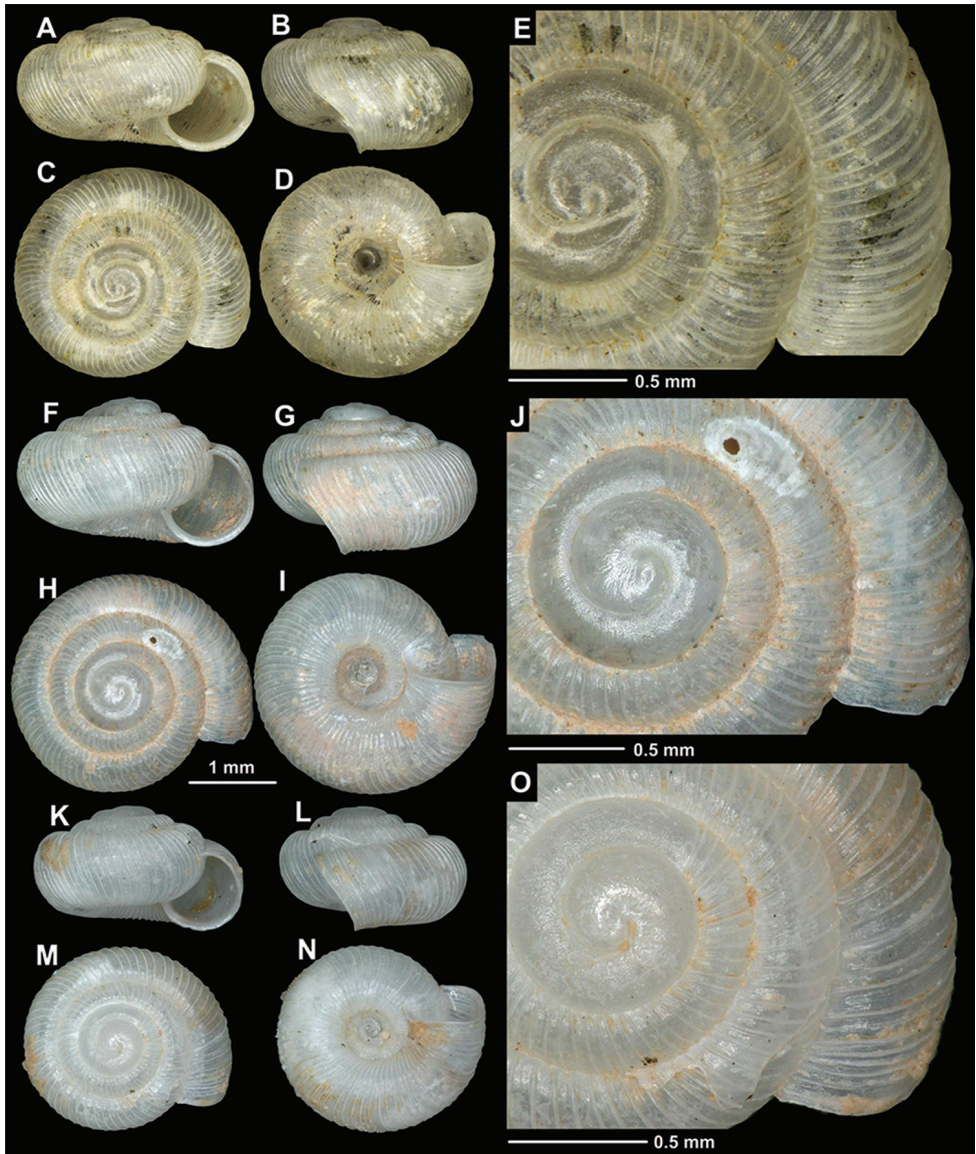


Figure 6. Shells of *Spelaediscus dejongi* Gittenberger, 1969. **A–E** holotype (NHMW 42517) **F–J** Montenegro, Gradiste Monastery (NHMW 112362) **K–O** Montenegro, 1.9 km (in a straight line) S of Virpazar (HNHM 103200).

DT/60–70, EZP/60–70, HA/60–70, HNHM 103201/28, PGB/60–70; Montenegro, SE of Virpazar, 7.3 km S(SE) of Đuravci, 1.6 km (in a straight line) NNW of Tejani, 455 m a.s.l., 42°06.803'N, 19°13.384'E (site code: 20171019I), leg. T. Deli, Z.P. Eröss, A. Hunyadi & B. Páll-Gergely, 19.10.2017, HNHM 103202/2; Montenegro, NNW of Virpazar, road between Rijeka Crnojevića and Virpazar, at the junc-

tion to Dupilo, 160 m a.s.l., 42°15.085'N, 19°04.987'E (site code: 20171020A), leg. T. Deli, Z.P. Eröss, A. Hunyadi & B. Páll-Gergely, 20.10.2017, HNHM 103203/1; Montenegro, S of Virpazar, 1.1 km (in a straight line) E of Limljani, one of the tunnels on the old road, 400 m a.s.l., 42°11.637'N, 19°06.309'E (site code: 20171021A), leg. T. Deli, Z.P. Eröss, A. Hunyadi & B. Páll-Gergely, 21.10.2017, DT/ca. 20, EZP/ca. 20, HA/ca. 20, HNHM 103204/6, PGB/ca. 20; Montenegro, S of Virpazar, 0.8 km (in a straight line) E of Limljani, above the village, 400 m a.s.l., 42°11.698'N, 19°06.217'E (site code: 20171021B), leg. T. Deli, Z.P. Eröss, A. Hunyadi & B. Páll-Gergely, 21.10.2017, DT/ca. 40, EZP/ca. 40, HA/ca. 40, HNHM 103205/8, PGB/ca. 40; Montenegro, NE of Bar, 1.2 km (in a straight line) NW of Tudjemili, 400 m a.s.l., 42°08.489'N, 19°08.144'E (site code: 20171021F), leg. T. Deli, Z.P. Eröss, A. Hunyadi & B. Páll-Gergely, 21.10.2017, DT/ca. 40, EZP/ca. 40, HA/ca. 40, HNHM 103206/10, PGB/ca. 40; Montenegro, 1.6 km (in a straight line) NE Petrovac, 0.3 km S of Novoselje, 470 m a.s.l., 42°13.032'N, 18°57.336'E (site code: 20171021G), leg. T. Deli, Z.P. Eröss, A. Hunyadi & B. Páll-Gergely, 21.10.2017, EZP/3; Montenegro, 2.8 km (in a straight line) NE Petrovac, 1.2 km E of Novoselje, 630 m a.s.l., 42°13.145'N, 18°58.245'E (site code: 20171021H), leg. T. Deli, Z.P. Eröss, A. Hunyadi & B. Páll-Gergely, 21.10.2017, DT/3, EZP/2, HA/4, HNHM 103207/1, PGB/2; Montenegro, Gradiste Monastery, 80 m a.s.l., 42°12.212'N, 18°57.772'E, leg. A. Reischütz, N. Reischütz & P. L. Reischütz, Jul. 2010, NHMW 112362/1 (photographed shell, Fig. 6F–J); REI/5; Montenegro, above Sv. Stefan south of Budva, 110 m a.s.l., 42°14.926'N, 18°54.131'E, leg. A. Reischütz, N. Reischütz & P. L. Reischütz, Mar. 2011, REI/4; Montenegro, Tudemili, 17 km towards Virpazar, Rumija Mts, 480 m a.s.l., 42°10.974'N, 19°6.546'E, leg. P. Subai, 15 Apr. 2009, NMBE 542070/56; Montenegro, Tudemili, 1 km towards Virpazar, Rumija Mts, 395 m a.s.l., 42°8.238'N, 19°8.388'E, leg. P. Subai, 25 Sep. 2005, NMBE 542069/1; Montenegro, Tudemili, 1 km towards Virpazar, Rumija Mts, 395 m a.s.l., 42°8.238'N, 19°8.388'E, leg. P. Subai, 25 Sep. 2005, NMBE 542068/3; Montenegro, Đuravci, 10 Km E, southern side of Mount Kronistar, 500 m a.s.l., 42°6.594'N, 19°13.908'E, leg. P. Subai, 16 Sep. 2006, NMBE 542067/1; Montenegro, Zoganje N 5 km, on the Ulcinj-Shkodër road, 80 m a.s.l., 41°58.762'N, 19°15.547'E (site code: 2015/32), leg. T. Deli, Z.P. Eröss & Z. Fehér, 27 May 2016, DT/ca. 50, HNHM 103208/22, NHMW 112363/ca. 50; Montenegro, Rumija Mts, Virpazar S 9 km (Virpazar–Bar road, between Boljevići and Tudemili), old tunnel, 440 m, 42°11.474'N, 19°06.489'E (site code: 2008/182), leg. Z. Fehér, J. Kontschán & D. Murányi, 14.10.2008, HNHM 103209/23; Montenegro, scree (talus) ca. 5 km east of Dobra Voda in direction of Vladimir, 220 m a.s.l., 42°1.508'N, 19°11.160'E, leg. A. Reischütz, N. Reischütz & P. L. Reischütz, Jul. 2010, REI/6; Montenegro, Donji Murići, above the village, at the junction of a minor road to Besa, 200 m a.s.l., 42°9.233'N, 19°12.930'E (site code 2017/007), leg. Z.P. Eröss & Z. Fehér 16.07.2017, HNHM 103492/1 (juvenile shell, identification uncertain).

Diagnosis. A small to medium sized species with dense, low ribs, smooth protoconch, and toothless aperture.

Description. Shell nearly flat, but spire somewhat always elevated; protoconch consists of 1.25–1.75 whorls, rather glossy; teleoconch with fine, equidistant, dense ribs; rib density variable (57–112 ribs on body whorl); between main ribs some fine wrinkles discernible; entire shell with 3.25–3.75 whorls; aperture semilunar; peristome slightly thickened and expanded; aperture toothless; umbilicus regular funnel-shaped, relatively narrow (width depends on spire height).

Measurements. SW: 1.9–3.4 mm (median = 2.3 mm), SH: 1.1–1.7 mm (median = 1.3 mm), AW: 0.7–1.3 mm (median = 0.9 mm), AH = 0.8–1.3 mm (median = 0.9 mm), AA = 56–68° (n = 15).

Differential diagnosis. See under *S. obodensis* and *S. hunyadii* sp. n.

Variation among specimens. This is a widely distributed species with numerous known populations, most of them with unique character states of spire height, shell size, and rib density.

Distribution. This species is distributed in the Rumija Mountain between the Shkodër Lake Basin and the Adriatic Sea. Northwards the range extends to the Cetinje area. According to the original labels, type material is of Slovenian origin, however, this species was never again found in Slovenia. It can be reasonably supposed that it is due to mislabelling and the ‘type locality’ is not the site where the type material actually came from (Gittenberger 1975). Welter-Schultes (2012) reports the species only from Slovenia, which is based on the originally incorrect type locality.

Conservation status. Assessed as Least Concern (LC) by Reischütz (2017a), because it is not an extremely rare species and there is no reason to suppose that the habitat quality, habitat extent or population are deteriorating or extremely fluctuating. Now, the number of known locations is more than 20, which confirms the LC status.

***Spelaeodiscus densecostatus* Páll-Gergely & A. Reischütz, sp. n.**

<http://zoobank.org/DDB4A406-1BF8-4062-A6F4-FB723C513FF8>

Figure 5M–R

Type material. Montenegro, Hotel/Restaurant Izvor north of Sutomore, no GPS available, leg. A. Reischütz, N. Reischütz & P. L. Reischütz, May 2015, NHMW 112364 (holotype: SW = 3.7 mm, SH = 1.8 mm, Figure. 5M–R), REI/1 juvenile/broken paratype.

Type locality. Montenegro, Hotel/Restaurant Izvor north of Sutomore.

Diagnosis. A large species with very low and dense ribs; aperture toothless.

Description. Spire slightly elevated; protoconch consists of slightly more than 1.5 whorls, rather glossy; teleoconch with very fine, low, equidistant riblets (approx. 112 on the body whorl); between main ribs some fine wrinkles discernible; entire shell with 3.75 whorls; aperture semilunar, peristome; peristome expanded and slightly reflected on the basal and umbilical areas; aperture toothless; umbilicus regular funnel-shaped, relatively wide.

Measurements. SW = 3.7 mm, SH = 1.8 mm, AW = 1.5 mm, AH = 1.4 mm (holotype).

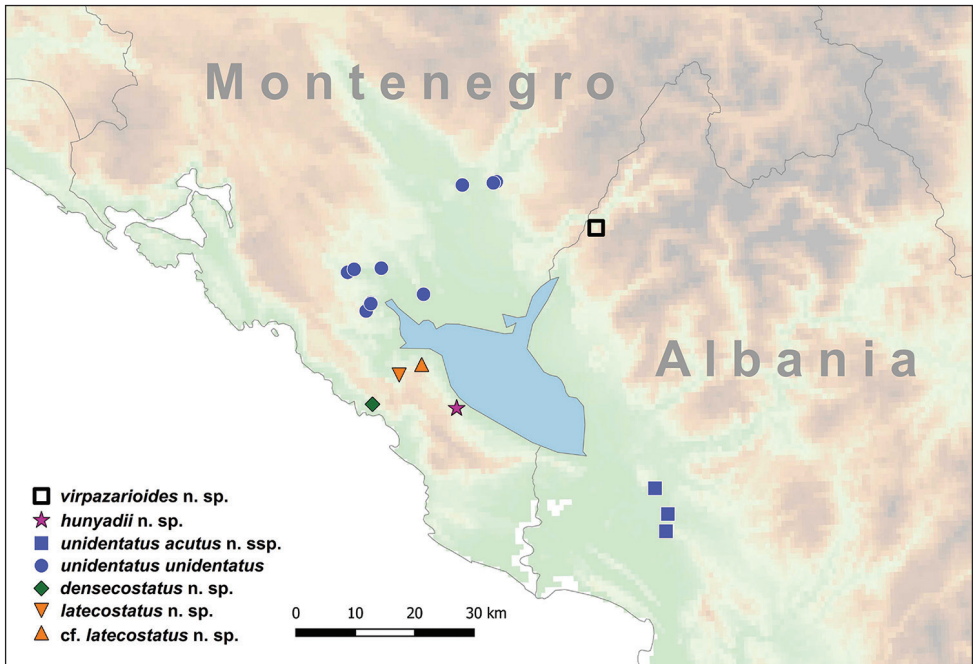


Figure 7. Distribution of *Spelaeodiscus* Brusina, 1886 species.

Differential diagnosis. *Spelaeodiscus densecostatus* sp. n. differs from *S. albanicus* by the smaller shell and the much denser and lower ribs on the teleoconch. Furthermore, *S. albanicus albanicus* has two basal and a palatal tooth in the aperture.

Variation among specimens. The only known adult shell is the holotype. Therefore, the morphological diversity within population is unknown.

Etymology. This new species is named for its dense ribs, which distinguishes it from the most similar *S. albanicus*.

Distribution. This species is known from the type locality only (Figure 7).

Conservation status. The number of known locations of this species is less than five (i.e. known from a single site) and AOO is smaller than 20 km², but there is no reason to suppose that AOO, EOO, number of locations, number of subpopulations or the number of mature individuals are declining or extremely fluctuating. Therefore, it should be assessed as Near Threatened (NT).

Spelaeodiscus hauffeni (Schmidt, 1855)

Figure 8A–O

Helix Hauffeni Schmidt, 1855: 3–4.

Patula Hauffeni — Clessin 1887: 104.

Aspasita Hauffeni — Sturany and Wagner 1914: 67, plate 2, figs 11a–c.

Spelaodiscus hauffeni — Pilsbry 1926: 185, Plate 22, Figs 9–11.

Spelaodiscus hauffeni — Bole 1965: 351–352, fig. 1b, 2a, Plate 76, fig. A.

Spelaodiscus (Spelaodiscus) hauffeni — Gittenberger 1969: 292–293, fig. 1.

Spelaodiscus hauffeni — Welter-Schultes 2012: 213.

Type material. Krain: Krimberg-Grotte, ex coll. Schmidt, SMF 53902/3 syntypes; No locality, (“Orig. Ex.”), NHMW 52776/2 syntypes (Figure 8A–E).

Other material. Velikajama, Soko Kod, Sela Dopilo (geographic position unknown), coll. Edlauer ex coll. Dabovič, NHMW 48473/2 shells (1 adult + 1 juvenile) (in brackets: neben 49.999, probably mistyped 48.999, because this was a mixed lot of *S. hauffeni* and *S. dejongi*; this is obviously incorrect locality for this species); Jama nadjama pri Gnezdu (Izilovice) (= Jama pri Gnezdu at 45.939°N, 14.271°E), coll. Edlauer ex coll. Kuščer, NHMW 49137(?) / 1 (incorrect locality); Krain, coll. Oberwimmer, NHMW 71640/O/00161/2; Carn., coll. Schmidt, NHMW 112346/2; Krain, coll. Kobelt ex coll. Ullepitsch, SMF 10663/2 adult+2 juvenile shells; Krain: Stubič, coll. C.R. Boettger, 1905, SMF 112878/1; Krainer Höhlen, coll. Kaltenbach ex coll. Müller, SMF 259470/1; Carniolia (= Krain), coll. Knobbe ex coll. Hauffen, SMF 53904/1; Höhle in Innerkrain, leg. Sever, coll. Ehrmann ex coll. Absolon, SMF 53905/1; Tekavičja jama (= Tkavčja jama, 45.824°N, 14.721°E), Dobropolje, NHMW 112350/2 strongly corroded shells; Krain, Tekavčja jama, Dobropolje, coll. Edlauer ex coll. Kuščer, NHMW 48468/3; Tekarija jama b. Dobropolje, coll. S.H. Jaeckel ex coll. Kuščer, SMF 200961/3; Krain, Tekavčja jama, Dobropolje, coll. Haas ex coll. Kuščer, SMF 53906/1; Krain, Berjakovo Brezno (= Malo Brezarjevo brezno, 46.080°N, 14.436°E), n. w. von Laibach, coll. Retaner (?), NHMW 12314/2; Berjakovo Brezno, nw v. Laibach, Krain, coll. Klemm ex coll. Edlauer, NHMW 79000/K/02938/2; Same data, coll. Schlickum, ex coll. Edlauer, SMF 275440/2; Berjakovo Brezno bei Dolnice n.w. von Ljubljana, coll. S.H. Jaeckel ex coll. Edlauer, SMF 200962/1; Radetina pečina, coll. Edlauer ex coll. Kuščer, NHMW 48751/6; Spodnja Skedevenica (at 45.854°N, 14.639°E), vel. Lašče, coll. Edlauer ex coll. Kuščer, NHMW 48883/15; Spodnja Skedevnica, coll. Edlauer ex coll. Kuščer, NHMW 48422/2; Spodnja Kedenrica, coll. W. Klemm ex coll. Kuščer, NHMW 33672/1 (figured shell, Fig. 8K–O); Sponja Skednevisa bei Preserje, coll. Edlauer ex coll. Kuščer, NHMW 48124/2; Am Eingang der Doline Jama bei Kompole (=Kompoljska jama at 45.800°N, 14.731°E), S. Oest. von Dobropolje, coll. Klemm, NHMW 112347/1; In der Raska Skedebnza bei Ponikve südl. von Dobropolje (= Skedenc at 45.89687418°N, 14.50100919°E), coll. Klemm, NHMW 112348/3; Reoteiner Grotte bei Poduzik (?) bei Ljubljana (Kalkofen) (Podutiško brezno at 46.076°N, 14.445°E), coll. Edlauer ex coll. Kuščer, NHMW 49111/1; Brezarjeva brezno pri Boduzik (?), coll. Edlauer ex coll. Kuščer, NHMW 48390/2; Brezno v. Leskovi dolini (at 45.941°N, 14.256°E), coll. Edlauer ex coll. Kuščer, NHMW 49200/1; Mašun b Gratenbrunn (probably Jama na Mašunu at 45.630°N, 14.373°E), Krain, leg. Schollmayer, NHMW 112349/2 juvenile shells; Duplica (=Dupliška jama at 45.963°N, 14.684°E), coll. Edlauer ex coll. Kuščer, NHMW 48576/16; Jama v Jurčelovih(?) (Jama 1 v Jurcetovih Percah at 46.09984722°N, 14.42093707°E or Jama 2 na Jurcetovih Percah at 46.101°N 14.418°E, the first is indi-

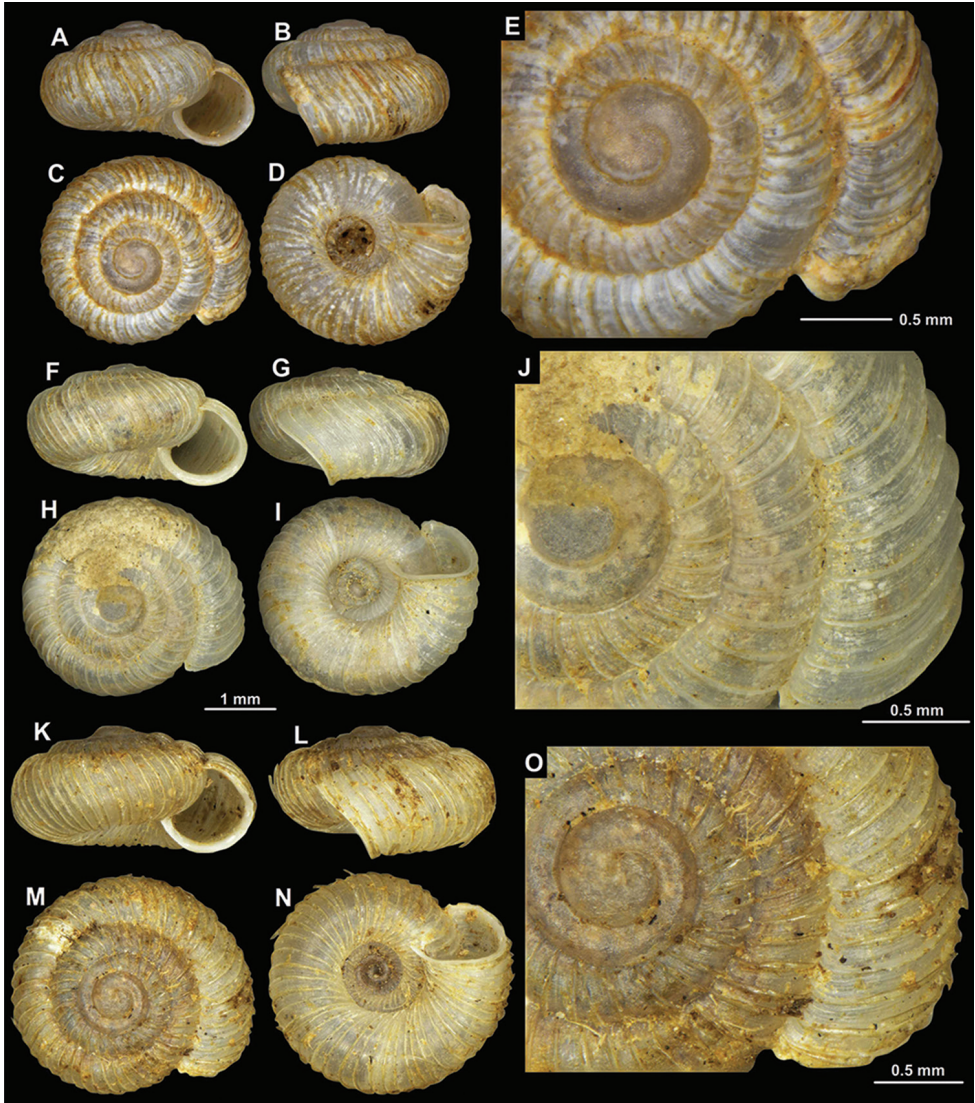


Figure 8. Shells of *Spelaeodiscus hauffeni* (Schmidt, 1855). **A–E** Syntype (NHMW 52776) **F–J** NHMW 71770/R/19 **K–O** Slovenia, Spodnja Kedenrica (NHMW 33672).

cated on the map), percah Tosko čelo, coll. Edlauer ex coll. Kuščer, NHMW 48688/16; Zakrita jama odd B (at 45.925°N, 14.293°E), coll. Edlauer ex coll. Kuščer, NHMW 48748/1 juvenile shell; Unterkrain: Grotte Thauzhia jama, coll. C. v. Heyden ex coll. N. Hoffmann, SMF 53903/1; Same data, coll. Gysser ex coll. Heynemann ex coll. C. v. Heyden, SMF 53901/2; Same data, coll. Heynemann ex coll. C. v. Heyden ex coll. N. Hoffmann, SMF 259469/3; Krain: Jeliarc-Grotte (maybe Jeliare or Jelice), coll. Th. Krüper, SMF 112877/1; Höhle Malo Bukuje bei Dobrova, Krain, coll. Dr. Leo Rušnov, ex coll. Dr. A. Oberwimmer, NHMW 71770/R/19 (1 photographed shell, Fig. 8F–J).

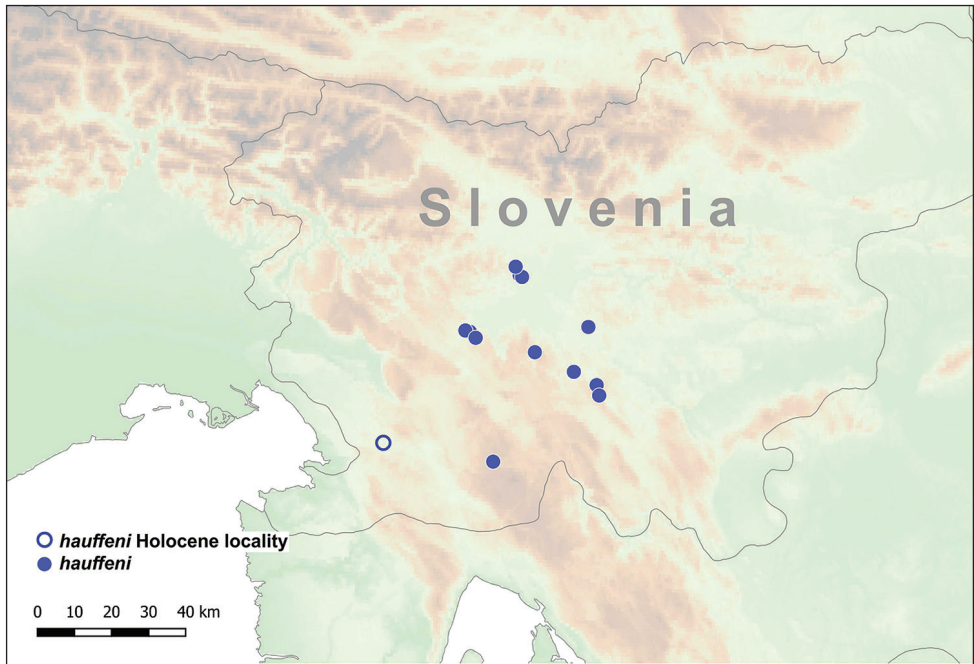


Figure 9. Distribution of *Spelaediscus hauffeni* (Schmidt, 1855).

Diagnosis. A medium sized species with very widely spaced, strong ribs, rounded, toothless aperture, and finely granular protoconch.

Description. Spire somewhat elevated; protoconch consists of 1.5–1.75 whorls, very finely granulated, rather matte, not glossy; teleoconch with strong ribs that are supported by fine periostracal filaments in fresh shells; ribbing less regular than in other congeneric species; ribs widely spaced (41–52 ribs on body whorl); between main ribs some fine wrinkles discernible; entire shell with 3.75–4.25 whorls; aperture toothless, semilunar/rounded; peristome slightly thickened, slightly reflected in direction of umbilicus; umbilicus regular funnel-shaped, relatively narrow.

Measurements. SW: 2.8–3.5 mm (median = 3.0 mm), SH: 1.7–1.9 mm (median = 1.8 mm), AW: 1.1–1.4 mm (median = 1.2 mm), AH: 1.0–1.3 mm (median = 1.1 mm), (n = 6; largest and smallest specimens of multiple populations measured).

Differential diagnosis. The most similar taxon to *Spelaediscus hauffeni* is *S. albanicus edentatus* ssp. n. in terms of shell size, shape, and rib density. However, the latter one is usually larger, has a glossier protoconch, a less rounded aperture caused by the straighter basal part, and the peristome edge on the palatal side is more strongly expanded (rather thickened only in *S. hauffeni*).

Variation among specimens. *Spelaediscus hauffeni* shows some variability in terms of shell size and spire height, but the rib density and the formation of the aperture are stable characters.

Distribution. This species is distributed in the southeastern Alps (Central Slovenia) relatively far from the ranges of its congeneric taxa. Slapnik (2005) found shells in the Škocjan Caves Regional Park, which are probably of Holocene age (Figure 9).

Conservation status. As there are several known locations and no reason to suppose that the habitat quality, habitat extent or population are deteriorating or extremely fluctuating, it was assessed as Least Concern (LC) by Reischütz (2017b).

***Spelaeodiscus hunyadii* Páll-Gergely & Deli, sp. n.**

<http://zoobank.org/5DB55567-0640-4C82-8BF3-B2A281366C7A>

Figure 10A–E

Type material. Montenegro, SE of Virpazar, 4.3 km (in a straight line) SSE of Đuravci, near Besa/Bes near Krone i Besit, 330 m a.s.l., 42°08.548'N, 19°13.165'E (site code: 20171019G), leg. T. Deli, Z.P. Eröss, A. Hunyadi & B. Páll-Gergely, 19.10.2017, HNHM 103210 (holotype, SW: 2.1 mm, SH: 1.2 mm, Fig. 10A–E), DT/40 paratypes, EZP/40 paratypes, HA/40 paratypes, HNHM 103211/3 paratypes, PGB/40 paratypes, NMBE 554178/3 paratypes, NHMW 112367/4 paratypes; Montenegro, Donji Murići junction S 2 km along the Virpazar-Ostros road, 320 m a.s.l., 42°8.544'N, 19°13.182'E (site code: 2017/009), leg. Z.P. Eröss & Z. Fehér, 16.07.2017, HNHM 103212/3 paratypes, EZP/3 paratypes.

Type locality. Montenegro, SE of Virpazar, 4.3 km (in a straight line) SSE of Đuravci, near Besa/Bes near Krone i Besit, 330 m a.s.l., 42°08.548'N, 19°13.165'E.

Diagnosis. A small, nearly flat species with strong, widely spaced ribs, glossy protoconch and strongly oblique, toothless aperture.

Description. Spire somewhat elevated; protoconch consists of 1.25–1.5 whorls, smooth, glossy; teleoconch with very strong (thick), equidistant, widely spaced ribs; rib density: 42–48 ribs on body whorl; between main ribs some fine wrinkles discernible; entire shell with 3.5–3.75 whorls; aperture semilunar, toothless, strongly oblique to shell axis; peristome slightly thickened and expanded in direction of umbilicus; umbilicus funnel-shaped, relatively narrow.

Measurements. SW: 2.1–2.2 mm (median = 2.2 mm), SH: 1.2–1.3 mm (median = 1.2 mm), AW: 0.8–0.9 mm (median = 0.9 mm), AH: 0.6–0.7 mm (median = 0.7 mm), AA = 47–52° (n = 4; largest and smallest specimens measured).

Differential diagnosis. *Spelaeodiscus obodensis* has a more conical shell and roughly sculptured protoconch. The most similar species to *Spelaeodiscus hunyadii* sp. n. is *S. dejongi*, which lives sympatrically with the new species. It differs from *Spelaeodiscus hunyadii* sp. n. in the less oblique aperture and the denser ribs. Some other populations of *S. dejongi* also possess widely spaced ribs, but their aperture is less oblique, thus, they can be distinguished from this new species. See also under *S. latecostatus* sp. n.

Variation among specimens. Specimens of the type sample show no notable conchological variability.

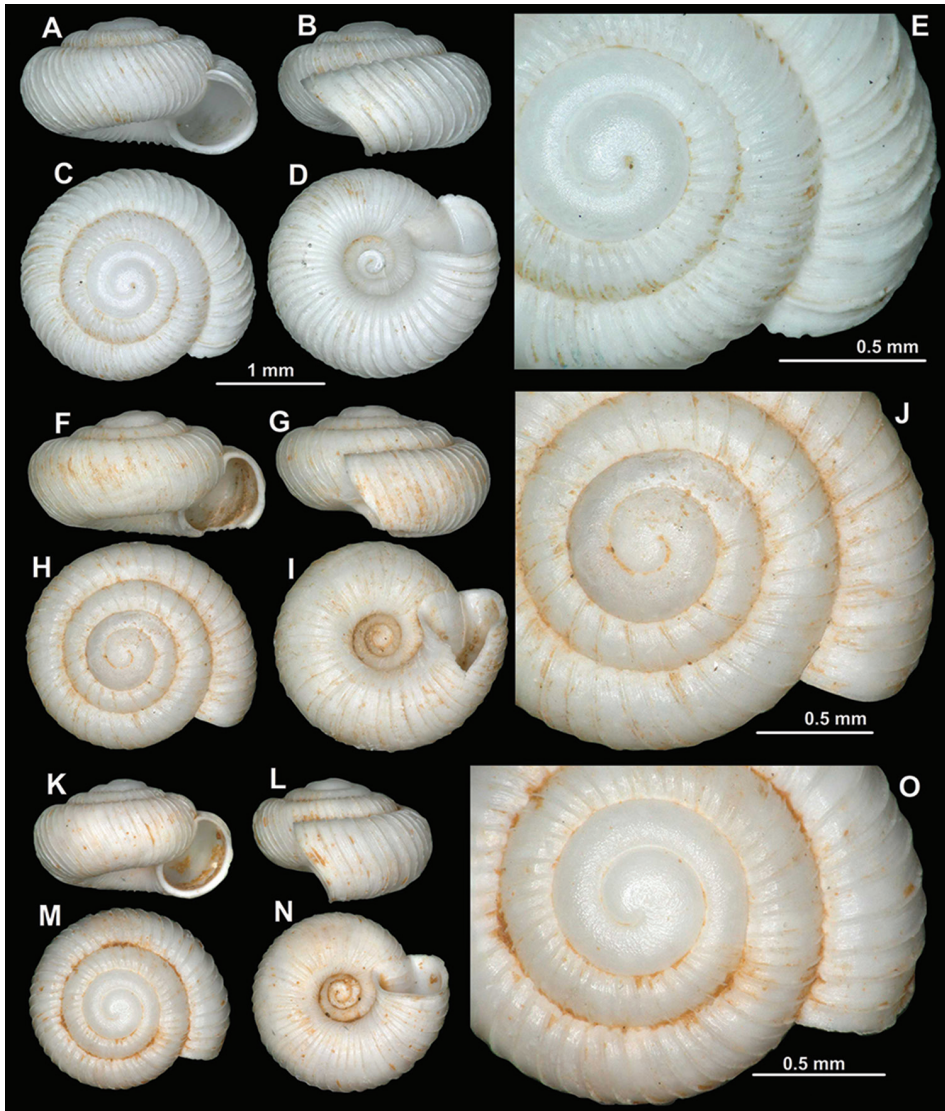


Figure 10. Shells of *Spelaediscus* Brusina, 1886 species. **A–E** *Spelaediscus hunyadi* sp. n., holotype (HNHM 103210) **F–J** *Spelaediscus latecostatus* sp. n., holotype (HNHM 103214) **K–O** *Spelaediscus* cf. *latecostatus* sp. n., Montenegro, Seoča S 1 km (HNHM 103213).

Etymology. This new species is named after our colleague and friend, András Hunyadi, who is one of those who first collected this species.

Distribution. This species is known from the type locality only (Figure 7).

Conservation status. To our present knowledge this species is very rare (currently known from a single location) and thus AOO is smaller than 20 km². However, there is no reason to suppose that AOO, EOO, number of locations, number of subpopulations or the number of mature individuals are declining or extremely fluctuating. Therefore, it might be assessed as Near Threatened (NT).

***Spelaodiscus latecostatus* Páll-Gergely & Erőss, sp. n.**

<http://zoobank.org/AEFE6B2C-573F-4C04-8353-4A413B536F24>

Figure 10F–O

Type material. Montenegro, S of Virpazar, 0.8 km (in a straight line) E of Limljani, above the village, 400 m a.s.l., 42°11.698'N, 19°06.217'E (site code: 20171021B), leg. T. Deli, Z.P. Erőss, A. Hunyadi & B. Páll-Gergely, 21.10.2017, HNHM 103214 (holotype, Fig. 10A–E).

Other material. Montenegro, Seoća S 1 km, along the Virpazar-Ostros road, 280 m a.s.l., 42°12.618'N, 19°9.000'E (site code: 2017/005), leg. Z.P. Erőss & Z. Fehér, 16.07.2017, HNHM 103213/3 shells, not paratypes (Fig. 10K–O).

Type locality. Montenegro, S of Virpazar, 0.8 km (in a straight line) E of Limljani, above the village, 400 m a.s.l., 42°11.698'N, 19°06.217'E (site code: 20171021B).

Diagnosis. A small, nearly flat species with strong, very widely spaced ribs, glossy protoconch and a toothless aperture.

Description of the holotype. Spire somewhat elevated; protoconch consists of ca 1.25–1.5 whorls (the holotype is corroded at the protoconch-teleoconch junction), rather smooth, moderately glossy; teleoconch with very strong, equidistant, widely spaced ribs (42 on the body whorl); between main ribs some fine wrinkles discernible; entire shell with 3.75 whorls; aperture semilunar, toothless; peristome slightly thickened and expanded; umbilicus funnel-shaped, relatively narrow.

Measurements. SW: 2.2 mm, SH: 1.2 mm, AW: 0.8 mm, AH: ca. 0.8 mm, AA = 63°(holotype).

Differential diagnosis. The widely spaced ribs are similar to *S. hunyadii* sp. n., but the less oblique aperture distinguishes *S. latecostatus* sp. n. from the other new species. *Spelaodiscus dejongi*, which lives sympatrically with *S. latecostatus* sp. n., is similar in shell shape and size and the formation of the aperture, but has much denser ribs.

Variation among specimens. See remarks.

Etymology. This new species is named after its remarkably widely spaced ribs.

Distribution. See under Remarks and Figure 7.

Remarks. The holotype of this species was found in a large sample of *S. dejongi*. Therefore, even if the shell shape does not differ from that species, the widely spaced ribs indicate that *S. latecostatus* sp. n. differs from *S. dejongi* on species level. Three shells from 1 km S of Seoća possess denser ribs than other *S. dejongi* populations (47–54 ribs on the body whorl), but obviously the rib density is lower than that of the holotype of *S. latecostatus* sp. n. Since the rib density of that population is intermediate between *S. dejongi* and *S. latecostatus* sp. n., it is not possible to decide which species it belongs to. More populations around the sample from 1 km S of Seoća site are necessary in order to provide a reliable identification. Here we provisionally identify those shells as *Spelaodiscus* cf. *latecostatus* sp. n.

Conservation status. To our present knowledge this species is very rare (currently known from two locations) and thus AOO is smaller than 20 km². However, there is no reason to suppose that AOO, EOO, number of locations, number of subpopulations or the number of mature individuals are declining or extremely fluctuating. Therefore, it might be assessed as Near Threatened (NT).

***Spelaeodiscus obodensis* Bole, 1965**

Figures 11, 12

Spelaeodiscus obodensis Bole, 1965: 350, plate 76, fig. D.*Spelaeodiscus (Spelaeodiscus) obodensis* — Gittenberger 1969: 296–297, fig. 1.*Spelaeodiscus obodensis* — Welter-Schultes 2012: 213. (partim: the photos show *S. unidentatus* specimens)**Type material.** Obodska pećina, Rij. Crnojevića, Mtg., September 1956, MZBI 1018 (2 adult and 3 juvenile/broken syntypes, photos were examined, Figure 12A).**Material examined.** Vodna jama (Lovćen), coll. Edlauer ex coll. Kuščer, NHMW 48543/2 (det. Gittenberger, 1973 Sep.); Same data, NHMW 49765/2; Montenegro, Ostrog, rocks below the upper parking lot, 820 m a.s.l., 42°40.534'N, 19°1.744'E, leg. A. Reischütz, P. L. Reischütz & N. Steiner-Reischütz, May 2017, REI/1; Montenegro, Ostrog, entrance of the penultimate parking lot, 770 m a.s.l., 42°40.510'N, 19°1.663'E, leg. A. Reischütz, P. L. Reischütz & N. Steiner-Reischütz, May 2017, NHMW 112365 (photographed shell, Fig. 11F–J), REI/1; Montenegro, Ostrog, 1 km north from Hotel Sokoline on the new street to Podgorica, 630 m a.s.l., 42°39.498'N, 19°2.188'E, leg. A. Reischütz, P. L. Reischütz & N. Steiner-Reischütz, May 2017, REI/2; Montenegro, 500 m south of the bridge over the Sitnica river, north of Podgorica, 45 m a.s.l., 42°27.473'N, 19°10.825'E, leg. A. Reischütz, N. Reischütz & P. L. Reischütz, Apr. 2012, NHMW 112366/1 (photographed shell, Fig. 11K–O), REI/2; Yugoslavia: Pećina u Peckom Brdu bg., above Začir, leg. L. Pintér & P. Subai, 20 Jul. 1972, HNHM 41127/2; Same data, HNHM 18062/3 (one of them is photographed, Fig. 11A–E); Montenegro, Pećina u peckom Brdu bei Začir (Brdu-cave at Začir), leg. H. Schütt, 06.06.1978, HNHM 42402/3.**Diagnosis.** A medium sized species with elevated spire, roughly sculptured protoconch, strong ribs on the teleoconch, and toothless aperture.**Description.** Spire elevated, shell low conical; protoconch consists of 1.25–1.5 whorls, roughly granulated/"hammered", matte, not glossy; teleoconch with strong, equidistant ribs that are supported by fine periostracal filaments in fresh shells; rib density variable (43–76 ribs on body whorl), usually widely spaced; between main ribs some fine wrinkles discernible; entire shell with 3.75–4 whorls; aperture semilunar, toothless; peristome slightly thickened and expanded, especially in direction of the umbilicus; umbilicus funnel-shaped, relatively narrow.**Measurements.** SW: 2.6–3.0 mm (median = 2.8 mm), SH: 1.6–1.9 mm (median = 1.7 mm), AW: 0.9–1.2 mm (median = 1.1 mm), AH: 1.0–1.2 mm (median = 1.1 mm), AA = 64–70° (n = 10; largest and smallest specimens of multiple populations measured).**Differential diagnosis.** The most similar species is *S. dejongi*, which usually has a lower spire, weaker ribs, and a glossy protoconch.**Variation among specimens.** This species is the most variable in terms of shell size and rib density.**Distribution.** This species is found northwest of the Shkodër Lake Basin, as well as in the Zeta River Valley between Podgorica and the Ostrog Monastery (Figure 4).

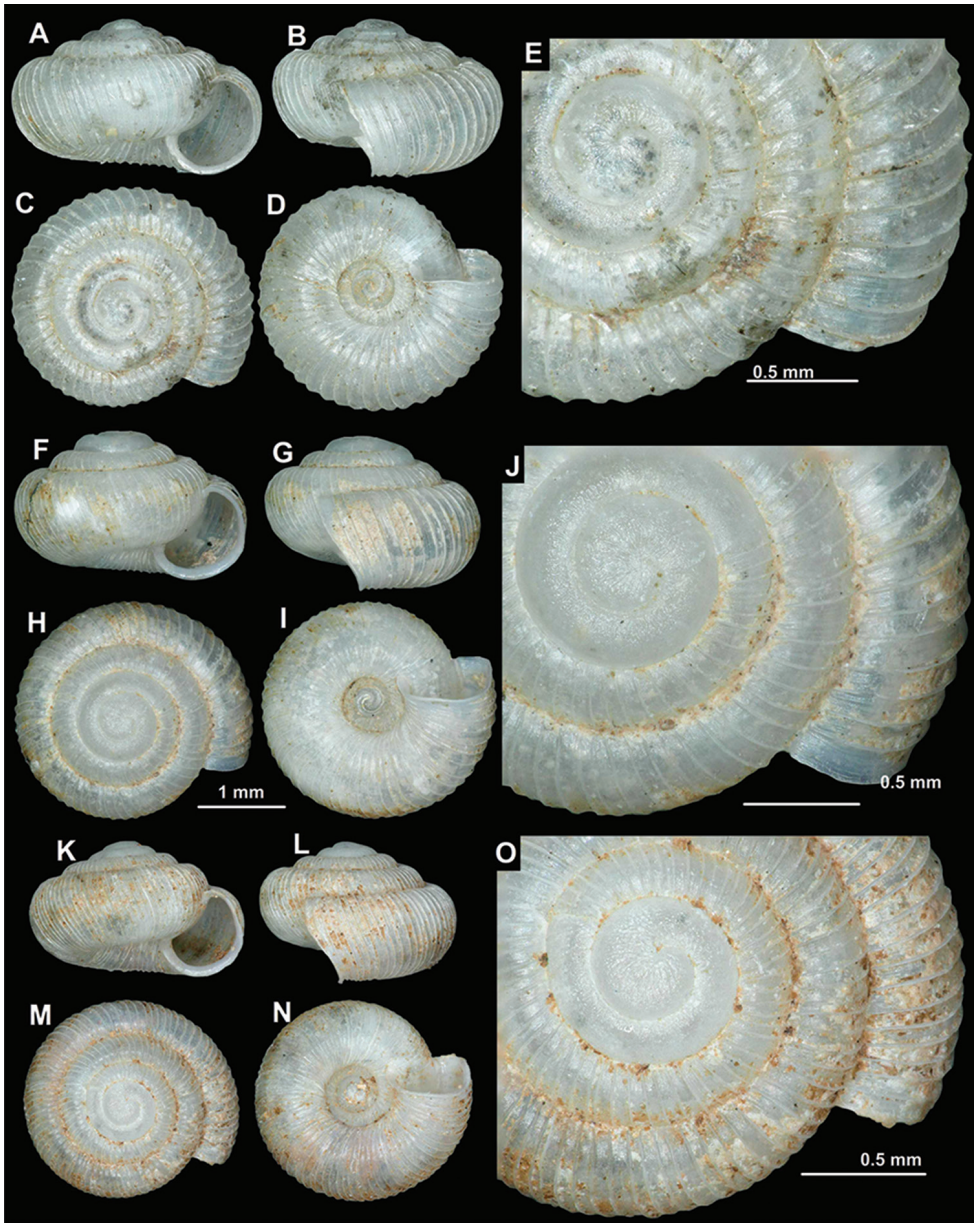


Figure 11. *Spelaeodiscus obodensis* Bole, 1965. **A–E** Pecina u Peckom Brdu cave, above Zacir (HNHM 18062) **F–J** Montenegro, Ostrog, entrance of the penultimate parking lot (NHMW 112365) **K–O** Montenegro, 500 m south of the bridge over the Sitnica river (NHMW 112366).

The Albanian record given by Reischütz et al. (2013) and referred by Reischütz (2017c) is actually *S. albanicus edentatus* ssp. n. So far, no Albanian occurrence is known.

Conservation status. As there are at least seven known locations and no reason to suppose that the habitat quality, habitat extent or population are deteriorating or extremely fluctuating, it was assessed as Least Concern (LC) by Reischütz (2017c).

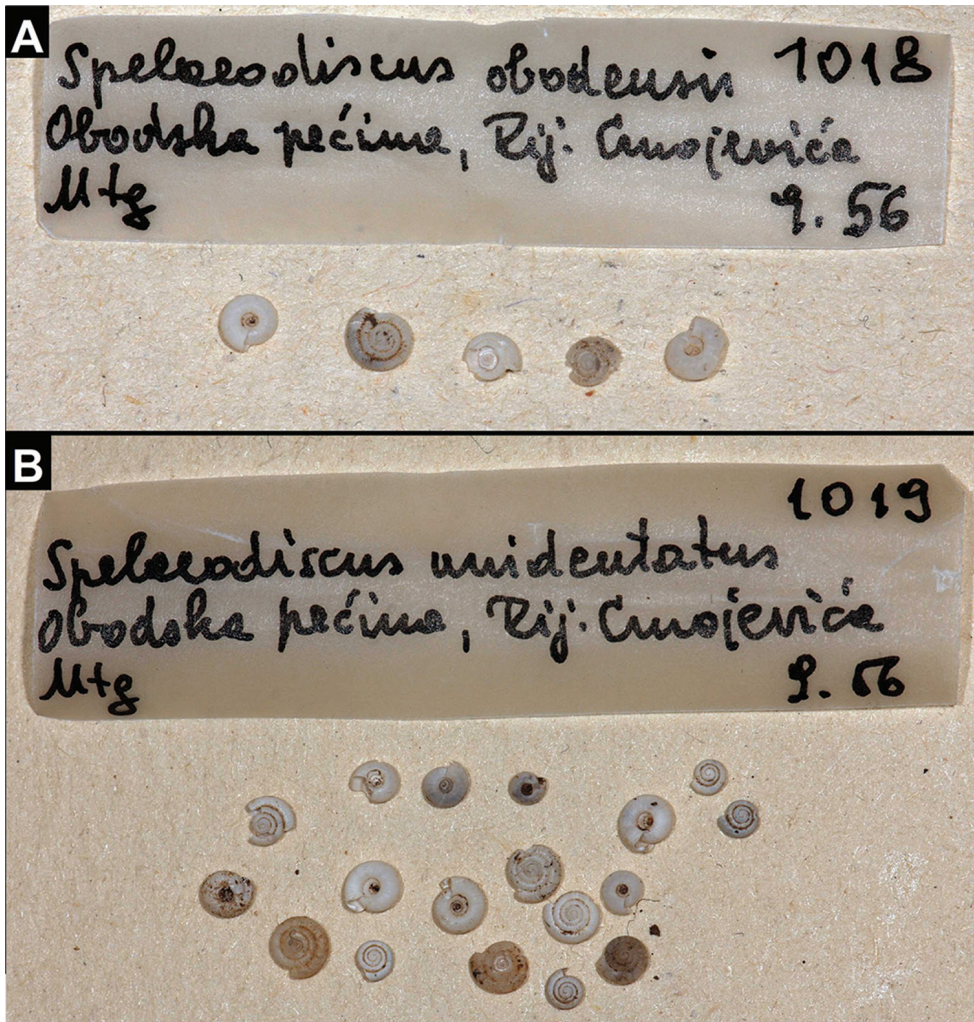


Figure 12. Type sample of *Speleodiscus obodensis* Bole, 1965 (A) and *Speleodiscus unidentatus unidentatus* Bole, 1961 (B).

Speleodiscus unidentatus Bole, 1961

Diagnosis. A small to medium sized species with dense riblets, and strong parietal and basal teeth/thickenings.

Differential diagnosis. This species differs from most other *Speleodiscus* species by the presence of two well-developed apertural teeth (a palatal and a basal). See also under *Speleodiscus albanicus*.

Conservation status. As there are more than five known locations and no reason to suppose that the habitat quality, habitat extent or population are deteriorating or extremely fluctuating, it was assessed as Least Concern (LC) by Reischütz (2017d).

***Spelaeodiscus unidentatus unidentatus* Bole, 1961**

Figure 13

Spelaeodiscus unidentatus Bole, 1961: 205 fig. 1a–d.*Spelaeodiscus unidentatus* — Bole 1965: 350–351, fig. 1a, 2b, plate 76, fig. C.*Spelaeodiscus (Spelaeodiscus) unidentatus* — Gittenberger 1969: 297, fig. 1.*Spelaeodiscus unidentatus* — Welter-Schultes 2012: 214.

Type material. Obodska pećina, Rij. Crnojevića, Mtg., 1956 September, MZBI 1019/6 adult syntypes and some juvenile syntypes (photos of the sample where examined, Figure 12B). See also Remarks.

Other material. Bioče, N Titograd, Mtg. 23.09.1978, MZBI 15443 (photos of the sample where examined); Megara, Toluši, Titograd, Mtg. MZBI 2335 (photos of the sample where examined); Pećina od Zavora, Peuta, Titograd, Mtg. 01.11.1963, MZBI 2338 (photos of the sample where examined); Höhle bei Virpazar, leg. Dabović, coll. Edlauer, NHMW 48881/1; Brošine cave (33), leg. Kuscer 10266/67, coll. Edlauer, NHMW 38874/a (20 juvenile shells, “schlechte Expl”); Same data, NHMW 58874/4 (“bessere Expl”); Virpazar, mit “oculus mundi”, leg. Dabović, coll. Edlauer, NHMW 78988/3 juvenile shells (det. Gittenberger, but identification not certain); Smarjetna gora + Grabočica cave (drawing of a cave on the label), (Trnovo), NHMW 78989/7; Same data, NHMW 48086/5; Vodna jama (Lovćen), coll. Edlauer ex coll. Kuščer, NHMW 48544/1; Same locality, coll. Edlauer, NHMW 49764/1 (labelled as “*Spelaeodiscus albanicus hadzii*”); Montenegro, NNW of Virpazar, road between Rijeka Crnojevića and Virpazar, 0.4 km (in a straight line) W of Poseljani, 130 m a.s.l., 42°18.361'N, 19°02.898'E (site code: 20171020F), leg. T. Deli, Z.P. Eröss, A. Hunyadi & B. Páll-Gergely, 20.10.2017, DT/ca. 15, EZP/ca. 15, HA/ca. 15, HNHM 103248/5, PGB/ca. 15; Montenegro, W of Rijeka Crnojevića, 1 km (in a straight line) NNE of Zaćir, above Obodska pećina, near the road, 320 m a.s.l., 42°21.168'N, 19°00.125'E (site code: 2017.10.20J), leg. T. Deli, Z.P. Eröss, A. Hunyadi & B. Páll-Gergely, 20.10.2017, DT/ca. 18, EZP/ca. 18, HA/ca. 18, HNHM 103249/5, PGB/ca. 18; Montenegro, 2 km north of Velje Brdo in the Zeta valley, north of Podgorica, 70 m a.s.l., 42°28.932'N, 19°14.454'E, leg. A. Reischütz, P. L. Reischütz & N. Steiner-Reischütz, May 2016, REI/5; Montenegro, Morača valley, after the exit to the “China Road and Bridge” camp N of Bioče, 70 m a.s.l., 42°29.167'N, 19°18.646'E, leg. A. Reischütz, P. L. Reischütz & N. Steiner-Reischütz, May 2016, NHMW 112368/1 (photographed shell, Fig. 13G–L), REI/10; Montenegro, road between Rijeka Crnojevića and Hrvasi, 180 m a.s.l., 42°21.491'N, 19°4.281'E, leg. A. Reischütz, N. Reischütz & P. L. Reischütz, Apr. 2012, REI/11; Montenegro, scree slope at the BMS-petrol station, south of the Morača gorge, 5 km south of Bioče, 90 m a.s.l., 42°29.064'N, 19°18.279'E, leg. A. Reischütz, N. Reischütz & P. L. Reischütz, Jul. 2008, REI/1; Montenegro, spring 1 km south of the junction towards Njive, south of Rijeka Crnojevića, 150 m a.s.l., 42°18.266'N, 19°2.900'E, leg. A. Reischütz, N. Reischütz & P. L. Reischütz, Mar. 2011, NHMW 112369/1 (photographed shell, Fig. 13M–R);

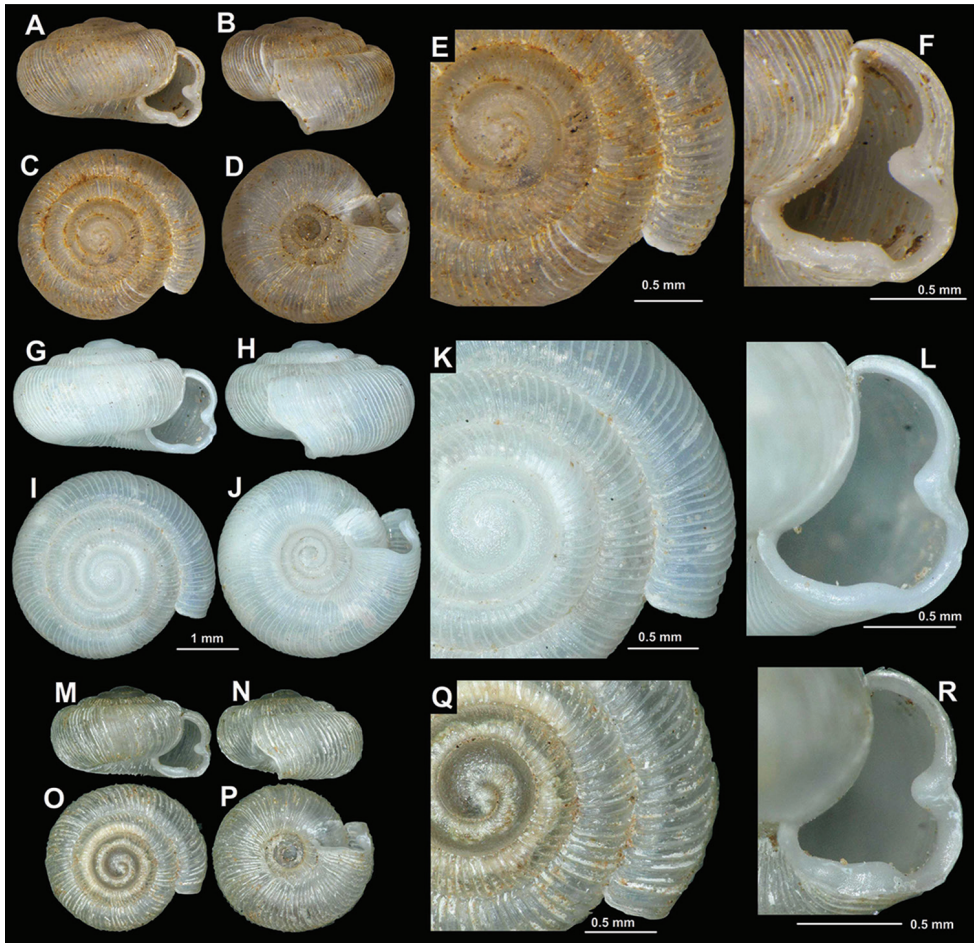


Figure 13. *Spelaeodiscus unidentatus unidentatus* Bole, 1961. **A–F** Pecina u Peckom Brdu cave, above Začir (HNHM 65187, topotypic specimen) **G–L** Montenegro, Morača valley, after the exit to the “China Road and Bridge” camp N of Bioče (NHMW 112368) **M–R** Montenegro, spring 1 km south of the junction towards Njive (NHMW 112369).

Montenegro, Žabljak Crnojevića, fortress, 50 m a.s.l., 42°19.030'N, 19°9.401'E (site code: 2015/007), leg. T. Deli, Z.P. Eröss & Z. Fehér, 25.05.2015, HNHM 103250/1 adult and several juvenile shells; Montenegro, Začir, “Pečina u pecko brdo” (cave), 450 m a.s.l., leg. L. Pintér, P. Subai, A. Szigeti, 20 Jul. 1972, NMBE 542072/76; Montenegro, Pečina u peckom, Brdu-bg Začirnál (Brdu-cave at Začir), leg. L. Pintér & P. Subai, 20 Jul. 1972, HNHM 65187/7 (one of them is photographed: Figs 13A–F); Montenegro, Pečina u peckom Brdu bei Začir (Brdu-cave at Začir), leg. H. Schütt, 06.06.1978, coll. Gy. Kovács, HNHM 65188/1; Same data, HNHM 42401/2; Montenegro, Rijeka Crnojevića, Obodska cave, 110 m a.s.l., 42°21.120'N, 19°0.318'E, leg. P. Subai & M. Szekeres, 23 Sep. 2006; NMBE 542071/1; Montenegro, Poseljani, on the Virpazar–Rijeka Crnojevića road, 150 m a.s.l., 42°18.347'N, 19°2.884'E (site

code: 2015/016), leg. T. Deli, Z.P. Eröss & Z. Fehér, 25.05.2015, HNHM 103251/8; NHMW 112370/8, DT/8.

Diagnosis. Basal tooth/thickening low, not pointed; palatal part of peristome with strong incision at the position of the palatal tooth, palatal region strongly “pushed” from outside.

Description. Spire elevated; protoconch consists of 1.5 whorls, roughly granulated/“hammered”, matte, not glossy; teleoconch with strong but dense, equidistant ribs that are supported by fine periostracal filaments in fresh shells; rib density variable (74–118 ribs on body whorl); between main ribs some fine wrinkles discernible; entire shell with 3.75–4.5 whorls; aperture semilunar or triangular due to straight basal part; peristome thickened, slightly expanded and slightly reflected on the palatal, basal and umbilical areas; palatal tooth strong, pointed; palatal region of peristome with strong outer incision (i.e. the position of the palatal tooth is indicated with a groove on the outer side); basal portion of peristome straight, thickened; occasionally two small denticles visible, sometimes only the one situated closer to the palatal side is developed as a low denticle; umbilicus funnel-shaped, wide to relatively narrow (width depends on spire height).

Measurements. SW: 2.4–3.2 mm (median = 2.7 mm), SH: 1.3–1.8 mm (median = 1.5 mm), AW: 0.9–1.1 mm (median = 1.0 mm), AH: 1.0–1.4 mm (median = 1.1 mm), (n = 11; largest and smallest specimens of multiple populations measured).

Differential diagnosis. See under *S. unidentatus acutus* ssp. n.

Variation among specimens. This subspecies is particularly variable in terms of shell size. The shape of the thickening of the basal part of the peristome is also slightly variable, although it never develops to a pointed tooth.

Distribution. This taxon is found north and northwest of the Shkodër Lake Basin in Montenegro (Figure 7). Albanian records given by Reischütz et al. (2013) actually refer to *S. unidentatus acutus* ssp. n.

Remarks. The only sample in the MZBI, which was collected before the original description is from Obodska pećina represent the type sample of this species (MZBI 1019). Bole collected both *S. obodensis* and *S. unidentatus* at Obodska pećina in September, 1956, but described only one (*S. unidentatus*) in 1961, and the other (*S. obodensis*) in 1965.

Formerly, Peuta Cave population was incorrectly referred to as *S. albanicus* and was taken into consideration in that species’ Red List assessment (Reischütz and Fehér 2017).

***Spelaeodiscus unidentatus acutus* Páll-Gergely & Fehér, ssp. n.**

<http://zoobank.org/90A2874A-9BE4-474F-A572-8A1FC36B6172>

Figure 14A–L

Spelaeodiscus unidentatus — Reischütz et al. 2013: 62, fig. 3.

Type material. Albania, rocks north of Hajmel at the bridge, north of Lezhe, 40 m a.s.l., 41°58.426'N, 19°38.683'E, leg. A. Reischütz, N. Reischütz & P. L. Reischütz,



Figure 14. Shells of *Spelaediscus*. **A–F** *Spelaediscus unidentatus acutus* ssp. n., holotype (HNHM 103252) **G–L** *Spelaediscus unidentatus acutus* ssp. n., Albania, rocks north of Hajmel at the bridge (NHMW 112371) **M–R** *Spelaediscus virpazariooides* sp. n., holotype (HNHM 103417).

Apr. 2012, NHMW 112371/1 (photographed paratype, Fig. 14G–L), REI/6 paratypes; Albania, rocks 1 km south of Hajmel, north of Lezhe, 50 m a.s.l., 41°56.848'N, 19°38.379'E, leg. A. Reischütz, N. Reischütz & P. L. Reischütz, Apr. 2012, REI/5 paratypes; Albania, Shkodër District, Vau i Dejës, Mjedë, near the dam, 45 m a.s.l., limestone rocks, 42°0.804'N, 19°37.188'E (site code: 2015/99), leg. Z.P. Eröss, Z. Fehér & J. Grego, 04 Jul. 2015, HNHM 103252 (holotype, SW: 2.9 mm, SH: 1.5 mm, Figs 14A–F), NHMW 112372/1 paratype, JG/1 paratype.

Type locality. Albania, Shkodër District, Vau i Dejës, Mjedë, near the dam, 45 m a.s.l., limestone rocks, 42°0.804'N, 19°37.188'E.

Diagnosis. Basal tooth pointed; palatal part of peristome with slight incision at the position of the palatal tooth, palatal region not or slightly “pushed” from outside.

Measurements. SW: 2.9–3.5 mm (median = 3.0 mm), SH: 1.4–1.8 mm (median = 1.5 mm), AW: 1.1–1.3 mm (1.2 mm), AH: 1.1–1.4 mm (median = 1.2 mm), (n = 9; largest and smallest specimens of multiple populations measured).

Differential diagnosis. *Spelaeodiscus unidentatus acutus* ssp. n. differs from the nominotypical subspecies by the strong, pointed basal tooth, which is blunt, or represented as a thickening of the basal peristome in the nominotypical subspecies. Moreover, the palatal region is not or only slightly “pushed” from the outside in the position of the palatal tooth. Rib density: 64–91 ribs on the body whorl.

Variation among specimens. This subspecies is variable in terms of shell size and spire height, i.e. one population has a nearly flat shell.

Etymology. This new subspecies is named after its pointed (Latin: *acutus*) basal tooth, which distinguishes it from the nominotypical subspecies.

Distribution. This subspecies is known from the southeastern side of the Shkodër Lake Basin in Albania (Figure 7).

***Spelaeodiscus virpazarioides* Páll-Gergely & Fehér, sp. n.**

<http://zoobank.org/6454FD89-D6C1-4607-9992-7F1CC7DBD617>

Figure 14M–R

Type material. Albania, Malësia district, a mountain pass 2 km N of Rraps-Starjë, 700 m a.s.l., 42°24.888'N, 19°30.240'E, leg. Eröss, Fehér, Szekeres, Grego, 27.06.2016, HNHM 103417 (holotype, SW = 3.45 mm, SH = 2.0 mm), HNHM 102765/4+1subadult+3fr (paratypes), NHMW 111672/3+2subadult+2fr; JG/3+2subadult+3fr (paratypes); same locality, leg. A. Reischütz, N. Reischütz & P. Reischütz, Apr. 2006, REI/1 juvenile paratype.

Type locality. Albania, Malësia district, a mountain pass 2 km N of Rraps-Starjë, 700 m a.s.l., 42°24.888'N, 19°30.240'E.

Diagnosis. A medium sized to large species with elevated spire, strong, very widely spaced ribs, fine spiral lines consisting of series of minute tubercles, hammered protoconch, weak basal thickening, weak parietal tooth, and a thickened parietal callus.

Description. Spire elevated; protoconch consists of ca. 1.25–1.75 whorls, roughly sculptured, “hammered”; teleoconch with very strong, equidistant, widely spaced ribs (40–70 on the body whorl; addition to the radial ribs very fine, dense spiral striation is visible on the entire teleoconch, consisting of minute tubercles; entire shell with 4–4.75 whorls; aperture subcircular/triangular; basal part with two low swellings (similar to those of *S. albanicus albanicus*), parietal wall with a weak tooth; parietal callus thickened, blunt; umbilicus funnel-shaped, relatively narrow.

Measurements. SW: 3.3–3.6 mm (median = 3.5 mm), SH: 1.95–2.25 mm (median = 2.1 mm), AW: 1.3–1.6 mm (median = 1.4 mm), SW: 1.4–1.5 mm (median = 1.4 mm), (n = 11).

Differential diagnosis. This new species can be distinguished from all congeners (especially the most similar *S. albanicus albanicus*) by the clearly visible spiral striation,

roughly sculptured protoconch and thickened parietal callus. All *Virpazaria* species possess an elevated parietal callus, but it is sharp in most (all?) species, and the aperture of those species are more slender, crescent-shaped.

Variation among specimens. The degree of the thickness of the parietal callus shows some recognisable variability within the single known population, but this trait might be due to the age (degree of development) of the examined shells.

Etymology. This new species is named after its resemblance to *Virpazaria* species based on the thickened parietal callus.

Distribution. *Spelaeodiscus virpazarioides* sp. n. is known from the type locality only (see also Figure 7).

Remarks. Initially we considered placing this species to the genus *Virpazaria* due to the thickened parietal callus, which was mentioned in the original description of the genus *Virpazaria*. However, the subcircular/triangular aperture indicates that it is better to be placed in *Spelaeodiscus*.

Formerly, this population was incorrectly referred to as *S. albanicus* and was taken into consideration in that species' Red List assessment (Reischütz and Fehér 2017)

Conservation status. To our present knowledge this species is very rare (currently known from a single location) and thus AOO is smaller than 20 km². However, there is no reason to suppose that AOO, EOO, number of locations, number of subpopulations or the number of mature individuals are declining or extremely fluctuating. Therefore, it might be assessed as Near Threatened (NT).

Discussion

Species recognition and biogeography

We examined all available *Spelaeodiscus* samples from the Western Balkan area (Slovenia, Montenegro, Albania). Our main aim was to delimit (sub)species based on conchological characters. We found that shell size, spire height and rib density is particularly variable within and between populations, and can be used only with caution for species recognition. Morphology of ribs, however (elevated or low, thin, lamella-like or strong, calcareous), the fine sculpture of the protoconch (glossy or granulate), and the obliqueness of the aperture to the shell axis are useful character in several cases. The two subspecies described here (*S. albanicus edentatus* ssp. n. and *S. unidentatus acutus* ssp. n.) are primarily recognized based on differences of the apertural teeth. The most important traits distinguishing the species delimited here are hardly or not quantifiable. Thus, no statistical tests are applied to verify our taxonomic decisions. We are aware of the limitations of the exclusively conchological approach, especially in case of species known from single shells or single populations. However, given the commonness of rarity, omitting the description of singletons would prevent the description of a very significant proportion of the species-level diversity (Lim et al. 2012).

Table 2. Co-occurrences of *Spelaeodiscus* species.

| Locality | co-occurring species |
|--|---|
| Montenegro, SE of Virpazar, 4.3 km (in a straight line) SSE of Đuravci, near Besa/Bes near Krone i Besit, 330 m a.s.l. | <i>S. hunyadii</i> sp. n. & <i>S. dejongi</i> |
| Yugoslavia: Pečina u Peckom Brdu cave above Začir | <i>S. unidentatus unidentatus</i> & <i>S. obodensis</i> |
| Obodska pećina, Rij. Crnojevića | <i>S. unidentatus unidentatus</i> & <i>S. obodensis</i> |
| Montenegro, S of Virpazar, 0.8 km (in a straight line) E of Limljani, above the village, 400 m a.s.l. | <i>S. latecostatus</i> sp. n. & <i>S. dejongi</i> |

Spelaeodiscus dejongi has the largest known area and is known from most numerous populations. In face of the large variability between populations we found no qualitative traits that would distinguish populations on species or subspecies level, therefore we treat it as a single, variable species. However, future studies should focus on the degree of differences on molecular level.

Although the majority of species is known from multiple populations of relatively large areas, three single-site endemic species (*S. densecostatus* sp. n., *S. hunyadii* sp. n., *S. latecostatus* sp. n.) are also described. The latter two new species were found in sympatry with the widely distributed *S. dejongi*, which is an evidence that none of them are conspecific with *S. dejongi* (see Table 2). More precise field collections should focus on the area they inhabit in order to examine the true extent of their range.

Habitat

Spelaeodiscus (in contrast to *Aspasita*) is obviously a subterranean genus. Up to the recent past, only a few populations were known and it was believed to be troglobiont, because – if not in fluvial flotsam – all findings were from or near caves. In the past decade, some other gastropod taxa, previously believed to be troglobiont, turned up in non-carbonate areas, or in limestone but assuredly outside of caves (Deli and Subai 2011, Subai 2011, Dedov 2015; Reischütz et al. 2016). These findings already demonstrated that *Agardhiella* Hesse, 1923, *Gyalina* Andreae, 1902, *Sciocochlea* C.R. Boettger, 1935 and *Tsoukatosia* Gittenberger, 2000 have affinity to the superficial underground compartments (also known as “Mesovoid Shallow Substratum” or “Milieu Souterrain Superficiel”, widely abbreviated as MSS, see e.g. Juberthie et al. 1980, 1981; Camacho 1992; Culver and Pipan 2009, Mammola et al. 2016).

We have collected all *Spelaeodiscus* samples in fissures or small cavities of bare limestone cliffs, from which fine granulated material could be yielded. Although we have found only empty shells, and therefore it is still not completely clear where they actually live, the abundance of *Spelaeodiscus* in these superficial fissures seems to be larger than in cave deposits. This prompted us to question whether *Spelaeodiscus* is truly troglobiont.

Literature data are very scarce about MSS dwelling gastropods, and still, that little is dealing mostly with scree slopes, habitats where fragments of rocks are accumulating at the bottom of rocky walls, and are covered over time by an evolving soil (Arndt



Figure 15. “Scratch and floatate” method to collect shells of subterranean species. **A–B** scratching out fine granulate soil material with handrakes **C** separating shells from soil particles by flotation **D** cursory visual inspection of the floated fraction **E** Storing the floated material in polyamide knee-sock.

and Subai 2013, Rendoš et al. 2014). Scree slopes were reported to harbour exclusively edaphic species, but Arndt and Subai (2013) presume that this was due to the applied passive sampling method (buried pitfall traps), which is ineffective for catching small sized and immobile snails.

Our sites represent a different sort of habitat type, similar to “bedrock MSS” according to the subdivision of Mammola et al. (2016), except that the rock surfaces of these sites are not covered by an evolving soil. Due to the nature of this habitat type, the use of pitfall traps or other sort of passive sampling devices was out of question. Therefore, we stayed with the “scratch and sieve” or “scratch and floatate” approach, i.e. we scratched out fine granulate material from the superficial fissures of rocks applying long and narrow hand rakes (Fig. 15A–B) and separated the shells by sieving or by flotation (Fig. 15C–E).

It is still disputed whether such a bedrock MSS habitat is characteristically different from caves or it can be considered just as the extension of the cave system, and therefore, its fauna is composed of troglobionts of wider ecological tolerance or

there are certain specialized elements exclusive of MSS (see Mammola et al. 2016 for review). The role of *Spelaeodiscus* remains unclear in this respect. However, our study indicates that the bedrock MSS habitats in the Balkans harbour a large and still largely undiscovered gastropod diversity.

Acknowledgements

We are grateful to Anita Eschner (NHMW) and Sigrid Hof (SMF) for access to museum collections at their care, to Eike Neubert (NMBE) for loaning shells for examination, to Tomi Trilar (Jovan Hadži Institute of Biology, Ljubljana) for sending photos of *Spelaeodiscus* samples housed in his museum collection, to Rajko Slapnik for identifying Slovenian localities, to Renáta Novák for translating the paper of Bole (1961), and to Oliver Macek (NHMW) for his help in photographing shells. Jozef Grego, Nicole Steiner-Reischütz, and Miklós Szekeres helped during field trips and Péter Subai provided inspiration and important information about collecting methods. This study was supported by the MTA (Hungarian Academy of Sciences) Premium Post Doctorate Research Program to B. Páll-Gergely and the Austrian Science Fund (FWF P-26581-B25) to Z. Fehér.

References

- Andreae A (1902) Zweiter Beitrag zur Binnenconchylienfauna des Miocäns von Oppeln in Schlesien. Mitteilungen aus dem Roemer-Museum Hildesheim 18: 1–31.
- Arndt E, Subai P (2013) Gastropoda from subterranean habitats in Greece. *Vernate* 31/2012: 213–224.
- Boettger CR (1935) Exploration biologique des cavernes de la Belgique et du Limbourg Hollandais. XXIIe contribution: Mollusca. *Zeitschrift für Karst- und Höhlenkunde (Mitteilungen über Höhlen- und Karstforschung)* 1935: 49–63.
- Bole J (1961) Nove vrste poszemeljskih polžev iz Črne Gore. II. jugoslavenski speleološki kongres Split 1958: 205–207.
- Bole J (1965) Die Vertreter der Gattung *Spelaeodiscus* Brusina 1886 (Gastropoda, Pulmonata) in Jugoslawien. *International Journal of Speleology* 1(3): 349–356. <https://doi.org/10.5038/1827-806X.1.3.9>
- Bouchet O, Rocroi J-P, Hausdorf B, Kaim A, Kano Y, Nützel A, Parkhaev P, Schrödl M, Strong EE (2017) Revised classification, nomenclator and typification of gastropod and monoplacophoran families. *Malacologia* 61 (1–2): 1–526. <https://doi.org/10.4002/040.061.0201>
- Brusina S (1886) Ueber die Mollusken-Fauna Oesterreich-Ungarns. *Mittheilungen des Naturwissenschaftlichen Vereins für Steiermark* 22[1885]: 29–56.
- Camacho AI (1992) The Natural History of Biospeleology. *Monografias del MNCN* 7. CSIC, Madrid, 680 pp.
- Clessin S (1887) Die Molluskenfauna Österreich-Ungarns und der Schweiz. Bauer & Raspe, Nürnberg, 858 pp.

- Dedov I (2015) A new *Gyralina* species from the Republic of Macedonia (Gastropoda: Pulmonata: Pristilomatidae). *Archiv für Molluskenkunde* 144(2): 239–242. <https://doi.org/10.1127/arch.moll/1869-0963/144/239-242>
- Deli T (2010) *Agardhiella tunde* spec. nov. (Gastropoda: Pulmonata: Argnidae), a new endemic land snail from Romania. *Journal of Conchology* 40 (3): 315–320.
- Deli T, Subai P (2011) Revision der *Vitrea*-Arten der Südkarpaten Rumäniens mit Beschreibung einer neuen Art (Gastropoda, Pulmonata, Pristilomatidae). *Contributions to Natural History* 19: 1–53.
- Gittenberger E (1969) Beiträge zur Kenntnis der Pupillacea I. Die Spelaediscinae. *Zoologische Mededelingen* 43 (22): 287–306.
- Gittenberger E (1975) Beiträge zur Kenntnis der Pupillacea. V. Die Spelaediscinae, erster Nachtrag. *Zoologische Mededelingen* 48 (23): 263–277.
- Gittenberger E (2000) Serrulininae in Greece, there may be more (Gastropoda, Pulmonata, Clausiliidae). *Basteria* 64 (4–6): 81–87.
- Harl J, Haring E, Sittenthaler M, Sattmann H, Asami T, Páll-Gergely B (2017) Molecular systematics of the land snail family Orculidae reveal paraphyly and deep splits within the clade Orthurethra (Gastropoda: Pulmonata). *Zoological Journal of the Linnean Society* 181: 778–794. <https://doi.org/10.1093/zoolinnean/zlx022>
- Hazay Gy (1883) Az Északi-Kárpátok és vidékének Mollusca faunája, etc. *Mathematikai és Természettudományi Közlemények* 19: 315–381.
- Hesse P (1923) Kritische Fragmente. *Archiv für Molluskenkunde* 55: 193–198.
- Hudec V (1965) Neue Erkenntnisse über den Geschlechtsapparat von *Argna bielzi* (Rossmässler) und Bemerkungen zur systematischen Stellung der Gattung *Argna*. *Archiv für Molluskenkunde* 94: 157–165.
- Hudec V (1970) Poznámky k anatomii nekterých plzu z Madarska. [Bemerkungen zur Anatomie einiger Schneckenarten aus Ungarn]. *Casopis Narodniho Muzea* 137 (3–4) [for 1968]: 33–43. [In Czech and German]
- Juberthie C, Delay B, Bouillon M (1980) Sur l'existence du milieu souterrain superficiel en zone non calcaire. *Comptes Rendus de l'Académie des Sciences de la France D* 290: 49–52.
- Juberthie CB, Dalay B, Bouillon M (1981) Sur l'existence d'un milieu souterrain superficiel en zone calcaire. *Mémoires de Biospéologie* 8: 77–93.
- Lim GS, Balke M, Meier R (2012) Determining Species Boundaries in a World Full of Rarity: Singletons, Species Delimitation Methods. *Systematic Biology* 61(1):165–169. <https://doi.org/10.1093/sysbio/syr030>
- Kerney MP, Cameron RAD (1979) *A Field Guide to the Land Snails of Britain and North-west Europe*. Collins, London, 288 pp.
- Kimakowicz M von (1884) Beitrag zur Mollusken-Fauna Siebenbürgens (Fortsetzung). *Verhandlungen und Mittheilungen des Siebenbürgischen Vereins für Naturwissenschaften in Hermannstadt* 34: 57–116.
- Mammola S, Giachino PM, Piano E, Jones A, Barberis M, Badino G, Isaia M (2016) Ecology and sampling techniques of an understudied subterranean habitat: the Milieu Souterrain Superficiel (MSS). *The Science of Nature* 103: 88. <https://doi.org/10.1007/s00114-016-1413-9>

- Pilsbry HA (1922–1926) *Manual of Conchology. Second Series: Pulmonata. Vol. 27. Pupillidæ (Orculinæ, Pagodulinæ, Acanthinulinæ, etc).* Conchological Section, Academy of Natural Sciences, Philadelphia, 369 pp.
- Reischütz A (2017a) *Spelaeodiscus dejongi*. The IUCN Red List of Threatened Species 2017: e.T171400A1325626. <http://dx.doi.org/10.2305/IUCN.UK.2017-3.RLTS.T171400A1325626.en> [Downloaded on 24 April 2018]
- Reischütz A (2017b) *Spelaeodiscus hauffeni*. The IUCN Red List of Threatened Species 2017: e.T170875A1318062. <http://dx.doi.org/10.2305/IUCN.UK.2017-3.RLTS.T170875A1318062.en> [Downloaded on 24 April 2018]
- Reischütz A (2017c) *Spelaeodiscus obodensis*. The IUCN Red List of Threatened Species 2017: e.T170912A1318600. <http://dx.doi.org/10.2305/IUCN.UK.2017-3.RLTS.T170912A1318600.en> [Downloaded on 24 April 2018]
- Reischütz A (2017d) *Spelaeodiscus unidentatus*. The IUCN Red List of Threatened Species 2017: e.T171630A1329127. <http://dx.doi.org/10.2305/IUCN.UK.2017-3.RLTS.T171630A1329127.en> [Downloaded on 24 April 2018]
- Reischütz A, Fehér Z (2017) *Spelaeodiscus albanicus*. The IUCN Red List of Threatened Species 2017: e.T170947A1319076. <http://dx.doi.org/10.2305/IUCN.UK.2017-3.RLTS.T170947A1319076.en> [Downloaded on 24 April 2018]
- Reischütz A, Reischütz PL (2009) Ein Beitrag zur Kenntnis der Molluskenfauna von Montenegro, nebst Beschreibung zweier neuer Arten der Gattung *Virpazaria* Gittenberger 1969. *Nachrichtenblatt der Ersten Vorarlberger Malakologischen Gesellschaft* 16: 51–60.
- Reischütz A, Reischütz N, Reischütz PL (2013) Beiträge zur Kenntnis der Molluskenfauna Albaniens. *Nachrichtenblatt der Ersten Vorarlberger Malakologischen Gesellschaft* 20: 61–64.
- Reischütz A, Reischütz PL, Szekeres M (2016) The Clausiliidae subfamily Phaedusinae (Gastropoda, Pulmonata) in the Balkans. *Nachrichtenblatt der Ersten Vorarlberger Malakologischen Gesellschaft* 23: 93–117.
- Rendoš M, Čejka T, Šteffek J, Mock A (2014) Land snails from subterranean traps exposed in a forested scree slope (Western Carpathians, Slovakia). *Folia Malacologica* 22 (4): 255–261. <https://doi.org/10.12657/folmal.022.022>
- Rossmässler EA (1838–1844) *Iconographie der Land- und Süßwassermollusken, mit vorzüglicher Berücksichtigung der europäischen noch nicht abgebildeten Arten.* Arnold, Dresden, Leipzig, book 7/8: [1–4], 1–44, book 9/10: [1–4], 1–66, book 11: [1–4], 1–15, book 12: [1–4], 1–37, Plate 31–60. <http://www.biodiversitylibrary.org/item/80434#page/77/mode/1up>
- Shileyko AA (1998) *Treatise on Recent Terrestrial Pulmonate Molluscs, Part 1. Achatinellidae, Amastridae, Orculidae, Strobilopsidae, Spelaeodiscidae, Valloniidae, Cochlicopidae, Pupillidae, Chondrinidae, Pyramidulidae.* Ruthenica, Supplement 2 (1): 1–127.
- Schmidt F (1855) Beschreibung zweier neuer Höhlenthiere, eines Käfers und einer Schnecke. *Verhandlungen des Zoologisch-Botanischen Vereins in Wien (Abhandlungen)* 5: 3–4.
- Slapnik R (2005) The molluscs (Mollusca) of Škocjan Caves Regional Park. *Annales, Series Historia Naturalis* 15: 265–276. [In Slovenian with English abstract]
- Steenberg CM (1925) Etudes sur l'anatomie et la systématique des maillots (fam. Pupillidae s. lat.). *Videnskabelige Meddelelser fra Dansk Naturhistorisk Forening i København* 80: 1–215.

- Sturany R, Wagner AJ (1915) Über schalentragende Landmollusken aus Albanien und Nachbargebieten. Denkschriften der kaiserlichen Akademie der Wissenschaften, mathematisch-naturwissenschaftliche Klasse 91: 19–138.
- Subai P (2011) Revision of the Argnidae, 2. The species of *Agardhiella* from the eastern part of the Balkan peninsula (Gastropoda: Pulmonata: Pupilloidea). Archiv für Molluskenkunde 140 (1): 77–121. <https://doi.org/10.1127/arch.moll/1869-0963/140/077-121>
- Subai P, Dedov I (2008) A review of the Bulgarian species of *Aspasita* Westerlund, 1889 (Gastropoda; Pulmonata; Spelaeodiscidae), with description of *A. bulgarica* spec. nov. Basteria 72: 111–118.
- Welter-Schultes FW (2012) European non-marine molluscs, a guide for species identification. Planet Poster Editions, Göttingen, 679 + 78 pp.
- Westerlund CA (1889) Fauna der in der paläarktischen Region (Europa, Kaukasien, Sibirien, Turan, Persien, Kurdistan, Armenien, Mesopotamien, Kleinasien, Syrien, Arabien, Egypten, Tripolis, Tunesien, Algerien und Marocco) lebenden Binnenconchylien. II. Gen. *Helix*. Friedländer, Berlin, 473 pp.

Sequence capture phylogenomics of eyeless *Cicurina* spiders from Texas caves, with emphasis on US federally-endangered species from Bexar County (Araneae, Hahniidae)

Marshal Hedin¹, Shahan Derkarabetian^{1,2}, Jennifer Blair³, Pierre Paquin⁴

1 Department of Biology, San Diego State University, 5500 Campanile Drive, San Diego CA, 92182, USA

2 Department of Organismic and Evolutionary Biology, Museum of Comparative Zoology, Harvard University, 26 Oxford St., Cambridge MA, 02138, USA

3 Blair Wildlife Consulting, 3815 Dacy Lane, Kyle TX, 78640, USA

4 Scienceinfuse Inc, 12 Saxby Sud, Shefford, QC, J2M 1S2, Canada

Corresponding author: Marshal Hedin (mhedin@sdsu.edu)

Academic editor: G. Blagoev | Received 14 April 2018 | Accepted 27 May 2018 | Published 26 June 2018

<http://zoobank.org/752922C5-DD18-42B6-9866-5716A341A94C>

Citation: Hedin M, Derkarabetian S, Blair J, Paquin P (2018) Sequence capture phylogenomics of eyeless *Cicurina* spiders from Texas caves, with emphasis on US federally-endangered species from Bexar County (Araneae, Hahniidae). ZooKeys 769: 49–76. <https://doi.org/10.3897/zookeys.769.25814>

Abstract

Morphological, mitochondrial, and nuclear phylogenomic data were combined to address phylogenetic and species delimitation questions in cave-limited *Cicurina* spiders from central Texas. Special effort was focused on specimens and cave locations in the San Antonio region (Bexar County), home to four eyeless species listed as US Federally Endangered. Sequence capture experiments resulted in the recovery of ~200–400 homologous ultra-conserved element (UCE) nuclear loci across taxa, and nearly complete COI mitochondrial DNA sequences from the same set of individuals. Some of these nuclear and mitochondrial sequences were recovered from “standard” museum specimens without special preservation of DNA material, including museum specimens preserved in the 1990s. Multiple phylogenetic analyses of the UCE data agree in the recovery of two major lineages of eyeless *Cicurina* in Texas. These lineages also differ in mitochondrial clade membership, female genitalic morphology, degree of troglomorphy (as measured by relative leg length), and are mostly allopatric across much of Texas. Rare sympatry was confirmed in Bexar County, where members of the two major clades sometimes co-exist in the same karst feature. Both nuclear phylogenomic and mitochondrial data indicate the existence of undescribed species from the San Antonio region, although further sampling and collection of adult specimens is needed to

explicitly test these hypotheses. Our data support the two following species synonymies (*Cicurina venii* Gertsch, 1992 = *Cicurina madla* Gertsch, 1992; *Cicurina loftini* Cokendolpher, 2004 = *Cicurina vespera* Gertsch, 1992), formally proposed here. Overall, our taxonomy-focused research has many important conservation implications, and again highlights the fundamental importance of robust taxonomy in conservation research.

Keywords

cave evolution, conservation, karst, mitochondrial by-catch, taxonomy, ultra-conserved element

Introduction

The limestone cave and karst habitats of Texas are home to hundreds of endemic cave-obligate animal species, including many eyeless spider species. The spider subgenus *Cicurella* (genus *Cicurina*) includes 60 described species, almost all endemic to Texas caves (Gertsch 1992, Cokendolpher 2004, Paquin and Dupérré 2009). Four eyeless Texas *Cicurina* species, all from Bexar County in the vicinity of San Antonio, are listed as US Federally Endangered (Service 2000). The listed species include *C. madla*, *C. baronia*, *C. vespera* and *C. venii*, the latter three of which are hypothesized single-cave endemic species. The conservation issues faced by these range-restricted taxa are unquestionable and ongoing, and include such threats as habitat destruction, chemical contamination, and invasive species (Service 2011).

Many authors have discussed the challenges of phylogenetic and taxonomic research in Texas cave *Cicurina* (Cokendolpher 2004, Paquin and Hedin 2004, Paquin et al. 2008, Paquin and Dupérré 2009, Hedin 2015). About 90% of collected specimens are immatures, and almost all adult specimens are females (Cokendolpher 2004, Paquin and Dupérré 2009). Given adult male rarity, males cannot be used reliably in species identification. Instead, adult females are primarily used for taxonomic decisions, but female genitalic morphology is variable both within and among caves, blurring the distinction between geographic variation and species level divergence (Paquin et al. 2008, Paquin and Dupérré 2009, Hedin 2015). This indistinct boundary between geographic variation and species level divergence also extends to the genome, because in naturally-fragmented karst habitats some level of genetic population structuring is an expectation (Hedin 2015). Finally, access to Texas caves is difficult, leading to small sample sizes and geographic sampling gaps, both of which impact phylogenetics and species delimitation, particularly molecular species delimitation (e.g., Niemiller et al. 2012, Carstens et al. 2013, Satler et al. 2013).

The special challenge of species delimitation in Texas cave *Cicurina* is exemplified by *Cicurina venii*. This federally endangered species is known only from a single adult female from the type locality (Bracken Bat Cave), the entrance to which has been buried since about 1990 (Cokendolpher 2004). Here is an example of an extremely important species hypothesis that is founded on fundamentally limited data, where the probability of sampling additional specimens (if the type population still persists, which is itself unknown) is very low because of habitat inaccessibility.

Hedin (2015) suggested that next-generation sequencing (NGS) methods, such as sequence capture of ultra-conserved elements (UCEs; ultraconserved.org/), might be used to help resolve challenging phylogenetic and taxonomic problems in eyeless *Cicurina*. The availability of conserved UCE probes makes it possible to capture hundreds of orthologous nuclear genetic regions (“loci”) from a set of specimens using cost-effective, scalable methods (Faircloth et al. 2012, Bossert and Danforth 2018). Within and between closely-related species, most phylogenetic information is coming from variable regions that flank the core UCE, and several recent publications have shown that such flanking regions carry enough phylogenetic information to robustly resolve species-level divergences (e.g., Smith et al. 2014, Blaimer et al. 2016a,b, McCormack et al. 2016, Zarza et al. 2016, Newman and Austin 2016, Starrett et al. 2017). Another potential benefit of UCE capture is that major portions of the mitochondrial genome are often included as “by-catch” in sequence reads (e.g., Zarza et al. 2016), further increasing phylogenetic return on investment.

An additional appeal of UCE-based phylogenomics is that the method has demonstrated applicability with degraded DNA (e.g., on “standard” museum specimens, without special preservation of DNA material). For example, hundreds or thousands of UCE loci have been captured from old bird museum specimens (McCormack et al. 2016), formalin-fixed snakes (Ruane and Austin 2017), and pinned insects (Blaimer et al. 2016a). Recently, Hedin et al. (2018) extended this utility to “standard” ethanol-preserved spider museum specimens. This type of utility would apply importantly to Texas cave *Cicurina*, as multiple regional collections house large numbers of both adult and immature specimens, many collected in the past 20–30 years. Given the natural rarity of eyeless *Cicurina* spiders, and general difficulty of cave access, the ability to use historical collections for sub-genomic phylogenomics could prove transformative. Here we combine morphological, mitochondrial, and UCE nuclear data to address phylogenetic and species delimitation questions in Texas cave *Cicurina*, focusing specifically on federally listed taxa from Bexar County.

Materials and methods

UCE specimen sampling and DNA extraction

Specimens and/or DNA extractions were made available from multiple institutions and persons, including the Texas Memorial Museum (TMM), Texas Tech University (TTU), ZARA Environmental, and the American Museum of Natural History (AMNH) (see Acknowledgements). In total, we attempted to gather UCE data for 83 eyeless *Cicurina* specimens, six of which were “standard” museum specimens (without special preservation of DNA material, Suppl. material 5), including holotype specimens of *C. venii* and *C. vespera*. Our sample emphasized species and populations from Bexar County, but we also included samples opportunistically from caves in counties to the northeast and west of San Antonio.

Many specimens used in this study were immatures, but could be tentatively identified to species in a *post hoc* manner based on phylogenetic placement into genetic clades including adult specimens, bolstered by locality data (i.e., caves from which adult *Cicurina* specimens have been collected in the past, including type locations). The assumption of no sympatry is fundamentally important here (i.e., one eyeless *Cicurina* species per cave). No sympatry is the rule for these spiders (Cokendolpher 2004, Paquin and Dupérré 2009), but as we show here (see Results), rare sympatry does occur. We acknowledge that the use of immatures is suboptimal, but in this system represents a clear trade-off. The inclusion of immatures brings some level of uncertainty, but exclusion results in a dramatic loss of information, again because immatures represent the bulk of collected specimens (Cokendolpher 2004, Paquin and Dupérré 2009).

For specimens preserved for DNA studies (preserved in high percentage ethyl alcohol at -80°C), genomic DNA was extracted from leg tissue using the Qiagen DNeasy Blood and Tissue Kit (Qiagen, Valencia, CA). For museum samples preserved in 70–80% EtOH we used standard phenol/chloroform extractions with a 24-hour incubation. All extractions were quantified using a Qubit Fluorometer (Life Technologies, Inc.) and quality was assessed via gel electrophoresis on a 1% agarose gel.

UCE data collection and matrix assembly

UCE data were collected in multiple library preparation and sequencing experiments. Up to 500 ng of genomic DNA was sonicated using a Covaris M220 Focused-ultrasonicator with treatment time of 60–65 s, Peak Incident Power of 50, 10% Duty Factor, and 200 cycles per burst. All museum samples were sonicated for 30 seconds using the same settings. Samples were electrophoresed on agarose gels to verify sonication success.

Library preparation followed Starrett et al. (2017), with minor modifications. Briefly, libraries were prepared using the KAPA Hyper Prep Kit (Kapa Biosystems), using up to 250 ng DNA (i.e., half reaction of manufacturer's protocol) as starting material. Ampure XP beads (Beckman Coulter) were used for all cleanup steps. For samples containing <250 ng total DNA, all available DNA was used in library preparation. After end-repair and A-tailing, universal adapters were ligated onto libraries at varying concentrations depending on amount of input DNA. Libraries were then amplified in a 50 μl reaction, with 15 μl adapter-ligated DNA, 1X HiFi HotStart ReadyMix, and 0.5 μM of each Illumina TruSeq dual-indexed primer (i5 and i7) with modified 8-bp indexes (Glenn et al. 2016). Amplification conditions were 98 $^{\circ}\text{C}$ for 45 s, then 18 cycles of 98 $^{\circ}\text{C}$ for 15 s, 60 $^{\circ}\text{C}$ for 30 s, and 72 $^{\circ}\text{C}$ for 60 s, followed by a final extension of 72 $^{\circ}\text{C}$ for 60 s. Samples were quantified again to ensure amplification success, and equimolar amounts of libraries were combined into 1000 ng total pools consisting of eight samples each (125 ng per sample).

Target enrichment was performed on pooled libraries using the MYbaits Arachnida 1.1K version 1 kit (Arbor Biosciences; Faircloth 2017) following the Target Enrichment

of Illumina Libraries v. 1.5 protocol (<http://ultraconserved.org/#protocols>). Hybridization was conducted at 60 or 65 °C for 24 hours. Following hybridization, pools were amplified in a 50 µl reaction consisting of 15 µl of hybridized pools, 1X Kapa HiFi Hot-Start ReadyMix, and 0.25 µM of each of TruSeq forward and reverse primers. Amplification conditions consisted of 98 °C for 45 s, then 16 or 18 cycles of 98 °C for 15 s, 60 °C for 30 s, and 72 °C for 60 s, followed by a final extension of 72 °C for 5 minutes. Following an additional cleanup, libraries were quantified using a Qubit fluorometer and equimolar mixes were prepared for sequencing on an Illumina HiSeq 2500 (Brigham Young University DNA Sequencing Center) using 125 bp PE reads.

Raw demultiplexed reads were processed using the PHYLUCE pipeline (Faircloth 2016). Quality control and adapter removal were conducted with the ILLUMIPROCESSOR wrapper (Faircloth 2013). Assemblies were created with VELVET (Zerbino and Birney 2008) using default settings. Contigs were matched to probes using minimum coverage and minimum identity values of 65. UCE loci were aligned with MAFFT (Kato and Standley 2013) and trimmed with GBLOCKS (Castresana 2000; Talavera and Castresana 2007) implemented in the PHYLUCE pipeline.

Individual UCE loci were imported into Geneious 10.1 (Biomatters Ltd.) for manual inspection. In particular, alignments with low % identical sites (less than 40%) were flagged for inspection. If exclusion of a single divergent sequence increased this value to > 75%, the locus was retained. Subsequently, all loci were inspected - individual sequences with large gaps in the core UCE region were excluded, and obvious alignment errors in flanking regions were manually adjusted.

UCE phylogenomic analyses

Concatenated data matrices with 50% and 70% occupancy (i.e., for any given locus, sequences for at least 50 or 70% of samples needed for locus inclusion in the final dataset) were assembled for phylogenomic analyses. Maximum likelihood analyses of both matrices were conducted using RAxML version 8.2 (Stamatakis 2014) with the GTRGAMMA model and 200 rapid bootstrap replicates. Bayesian analyses were run on the concatenated 70% matrix using BEAST 2.4.0 (Bouckaert et al. 2014) with the molecular model estimated using PartitionFinder 1.1.1 (Lanfear et al. 2012). This analysis was run for 10 million generations, logging every 1000. Stationarity was assessed using Tracer (Rambaut and Drummond 2007) to ensure all ESS values were above 200. Two coalescent analyses were also conducted for both 50% and 70% matrices. First, ASTRAL-II (Mirarab et al. 2014; Mirarab and Warnow 2015) was used with individual gene trees estimated in RAxML with 500 bootstrap replicates. We also used SVDquartets (Chifman and Kubatko 2014, 2015) with $n = 500$ bootstraps, as implemented in PAUP* 4.0 (Swofford 2003). RAxML phylogenies were midpoint rooted, while BEAST trees were rooted according to the implemented clock model.

Mitochondrial phylogenetics

Using a sample of eyed and eyeless *Cicurina* spiders from Texas and other US states, Paquin and Hedin (2004) recovered a “Texas eyeless” mitochondrial cytochrome oxidase I (COI) clade. We downloaded representative sequences for this clade from GenBank. We also used Geneious BLAST searches to extract COI sequences from UCE VELVET assemblies, using Texas eyeless clade Sanger data as query sequences (blastn, no low complexity filter, max e-value of 1e-5). For any single specimen these searches sometimes returned multiple sequences covering the same region; here, large differences in contig coverage values were used to discard putatively non-homologous contigs. After assembly of the Sanger plus UCE “by-catch” matrix (984 basepairs × 132 taxa), a partitioned (by codon position) RAxML analysis was conducted with the GTRGAMMA model and 200 rapid bootstrap replicates. Following Paquin and Hedin (2004), we rooted the mitochondrial tree using sequences from *Cicurina pampa*, a six-eyed species from Texas.

Morphological study

Cokendolpher (2004) showed that cave-dwelling *Cicurina* from Bexar County fall into two distinct morphological groups that differ in degree of troglomorphy, as measured by the ratio of first leg length / carapace length. Species with a high “troglomorphy index” (TI) are relatively long-legged as compared to taxa with a lower TI. Although Cokendolpher (2004) measured only adult specimens, we wondered whether this TI difference also applied to immatures. Focusing on Bexar County taxa, we measured adult and immature specimens from multiple species (see Suppl. material 6). Measurements were taken using an Olympus SZ40 dissecting scope fitted with an ocular micrometer, as specified in Suppl. material 6.

For adult specimens used in UCE experiments we imaged genitalia using a Visionary Digital BK plus system (<http://www.visionarydigital.com>). Individual images were merged into a composite image using Helicon Focus 6.2.2 software (<http://www.heliconsoft.com/heliconfocus.html>). Because we did not have access to all specimens borrowed from TTU (some loans were DNA only), we were not able to image all adult specimens used in this study.

Results

Suppl. material 5 includes specimen voucher information, DNA quantities, number of raw Illumina reads passing quality filter, VELVET contig numbers, and SRA accession numbers. We generated UCE data for six total museum specimens, but BLAST searches of both raw reads and VELVET contigs for the *C. venii* and *C. vespera* holotype specimens returned only bacterial, fungal, or human sequences. For 81 remaining specimens we

analyzed both 50% (399 loci, 94379 basepairs) and 70% occupancy (238 loci, 61054 basepairs) nuclear UCE matrices (Suppl. material 5). Raw Illumina reads are available at the NCBI Short-Read Archive (BioProject PRJNA471846), with aligned matrices and .tre files available at Dryad (<https://doi.org/10.5061/dryad.28fg251>).

Using molecular clock or mid-point rooting, all nuclear phylogenomic analyses result in recovery of two primary Texas eyeless *Cicurina* clades (Figures 1, 2; Suppl. material 1–3). A relatively broadly distributed clade includes species with adult females possessing mostly elongate spermathecae (see Cokendolpher 2004, Paquin and Dupérré 2009), hereafter called the ME clade. This clade is found in multiple Texas counties that include Edwards Plateau caves (Figure 1). A more narrowly distributed clade includes species with adult females possessing rounded spermathecae (Cokendolpher 2004, Paquin and Dupérré 2009), hereafter called the R clade. Given our taxon sample, the R clade appears restricted to caves in Bexar and adjacent southern Comal counties (Figure 1).

We recovered mitochondrial COI sequences from UCE assemblies for all but two specimens (TMM_9790, TK_190994), with an overall matrix completeness above 97%. All UCE-derived COI sequences were in frame and lacked stop codons or ambiguities, and when directly compared to previously published Sanger data (e.g., from same cave or sometimes same specimen), were found to be identical (Figure 3). The aligned COI matrix is available at Dryad (<https://doi.org/10.5061/dryad.28fg251>).

Maximum likelihood trees, rooted with the eyed taxon *C. pampa*, include an R clade, but the poorly supported placement of two ME sequences renders this latter group paraphyletic (Figure 3). We note that both ME and R clades were recovered in Paquin and Hedin (2004), although with more limited taxon sampling. The COI dataset includes some species and populations not included in nuclear analyses, including *C. puentecilla* and *C. platypus*, placed into the mitochondrial ME group. Cokendolpher (2004) discussed the unique morphology of *C. platypus* spermathecae, perhaps best described as a third morphological type (large, even-sized, rounded); *C. puentecilla* has a genital morphology very similar to *C. platypus* (Paquin and Dupérré 2009). The COI phylogeny includes higher resolution (not necessarily accuracy) within some species, but generally lacks support at deeper nodes (Figure 3). As such, most discussion below focuses on the highly supported nuclear UCE results.

Within the ME clade, nuclear phylogenomic relationships are structured geographically, with western, northeastern, and Bexar county groupings (Figure 1). Female morphology is mostly consistent across these groups (Figure 4), and we predict that described *Cicurina* species with similar genital morphologies not sampled here will ultimately fall into the ME genetic clade (e.g., *C. sansaba*, many species from western counties, etc.; see Paquin and Dupérré 2009). Figure 5 shows the distribution of *C. madlla* and *C. cf. madlla* in Bexar and adjacent Medina and Bandera counties. Consistent with Paquin and Hedin (2004) and new mitochondrial results, sampled populations of *C. madlla* are found in multiple karst faunal regions (KFRs) of northwestern Bexar county. A novel result is the placement of multiple samples from the northern Culebra Anticline KFR in the *C. madlla* clade (Figure 5). This unexpected

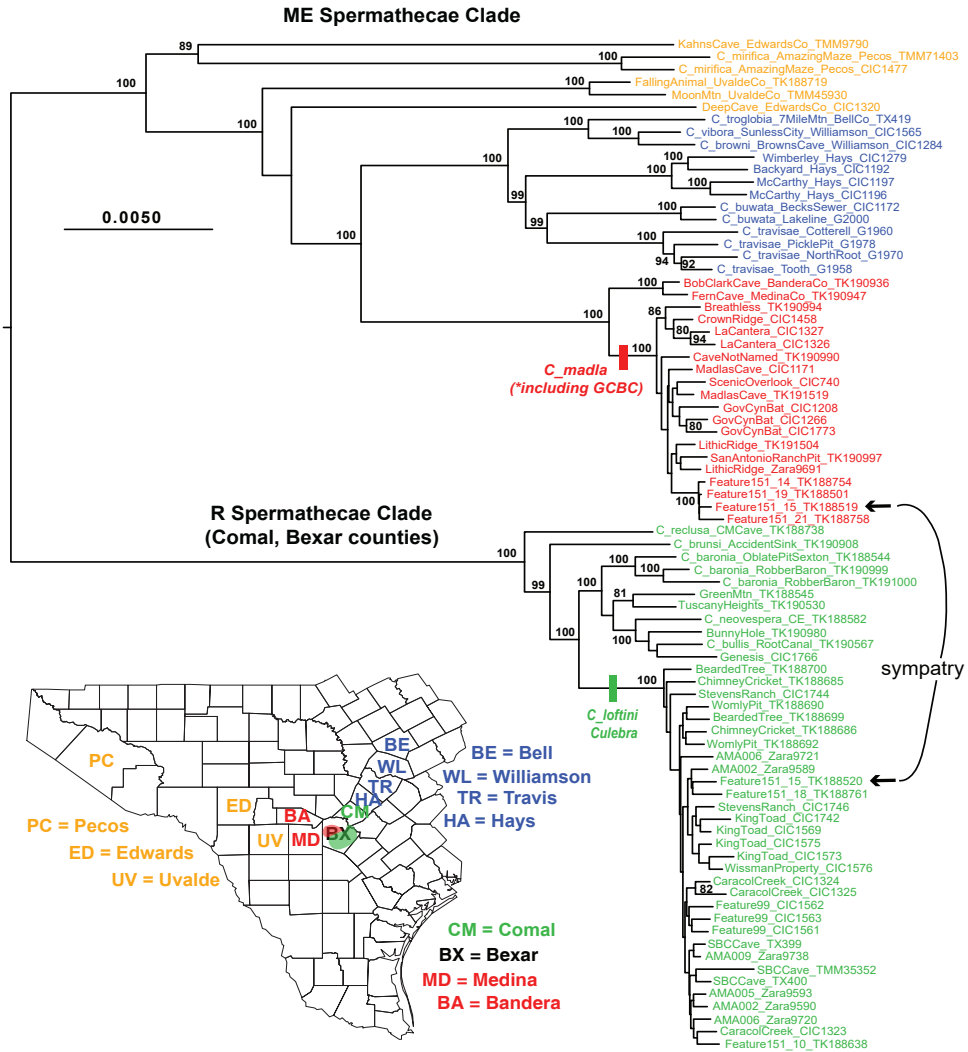


Figure 1. Phylogenetic tree from RAxML analysis of 399 UCE loci, 70% (399/70) occupancy matrix. Bootstrap values below 75 not shown. Geography and morphology highlighted. Abbreviations: ME (= mostly elongate) spermathecae clade, R (= rounded) spermathecae clade. Further details regarding specimen codes and locations found in Suppl. material 5. Inset: sampled Texas counties.

distribution across disjunct and geologically isolated KFRs is also seen in the eyeless leptonetid spider *Tayshaneta whitei* (Ledford et al. 2012, fig. 63). At one location in the northern Culebra Anticline (location = “feature 151_15”), members of ME and R clades are found in apparent sympatry, rare in TX cave *Cicurina* (Cokendolpher 2004, Paquin and Dupérré 2009).

Figure 6 shows the morphology of adult specimens from the *C. madla* clade, including specimens from the sympatric location. This morphology is consistent with

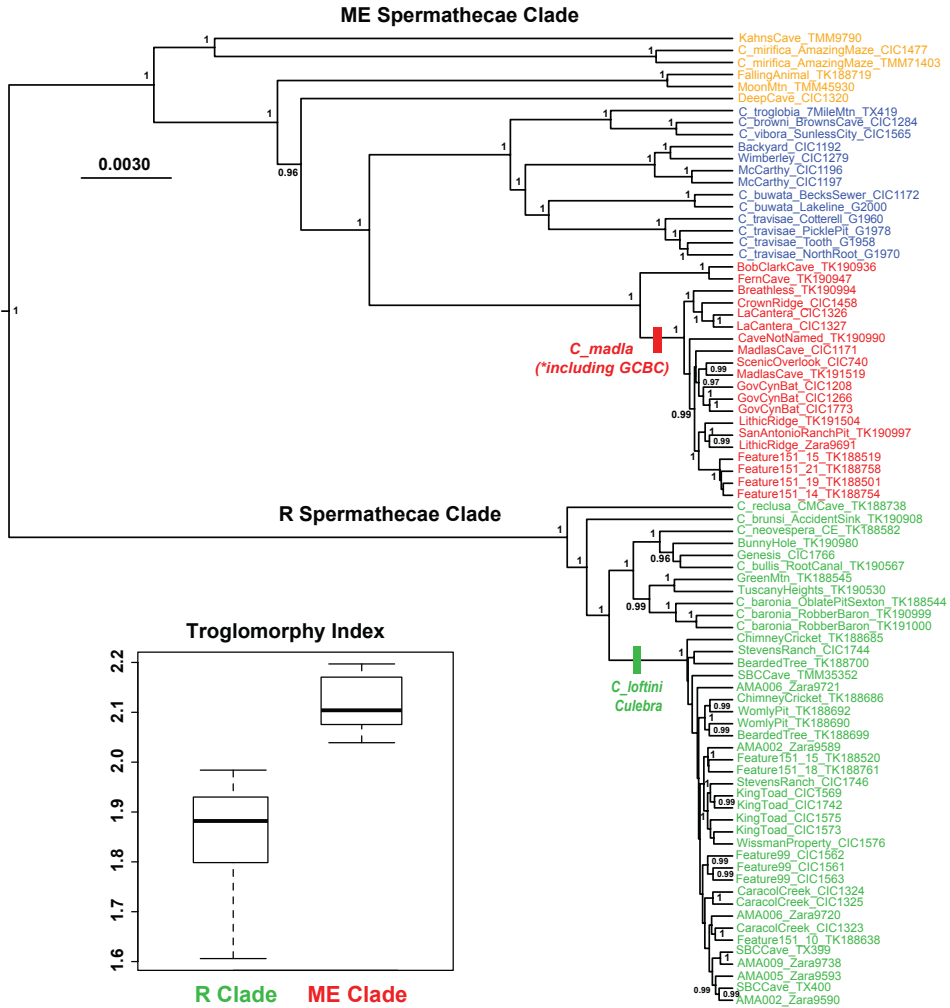


Figure 2. Phylogenetic tree from BEAST analysis of 399_70 UCE matrix. Posterior probability values above 0.95 shown. Inset: Boxplots of TI values (from Suppl. material 6) for ME and R clade members from Bexar County (for ME clade, two small juveniles and Stahl Cave specimens not included).

the description for *C. madla*. We note that many additional adult *C. madla* specimens have been collected from sampled (or nearby sampled) caves not shown here (Coken-dolpher 2004, Paquin and Dupérré 2009).

We gathered nuclear UCE data for three specimens from Government Canyon Bat Cave (GCBC, the stated type locality of *C. vespera*), all of which fall into the *C. madla* UCE genetic clade. This nesting of GCBC specimens inside a *C. madla* clade also applies to the COI dataset, which also includes two additional Sanger GCBC specimens (Figure 6). In total, five specimens from GCBC have been included in this or prior genetic studies (Paquin and Hedin 2004), and all are genetically allied with *C. madla*.

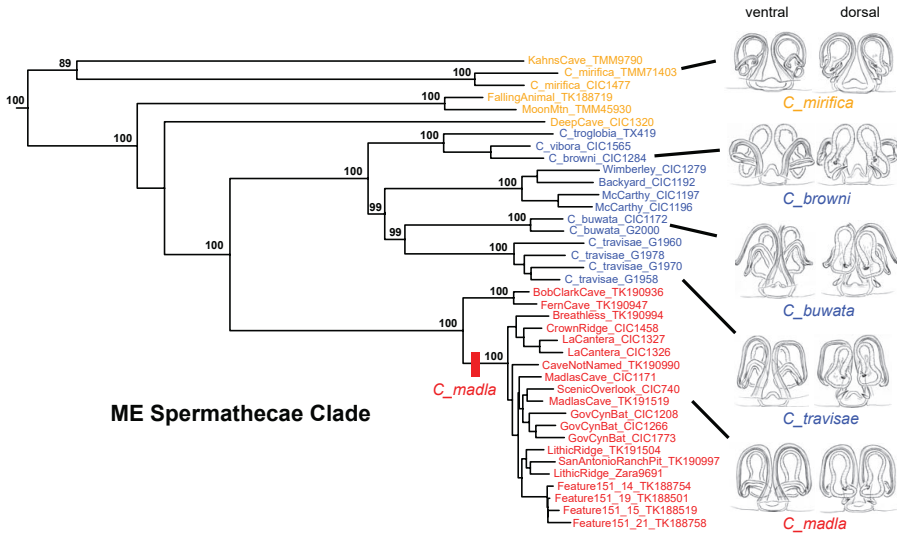


Figure 4. Morphology of ME clade with corresponding 399_70 UCE RAXML phylogeny (not all bootstrap values shown). Holotype female spermathecal images from Paquin and Dupérré (2009), used with permission. Images not to scale.

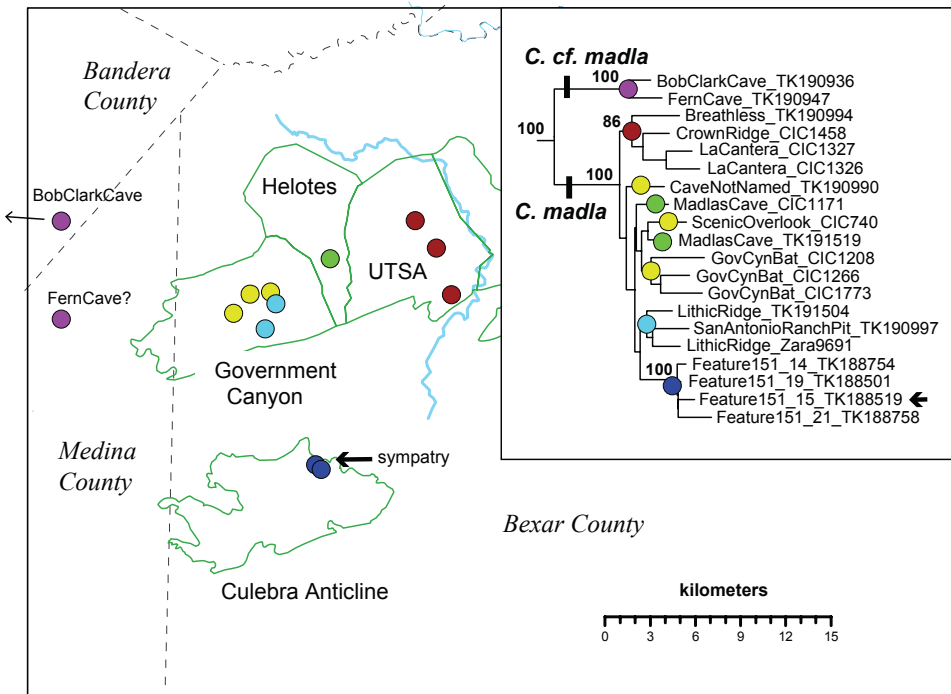


Figure 5. Distribution of *C. madla* and *C. cf. madla* in Bexar and adjacent counties, with corresponding 399_70 RAXML UCE phylogeny (not all bootstrap values shown). Different geographic populations designated by different colors. Cave locations approximate.

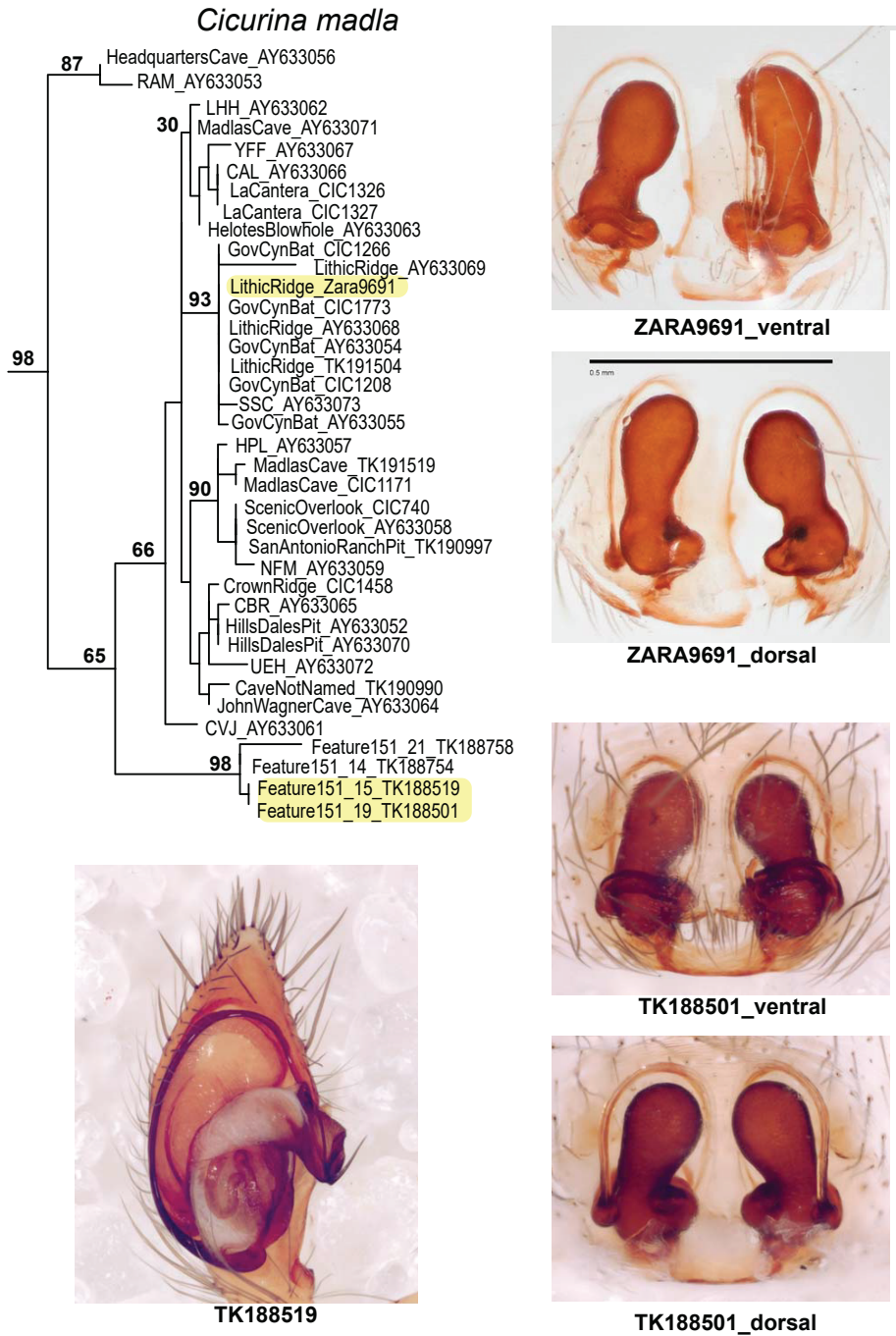


Figure 6. Morphology of adult *C. madla* with corresponding COI RAXML phylogeny. Previously published sequences with corresponding GenBank numbers (AY#), some with cave location codes as in Paquin and Hedin (2004). Imaged specimens highlighted on phylogeny; images of specimens TK_188519 and TK_188501 from Joel Ledford. Scale bar: 0.5 mm.

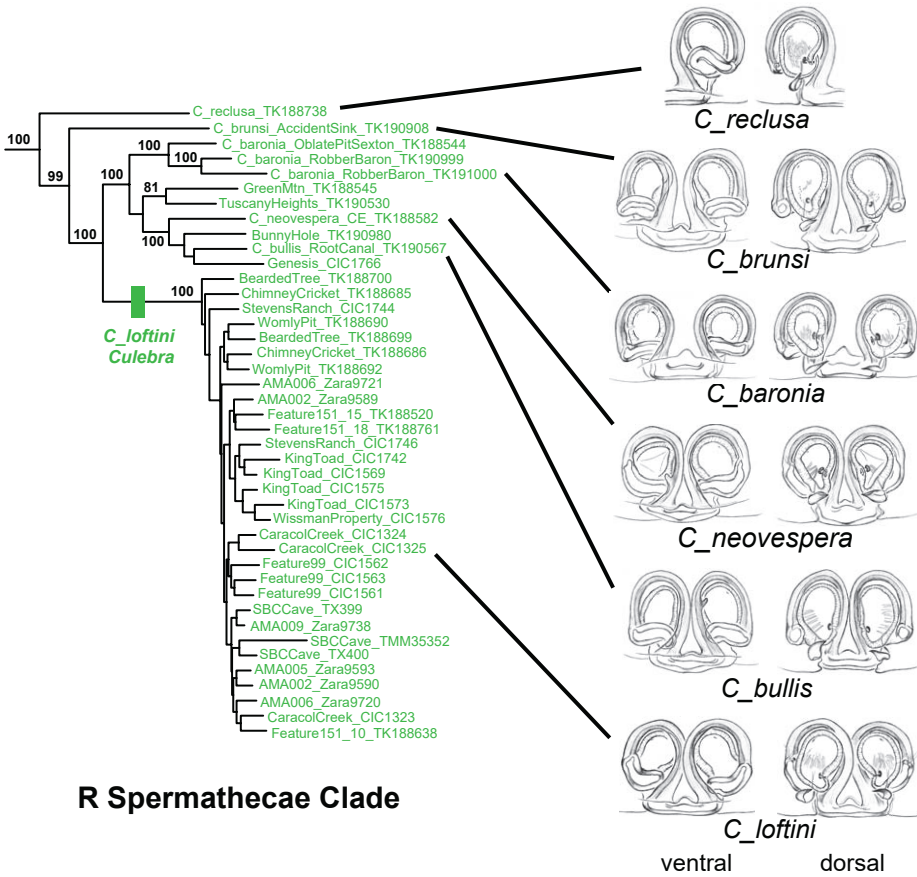


Figure 7. Morphology of R clade with corresponding 399_70 UCE RAxML phylogeny (not all bootstrap values shown). Holotype female spermathecal images from Paquin and Dupérré (2009), used with permission. Images not to scale.

The R clade includes six described species with very similar genitalic morphologies (Figure 7), with a distribution that spans from southern Comal to southwestern Bexar County (Figure 8). These nuclear phylogenomic results agree with Cokendolpher's (2004) hypothesis regarding the morphological affinities of R clade members, although UCE data do not recover his internal groupings of *C. baronia*, *C. brunsi*, *C. bullis* (rounded spermathecal lobes of unequal size; spermathecal stalk transverse) versus *C. loftini*, *C. neovespera*, and *C. vespera* (rounded spermathecal lobes of unequal size; spermathecal stalk oblique). Both UCE and mitochondrial results confirm a new population for *C. baronia* (=OblatePitSexton), which is important because this Federally endangered species was previously known only from the highly impacted type locality. One area of uncertainty in the R clade involves the species status and phylogenetic placement of specimens from Genesis, GreenMtn and Tuscany Heights locations, with different placements across nuclear and COI analyses (Figure 8; Suppl. material 4).

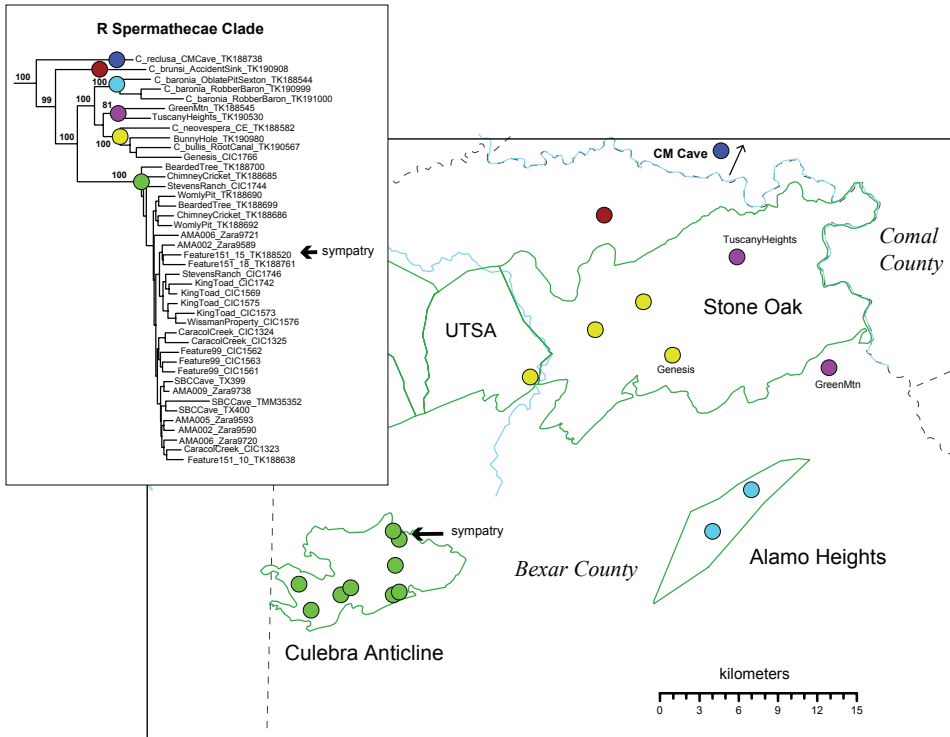


Figure 8. Distribution of R clade in Bexar and Comal counties, with corresponding 399_70 UCE RAxML phylogeny. Different species designated by different colors. Cave locations approximate.

Cicurina loftini is found only in the Culebra Anticline KFR (Figure 8). Some populations at the northern edge of this range are in sympatry or close parapatry with *C. madla*, as highlighted in the text above. Figure 9 shows the morphology of adult specimens from *C. loftini*, including adult specimens from the sympatric location; this morphology is consistent with the description for *C. loftini* (Cokendolpher 2004, Paquin and Dupérré 2009). Fine-scale mitochondrial structuring within *C. loftini* appears to closely follow karst geology within the Culebra Anticline KFR, as individual or adjacent caves form distinct and well-supported mitochondrial subclades (Figure 10).

We measured TI values for 49 total specimens, some of which were included in UCE experiments (Suppl. material 6). For 23 specimens representing the R clade, all measured specimens have a TI value (= partial leg I length / carapace length) below 1.98 (Figure 2). This is consistent with the measurements of Cokendolpher (2004, table 1) for *C. baronia*, *C. brunsi*, *C. bullis*, *C. loftini*, *C. neovespera*, and the *C. vespera* holotype, all with TI values below 1.98.

For 25 specimens representing the ME clade, all but two specimens have TI values above 2.04 (Figure 2), consistent with the measurements of Cokendolpher (2004, table 1) for *C. madla* and the *C. venii* holotype. This relatively high TI does not pertain for two very small immature specimens (carapace length below 1 mm) that are sus-

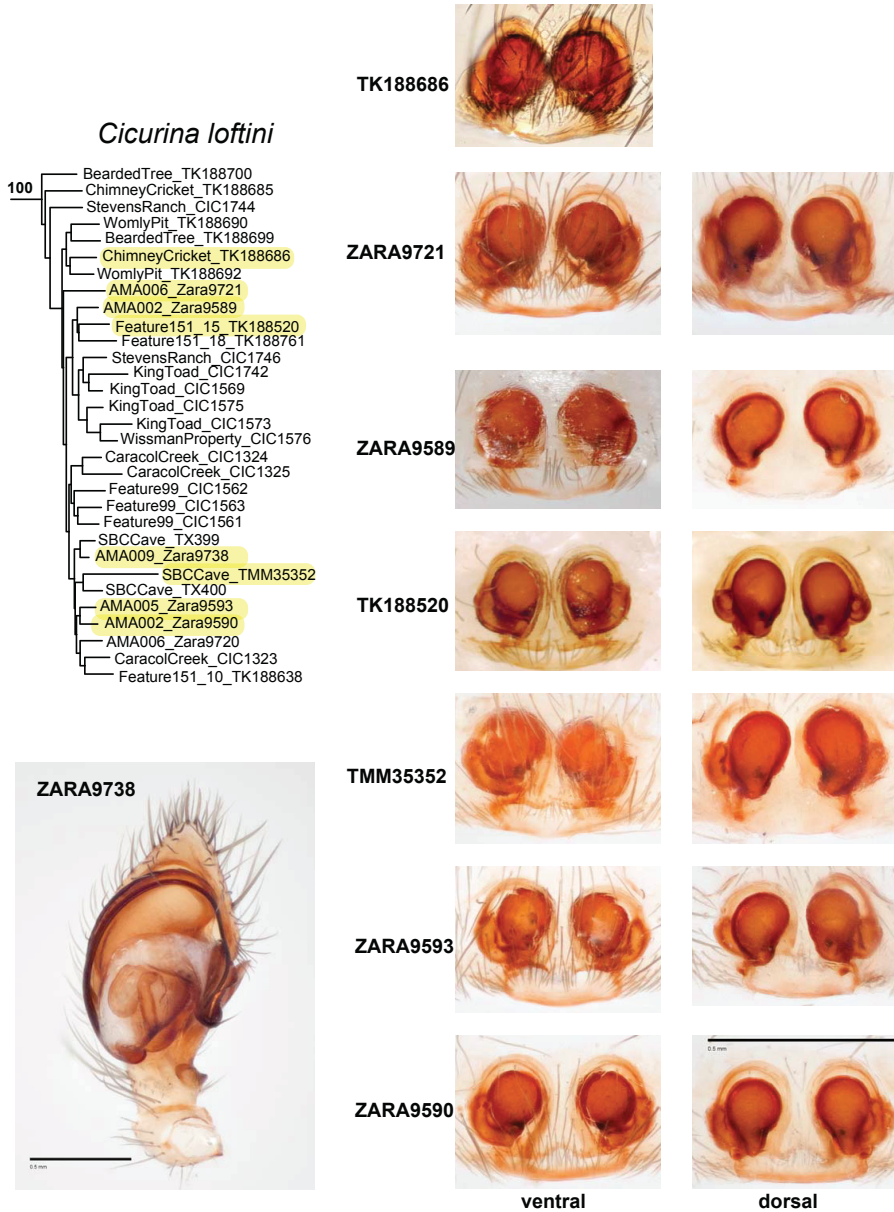


Figure 9. Morphology of adult *C. loftini* with corresponding 399_70 UCE RAxML phylogeny. Imaged specimens highlighted on phylogeny; images of specimen TK_188520 from J. Ledford, specimen TK_188686 from J. Cokendolpher (via Symbiota Collections of Arthropods Network). Scale bar: 0.5 mm.

pected members of the ME clade, based on cave location (Suppl. material 6). Also, we measured two specimens from GCBC (different from genetic specimens), the stated type locality of the R morphology, low TI *C. vespera* holotype specimen. Both of these

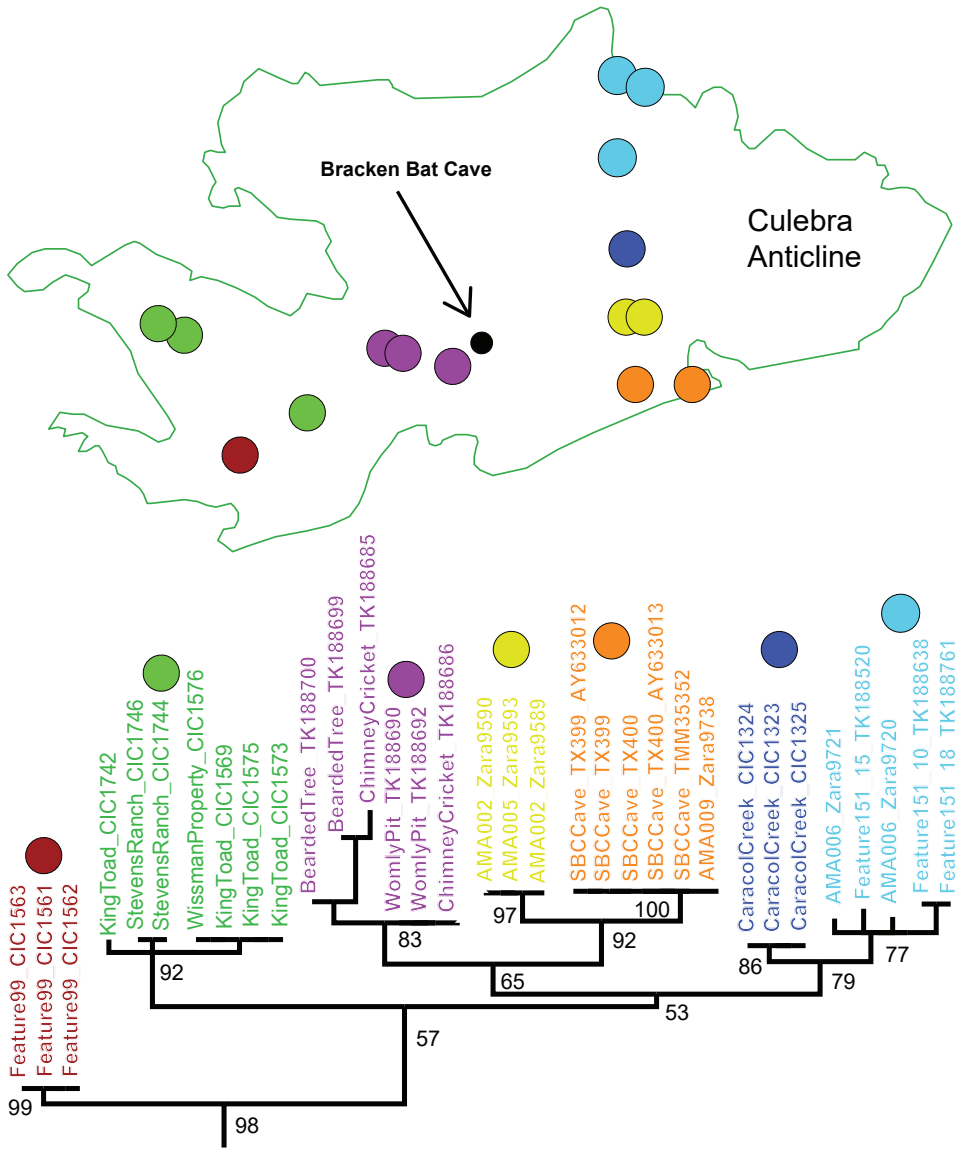


Figure 10. Distribution of *C. loftini* in Culebra Anticline KFR, with corresponding COI RaXML phylogeny. Different mtDNA microclades designated by different colors. Cave locations approximate.

specimens have a TI value above 2.08 (Suppl. material 6). A single immature specimen from Stahl Cave is potentially anomalous. This specimen is from the type locality of the R clade member *C. brunsi*, but has a high TI (2.34) indicative of an ME species (Suppl. material 6). We hypothesize that this represents a potential case of previously unreported sympatry; generation of UCE data for this specimen, or further collecting from this location would provide a test of this hypothesis.

Discussion

The spider genus *Cicurina* includes over 130 described species known from multiple regions in the northern hemisphere (World Spider Catalog 2018), with many taxa showing troglomorphic modifications associated with cave life (Paquin and Dupérré 2009). It was not our goal to conduct a generic-level phylogenetic analysis, and we acknowledge that we have largely assumed the monophyly of a “Texas eyeless” lineage, as found in the molecular phylogenetic research of Paquin and Hedin (2004), and supported by morphology (subgenus *Cicurella* Chamberlin and Ivie, Gertsch 1992, Cokendolpher 2004, Paquin and Dupérré 2009). We hypothesize that two primary lineages exist in a larger “Texas eyeless” clade, but much denser taxonomic and phylogenomic sampling is needed to rigorously test this idea, particularly sampling of more eyeless species from west Texas and northeastern Mexico. We note that Cokendolpher (2004) also hypothesized common ancestry for members of the R clade, based on comparative analysis of morphology.

The capture-based DNA sequencing strategy implemented here provides a foundation for ultimately collecting nuclear phylogenomic data for all described eyeless *Cicurina* species in Texas. Collection of such data would be extremely important for testing existing species hypotheses, many of which are based on limited material and represent fundamentally weak hypotheses (see Paquin and Dupérré 2009). Also, although collection of UCE data from “standard” museum specimens was not successful in all cases (Suppl. material 5), it is clear that such samples will represent an important resource for capture-based phylogenomics research moving forward. For example, it remains possible that new DNA extraction methods (e.g., Tin et al. 2014), in combination with targeted sequence capture, will ultimately allow for the collection of useable DNA sequence data from older ethanol-preserved museum specimens.

Species sympatry

Examples of eyed- and eyeless *Cicurina* taxa from the same Texas cave are numerous (e.g., Cokendolpher 2004), but well-supported examples of eyeless taxa sympatry in the same cave are scarce. North of Bexar County, Gertsch (1992) hypothesized sympatry of *C. reddelli* and *C. buwata*, while Cokendolpher and Reddell (2001) hypothesized sympatry of *C. caliga* and *C. hoodensis*. All of these taxa are members of a “northeast” clade within the larger ME clade (Figure 1), and thus are relatively closely related, making sympatry potentially less likely. Indeed, Cokendolpher and Reddell (2001) disclaimed the *C. reddelli* / *C. buwata* case, and the species *C. caliga* and *C. hoodensis* are genetically extremely similar (Figure 3) and are possibly conspecific (see also Paquin and Hedin 2004).

Our discovery of divergent ME and R genetic lineages, with corresponding differences in degree of troglomorphy (Figure 2), helps to now explain several cases of apparently bonafide sympatry. Cokendolpher (2004) first hypothesized sympatry

between *C. platypus* (unique genitalia, ME mitochondrial clade, high TI) and *C. bullis* (R clade, low TI) in the Stone Oak KFR (Figure 8). We have hypothesized sympatry in Stahl Cave (east of Accident Sink, see Figure 8) between low TI *C. brunsi* and an unidentified member of the ME clade (possibly *C. platypus*), and have convincingly shown sympatry in the northern Culebra Anticline between *C. madla* and *C. loftini* (Figs 5 and 8). This sympatry, at karst “feature 151_15”, includes spiders collected from the same very small ($\sim 2 \times 6$ meter) solutionally enlarged fracture. The three cases above all occur in Bexar County where divergent members of the ME and R come into secondary contact, typically at the edge of species distributions. Cokendolpher (2004) hypothesized that less troglomorphic R clade taxa may be younger than taxa with elongate spermathecae; our phylogenomic topologies are consistent with this idea (e.g., Figure 2), although we have not formally conducted clock analyses.

Immatures, new populations, likely new species

The current study was partially constrained in two ways – first, we often used immature specimens, again because about 90% of collected eyeless specimens are immature (Cokendolpher 2004, Paquin and Dupérré 2009). We felt that return on investment by inclusion was higher than complete exclusion. Also, we did not have access to all specimens borrowed from TTU (some loans were DNA only), some of which were adults. Acknowledging these limitations, our results provide important new population or species-level information in several cases, even when based on immature specimens. Put simply, our findings offer new hope in increasing the systematic information content of 100s of “unidentifiable” immature eyeless *Cicurina* that reside in regional collections (e.g., see records in Cokendolpher 2004, Paquin and Dupérré 2009).

We have shown that immatures of ME and R clade species from Bexar County differ in TI index (Figure 2), which implies that many immature museum specimens (above a certain instar) might be broadly placed into these primary lineages. This could be useful in conservation-focused identifications, or cases of sympatry where the relative abundance of sympatric individuals remains largely unstudied because of low adult spider sample sizes.

Within the ME clade, immature spiders from Bob Clark Cave (Bandera Co.) and Fern Cave (Medina Co.) represent a *potentially* undescribed sister species of *C. madla*, herein called *C. cf. madla* (Figure 5). This result is supported by high and congruent divergence in both nuclear (Figure 5) and mitochondrial genomes (Figure 3). We are unaware of adult spiders from these caves, but hypothesize an ME morphology similar to *C. madla*. We stress *potentially*, as these cave samples might alternatively represent new populations of an already described western species (e.g., *C. watersi*, *C. obscura*,

etc. – see Paquin and Dupérré 2009, fig. 135). Collection of samples from cave habitats in the geographic region between the Government Canyon KFR and the above more westerly cave locations (Figure 5) should be prioritized.

Within the R clade, immature spiders from the “Oblate Pit Sexton” location clearly represent a second known population for the federally endangered species *C. baronia* (Figs 3, 8, Suppl. material 4), possibly indicating a previously undocumented karst connection within the Alamo Heights KFR. Robber Baron Cave is surrounded in the urban matrix of San Antonio, and as such is highly impacted (Cokendolpher 2004). The Oblate Pit Sexton location, and any karst features in the adjacent area, become extremely important from a conservation perspective. As discussed above, the species status and phylogenetic placement of immature specimens from Genesis, GreenMtn and Tuscany Heights locations requires further study (Figure 8; Suppl. material 4). Collection of adults from these locations, and sampling of phylogenomic data from more regional caves would help clarify the status of both potentially undescribed and described R clade taxa (*C. bullis*, *C. neovespera*, *C. baronia*; Figure 8; Suppl. material 4).

The status of federally-listed *C. vespera* and *C. venii*

Both *C. vespera* and *C. venii* are single-site endemic species listed as US federally endangered (Figure 11). The female morphology and TI index of the *C. vespera* holotype (type location stated as GCBC) is like *C. loftini* (R clade), although GCBC is surrounded by *C. madlla* populations (ME clade). Of seven total specimens collected from GCBC for which we have either morphological or genetic data, all are allied with *C. madlla*, except for the holotype specimen of *C. vespera*. In fact, the *C. vespera* holotype remains the single known R clade specimen known from the Government Canyon, Helotes, or UTSA KFRs, all with caves inhabited by *C. madlla*.

Conversely, the female morphology and TI index of the *C. venii* holotype (type location stated as Bracken Bat Cave) is like *C. madlla* (Cokendolpher 2004), although Bracken Bat is surrounded by *C. loftini* populations, including other caves within 100s of meters from this location (Figs 10 and 11). Because the entrance of Bracken Bat has been sealed, additional samples from this cave for genetics research have never been available.

A key to resolving the above anomalous morphological and distributional data would have been successful collection of nuclear UCE data (or by-catch COI data) from the type specimens. We were unable to secure such data from the old holotype specimens. Given this lack of direct evidence for species status of the anomalous holotypes, we propose two alternative scenarios: 1) Gertsch (1992) either switched the labels or specimens in vials, or 2) both anomalous geographic cases represent additional examples of ME and R clade sympatry. Under either hypothesis, the species synonymies proposed below remain valid.

Taxonomy

Family Hahniidae Bertkau, 1878

Genus *Cicurina* Menge, 1871

Subgenus *Cicurella* Chamberlin & Ivie, 1940

Cicurina (Cicurella) madla Gertsch, 1992

Figs 1–6, 10–12, Suppl. materials 1–3, 5–6.

Cicurina madla Gertsch, 1992: 109, figs 91–92.

Cicurina madla Cokendolpher, 2004: 42, figs 7, 40–47.

Cicurina madla Paquin & Dupérré, 2009: 28, figs 50–51, 134–135.

Cicurina venii Gertsch, 1992: 111, figs 95–96; **syn. n.**

Cicurina venii Cokendolpher, 2004: 52, figs 63–64; **syn. n.**

Cicurina venii Paquin & Dupérré, 2009: 52, figs 116–117; **syn. n.**

Diagnosis. The adult morphology of a potentially undescribed sister species (*C. cf. madla*) remains unknown. ME clade members from the neighboring Stone Oak KFR (*C. platypus*, *C. puentecilla*) have different spermathecal morphologies (large, even-sized, rounded; Cokendolpher 2004, Paquin and Dupérré 2009). *Cicurina madla* is easily distinguished from neighboring or sympatric R clade members using genetic data, spermathecal morphology, male palpal morphology, or TI index.

Description. Female spermathecal morphology as described in Paquin and Dupérré (2009). Male palpus with relatively narrow, elongate cymbium, oblong tegulum, origin of embolus at ~ 6 o'clock (Figs 6, 12).

Distribution. ME clade member known from approximately 25 caves or karst features in the Government Canyon, Helotes, UTSA and northern Culebra Anticline KFRs (Figure 5), plus two populations in Stone Oak KFR and Uvalde County (Figure 6, also figure 4 of Paquin and Hedin 2004).

Discussion. The high TI index, elongate spermathecae holotype *C. venii* type specimen is either 1) actually from GCBC, but was mislabeled or placed into an incorrect vial, or 2) is actually from Bracken Bat Cave, and represents a further southern (but currently unknown) extension of the *C. madla* Culebra Anticline subclade (Figure 11). If the latter, sympatry with *C. vespera* is likely in this central region of the Culebra Anticline.

Cicurina (Cicurella) vespera Gertsch, 1992

Figs 1–3, 7–12, Suppl. materials 1–6.

Cicurina vespera Gertsch, 1992: 111, figs 93–94.

Cicurina vespera Cokendolpher, 2004: 53, figs 65–66.

Cicurina vespera Paquin & Dupérré, 2009: 53, figs 118–119, 134.

Cicurina loftini Cokendolpher, 2004: 41, figs 5, 10, 37–39; **syn. n.**

Cicurina loftini Paquin & Dupérré, 2009: 27, figs 46–47, 134; **syn. n.**

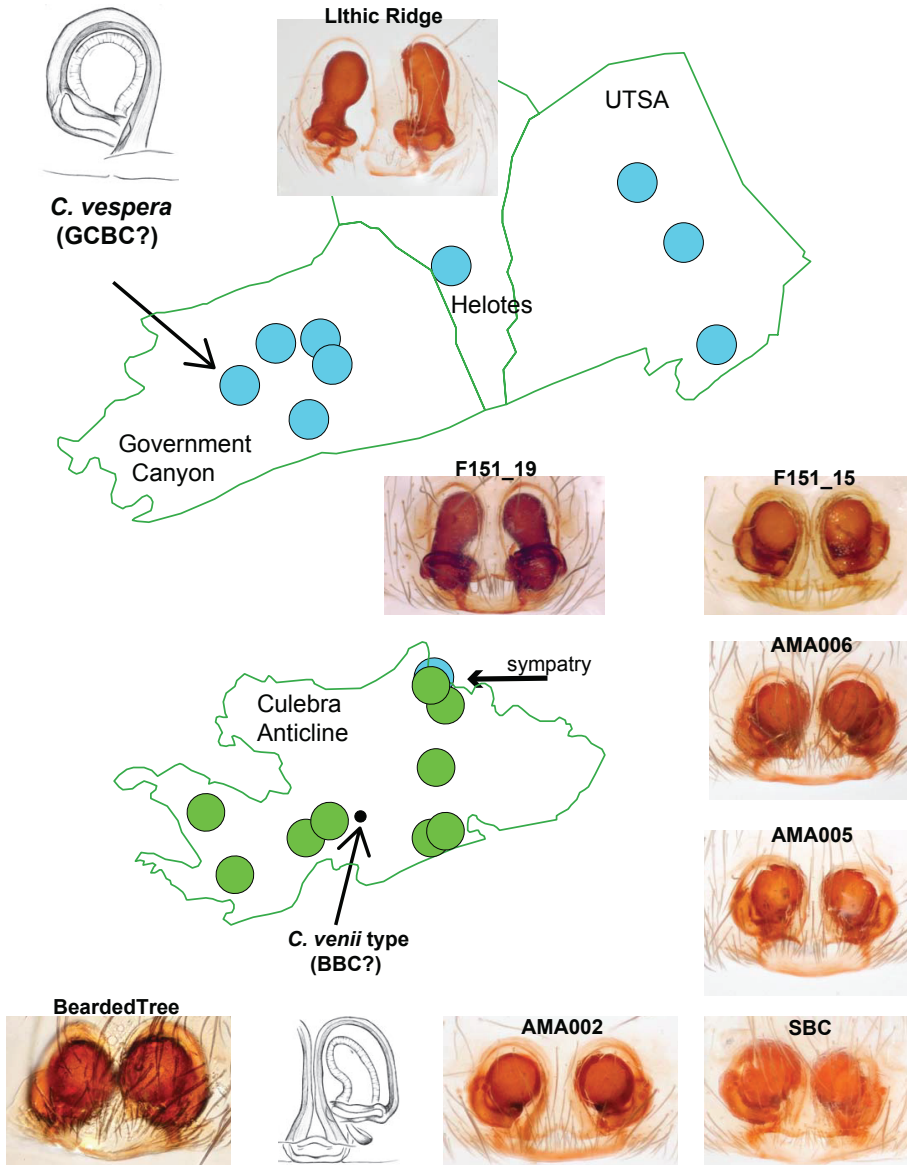


Figure 11. Anomalous geographic distribution of *C. venii* and *C. vespera* type specimens. All views ventral.

Diagnosis. Based on well-supported nuclear phylogenomic analyses (Figs 1–2, 7), sister taxon to a clade including *C. baronia*, *C. neovespera*, and *C. bullis*. *Cicurina vespera* is morphologically very similar to the above taxa (Figure 7, Cokendolpher 2004, Paquin and Dupérré 2009), best separated by geographic allopatry (Figure 8). This species can be distinguished from neighboring or sympatric ME clade members using genetic data, spermathecal morphology, male palpal morphology, or TI index.

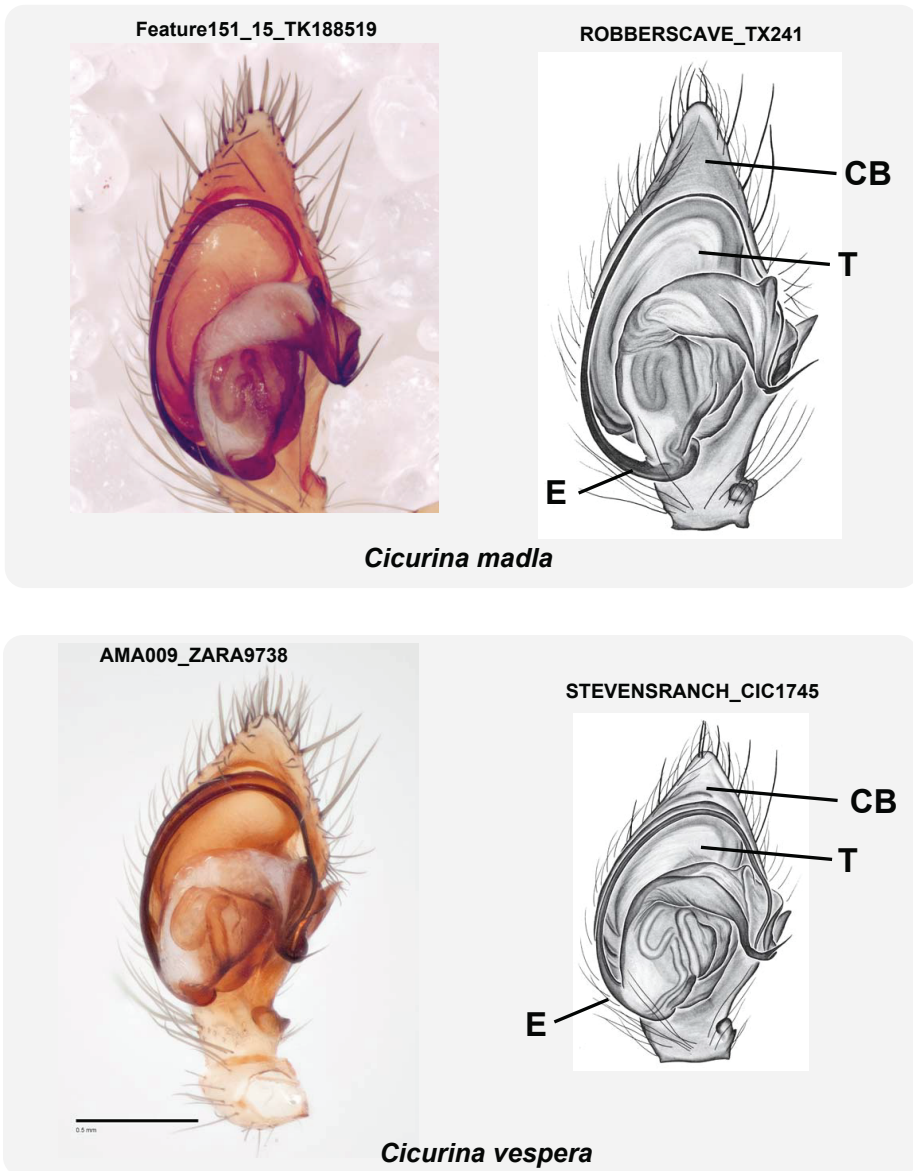


Figure 12. Male palpal morphology of *C. madla* and *C. vespera* (left palp, ventral view). Specimens from Stevens Ranch Trash Hole Cave (CIC_1745) and Robbers Cave (TX_241) from PP personal collection. Image of specimen TK_188519 from Joel Ledford. Abbreviations: CB = cymbium, T = tegulum, E = embolus. Scale bar: 0.5 mm.

Description. Female spermathecal morphology as described in Paquin and Dupérré (2009) and Cokendolpher (2004). Male palpus with relatively broad, truncate cymbium, compact tegulum, origin of embolus rotated slightly clockwise from 6 o'clock (Figs 9, 12).

Distribution. R clade member known from 16 cave or karst features in the Culebra Anticline KFR (Figure 10); possibly also from GCBC.

Discussion. The low TI index, rounded spermathecae holotype *C. vespera* type specimen is either 1) actually from Bracken Bat Cave, but was mislabeled or placed into an incorrect vial, or 2) is actually from GCBC, and represents a northern disjunct from most Culebra Anticline *C. vespera* populations, although we note that direct evidence for such an extension does not exist in the Government Canyon KFR (Figure 11). If the latter, rare sympatry must exist in GCBC, as other known specimens from this location represent *C. madlla*.

Acknowledgements

We would like to thank James Cokendolpher, Kathy MacDonald, Heath Garner, and Caleb Phillips from the Museum of Texas Tech University, James Reddell from the Texas Memorial Museum, Jean Krejca and Rachel Barlow from ZARA Environmental, and Louis Sorkin and Lorenzo Prendini from the American Museum of Natural History. We also thank the many other persons who have collected *Cicurina* specimens ultimately used in this research (Suppl. material 5 and 6). We sincerely thank Nadine Dupérré for specimen illustrations. Joel Ledford and James Cokendolpher shared specimen images. Research was funded by a contract to MH from the Southern Edwards Plateau Habitat Conservation Plan (Bexar County, Texas and the City of San Antonio, Texas) as part of the SEP-HCPs ongoing research program. Comments of Ingi Agnarsson, Gergin Blagoev, Shuqiang Li, and Victor Fet helped to improve the manuscript.

References

- Blaimer BB, Lloyd MW, Guillory WX, Brady SG (2016a) Sequence capture and phylogenetic utility of genomic ultraconserved elements obtained from pinned insect specimens. *PLoS ONE* 11(8): e0161531. <https://doi.org/10.1371/journal.pone.0161531>
- Blaimer BB, LaPolla JS, Branstetter MG, Lloyd MW, Brady SG (2016b) Phylogenomics, biogeography and diversification of obligate mealybug-tending ants in the genus *Acropyga*. *Molecular Phylogenetics and Evolution* 102: 20–29. <https://doi.org/10.1016/j.ympev.2016.05.030>
- Bossert S, Danforth BN (2018) On the universality of target enrichment baits for phylogenomic research. *Methods in Ecology and Evolution*. <https://doi.org/10.1111/2041-210X.12988>
- Carstens BC, Pelletier TA, Reid NM, Satler JD (2013) How to fail at species delimitation. *Molecular Ecology* 22: 4369–4383. <https://doi.org/10.1111/mec.12413>
- Castresana J (2000) Selection of conserved blocks from multiple alignments for their use in phylogenetic analysis. *Molecular Biology and Evolution* 17: 540–552. <https://doi.org/10.1093/oxfordjournals.molbev.a026334>
- Chifman J, Kubatko L (2014) Quartet inference from SNP data under the coalescent. *Bioinformatics* 30: 3317–3324. <https://doi.org/10.1093/bioinformatics/btu530>

- Chifman J, Kubatko L (2015) Identifiability of the unrooted species tree topology under the coalescent model with time-reversible substitution processes, site-specific rate variation, and invariable sites. *Journal of Theoretical Biology* 374: 35–47. <https://doi.org/10.1016/j.jtbi.2015.03.006>
- Cokendolpher JC, Reddell JR (2001) Cave spiders (Araneae) of Fort Hood, Texas, with descriptions of new species of *Cicurina* (Dictynidae) and *Neoleptoneta* (Leptonetidae). Texas Memorial Museum, Speleological Monographs 5: 35–55.
- Cokendolpher JC (2004) *Cicurina* spiders from caves in Bexar County, Texas. Texas Memorial Museum Speleological Monographs, 6. Studies on the cave and endogean fauna of North America IV: 13–58.
- Faircloth BC, McCormack JE, Crawford NG, Harvey MG, Brumfield RT, Glenn TC (2012) Ultraconserved elements anchor thousands of genetic markers spanning multiple evolutionary timescales. *Systematic Biology* 61: 717–726. <https://doi.org/10.1093/sysbio/sys004>
- Faircloth BC (2013) illumiprocessor: a trimmomatic wrapper for parallel adapter and quality trimming. <http://dx.doi.org/10.6079/J9ILL>
- Faircloth BC, Branstetter MG, White ND, Brady SG (2015) Target enrichment of ultraconserved elements from arthropods provides a genomic perspective on relationships among Hymenoptera. *Molecular Ecology Resources* 15: 489–501. <https://doi.org/10.1111/1755-0998.12328>
- Faircloth BC (2016) PHYLUCE is a software package for the analysis of conserved genomic loci. *Bioinformatics* 32: 786–788. <https://doi.org/10.1093/bioinformatics/btv646>
- Faircloth BC (2017) Identifying conserved genomic elements and designing universal probe sets to enrich them. *Methods in Ecology and Evolution* 8: 1103–1112. <https://doi.org/10.1111/2041-210X.12754>
- Gertsch WJ (1992) Distribution patterns and speciation in North American cave spiders with a list of the troglobites and revision of the cicurinas of the subgenus *Cicurella*. Texas Memorial Museum Speleological Monographs 3. Studies on the endogean fauna of North America 2: 75–122.
- Glenn TC, Nilsen R, Kieran TJ, Finger JW, Pierson TW, Bentley KE, Hoffberg S, Louha S, Garcia-De-Leon FJ, del Rio Portilla MA, Reed K, Anderson JL, Meece JK, Aggery S, Reakaya R, Alabady M, Belanger M, Winker K, Faircloth BC (2016) Adapterama I: universal stubs and primers for thousands of dual-indexed Illumina libraries (iTru and iNext). [bioRxiv. https://doi.org/10.1101/049114](https://doi.org/10.1101/049114)
- Hedin M (2015) High stakes species delimitation in eyeless cave spiders (*Cicurina*, Dictynidae, Araneae) from central Texas. *Molecular Ecology* 24: 346–361. <https://doi.org/10.1111/mec.13036>
- Hedin M, Derkarabetian S, Ramírez MJ, Vink C, Bond J (2018) Phylogenomic reclassification of the world's most venomous spiders (Mygalomorphae, Aracninae), with implications for venom evolution. *Scientific Reports* 8: 1636. <https://doi.org/10.1038/s41598-018-19946-2>
- Katoh D, Standley DM (2013) MAFFT multiple sequence alignment software version 7: improvements in performance and usability. *Molecular Biology and Evolution* 30: 772–780. <https://doi.org/10.1093/molbev/mst010>
- Ledford J, Paquin P, Cokendolpher J, Campbell J, Griswold C (2012) Systematics, conservation and morphology of the spider genus *Tayshaneta* (Araneae, Leptonetidae) in central Texas caves. *ZooKeys* 167: 1–102. <https://doi.org/10.3897/zookeys.167.1833>

- McCormack JE, Tsai WLE, Faircloth BC (2016) Sequence capture of ultraconserved elements from bird museum specimens. *Molecular Ecology Resources* 16: 1189–1203. <https://doi.org/10.1111/1755-0998.12466>
- Mirarab S, Reaz R, Bayzid MS, Zimmermann T, Swenson MS, Warnow T (2014) ASTRAL: genome-scale coalescent-based species tree estimation. *Bioinformatics* 30: i541–i548. <https://doi.org/10.1093/bioinformatics/btu462>
- Mirarab S, Warnow T (2015) ASTRAL-II: coalescent-based species tree estimation with many hundreds of taxa and thousands of genes. *Bioinformatics* 31: i44–i52. <https://doi.org/10.1093/bioinformatics/btv234>
- Niemiller ML, Near TJ, Fitzpatrick BM (2012) Delimiting species using multilocus data: diagnosing cryptic diversity in the southern cavefish *Typhlichthys subterraneus* (Teleostei: Amblyopsidae). *Evolution* 66: 846–866. <https://doi.org/10.1111/j.1558-5646.2011.01480.x>
- Paquin P, Hedin M (2004) The power and perils of ‘molecular taxonomy’: a case study of eyeless and endangered *Cicurina* (Araneae: Dictynidae) from Texas caves. *Molecular Ecology* 13: 3239–3255. <https://doi.org/10.1111/j.1365-294X.2004.02296.x>
- Paquin P, Dupérré N (2009) A first step towards the revision of *Cicurina*: redescription of type specimens of 60 troglobitic species of the subgenus *Cicurella* (Araneae: Dictynidae), and a first visual assessment of their distribution. *Zootaxa* 2002: 1–67.
- Paquin P, Dupérré N, Cokendolpher JC, White K, Hedin M (2008) The fundamental importance of taxonomy in conservation biology: the case of the eyeless *Cicurina bandida* (Araneae: Dictynidae) of central Texas, including new synonyms and the description of the male of the species. *Invertebrate Systematics* 22: 139–149. <https://doi.org/10.1071/IS07044>
- Ruane S, Austin CC (2017) Phylogenomics using formalin-fixed and 100+ year-old intractable natural history specimens. *Molecular Ecology Resources* 17: 1003–1008. <https://doi.org/10.1111/1755-0998.12655>
- Satler JD, Carstens BC, Hedin M (2013) Multilocus species delimitation in a complex of morphologically conserved trapdoor spiders (Mygalomorphae, Antrodiaetidae, *Aliatypus*). *Systematic Biology* 62: 805–823. <https://doi.org/10.1093/sysbio/syt041>
- Service [U.S. Fish and Wildlife Service] (2000) Endangered and threatened wildlife and plants; final rule to list nine Bexar County, Texas invertebrate species as endangered. *Federal Register* 65: 81419–81433.
- Service [U.S. Fish and Wildlife Service] (2011) Bexar County Karst Invertebrates Recovery Plan. U.S. Fish and Wildlife Service, Albuquerque, NM.
- Smith BT, Harvey MG, Faircloth BC, Glenn TC, Brumfield RT (2014) Target capture and massively parallel sequencing of ultraconserved elements (UCEs) for comparative studies at shallow evolutionary time scales. *Systematic Biology* 63: 83–95. <https://doi.org/10.1093/sysbio/syt061>
- Stamatakis A (2014) RAxML version 8: a tool for phylogenetic analysis and post-analysis of large phylogenies. *Bioinformatics* 30: 1312–1313. <https://doi.org/10.1093/bioinformatics/btu033>
- Starrett J, Derkarabetian S, Hedin M, Bryson Jr RW, McCormack JE, Faircloth BC (2017) High phylogenetic utility of an Ultraconserved element probe set designed for Arachnida. *Molecular Ecology Resources* 17: 812–823. <https://doi.org/10.1111/1755-0998.12621>

- Swofford DL (2003) PAUP*: phylogenetic analysis using parsimony, version 4.0 b10.
- Talavera G, Castresana J (2007) Improvement of phylogenies after removing divergent and ambiguously aligned blocks from protein sequence alignments. *Systematic Biology* 56: 564–577. <https://doi.org/10.1080/10635150701472164>
- Tin MM-Y, Economo EP, Mikheyev AS (2014) Sequencing degraded DNA from non-destructively sampled museum specimens for RAD-Tagging and low-coverage shotgun phylogenetics. *PLoS ONE* 9(5): e96793. <https://doi.org/10.1371/journal.pone.0096793>
- World Spider Catalog (2018) World Spider Catalog (version 19.0). Natural History Museum Bern. <http://wsc.nmbe.ch> [accessed on 13 March 2018]
- Zarza E, Faircloth BC, Tsai W, Bryson Jr R, Klicka J, McCormack JE (2016) Hidden histories of gene flow in highland birds revealed with genomic markers. *Molecular Ecology* 25: 5144–5157. <https://doi.org/10.1111/mec.13813>
- Zerbino DR, Birney E (2008) Velvet: Algorithms for de novo short read assembly using de Bruijn graphs. *Genome Research* 18: 821–829. <https://doi.org/10.1101/gr.074492.107>

Supplementary material 1

Figure S1. SVD Quartets, 50 & 70% matrices

Authors: Marshal Hedin, Shahan Derkarabetian, Jennifer Blair, Pierre Paquin

Data type: image

Copyright notice: This dataset is made available under the Open Database License (<http://opendatacommons.org/licenses/odbl/1.0/>). The Open Database License (ODbL) is a license agreement intended to allow users to freely share, modify, and use this Dataset while maintaining this same freedom for others, provided that the original source and author(s) are credited.

Link: <https://doi.org/10.3897/zookeys.769.25814.suppl1>

Supplementary material 2

Figure S2. ASTRAL, 50 & 70% matrices

Authors: Marshal Hedin, Shahan Derkarabetian, Jennifer Blair, Pierre Paquin

Data type: image

Copyright notice: This dataset is made available under the Open Database License (<http://opendatacommons.org/licenses/odbl/1.0/>). The Open Database License (ODbL) is a license agreement intended to allow users to freely share, modify, and use this Dataset while maintaining this same freedom for others, provided that the original source and author(s) are credited.

Link: <https://doi.org/10.3897/zookeys.769.25814.suppl2>

Supplementary material 3

Figure S3. RAxML, 50% matrix

Authors: Marshal Hedin, Shahan Derkarabetian, Jennifer Blair, Pierre Paquin

Data type: image

Copyright notice: This dataset is made available under the Open Database License (<http://opendatacommons.org/licenses/odbl/1.0/>). The Open Database License (ODbL) is a license agreement intended to allow users to freely share, modify, and use this Dataset while maintaining this same freedom for others, provided that the original source and author(s) are credited.

Link: <https://doi.org/10.3897/zookeys.769.25814.suppl3>

Supplementary material 4

Figure S4. Relationships within *C. baronia* + *C. bullis* - *C. neovespera* clade

Authors: Marshal Hedin, Shahan Derkarabetian, Jennifer Blair, Pierre Paquin

Data type: image

Copyright notice: This dataset is made available under the Open Database License (<http://opendatacommons.org/licenses/odbl/1.0/>). The Open Database License (ODbL) is a license agreement intended to allow users to freely share, modify, and use this Dataset while maintaining this same freedom for others, provided that the original source and author(s) are credited.

Link: <https://doi.org/10.3897/zookeys.769.25814.suppl4>

Supplementary material 5

Table S1. Voucher and genetic information

Authors: Marshal Hedin, Shahan Derkarabetian, Jennifer Blair, Pierre Paquin

Data type: occurrence, genomic

Copyright notice: This dataset is made available under the Open Database License (<http://opendatacommons.org/licenses/odbl/1.0/>). The Open Database License (ODbL) is a license agreement intended to allow users to freely share, modify, and use this Dataset while maintaining this same freedom for others, provided that the original source and author(s) are credited.

Link: <https://doi.org/10.3897/zookeys.769.25814.suppl5>

Supplementary material 6**Table S2. Troglomorphy Index data**

Authors: Marshal Hedin, Shahan Derkarabetian, Jennifer Blair, Pierre Paquin

Data type: morphological

Copyright notice: This dataset is made available under the Open Database License (<http://opendatacommons.org/licenses/odbl/1.0/>). The Open Database License (ODbL) is a license agreement intended to allow users to freely share, modify, and use this Dataset while maintaining this same freedom for others, provided that the original source and author(s) are credited.

Link: <https://doi.org/10.3897/zookeys.769.25814.suppl6>

A new species of deep-water spider crab of the genus *Paramaya* De Haan, 1837 from the Bay of Bengal, India (Crustacea, Brachyura, Majidae)

Peter K. L. Ng¹, M. Prema², S. Ravichandran²

1 Lee Kong Chian Natural History Museum, 2 Conservatory Drive, National University of Singapore, Singapore 117377, Republic of Singapore **2** Centre of Advanced Study in Marine Biology, Annamalai University, Parangipettai 608 502, India

Corresponding author: Peter K. L. Ng (peterng@nus.edu.sg)

Academic editor: I. Wehrtmann | Received 24 April 2018 | Accepted 11 June 2018 | Published 26 June 2018

<http://zoobank.org/B403C281-6BE4-40D1-972D-DC351B7ACD44>

Citation: Ng PKL, Prema M, Ravichandran S (2018) A new species of deep-water spider crab of the genus *Paramaya* De Haan, 1837 from the Bay of Bengal, India (Crustacea, Brachyura, Majidae). ZooKeys 769: 77–88. <https://doi.org/10.3897/zookeys.769.26152>

Abstract

The identity of the majid species of *Paramaya* De Haan, 1837, in the Indian Ocean is clarified with the collection of fresh specimens from the Bay of Bengal. Previously identified as *P. spinigera* (De Haan, 1837) which is known only from Japan, Taiwan, and Korea, the material from eastern India is here referred to a new species, *P. mulli* sp. n. The new species can easily be distinguished from all congeners by its relatively shorter pseudorostral and carapace spines, more swollen branchial regions, distinctly granulated male thoracic sternum, and the G1 is not prominently curved with the dorsal projection on the sub distal part short and the tip rounded.

Keywords

deep-water, Indian Ocean, Majoidea, new species, taxonomy, spider crab

Introduction

Ng and Richer de Forges (2015) revised the majid genus *Maja* Lamarck, 1801, and recognised *Paramaya* De Haan, 1837, as a valid taxon from the Indo-West Pacific. Three species of *Paramaya* are currently known: *P. coccinea* Ng & Richer de Forges, 2015 [Vanuatu], *P. ouch* Ng & Richer de Forges, 2015 [Philippines], and *P. spinigera* (De Haan, 1837) [Japan, Taiwan, and Korea] (Ng and Richer de Forges 2015; Ko and Lee 2015). There is a record of *Paramaya spinigera* from Beluchistan in Pakistan in the Indian Ocean by Alcock (1895) and Alcock and Anderson (1898) with Ng and Richer de Forges (2015) recording a specimen from Sri Lanka. None of these specimens, however, could be examined, and Ng and Richer de Forges (2015: 156) noted that “although on the basis of geography, they are probably different species [from the Pacific ones]. For the moment, we do not know their precise identities.”

Collections from deep-water ports in India have obtained numerous interesting new brachyurans over the last few years (Ng and Kumar 2015, 2016, Mendoza and Suvarna Devi 2017, Ng et al. 2017a–c, Prema et al. 2018; Ng et al. 2018) and pair of *Paramaya* were recently obtained from Pazhayar, near Chennai in eastern India. These specimens now allow resolving the identity of the Indian Ocean *Paramaya*. Not surprisingly, they represent a new species, and though superficially similar to *Paramaya spinigera* s. str., it nevertheless differs from congeners in various carapace features, ambulatory leg proportions as well as the structures of the male thoracic sternum and gonopods. They are here described as *Paramaya mulli* sp. n.

Material and methods

The terminology used in this paper follows Ng and Richer de Forges (2015) and Davie et al. (2015), and the measurements provided (in millimetres) are of the post-pseudorostral carapace length (from the base of spines to the posterior carapace margin, not including median posterior spines) against the maximum carapace width, respectively. Specimens examined are deposited in the Centre of Advanced Study in Marine Biology, Annamalai University (CASAU), Parangipettai, Tamil Nadu, India; and the Zoological Reference Collection of the Lee Kong Chian Natural History Museum (ZRC), National University of Singapore.

Systematics

Family Majidae Samouelle, 1819

Genus *Paramaya* De Haan, 1837

Type species. *Pisa (Paramaya) spinigera* De Haan, 1837; by monotypy.

***Paramaya mulli* sp. n.**

<http://zoobank.org/694A5779-FC41-4105-B536-9FB7DC23D65D>

Figs 1, 2A–C, 3A–C, 4A, B, 5A–D, H, 6, 7

Maia spinigera – Alcock 1895: 239; Alcock and Anderson 1898: pl. 34, fig. 3.

“*Maja spinigera*” – Ng and Richer de Forges 2015: 156, fig. 22B–D.

Non *Pisa* (*Paramaya*) *spinigera* De Haan, 1837.

Material examined. Holotype: male (70.4 × 61.4 mm) (CASAU), Pazhayar fish landing centre, facing Bay of Bengal, Tamil Nadu, India, 11°21'11.5"N, 79°45'26.3"E, from trawls, coll. M. Prema and S. Ravichandran, 7 February 2018. Paratype: 1 female (40.0 × 33.5 mm) (CASAU), same data as holotype.

Comparative material examined. *Paramaya spinigera* (De Haan, 1837): 7 males (85.0 × 66.4 mm, 78.2 × 62.1 mm, 73.6 × 55.3 mm, 68.3 × 53.4 mm, 73.8 × 58.4 mm, 62.8 × 49.0 mm, 72.8 × 57.3 mm), 1 ovigerous female (63.0 × 48.6 mm) (ZRC 1999.738), Longtong, near Keelung, northern Taiwan, in tangle nets for lobsters, coll. S-H Wu, May 1999. For other material of *Paramaya* species, see Ng and Richer de Forges (2015).

Diagnosis. Pseudorostral horns relatively short (Figs 2A, 3A, B); hepatic, lateral and branchial spines long; median row with 5 spines: 3 gastric, 1 cardiac, 1 intestinal; 2 spines on posterior carapace margin (Figs 2A, 3A); adult branchial region distinctly swollen (Fig. 3A, C); intercalated tooth on carapace relatively broad (Figs 3B, 4A, B); epistome quadrate (Fig. 5A, B); surface of thoracic sternum not prominently setose, with numerous prominent rounded granules (Figs 5C, 6B); chela of adult male with distinct carina on dorsal and ventral margins (Figs 2A, 6D); ambulatory meri in adult males relatively slender, long (Figs 2A, 5D); G1 gently curved, dorsal projection on the sub distal part low, tip distinctly rounded (Fig. 7A–C).

Colour. Freshly obtained specimens have the dorsal surfaces orangish-red, with red and white bands on ambulatory legs; chelipeds yellowish-orange with white fingers; ventral surfaces white with patches of orange (Fig. 1).

Etymology. The species is named after the famous Mulli plant in Tamil mythology, from the classic poetic work *Kurunthogai*. Mulli is a coastal plant (*Spinifex littoreus* (Burm.f.) Merr., family Poaceae) with very sharp spines (mulli is the Tamil word for spiny), a character shared with the present species. The name is used as a noun in apposition.

Remarks. Compared to *P. spinigera*, the branchial region of adult male *P. mulli* sp. n. is more swollen (Fig. 3A, C) (versus gently convex in *P. spinigera*; Fig. 3D, F); the intercalated tooth on the carapace is relatively broader (Figs 3B, 4A, B) (versus more acutely triangular in *P. spinigera*; Figs 3E, 4C, D); the epistome is more quadrate (Fig. 5A, B) (versus more transversely rectangular in *P. spinigera*; Fig. 5E, F); the surface of the male thoracic sternum, especially the areas adjacent to the sternopleonal cavity is distinctly granulated with scattered setae (Fig. 5C) (versus surfaces weakly granulate with dense setae in *P. spinigera*; Fig. 5G); and the G1 has the dorsal projection on the subdistal part relatively small with the tip more prominently rounded (Fig. 7A–C)

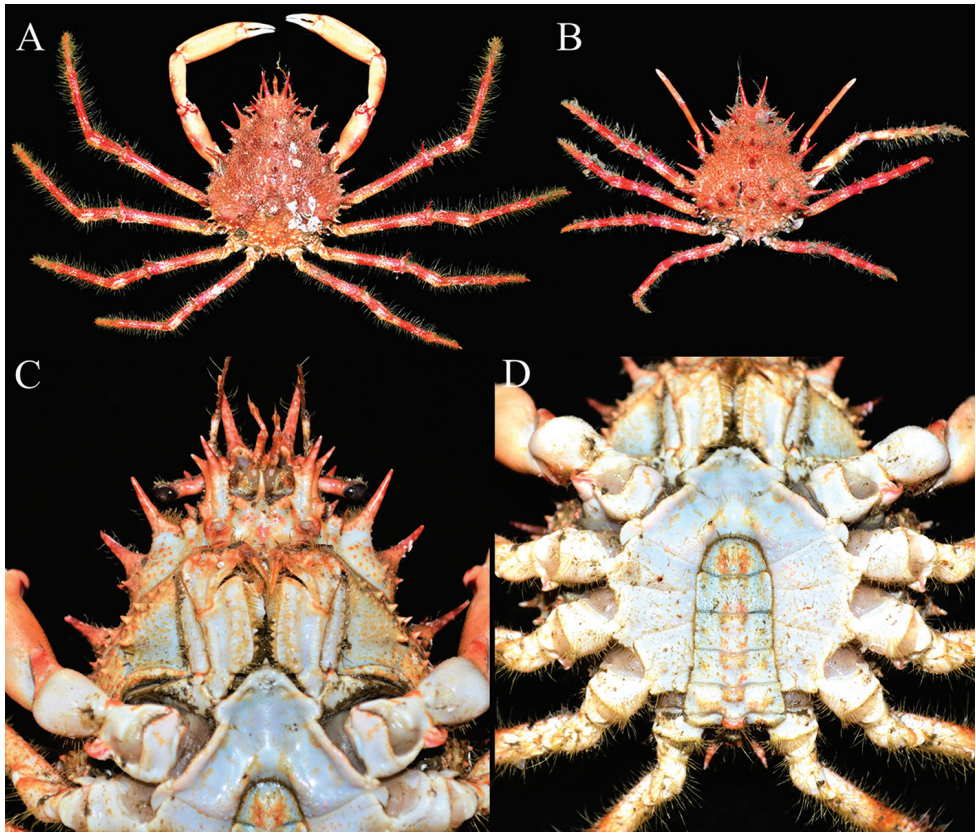


Figure 1. Colours in life. *Paramaya mulli* sp. n. **A, C, D** holotype male (70.4 × 61.4 mm) (CASAU), India **B** paratype female (40.0 × 33.5 mm) (CASAU), India **A, B** overall habitus **C** buccal cavity, epistome, antennae and antennules **D** thoracic sternum and pleon.

(versus dorsal projection on the subdistal part more developed with the tip gently tapering in *P. spinigera*; Ng and Richer de Forges 2015: fig. 23A–C).

There is variation in the proportions of the ambulatory legs of *Paramaya* species. In the series of specimens of *P. spinigera* on hand, females generally have relatively shorter ambulatory legs compared to males. In addition, for each sex, smaller specimens have proportionately shorter and stouter legs (Fig. 5I) compared to larger ones (Fig. 5J). When comparing the holotype male *P. mulli* sp. n. (70.4 × 61.4 mm, CASAU) with a similar size male of *P. spinigera* from Taiwan (73.6 × 55.3 mm, ZRC 1999.738), the merus, propodus and dactylus of *P. mulli* sp. n. (Fig. 5D) is significantly more slender and longer than that of *P. spinigera* (Fig. 5I). In larger male specimens of *P. spinigera* from Taiwan (85.0 × 66.4 mm, ZRC 1999.738), the merus is proportionately longer but is still relatively stouter (Fig. 5J). Females of both species have relatively shorter and stouter ambulatory legs compared to males (Fig. 5H).

Ng and Richer de Forges (2015: 156) noted that the specimen mentioned and figured by Alcock (1895) and Alcock and Anderson (1898) as “*P. spinigera*” has short

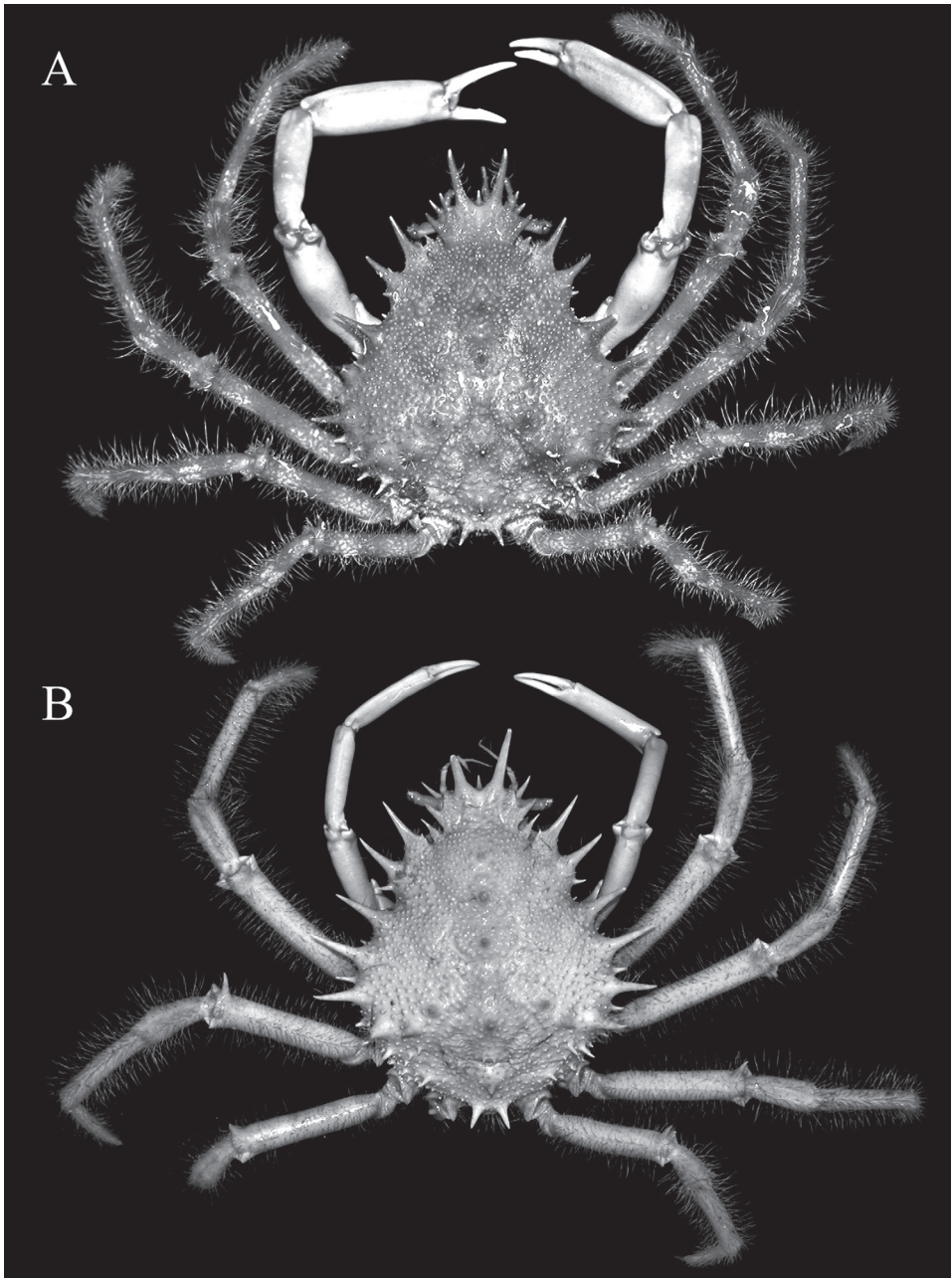


Figure 2. Overall habitus **A** *Paramaya mulli* sp. n., holotype male (70.4 × 61.4 mm) (CASAU), India
B *P. spinigera* (De Haan, 1837), male (73.6 × 55.3 mm) (ZRC 1999.738), Taiwan.

ambulatory meri, but this is probably because this specimen was small; and the larger specimen from Sri Lanka they examined a photograph has proportionately longer ambulatory legs. As discussed above, the proportions of the ambulatory meri is clearly

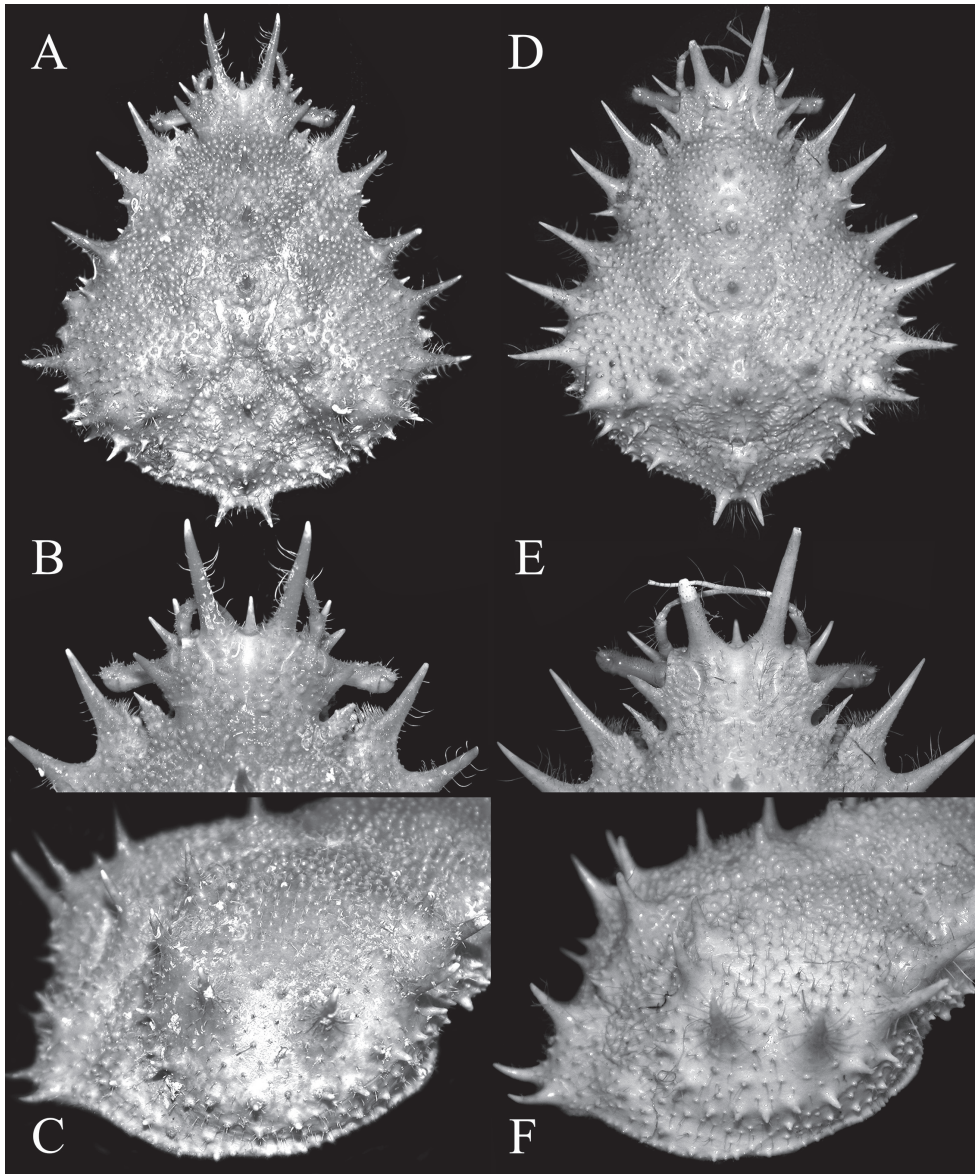


Figure 3. **A–C** *Paramaya mulli* sp. n., holotype male (70.4 × 61.4 mm) (CASAU), India **D–F** *P. spinigera* (De Haan, 1837), male (73.6 × 55.3 mm) (ZRC 1999.738), Taiwan **A, D** dorsal view of carapace **B, E** frontal part of carapace **C, F** lateral view of branchial region of carapace.

correlated with size. Noteworthy is that the Sri Lankan specimen also has relatively more inflated branchial regions, and as such, is almost certainly conspecific with what is described here as *P. mulli* sp. n.

The distinctly granulated thoracic sternum of *P. mulli* sp. n. (Fig. 5C) allies the species with *P. ouch* (Ng and Richer de Forges 2015: fig. 50B), but in *P. ouch*, the

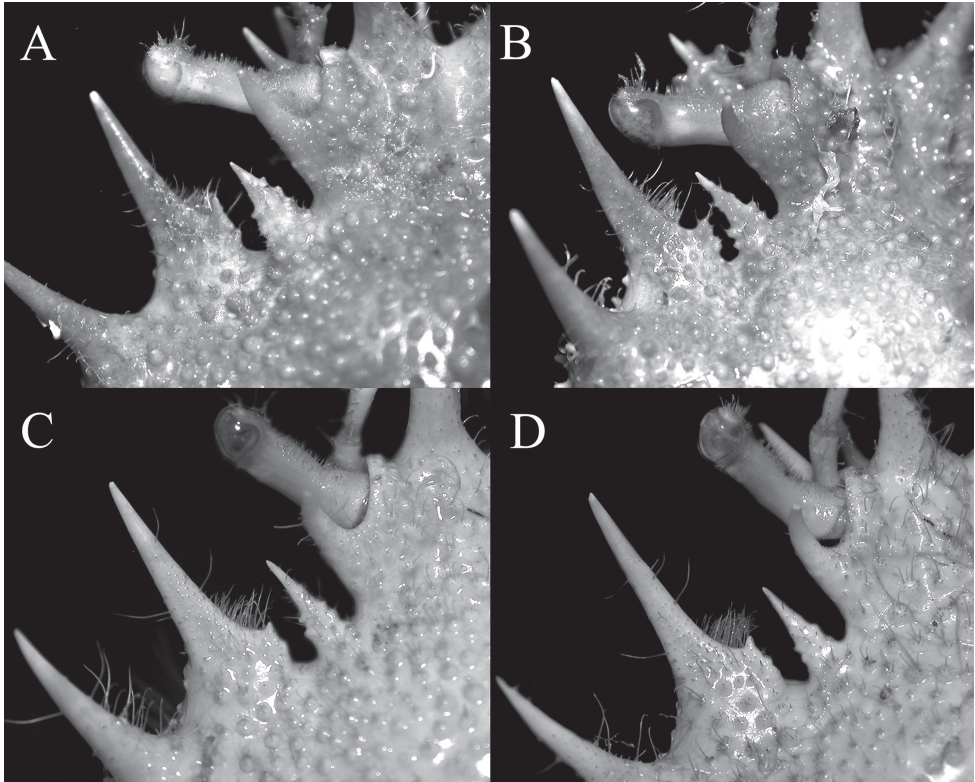


Figure 4. Intercalated spine **A** *Paramaya mulli* sp. n., holotype male (70.4 × 61.4 mm) (CASAU), India **B** *P. mulli* sp. n., paratype female (40.0 × 33.5 mm) (CASAU), India **C** *P. spinigera* (De Haan, 1837), male (73.6 × 55.3 mm) (ZRC 1999.738), Taiwan **D** *P. spinigera* (De Haan, 1837), male (85.0 × 66.4 mm) (ZRC 1999.738), Taiwan.

branchial region is not distinctly swollen, and the pseudorostral and carapace spines are proportionately longer across all size ranges in both sexes (cf. Ng and Richer de Forges 2015: figs 21E, F, 37B) (versus branchial regions more swollen and the spines are proportionately shorter in *P. mulli* sp. n.; Figs 2A, 3A–C, 6E). In addition, the distal part of the G1 in *P. ouch* is more strongly curved (Ng and Richer de Forges 2015: fig. 23D) with the dorsal projection on the subdistal part prominent and the tip is relatively more angular (Ng and Richer de Forges 2015: fig. 23E, F) (versus distal part of G1 less curved with the dorsal projection low and tip rounded in *P. mulli* sp. n.; Fig. 7A–C). Compared to *P. mulli* sp. n., *P. coccinea* has proportionately longer pseudorostral and carapace spines with the branchial region not distinctly swollen (Ng and Richer de Forges 2015: figs 22A, 37C), the male thoracic sternum is almost smooth with the granules low (Ng and Richer de Forges 2015: fig. 50C) and the dorsal projection on the subdistal part of the G1 is prominent with the tip relatively more angular (Ng and Richer de Forges 2015: fig. 23H, I) (cf. pseudorostral and carapace spines proportionately shorter, the male thoracic sternum is distinctly granulated and the dorsal

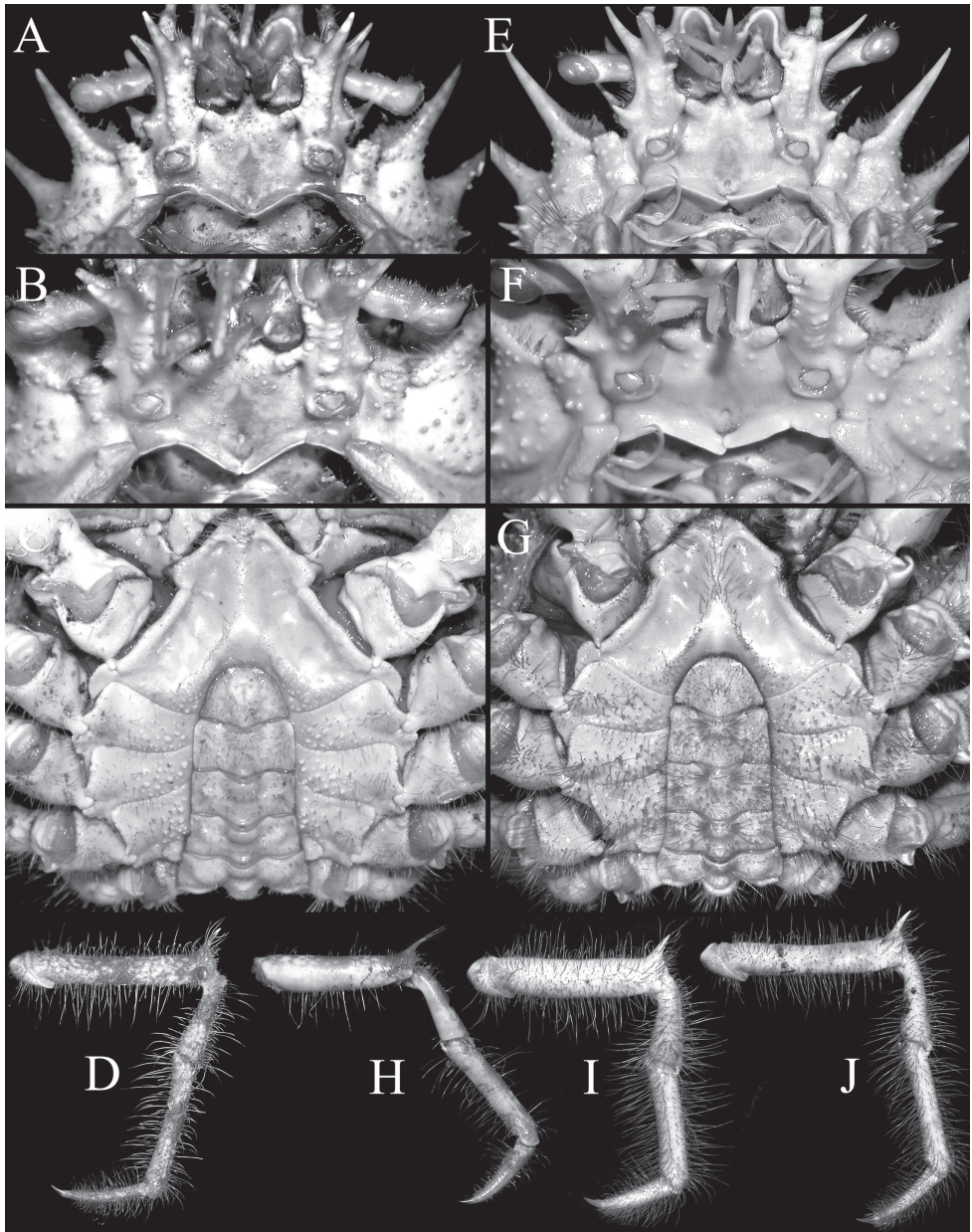


Figure 5. **A–D** *Paramaya mulli* sp. n., holotype male (70.4 × 61.4 mm) (CASAU), India **H** *P. mulli* sp. n., paratype female (40.0 × 33.5 mm) (CASAU), India **E–G, I** *P. spinigera* (De Haan, 1837), male (73.6 × 55.3 mm) (ZRC 1999.738), Taiwan **J** *P. spinigera* (De Haan, 1837), male (85.0 × 66.4 mm) (ZRC 1999.738), Taiwan **A, B, E, F** epistome, basal antennal article and antennules **C, G** thoracic sternum and pleon **D–J** right fourth ambulatory leg.

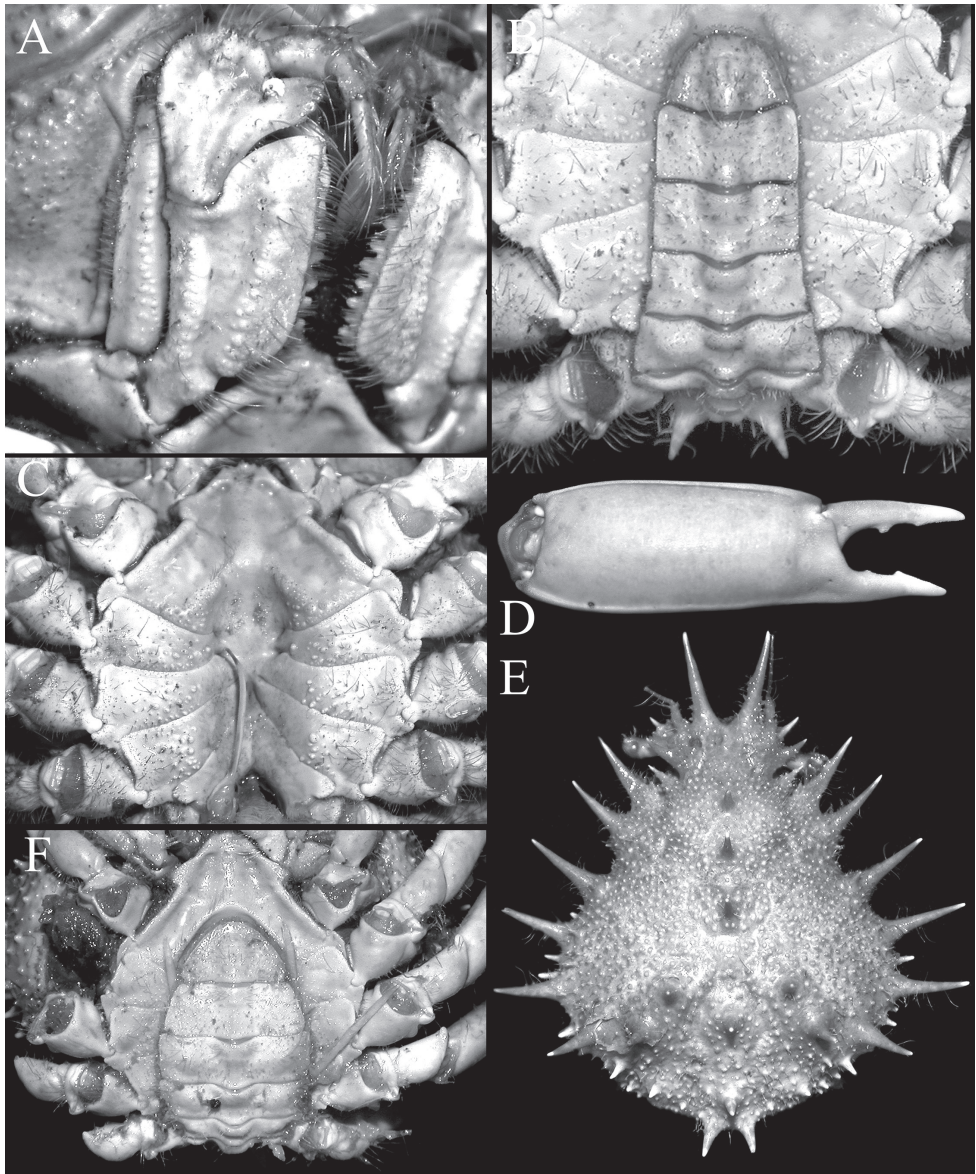


Figure 6. **A–D** *Paramaya mulli* sp. n., holotype male (70.4 × 61.4 mm) (CASAU), India **E, F** *P. mulli* sp. n., paratype female (40.0 × 33.5 mm) (CASAU), India **A** right third maxilliped **B** thoracic sternum and pleon; **C**, sternopleonal cavity **D** outer view of right chela **E** dorsal view of carapace **F** thoracic sternum and pleon.

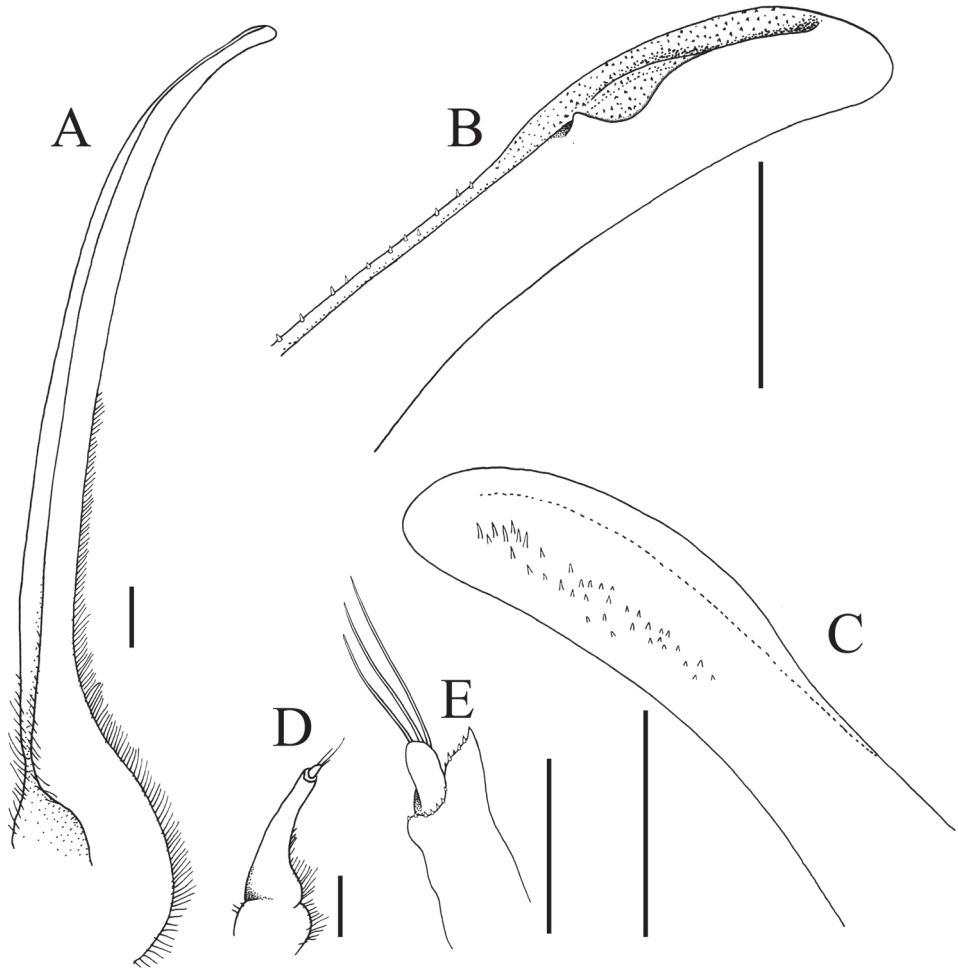


Figure 7. *Paramaya mulli* sp. n., holotype male (70.4 × 61.4 mm) (CASAU), India **A** left G1 (ventral view) **B** distal part of left G1 (ventral view) **C** distal part of left G1 (dorsal view) **D** left G2 **E** distal part of left G2. Scale bars: **A, D** 1.0 mm **B, C, E** 0.5 mm.

projection on the G1 subdistal part is low with the tip rounded; Figs 2A, 3A–C, 5C, 6E, 7A–C). In addition, even though the holotype male and only known specimen of *P. coccinea* is about the same size as the holotype male of *P. mulli* sp. n., the ambulatory meri are proportionately much longer (cf. Ng and Richer de Forges 2015: figs 22A, 70B) (versus distinctly shorter in *P. mulli* sp. n.; Figs 2A, 5D).

Like other *Paramaya* species, the preferred habitat of *P. mulli* sp. n. is probably relatively steep and rocky areas that are difficult to sample except with tangle nets (see Ng et al. 2009, Mendoza et al. 2010). As such, normal fishery operations using trawls are less likely to obtain them and could explain their apparent rarity in Indian waters.

Acknowledgements

The second and third authors are grateful to UGC - BSR (BININ00449691) and DBT, Government of India (BT/PR5769/AAQ/3/597/2012) for financial support. The authors also thank Mr. P. Vigneshwaran for help in obtaining specimens in the field. The authors are grateful to Bertrand Richer de Forges and Ingo Wehrtmann for reading the manuscript and their many helpful comments.

References

- Alcock A (1895) Materials for a carcinological fauna of India, 1. The Brachyura Oxyrhyncha. *Journal of the Asiatic Society of Bengal, Calcutta*, 64: 157–291. [pls 3–5]
- Alcock A, Anderson ARS (1898) Illustrations of the Zoology of the Royal Indian Marine Survey Ship Investigator, under the command of Commander T. H. Heming, R.N. Fishes.-Part V, Plates XVIII–XXIV. Crustacea.-Part VI, Plates XXXIII–XXXV. Mollusca.-Part H, Plates VII–VIII. Published under the Authority of Captain W. S. Goodridge, R.N., Director of the Royal Indian Marine, Calcutta.
- Davie PJF, Guinot D, Ng PKL (2015) Anatomy and functional morphology of Brachyura. In: Castro P, Davie PJF, Guinot D, Schram FR, von Vaupel Klein JC (Eds) *Treatise on Zoology – Anatomy, Taxonomy, Biology. The Crustacea. Volume 9C–I. Decapoda: Brachyura* (Part 1), 11–163. https://doi.org/10.1163/9789004190832_004
- Ko H-S, Lee S-H (2015) *Invertebrate Fauna of Korea Volume 21, Number 41. Arthropoda: Crustacea: Decapoda: Brachyura: Majoidea Crabs and Zoeas IV*. National Institute of Biological Resources, Ministry of Environment, Korea, 78 pp.
- Mendoza JCE, Suvarna Devi S (2017) A new species of the swimming crab genus, *Laleonectes* Manning & Chace, 1990 (Crustacea: Brachyura: Portunidae), from the western Indian Ocean. *Zootaxa* 4323(2): 219–228. <https://doi.org/10.11646/zootaxa.4323.2.5>
- Mendoza JCE, Naruse T, Tan S-H, Chan T-Y, Richer de Forges B, Ng PKL (2010) Case studies on decapod crustaceans from the Philippines reveal deep, steep underwater slopes as prime habitats for ‘rare’ species. *Biodiversity and Conservation* 19(2): 575–586. <https://doi.org/10.1007/s10531-009-9744-x>
- Ng PKL, Kumar AB (2015) The species of *Moloha* Barnard, 1946, from the western Indian Ocean, with the description of a new species from India (Crustacea: Brachyura: Homolidae). *European Journal of Taxonomy* 166: 1–25. <https://doi.org/10.5852/ejt.2015.166>
- Ng PKL, Kumar AB (2016) *Carcinoplax fasciata*, a new species of deep-water goneplacid crab from southwestern India (Crustacea: Decapoda: Brachyura: Goneplacoidea). *Zootaxa* 4147(2): 192–200. <https://doi.org/10.11646/zootaxa.4147.2.6>
- Ng PKL, Mendoza JCE, Manuel-Santos M (2009) Tangle net fishing, an indigenous method used in Balicasag Island, central Philippines. *Raffles Bulletin of Zoology, Supplement* 20: 39–46.
- Ng PKL, Prema M, Tan SH, Ravichandran S (2017a) The taxonomy of two poorly known species of elbow crabs, *Daldorfia spinosissima* (A. Milne-Edwards, 1862), and *D. triangula-*

- ris* Sakai, 1974 (Brachyura, Parthenopidae). *Crustaceana* 90(14): 1779–1791. <https://doi.org/10.1163/15685403-00003721>
- Ng PKL, Ravinesh R, Ravichandran S (2017b) A new large oregoniid spider crab of the genus *Pleistacantha* Miers, 1879, from the Bay of Bengal, India (Crustacea, Brachyura, Majoidea). *Zookeys* 716: 127–146. <https://doi.org/10.3897/zookeys.716.21349>
- Ng PKL, Suvarna Devi S, Kumar AB (2017c) *Typhlocarcinus kerala*, a new species of rhizopine crab from southwestern India, and the identity of *T. craterifer* Rathbun, 1914 (Crustacea: Brachyura: Pilumnidae). *Zootaxa* 4272(1): 131–141. <https://doi.org/10.11646/zootaxa.4272.1.7>
- Ng PKL, Suvarna Devi S, Kumar AB (2018) The genus *Parilia* Wood-Mason, in Wood-Mason & Alcock, 1891, with description of a new species and establishment of a new genus for *P. tuberculata* Sakai, 1961 (Crustacea, Brachyura, Leucosiidae). *Raffles Bulletin of Zoology* 66: 300–319.
- Ng PKL, Richer de Forges B (2015) Revision of the spider crab genus *Maja* Lamarck, 1801 (Crustacea: Brachyura: Majoidea: Majidae), with descriptions of seven new genera and 17 new species from the Atlantic and Indo-West Pacific. *Raffles Bulletin of Zoology* 63: 110–225.
- Prema M, Ravichandran S, Ng PKL (2018) Redescription of *Parilia alcocki* Wood-Mason, in Wood-Mason & Alcock, 1891 (Decapoda, Brachyura, Leucosiidae) from southeast India. *Zootaxa* 4378(1): 111–120. <https://doi.org/10.11646/zootaxa.4378.1.7>

Two new species of crayfish of the genus *Cherax* from Indonesian New Guinea (Crustacea, Decapoda, Parastacidae)

Christian Lukhaup¹, Rury Eprilurahman², Thomas von Rintelen³

1 Waldstrasse 5a, 66999 Hinterweidenthal, Germany **2** Animal Systematics Laboratory, Faculty of Biology, Universitas Gadjah Mada Jl. Teknika Selatan, Sekip Utara Yogyakarta 55281, Indonesia **3** Museum für Naturkunde – Leibniz Institute for Evolution and Biodiversity Science, Invalidenstrasse 43, 10115 Berlin, Germany

Corresponding author: *Christian Lukhaup* (craykeeper@gmx.de)

Academic editor: *S. De Grave* | Received 23 April 2018 | Accepted 7 June 2018 | Published 26 June 2018

<http://zoobank.org/1B07A81E-7CEE-4865-98FD-6E0D7AD548BA>

Citation: Lukhaup C, Eprilurahman R, von Rintelen T (2018) Two new species of crayfish of the genus *Cherax* from Indonesian New Guinea (Crustacea, Decapoda, Parastacidae). *ZooKeys* 769: 89–116. <https://doi.org/10.3897/zookeys.769.26095>

Abstract

Two new species of the genus *Cherax* are described and illustrated. *Cherax mosessalossa* **sp. n.**, endemic to the Klademak Creek drainage in Sorong, in the western part of the Kepala Burung (Vogelkop) peninsula, West Papua, Indonesia, is described, figured and compared with its closest relatives, *Cherax misolicus* Holthuis, 1949 and *Cherax warsamsonicus*. The new species may be easily distinguished from both by the shape of the rostrum, the shape of the chelae, the presence of five cervical spines, the shape of the scaphocerite, and short scattered hairs on the carapace. *Cherax alyciae* **sp. n.**, endemic to creeks in the Digul River drainage in the eastern part of the Boven Digoel Regency, Papua, Indonesia, is described, figured, and compared with its closest relative, *Cherax peknyi* Lukhaup & Herbert, 2008. The new species may be easily distinguished from *Cherax peknyi* by the shape of the chelae, presence of a soft patch on the chelae of the males, and colouration. A molecular phylogeny based on two mitochondrial gene fragments, 16S and COI, supports the morphology-based description of the two new species, which can also be clearly distinguished by sequence differences.

Keywords

freshwater, morphology, molecular phylogeny, New Guinea, taxonomy

Introduction

The crayfishes of the island of New Guinea were extensively studied by Holthuis (1949, 1956, 1958, 1982, 1986, 1996), with additions by Lukhaup and Pekny (2006, 2008a), Lukhaup and Herbert (2008), Lukhaup (2015), Lukhaup et al. (2015), Patoka et al. (2015), Lukhaup et al. (2017) and Patoka et al. (2017).

In January 2016 the first author visited Sorong Regency and South Sorong Regency, West Papua, Indonesia, to clarify the distribution of some crayfish species present in the pet trade. During the stay in Sorong, we also had the chance to visit a creek at the edge of the city where our guide, Marten Luter Salossa, showed us a *Cherax* species. In the present contribution, this species is described as new to science. *Cherax mosessalossa* sp. n. is genetically and morphologically most similar to *Cherax misolicus* Holthuis, 1949 endemic to the Island of Misool, one of four major islands in the Raja Ampat Islands in West Papua, Indonesia and to *Cherax warsamsonicus* endemic to the Warsamson River drainage, in the western part of the Kepala Burung (Vogelkop) peninsula.

Cherax mosessalossa sp. n. may be easily distinguished from both by using sequence divergence, by colouration and pattern of live individuals, by the shape of the chelae, the shape of rostrum, and presence of setae on the carapace in *C. mosessalossa* which is absent in *C. misolicus* and *C. warsamsonicus*. *Cherax alyciae* sp. n. is genetically and morphologically most similar to *Cherax peknyi* Lukhaup & Herbert, 2008, from Tamu Creek, in the Fly River drainage, Papua New Guinea. *Cherax alyciae* sp. n. may be easily distinguished from *Cherax peknyi* by colouration and pattern of live individuals, by the shape of the chelae and a soft patch present on the chelae of the males, the shape of rostrum, fewer setae on the ventral side of the chelae, and by using sequence divergence.

Materials and methods

Samples of *Cherax mosessalossa* sp. n., *Cherax alyciae* sp. n., and *C. peknyi* were collected from creeks in West Papua and Papua provinces (Table 1). Holotypes and allotypes were photographed and kept alive in indoor tanks until samples were obtained for DNA analysis. After this procedure, the animals were preserved in 70% ethanol. Morphometric parameters of all individuals were taken using an electronic digital caliper with an accuracy of 0.1 mm. For the molecular analyses, sequences from an additional ten species of *Cherax* and from two other parastacid genera used as outgroup were downloaded from GenBank (see Table 1).

All material has been deposited at the Museum Zoologicum Bogoriense (= Bidang Zoologi) Research Centre for Biology (= Pusat Penelitian Biologi), Indonesian Institute of Sciences (= LIPI), Jalan Raya Jakarta-Bogor Km 46 Cibinong 16911, Indonesia.

DNA was purified from approximately 2 mm³ of muscle tissue with a Qiagen BioSprint 96 using the manufacturer's protocol. Polymerase chain reaction (PCR) was used to amplify two mitochondrial gene fragments, a ~535 bp region of the 16S ribosomal RNA gene (16S) using primers 1471 and 1472 (Crandall and Fitzpatrick 1996)

Table 1. Material studied with GenBank accession numbers. Sequences of species represented by more than one sequence are listed consecutively as labelled in Figure 19.

| Species/sample | Location | GenBank acc. nos | |
|-------------------------------|---|------------------|----------|
| | | COI | 16S |
| <i>C. boesemani</i> | Ajamaru Lake, Papua Barat; 1°17'19.97"S, 132°14'49.14"E; January 23, 2016 | KY654084 | KY654089 |
| | | KY654085 | KY654090 |
| <i>C. alyciae</i> sp. n. | Unnamed creek, Boven Digoel Regency, West Papua, Indonesia; December 7, 2016 | MH457597 | MH457588 |
| | | MH457599 | MH457590 |
| | | MH457598 | MH457589 |
| <i>C. communis</i> | Lake Paniai | – | MH457602 |
| <i>C. gherardiae</i> | Pet trade | KU821417 | KU821417 |
| <i>C. holthuisi</i> | Papua Barat | KU821419 | KU821433 |
| <i>C. misolicus</i> | Misool Island, South of Papua Barat (Leiden Museum) | – | KJ920813 |
| <i>C. monticola</i> | Baliem River, Wamena, Papua | KF649851 | KF649851 |
| | | – | KJ920818 |
| <i>C. mosessalossa</i> sp. n. | Klademak Creek, Sorong City 0°52'23.59"S, 131°16'24.40"E; January 26, 2016 | MH457602 | MH457594 |
| | | MH457602 | MH457595 |
| <i>C. paniaicus</i> | Lake Tage, Papua (Field collection) | KJ950528 | KJ920830 |
| <i>C. peknyi</i> | Unnamed Creek, tributary of Fly River, Papua New Guinea | MH457600 | MH457591 |
| | | MH457601 | MH457592 |
| | | MH457604 | MH457596 |
| <i>C. pulcher</i> | Hoa Creek (Teminabuan), Papua Barat; 1°28'32.73"S, 132°3'54.94"E; January 23, 2016 | KY654083 | KY654088 |
| <i>C. snowden</i> | Oinsok (Ainsok River Drainage), Papua Barat; 1°11'40.07"S, 131°50'1.14"E; January 24, 2016 | KY654082 | KY654087 |
| <i>C. warsamsonicus</i> | Small tributary to Warsamson River; 0°49'16.62"S, 131°23'3.34"E; January 20, 2016 | KY654086 | KY654091 |
| | Papua Barat | KU821424 | KU821438 |
| | | KU821426 | KU821437 |
| <i>Engaeus strictifrons</i> | Crawford River, Victoria, Australia | AF493633 | AF492812 |
| <i>Euastacus bispinosus</i> | Crawford River, Victoria, Australia | AF493634 | AF492813 |

and a 710 bp fragment of the Cytochrome Oxidase subunit I gene (COI) using primers LCO1490 and HCO2198 (Folmer et al. 1994).

PCR was performed in 25 µl volumes containing 1x Taq buffer, 1.5 mM MgCl₂, 200 µM each dNTP, 1 U Taq polymerase, ca. 50-100 ng DNA and ddH₂O. After an initial denaturation step of 3 min at 94 °C, cycling conditions were 35 cycles at 94 °C for 35 s, 45 °C (COI) or 50 °C (16S) for 60 s, and 72 °C for 1 min (COI) or 90 s (16S), with a final elongation step of 5 min at 72 °C. The same primers were used in PCR and sequencing. PCR products were sent to Macrogen Europe for purification and cycle sequencing of both strands of each gene.

Sequences were aligned by eye (COI) and with MAFFT (16S) using the G-INS-i strategy suitable for thorough alignments of sequences with global homology (Kato et al. 2002). The resulting alignments had a length of 658 bp (COI) and 542 bp (16S), respectively. To determine the best substitution model for Bayesian information analyses (see below), hierarchical likelihood ratio tests were carried out with jModelTest (Posada 2008) on both sequence sets (24 models tested). Based on the Akaike Information

Criterion and the Bayesian Inference Criterion, the GTR + I + G (COI) (BIC: HKY + I + G; more complex model chosen) and the HKY + G (16S) models were chosen. The two sequence datasets were subsequently analysed both separately and combined.

Phylogenetic trees were reconstructed by maximum parsimony (MP) using the heuristic search algorithm as implemented in PAUP* (Swofford 2002), with gaps treated as fifth base. Support for nodes was estimated by bootstrap analysis (1,000 bootstrap replicates with 10 random addition sequence replicates each). Maximum Likelihood (ML) analyses were conducted with RAxML (Stamatakis et al. 2008; RAxML Black-Box; 100 bootstrap replicates) under the GTR + (I) + G model of sequence evolution. In addition, Bayesian inference was employed to infer phylogeny by using MrBayes 3.2.2 (Ronquist and Huelsenbeck 2003). The MCMCMC-algorithm was run with four independent chains for 10,000,000 generations, samplefreq = 500, and burnin = 10,001) using the models specified above. The combined dataset was subjected to a partitioned analysis (ML and BI) using the different models for the two genes in the BI analyses. Genetic distances were calculated using MEGA 7.0 (Kumar et al. 2016.). All new sequences have been deposited in GenBank (see Table 1).

Systematics

Parastacidae Huxley, 1879

Genus *Cherax* Erichson, 1846

Cherax mosessalossa sp. n.

<http://zoobank.org/B14DD6CD-7368-451A-A91A-4C97F0F8F54A>

Figs 1–5

Material examined. Holotype: male (MZB Cru 4675), under rocks and among roots along banks of Klademak Creek, Sorong City, 0°52'23.59"S, 131°16'24.40"E, West Papua, Indonesia, coll. Christian Lukhaup, Marten Luter Salossa and Salvatore a`Paulo Narahawarin, January 26, 2016. **Allotype:** female (MZB Cru 4676), same data as holotype. **Paratypes:** (MZB Cru 4677), same data as holotype.

Diagnosis. Carapace surface smooth with scattered fine hairs, five small spiniform tubercles posterior to cervical groove on lateral carapace. Eyes large, pigmented. Cornea slightly broader than eyestalk. Rostrum triangular in shape with elevated margins, setose in the anterior half. Rostral margins with three prominent teeth. Rostral carinae prominent. Postorbital ridges prominent with one acute tubercle at anterior terminus. Uncalcified patch on lateral margin of chelae of adult male white, translucent. Propodal cutting edge with row of small granules and one larger tubercle. Chelipeds blue-grey lateral margins white, posterior lateral part sometimes orange. Fingers dark black blue with hooked yellow tips. Other walking legs blue-gray. Pleon blue-grey with yellow transverse lines.

Description of male holotype (Figs 2–5). Body and eyes pigmented. Eyes not reduced. Body subovate, slightly compressed laterally. Pleon narrower than cephalothorax



Figure 1. *Cherax moesselossa* sp. n. **A** holotype male (MZB Cru 4675) from Klademak Creek, Sorong City **B** idem, side view.

mm long and 2.7 mm wide. Proximal margins setose. Antennulae and antennae typical for genus. Antennae approx. 10 % longer than body. Antennular peduncle reaching slightly behind acumen, antennal peduncle reaching slightly behind apex of scapho-



Figure 2. *Cherax mosessalossa* sp. n. holotype male (MZB Cru 4675). Scale bar: 10 mm.

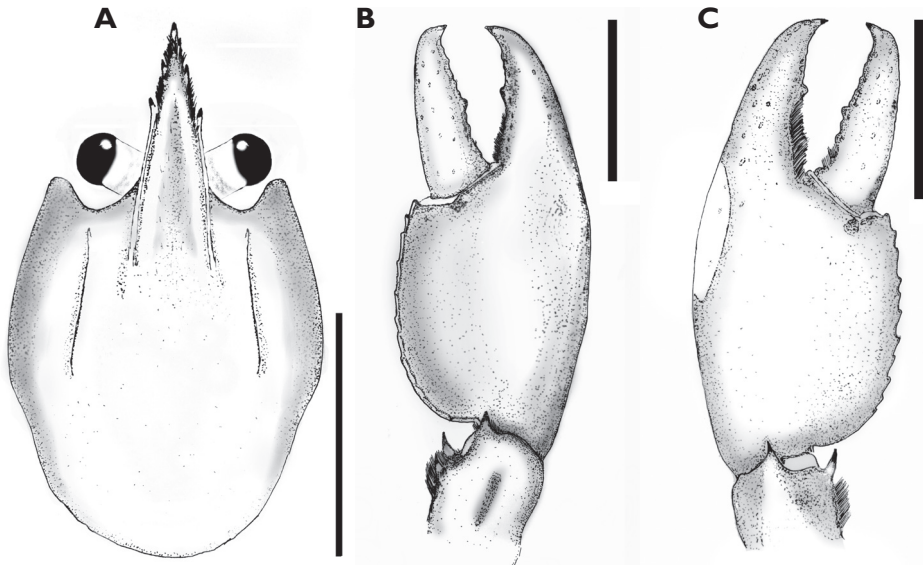


Figure 3. *Cherax moessalossa* sp. n. holotype male (MZB Cru 4675). **A** dorsal view of carapace **B** dorsal view of right chelae **C** ventral view of right chelae. Scale bars: 10 mm.

(width 12.9 mm and 13.6 mm, respectively). Rostrum (Figure 3A) broad in shape, reaching nearly to end of ultimate antennular peduncle more than three times longer than wide (width 3.3 mm at base, length 10.9 mm). Upper surface smooth, short scattered hairs present. Margins slightly elevated continuing in rostral carinae on carapace, almost straight in basal part, distally rather moderately tapering towards apex. Scattered, short, fine hairs present on rostrum surface. Lateral rostral margin bearing three prominent teeth in distal half on right side and two on left, pointing upwards at angle of approximately 45°. Few short hairs present on distal half of outer margins. Acumen with anteriorly orientated spine.

Rostral carinae extending as slight elevation posteriorly on carapace terminating at ending of postorbital ridges. Postorbital ridges well developed, terminating in spiniform tubercle anteriorly, fading at two-thirds of occipital carapace length, posteriorly. (Figure 4) Dorsal surface of carapace smooth, scattered fine short hairs present after cervical groove. Cervical and branchiocardiac grooves distinct, setose at middle part, three prominent corneous spine and two smaller spines present at middle part behind cervical groove on lateral sides of carapace.

Areola length 9.3 mm, narrowest width 5.1 mm. Length of areola 31.8% of total length of carapace (31.17 mm).

Ventrolateral parts smooth with scattered short hairs; anterior margin strongly produced, rounded upper margin directed inward.

Scaphocerite broadest at midlength, convex in distal part becoming narrower in basal part; thickened lateral margin terminating in large corneous spine, almost reaching distal margin of ultimate segment of antennular peduncle. Right scaphocerite 7.7



Figure 4. *Cherax mosessalossa* sp. n. holotype male (MZB Cru 4675), dorsal view of cephalothorax. Scale bar: 10 mm.

cerite. Antennal protopodite with spine anteriorly; basicerite with one lateral and one ventral spine.

Mouthparts typical for the genus. Epistome with subcordiform cephalic lobe anteriorly bearing lanceolate cephalomedian projection constricted at base. Lateral margins of lobe not thickened; each lateral margin with two groups of 5–6 tubercles separated by a smooth place. Central part smooth, not pitted, excavate. Eyes rather large; cornea globular, darkly pigmented, nearly as long as eyestalk; eyestalk slightly narrower than cornea.

First pereopod equal in form, chela slightly gaping, equal in size, right cheliped (24.6 mm long, 5.2 mm high, 11.2 mm wide). Right chelae (Figure 3B, C), strongly compressed. Fingers shorter than palm (dactylus 10.4 mm long). Dactylus broad at base (3.5 mm), tapering slightly towards tip. Tip with sharp, corneous, hooked tooth pointing outwards at an angle of 45°. Cutting edge of dactyl with continuous row of rather small granular teeth and one prominent larger tooth at middle of cutting edge. Ventral and dorsal surface of movable finger with scattered punctuation. Fixed finger

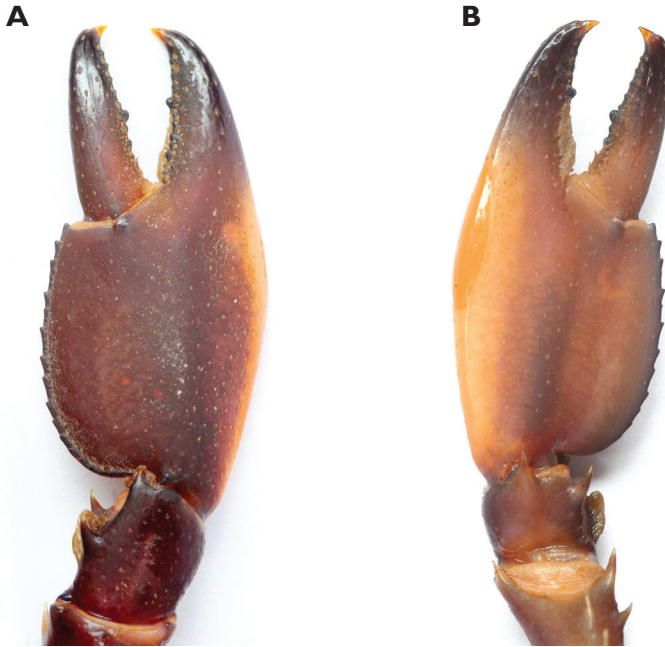


Figure 5. *Cherax mosessalossa* sp. n. holotype male (MZB Cru 4675). **A** right first chela, dorsal aspect **B** right first chela, ventral aspect. Scale bars: 10 mm.

triangular, merging gradually into palm, ending in sharp, corneous, hooked tooth, standing almost perpendicular to axis of finger. Tips of fingers slightly crossing when fingers clasp. Upper surface of palm practically smooth, slightly pitted, more densely pitted at margins. Fixed finger with approximately same width as dactyl at base (5.0 mm). Dense, short setae present in posterior ventral part of fixed finger. Cutting edge of fixed finger with row of rather small granular teeth at posterior half and one at middle of anterior part. Scattered, short hairs present in posterior ventral half of dactylus.

Dorsal surface of *carpus* (8.7 mm) smooth and pitted, with slight excavation in middle part and with a well-developed mesial carpal spine. Ventral carpal surface margins slightly elevated, setose at inner margin and with fovea; inner margin with well-developed ventral carpal spine and ventromesial carpal spine oriented in angle of approx. 45°. Outer lateral margin of chelae with swollen soft and uncalcified patch (7.3 mm) which extends from approx. first third of palm to approx. beginning of the movable finger. Mesial margin of palm slightly elevated, forming slender serrated ridge with row of 10-11 small granular teeth (Figure 5A, B).

Merus (13 mm) laterally depressed in basal part; surface slightly pitted; small dorsal meral spine present. Inner ventrolateral margin densely covered with small granules, four sharp ventral meral spines present, one at midlength, other in middle of anterior part, third and fourth on distal ventrolateral inner margin.

Ischium (7.8 mm) smooth with two small spines and two granules at midlength of ventrolateral inner margin.

Second pereopod reaching anteriorly to approximately corneous spine of scaphocerite. Finger (3.5 mm) slightly shorter as palm (4.0mm), of same height. Scattered short setae present on dactyl and fixed finger. Cutting edge of fixed finger and carpus with row of dense, short setae. Carpus (5.4 mm), smooth, slightly pitted, longer than palm. Merus (9.5 mm) 1.75 times longer than carpus. Ischium (4.6 mm) approx. as half as long as merus.

Third pereopod overreaching second by length of finger of second pereopods. Fingers shorter than palm.

Fourth pereopod reaching distal margin of scaphocerite. Dactylus with corneous tip. Short scattered setae present. Propodus more than twice as long as dactylus, nearly 1.5 times as long as carpus; somewhat flattened, carrying many stiff setae on lower margin. Merus just slightly longer than propodus.

Fifth pereopod similar to fourth, slightly shorter.

Dorsal surface of pleon smooth, with scattered pits; abdominal segments with short setae present on caudal margins.

Telson with posterolateral spines, dense short setae present in posterior third. Posterior margins setose. Uropodal protopod with two distal spines on mesial lobe. Exopod of uropod with transverse row of posteriorly directed diminutive spines ending in one more prominent spine, posteriorly directed on outer margin of mesial lobe. Terminal half of exopod with small tubercles and short hairs, slightly corrugated. Endopod of uropod smooth. Short scattered hairs present on posterior third of dorsal exopod. Postrolateral spine on outer margin present. Second spine on medial dorsal surface present, directed posteriorly.

Description of allotype female (Figure 6). Chela of first pereopods equal, 2.6 times as long as broad (28.6 mm and 10.9 mm respectively). Mesial margin of palm slightly elevated, forming slender serrated ridge with row of 12–13 small granular teeth. Cutting edge of dactylus with 4–5 rather small granular teeth. Cutting edge of fixed finger with 84–5 small granules. Small scattered short setae visible along ventral cutting edge of chelae, denser and long in ventral posterior area. Tips of fingers slightly crossing when fingers clasp, not gaping. Cervical groove distinct, short setae present at middle part. One prominent corneous spine and two smaller granules present at middle part behind cervical groove on lateral sides of carapace. Pleon just slightly narrower than cephalothorax (widths 12 mm and 12.5 mm respectively). Same colour pattern as in males, less intense.

Size. The largest male examined is the holotype with a carapace length of 31.3 mm, and a total length of 79 mm; the paratype male has a total length of 66.3 mm and the other male has a total length of 59 mm; the allotype female has a carapace length of 40 mm and a total length of 87.7 mm (n = 6).

Colour. The living animals (Figure 1A, B) are coloured as follows. Male: Chelae dark blue with white margins and white patch. Anterior part usually dark blue. Corneous tooth on tip of fingers orange. Cephalothorax brown-black, with creamy spots laterally. Dark reddish patch on dorsolateral side of the carapace between rostral carinae and cervical groove. Segments of pleon dark blue or brown with yellowish cream transversal band. Lateral pleura slightly lighter with some yellowish cream spots. Walk-



Figure 6. *Cherax mosessalossa* sp. n., allotype female (MZB Cru 4676).

ing legs dark bluish grey. Distal margin of tail-fan creamy orange to light yellowish. Females: usually same colour as males somewhat less colourful.

Molecular phylogenetic results. *Cherax mosessalossa* sp. n. is sister species to *Cherax misolicus* (16S only, Figure 19), both are in turn sister group to *C. warsamsonicus*. *Cherax mosessalossa* sp. n. is well isolated from both *C. misolicus* with a sequence divergence (p-distance, 16S) of 1.8 % and from *C. warsamsonicus* with a sequence divergence of 2.6 % (16S) and 6.6–7.0 % (COI), respectively, supporting the morphology-based description of *C. mosessalossa* as a new species.

Systematic remarks. Among all species of the northern group, *C. mosessalossa* sp. n. is most similar to *C. misolicus*, a species that is endemic to Misool Island, one of four major islands in the Raja Ampat Islands in West Papua, Indonesia, and to *C. warsamsonicus*, a species that is endemic to the Warsamson River ca. 50 km north of Sorong. *Cherax mosessalossa* sp. n. differs from *C. misolicus* and *C. warsamsonicus* in several characters (see Table 2).

Etymology. *Cherax mosessalossa* sp. n. is named after the son of our guide Marten Luther Salossa, Moses Yorof Salossa, who died of malaria at the age of 2.

Ecology. Known only from the Klademak Creek, South Sorong Regency, in the central part of the Kepala Burung (Vogelkop) peninsula. (Figure 8) At the sampling site the creek is shallow (20–50 cm) with a moderate flow and had a pH of approximately 6.5. In most parts no water plants are present. The substrate of the creek is

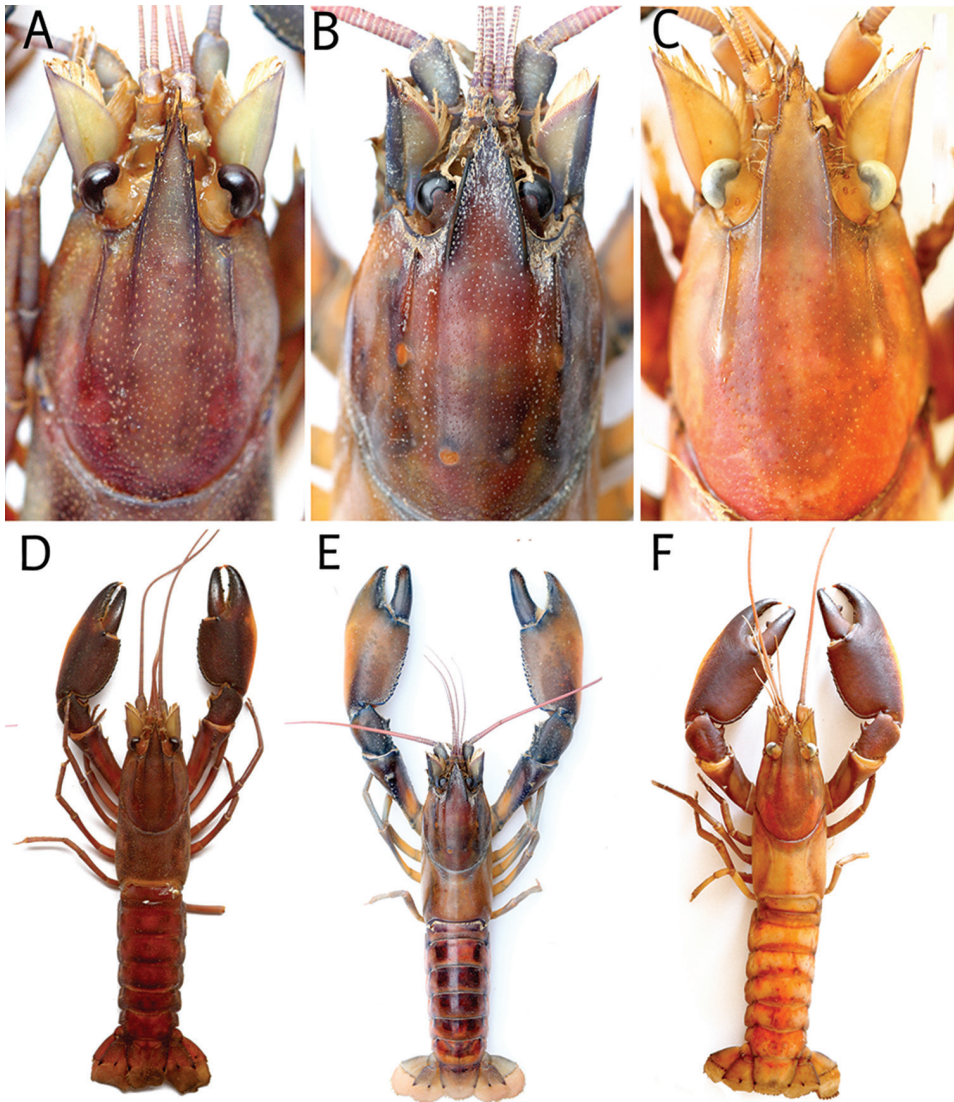


Figure 7. Rostrum dorsal view **A** *Cherax moessalossa* sp. n. holotype male (MZB Cru 4675) **B** *Cherax misolicus* (this study) **C** *Cherax warsamsonicus*, holotype male, (MZB Cru 4529) Dorsal view **D** *Cherax moessalossa* sp. n. holotype male (MZB Cru 4675). **E** *Cherax misolicus* (this Study) **F** *Cherax warsamsonicus*, holotype male, (MZB Cru 4529)

gravel or sand and soil mostly covered with silt and detritus, stones and larger rocks (Figure 9). Crayfish hide in short borrows in the creek bank, under larger rocks or in detritus that gathers in slower flowing parts of the creek. To improve the knowledge of the ecology and distribution of the species more field surveys will be necessary.

Common name. As common name for this crayfish we propose Klademak Creek Crayfish.

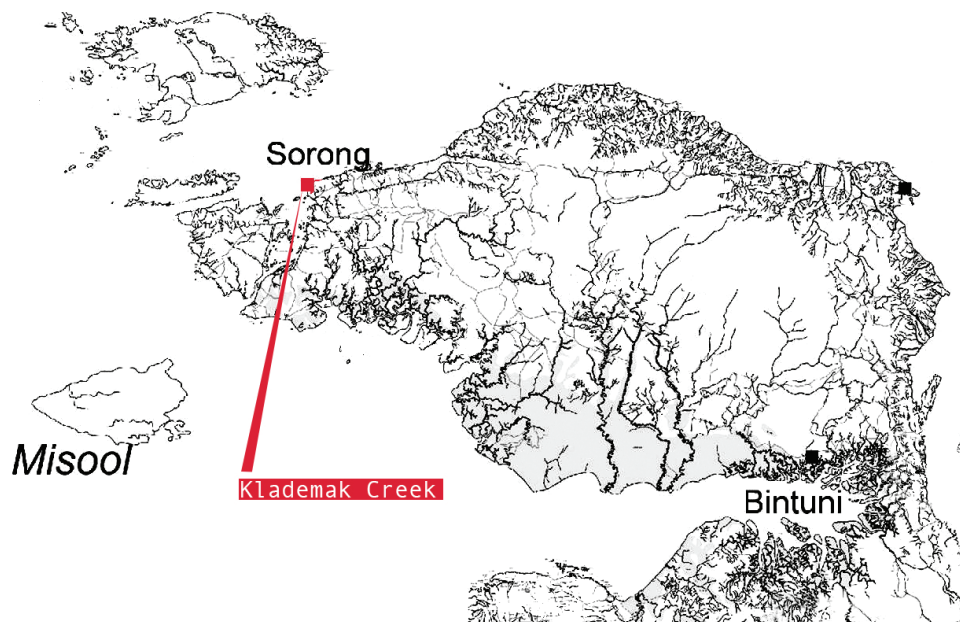


Figure 8. The Bird's Head Peninsula, West Papua, Indonesia with the type locality, Klademak Creek, indicated.



Figure 9. Klademak Creek, habitat of the new species.

Table 2. Comparison of morphological features of *C. mosesalossa* sp. n., *C. misolicus*, and *C. warsamsonicus*.

| | <i>C. mosesalossa</i> sp. n. | <i>C. misolicus</i> | <i>C. warsamsonicus</i> |
|---|--|--|--|
| Chelae | 4.5–4.7 times as long as height, 2.0–2.1 times as broad as height. | 4.0–4.2 times as long as height, 1.6–1.7 times as broad as height. | 4.6 times as long as height, 2.3 times as broad as height |
| Rostrum | 3 times as long as broad, rather straight | 2 times as long as broad, rather straight | 2.5 times as long as broad, clearly bent outwards at middle part. |
| Lateral sides of the carapace | 3 prominent corneous spines, 2 smaller spines on middle part behind cervical groove | 6–7 very small tubercles on middle part behind cervical groove | 1 prominent corneous spine and 3 tubercles on middle part behind cervical groove |
| Setae | Rostrum: less setose, Chelae: setae on the ventral side of the cutting edges of the chelae, Carpus: setae present on the inner margin Carapax :short fine hairs present. | Rostrum: setose Chelae: ventral side with short setae on edge of fixed finger and movable finger. Carapax; fine short hairs present. | Rostrum: non setose, few bristles. Chelae: ventral side of cutting edged not setose, few short bristles Carapax: non setose. |
| Coloration of the chelae | dark grey blue, whiter at the margins, with a white patch. | light blue with yellow creamy margins and a white patch. | dark blue chelae, white coloured lateral margin, white patch. |
| Coloration of the body | dark brown with white spots. | creamy to brown and yellow. | greenish grey with red to pink patches dorsally. |
| Coloration of the cephalothorax | brown grey with creamy spots laterally. | creamy to yellow. | greenish black, with small slightly darker spots laterally and ventrally fading to grey-green. |
| Coloration of the segments of the pleon | dark blue or brown with cream yellowish transversal bands. | creamy to yellow, light green dorsally with a black pattern. | with pink red band anteriorly becoming black. |

***Cherax alyciae* sp. n.**

<http://zoobank.org/A18FE24A-8259-4B98-9CE4-C5112C47E6A5>

Figs 10–14

Material examined. Holotype: male (MZB Cru 4672), under rocks, among roots and in debris along banks of a nameless creek, Boven Digoel Regency, West Papua, Indonesia. coll. local catchers and fisherman, December 7, 2016. **Allotype:** female (MZB Cru 4673), same data as holotype. **Paratypes:** (MZB Cru 4674) and (ZMB 30708), same data as holotype. Exact location stored with type material to protect population in its natural habitat.

Diagnosis. Carapace surface covered with small granules, areola pitted, no spines present posterior to cervical groove on lateral carapace. Eyes large, pigmented. Cornea slightly broader than eyestalk. Rostrum triangular in shape with elevated margins, setose in the anterior marginal half. Rostral margins with two prominent teeth, rostral carinae prominent. Postorbital ridges prominent with one acute tubercle at anterior terminus. Carapace blue, dorsal usually darker blue to green. Uncalcified patch on



Figure 10. *C. alyciae* sp. n. **A** holotype male (MZB Cru 4672) from nameless creek, Boven Digoel Regency **B** idem, colour variation.

lateral margin of chelae of adult male white, translucent. Propodal cutting edge with row of small granules and one larger tubercle. Chelipeds blue, lateral margins white, posterior lateral part sometimes orange. Fingers blue, in posterior third dark blue with

hooked orange tips. Other walking legs blue-green with orange joints. Pleon dark blue with light blue transverse lines.

Description of male holotype (Figs 11–14). Body and eyes pigmented. Eyes not reduced. Body subovate, slightly compressed laterally. Pleon narrower than cephalothorax (width 21.8 mm and 24.9 mm respectively). Rostrum (Figure 12A) broad in shape, reaching nearly to end of ultimate antennular peduncle and approx. twice as long than wide (width 6.1 mm at base, length 11.7 mm). Margins slightly elevated continuing in rostral carinae on carapace, almost straight in basal part, distally rather moderately tapering towards apex. Lateral rostral margin bearing two prominent teeth in distal half, pointing upwards at angle of approximately 45°. Few short hairs present on distal half of outer margins between the first teeth and the acumen. Acumen with anteriorly orientated spine.

Rostral carinae extending as slight elevation posteriorly on carapace terminating at ending of postorbital ridges. Postorbital ridges well developed, terminating in spiniform tubercle anteriorly, fading at two-thirds of occipital carapace length, posteriorly. Postorbital ridges approx. 1/3 of CL. Cervical and branchiocardiac grooves distinct, non-setose, six tiny and weak developed tubercles present at middle part behind cervical groove on lateral sides of carapace. Carapace surface densely covered with tiny granules, anterior margin strongly produced, rounded upper margin directed inward.

Areola length 18.4 mm, narrowest width 8.0 mm. Length of areola 34.7% of total length of carapace (54 mm). Densely pitted.

Scaphocerite (Figure 12B), broadest at posterior third, convex in distal part becoming narrower in basal part; thickened lateral margin terminating in corneous spine, almost reaching distal margin of ultimate segment of antennular peduncle. Right scaphocerite 12.0 mm long and 3.9 mm wide. Proximal margins setose. Antennulae and antennae typical for genus. Antennae slightly longer than body. Antennular peduncle reaching slightly behind acumen, antennal peduncle reaching slightly behind apex of scaphocerite. Antennal protopodite with spine anteriorly; basicerite with one lateral and one ventral spine.

Mouthparts typical for the genus. Epistome with sub-cordiform cephalic lobe anteriorly bearing lanceolate cephalomedian projection constricted at base. Lateral margins of lobe not thickened; each lateral margin with two groups of 8–9 tubercles separated by a smooth place. Central part smooth, not pitted, excavate. Eyes rather large; cornea globular, darkly pigmented, nearly as long as eyestalk; eyestalk slightly narrower than cornea.

First pereopod equal in form, chela slightly gaping. Right cheliped 56 mm long, 12 mm high, 21 mm wide. Left chelae (Figure 12C, D) 51.8 mm long and 10.4 mm high, 20.6 mm wide, strongly compressed. Fingers shorter than palm (right dactylus 25.4 mm long). Dactylus broad at base (7.8 mm), tapering slightly towards tip.

Tip with sharp, corneous, hooked tooth pointing outwards at an angle of 45°. Cutting edge of dactyl with continuous row of rather small granular teeth and one prominent larger tooth at middle of cutting edge. Ventral and dorsal surface of movable finger with scattered punctuation. Ventral posterior half of cutting edge with with dense setae reaching from base to prominent larger tooth. Fixed finger triangular, merging



Figure 11. *C. abyciae* sp. n. holotype male (MZB Cru 4672). Scale bar: 10 mm.

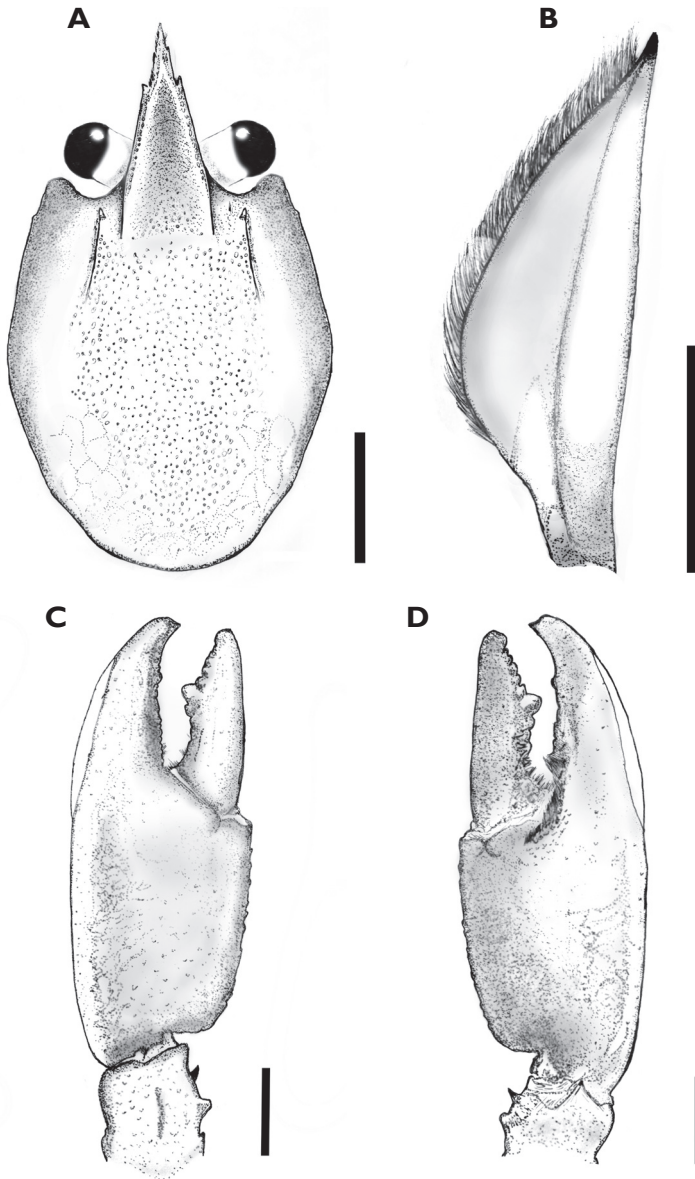


Figure 12. *C. abyciae* sp. n. holotype male (MZB Cru 4672) **A** dorsal view of carapace **B** scaphocerite **C** dorsal view of left chelae **D** ventral view of left chelae. Scale bars: 10 mm (**A, C, D**), 5 mm (**B**).

gradually into palm, ending in sharp, corneous, hooked tooth, standing almost perpendicular to axis of finger. Tips of fingers slightly crossing when fingers clasp. Upper surface of palm practically smooth, slightly pitted, more densely pitted at margins. Fixed finger slightly broader than dactyl at base (11.3 mm). Dense, short setae present in posterior ventral part of fixed finger, reaching from base to midlength. Cutting edge of fixed finger with row of rather small granular teeth at posterior half and one bigger



Figure 13. *C. alyciae* sp. n. holotype male (MZB Cru 4672), dorsal view of cephalothorax. Scale bar: 10 mm.

one at midlength. Outer lateral margin of chelae with swollen soft and uncalcified patch (23 mm) which extends from about middle of palm to midlength of opposable dactylus. Row of 20-21 mesial probodal granules at dorsolateral margin. Dorsolateral margins slightly elevated.

Dorsal surface of *carpus* (14.4 mm) smooth and pitted, with slight excavation in middle part and with a well-developed mesial carpal spine. Ventral carpal surface margins slightly elevated, non-setose and with fovea; inner margin with well-developed ventral carpal spine and ventromesial carpal spine oriented in angle of approx. 45°.

Merus (24.7 mm) laterally depressed in basal part; surface slightly pitted; small dorsal meral spine present. Inner ventrolateral margin densely covered with small granules, three ventral meral spines present, one at midlength other in middle of anterior part, third on distal ventrolateral inner margin.

Ischium (14.69 mm) smooth with two small spines and eleven granules at midlength of ventrolateral inner margin.

Second pereopod reaching anteriorly to approximately corneus spine of scaphocerite. Finger (7.0 mm) slightly longer as palm (6.6mm), of same height. Scattered short setae pre-

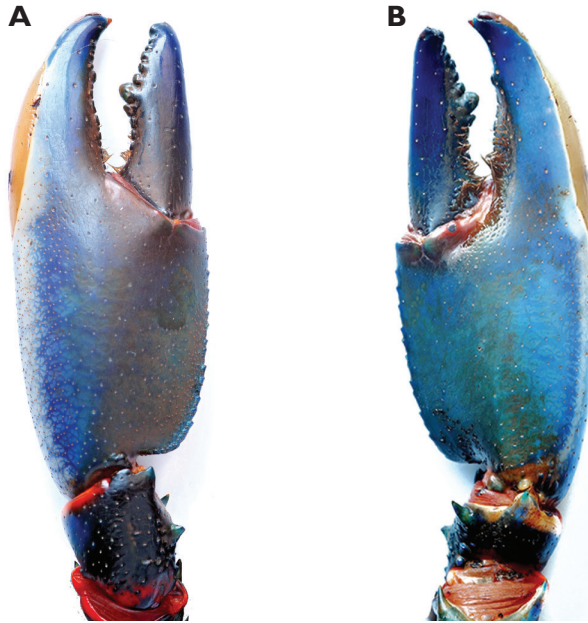


Figure 14. *C. alyciae* sp. n. holotype male (MZB Cru 4672) **A** left first chela, dorsal aspect **B** left first chela, ventral aspect. Scale bars: 10 mm.

sent on dactyl and fixed finger. Cutting edge of fixed finger and carpus with row of dense, short setae. Carpus (9.3 mm), smooth, slightly pitted, longer than palm. Merus (17.4 mm) 1.87 times longer than carpus. Ischium (8.3 mm) about as half as long as merus.

Third pereopod overreaching second by length of finger of second pereopods. Fingers shorter than palm.

Fourth pereopod reaching distal margin of scaphocerite. Dactylus with corneous tip. Short scattered setae present. Propodus more than twice as long as dactylus, nearly 1.5 times as long as carpus; somewhat flattened, carrying many stiff setae on lower margin. Merus just slightly longer than propodus.

Fifth pereopod similar to fourth, slightly shorter.

Dorsal surface of pleon smooth, with scattered pits; abdominal segments with short setae present on caudal margins.

Telson with posterolateral spines, dense short setae present in posterior third. Posterior margins setose. Uropodal protopod with two distal spines on mesial lobe. Exopod of uropod with transverse row of posteriorly directed diminutive spines ending in one more prominent spine, posteriorly directed on outer margin of mesial lobe. Terminal half of exopod with small tubercles and short hairs, slightly corrugated. Endopod of uropod smooth. Short scattered hairs present on posterior third of dorsal exopod. Posterolateral spine on outer margin present. Second spine on medial dorsal surface present, directed posteriorly.

Description of allotype female (Figure 15). Chela of first pereopods equal, 2.7 times as long as broad (30.6 mm and 11.2 mm respectively). Mesial margin of palm



Figure 15. *C. alyciae* sp. n. allotype female (MZB Cru 4673). Scale bar: 10 mm.

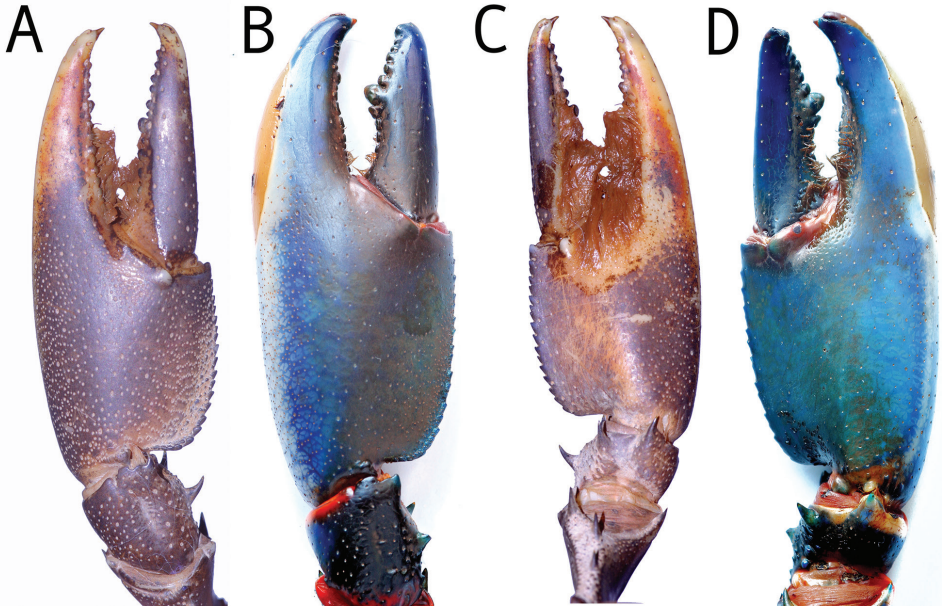


Figure 16. Dorsal view chelae. **A** *Cherax peknyi*, holotype male (QMW28267) **B** *C. ablyciae* sp. n. holotype male (MZB Cru 4672) ventral view chelae **C** *Cherax peknyi*, holotype male, (QMW28267) **D** *C. ablyciae* sp. n. holotype male (MZB Cru 4672).

slightly elevated, forming slender serrated ridge with row of 24–25 small granular teeth. Cutting edge of dactylus with 16–17 rather small granular teeth. Cutting edge of fixed finger with 16 small granules. Small scattered short setae visible along ventral cutting edges of chelae, denser and long in ventral posterior area. Tips of fingers slightly crossing when fingers clasp, not gaping. Cervical groove distinct, non-setose. Pleon just slightly narrower than cephalothorax (widths 16.2 mm and 16.6 mm respectively). Same colour pattern as in males. No soft patch in females observed ($n = 120$).

Size. The largest male examined has a carapace length of 56 mm and a total length of 122 mm; the holotype male has a total length of 117 mm; the other males have a total length between 78 mm and 119 mm; the allotype has a carapace length of 39 mm and a total length of 86 mm ($n = 11$).

Colour. The living animals (Figure 1A, B) are coloured as follows. Male: Chelae light to dark blue with white margins and white patch. Anterior part usually dark blue, more intense coloured. Corneous tooth on tip of fingers orange. Cephalothorax bright blue, dorsally more intense from purple to greenish blue, fading ventrally to light blue. Joints between propodus and carpus and between carpus and merus bright orange-red. Segments of pleon dark blue to black, lateral pleura lighter becoming blueish green. Light blue transverse bands in the posterior part of each pleonary somite. Walking legs light blue with orange joints. Distal margin of tail-fan creamy orange to orange. Some animals are darker and differ in the colouration of chelae. Chelae dark blue to black, becoming orange-red at the outer lateral margin. Dorsolateral margins light



Figure 17. Unnamed Creek, Boven Digoel Regency, habitat of the new species.

blue. These males have usually also orange or yellow rostral margins. Females: same colour as males, sometimes less intense.

Molecular phylogenetic results. *Cherax alyciae* sp. n. is sister species to *Cherax peknyi* (Figure 19), both are in turn sister group to *C. warsamsonicus*. *Cherax alyciae* sp. n. is well isolated from *C. peknyi* with a sequence divergence (p-distance) of 2.1–2.8 % (16S) and 5.7–6.3 % (COI), respectively, supporting the morphology-based description of *C. alyciae* as a new species.

Deposition of types. The holotype (MZB Cru 4672), allotype (MZB Cru 4673) and paratypes (MZB Cru 4674) are deposited at the Museum Zoologicum Bogoriense (= Bidang Zoologi) Research Centre for Biology (= Pusat Penelitian Biologi), Indonesian Institute of Sciences (= LIPI), Jalan Raya Jakarta-Bogor Km 46 Cibinong 16911, Indonesia. Additional Paratypes are deposited at the Museum für Naturkunde, Leibniz Institute for Evolution and Biodiversity Science, Berlin (ZMB 30708).

Systematic position. Holthuis (1949) in his publication on the New Guinea *Cherax* considered species should be placed into two groups. One with the rostral and median carinae absent or weakly developed and referred to as the *Cherax* group following the characteristics of the type species, *C. preissii* (Erichson, 1846) from southwest Australia. The other group contains species that have the rostral and sometimes the median carina well developed and referred to as the *Astaconephrops* group with Nobili's (1899)

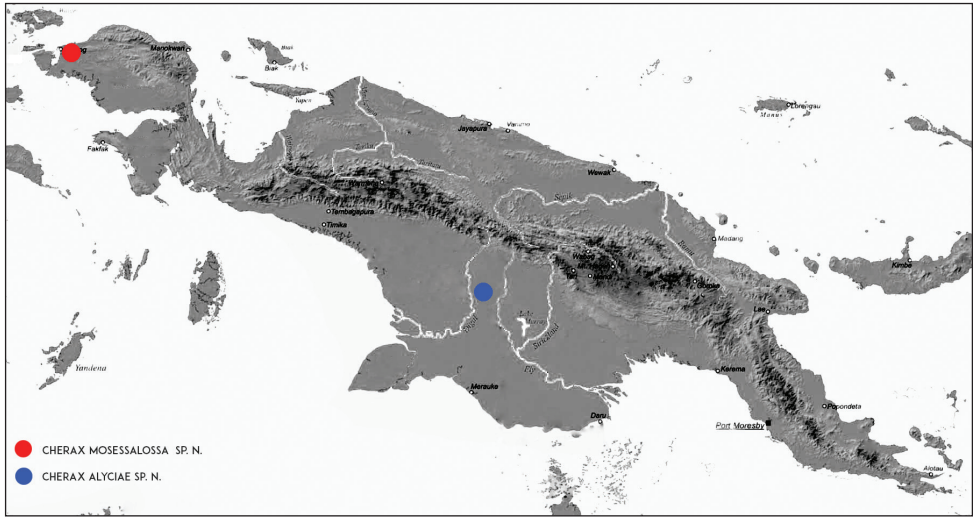


Figure 18. Map of Papua New Guinea, with the type localities indicated.

Astaconephrops albertisii as the type. Newly described species have been placed into one or the other of the two subgenera (Lukhaup and Pekny 2006; Lukhaup and Pekny 2008; Lukhaup and Herbert 2008; Lukhaup 2015, Lukhaup et al. 2015; Patoka et al. Kouba 2015). Munasinghe et al. (2004a, b), Austin (1996); and Austin et al. (1996) however, identified three lineages with different geographic ranges within *Cherax* based on molecular genetics and phylogenetic studies. These consist of a southwestern group, an eastern group and a northern group. Support for the latter group, however, was based on only very limited sampling (e.g., single samples of *C. quadricarinatus*, *C. rhynchotus*, and *C. peknyi* in Munasinghe et al. (2003). Munasinghe et al. (2004b) indicate that the division of *Cherax* into two subgenera, as conceived by Holthuis and subsequent authors dealing with New Guinea crayfish, has to be reconsidered. Based on Munasinghe et al. (2004a, b), Austin (1996), and Austin et al. (1996), *Cherax warsamsonicus* sp. n. and *Cherax alyciae* sp. n. belong to the northern species group lineage consisting of 25 species: *C. acherontis* Patoka, Bláha & Kouba, 2017, *C. albertisii* (Nobili, 1899), *C. alyciae* sp. n. (this study), *C. boesemani* Lukhaup & Pekny, 2008, *C. boschmai* Holthuis, 1949, *C. buitendijkae* Holthuis, 1949, *C. communis* Holthuis, 1949, *C. gherardii* Patoka, Bláha & Kouba, 2015, *C. holthuisi* Lukhaup & Pekny, 2006, *C. lorentzi aruanus* (Roux, 1911), *C. lorentzi lorentzi* (Roux, 1911), *C. longipes* Holthuis, 1949, *C. misolicus* Holthuis, 1949, *C. murido* Holthuis, 1949, *C. monticola* Holthuis, 1950, *C. moessalossa* sp. n. (this study), *C. minor* Holthuis, 1996, *C. peknyi* Lukhaup & Herbert, 2008, *C. pallidus* Holthuis, 1949, *C. papuanus* Holthuis, 1949, *C. paniaicus* Holthuis, 1949, *C. pulcher* Lukhaup, 2015, *C. solus* Holthuis, 1949, *C. snowden* Lukhaup, Panteleit & Schrimpf, 2015, and *C. warsamsonicus* Lukhaup, Eprilurahman & von Rintelen, 2017.

Systematic remarks. In comparison to all species of the northern group the new species, *C. alyciae* sp. n. is most similar to *C. peknyi*, a species that is known from the Fly River drainage, close to the City of Kiunga, Papua New Guinea. *Cherax alyciae* sp. n.

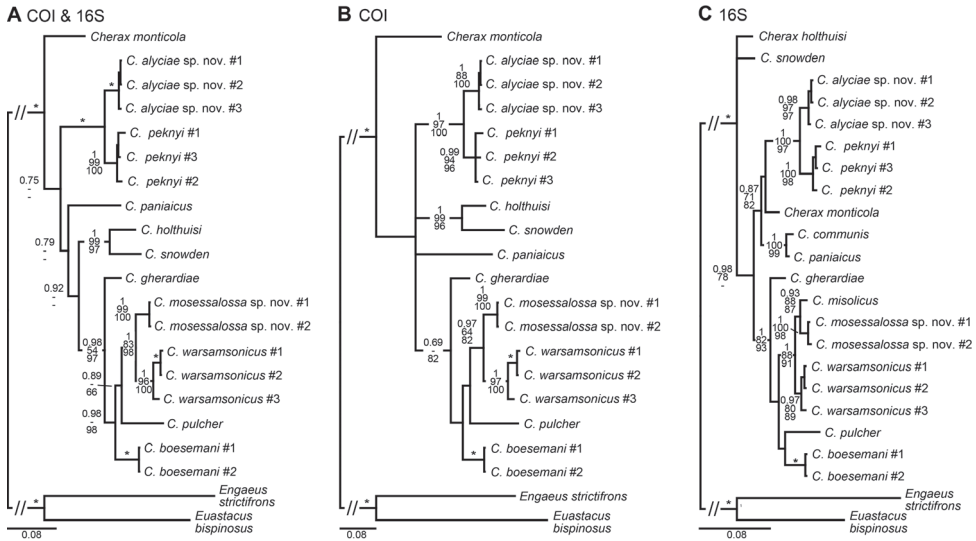


Figure 19. Phylogenetic relationships of *Cherax mosessalossa* sp. n. and *C. alyciae* sp. n. within the northern New Guinea *Cherax* lineage, reconstructed by BI analyses of two mitochondrial gene fragments. Number on branches show, from top, Bayesian posterior probabilities (>0.7) and ML/MP bootstrap values (>50). An asterisk indicates nodes with full support (1/100/100) in all analyses. The scale bar indicates the substitution rate. See Table 1 for information on the sequenced specimens. **A** Topology based on concatenated COI and 16S dataset **B** Topology based on COI dataset **C** Topology based on 16S dataset.

differs from *C. peknyi* in the following characters: shape of the chelae (Figure 16A–D), the presence of a soft patch in the chelae of males and in colouration. The rostrum of *Cherax alyciae* sp. n. is rather straight, triangular shaped, while the rostrum of *Cherax peknyi* is clearly bent outwards at the middle part. *Cherax peknyi* has 3–4 anteriorly directed spines present at middle part behind cervical groove on lateral sides of carapace while *C. alyciae* sp. n. has six tiny and weak developed tubercles there. *Cherax peknyi* has usually red to orange chelae becoming white posteriorly with blue fingertips, the carapace is orange yellow becoming dark red dorsally while the pleon is dark green with orange yellow transverse bands. None of the males of *C. peknyi* had a soft patch. Furthermore, the presence of dense setae on the ventral chelae in *C. peknyi* while *C. alyciae* sp. n. has just very few setae there. *Cherax peknyi* is endemic in the Fly River drainage in Papua New Guinea, while *C. alyciae* sp. n. is found in creeks and rivers of the Digul River drainage in the eastern part of the Boven Digoel Regency, Papua, Indonesia.

Etymology. *Cherax alyciae* sp. n. is named after Alycia Evanya, the daughter of Christian Jeffrey (Maju Aquarium) who brought the species to our attention.

Ecology. Known only from several nameless creeks in the Boven Digoel Regency in the eastern Part of Papua Province, Indonesia, close to the border of Papua New Guinea. The creek harbouring these crayfish is shallow (20–70 cm) with a moderate flow and had a pH of approximately 5.0. The temperature is around 25–27 °C and 12 µS/cm. In most parts no water plants are present. The substrate of the creek is gravel or sand and soil mostly covered with silt and detritus, stones and larger rocks (Figure 17).

Crayfish hide in short borrows in the riverbank, under larger rocks or in detritus that gathers in slower flowing parts of the creek. To improve the knowledge of the distribution of the species more field surveys will be necessary.

Common name. As common name for this crayfish we propose Blue Kong Crayfish as it is already known under this name in the pet trade.

Acknowledgements

Marten Luter Salossa is thanked for bringing *Cherax mosessalossa* sp. n. to our attention. Christian Jeffrey from Maju Aquarium in Jakarta is thanked for bringing *Cherax alyciae* sp. n. to our attention. We are grateful to Hans Georg Evers for providing details on the habitat and species location of *Cherax alyciae* sp. n., and we would like to thank Aquarium Dietzenbach for helping to obtain the species. We also thank Sammy de Grave, Charles Franssen, and Zachary Loughman for their helpful comments.

References

- Austin CM (1996) Systematics of the freshwater crayfish genus *Cherax* Erichson (Decapoda: Parastacidae) in northern and eastern Australia: electrophoretic and morphological variation. *Australian Journal of Zoology* 44: 259–296. <https://doi.org/10.1071/ZO9960259>
- Austin CM, Knott B (1996) Systematics of the freshwater crayfish genus *Cherax* Erichson (Decapoda: Parastacidae) in south-western Australia: electrophoretic, morphological and habitat variation. *Australian Journal of Zoology* 44: 223–258. <https://doi.org/10.1071/ZO9960223>
- Crandall KA, Fitzpatrick JF (1996) Crayfish molecular systematics: using a combination of procedures to estimate phylogeny. *Systematic Biology* 45: 1–26. <https://doi.org/10.1093/sysbio/45.1.1>
- Erichson WF (1846) Übersicht der Arten der Gattung *Astacus*. *Archiv für Naturgeschichte* 12: 86–103, 375–377.
- Folmer O, Black M, Hoeh W, Lutz R, Vrijenhoek R (1994) DNA primers for amplification of mitochondrial cytochrome c oxidase subunit I from diverse metazoan invertebrates. *Molecular Marine Biology and Biotechnology* 3: 294–299.
- Gan HM, Tan MH, Eprilurahman R, Austin CM (2014) The complete mitogenome of *Cherax monticola* (Crustacea: Decapoda: Parastacidae), a large highland crayfish from New Guinea. *Mitochondrial DNA Part A* 27: 337–338. <https://doi.org/10.3109/19401736.2014.892105>
- Holthuis LB (1949) Decapoda Macrura with a revision of the New Guinea Parastacidae. *Zoological results of the Dutch New Guinea Expedition 1939*. No. 3. *Nova Guinea* (n. ser.) 5: 289–330.
- Holthuis LB (1956) Native fisheries of freshwater Crustacea in Netherlands New Guinea. *Contributions to New Guinea Carcinology*. I. *Nova Guinea* (n. ser.) 7 (2): 123–137. [figs 1–3]

- Holthuis LB (1958) Freshwater crayfish in Netherlands New Guinea Mountains. South Pacific Commission Quarterly Bulletin 8 (2): 36–39. [7 figs]
- Holthuis LB (1982) Freshwater Crustacea Decapoda of New Guinea. In: Gressitt JL (Ed.) Biogeography and Ecology of New Guinea (Vol. 2). Monographiae Biologicae 42: 603–619. https://doi.org/10.1007/978-94-009-8632-9_28
- Holthuis LB (1986) The freshwater crayfish of New Guinea. Freshwater Crayfish 6: 48–58.
- Holthuis LB (1996) *Cherax (Astaconephrops) minor* new species, a parastacid from the mountains of Irian Jaya (W. New Guinea) Indonesia (Crustacea: Decapoda: Parastacidae). Zoologische Mededelingen Leiden 70 (24): 361–366.
- Huxley TH (1879) The Crayfish: an Introduction to the Study of Zoology. C. Kegan Paul & Co, London, 371 pp.
- Katoh K, Misawa K, Kuma K-I, Miyata T (2002) MAFFT: a novel method for rapid multiple sequence alignment based on fast Fourier transform. Nucleic Acids Research 30: 3059–3066. <https://doi.org/10.1093/nar/gkf436>
- Kumar S, Stecher G, Tamura K (2016) MEGA7: Molecular Evolutionary Genetics Analysis version 7.0 for bigger datasets. Molecular Biology and Evolution 33: 1870–1874. <https://doi.org/10.1093/molbev/msw054>
- Lukhaup C, Pekny R (2006) *Cherax (Cherax) holthuisi*, a new species of crayfish (Crustacea: Decapoda: Parastacidae) from the centre of the Vogelkop Peninsula in Irian Jaya (West New Guinea), Indonesia. Zoologische Mededelingen Leiden 80–1 (7): 101–107.
- Lukhaup C, Pekny R (2008) *Cherax (Astaconephrops) boesemani*, a new species of crayfish (Crustacea: Decapoda: Parastacidae) from the centre of the Vogelkop Peninsula in Irian Jaya (West New Guinea), Indonesia. Zoologische Mededelingen Leiden 82 (33): 331–340.
- Lukhaup C, Herbert B (2008) *Cherax (Cherax) peknyi* sp. nov., a new species of crayfish (Crustacea: Decapoda: Parastacidae) from the Fly River Drainage, Western Province, Papua New Guinea. Memoirs of the Queensland Museum 52 (2): 213–219.
- Lukhaup C (2015) *Cherax (Astaconephrops) pulcher*, a new species of freshwater crayfish (Crustacea, Decapoda, Parastacidae) from the Kepala Burung (Vogelkop) Peninsula, Irian Jaya (West Papua), Indonesia. ZooKeys 502: 1–10. <https://doi.org/10.3897/zookeys.502.9800>
- Lukhaup C, Panteleit J, Schrimpf A (2015) *Cherax (Astaconephrops) snowden* a new species of freshwater crayfish (Crustacea, Decapoda, Parastacidae) from the Kepala Burung (Vogelkop) Peninsula, Irian Jaya (West Papua), Indonesia. ZooKeys 518: 1–14. <https://doi.org/10.3897/zookeys.518.6127>
- Lukhaup C, Eprilurahman R, Rintelen T (2017) *Cherax warsamsonicus*, a new species of crayfish from the Kepala Burung (Vogelkop) peninsula in West Papua, Indonesia (Crustacea, Decapoda, Parastacidae). ZooKeys 660: 151–167. <https://doi.org/10.3897/zookeys.660.11847>
- Munasinghe DHN, BurrIDGE CP, Austin CM (2004a) The systematics of freshwater crayfish of the genus *Cherax* Erichson (Decapoda: Parastacidae) in eastern Australia re-examined using nucleotide sequences from 12S rRNA and 16S rRNA genes. Invertebrate Systematics 18: 215–225. <https://doi.org/10.1071/IS03012>
- Munasinghe DHN, BurrIDGE CP, Austin CM (2004b) Molecular phylogeny and zoogeography of the freshwater crayfish genus *Cherax* Erichson (Decapoda: Parastacidae) in Australia.

- Biological Journal of the Linnean Society 81: 553–563. <https://doi.org/10.1111/j.1095-8312.2003.00299.x>
- Munasinghe DHN, Murphy NP, Austin CM (2003) Utility of mitochondrial DNA sequences from four gene regions for systematic studies of Australian freshwater crayfish of the genus *Cherax* (Decapoda: Parastacidae). *Journal of Crustacean Biology* 23: 402–417. <https://doi.org/10.1163/20021975-99990350>
- Nobili DG (1899) Contribuzioni alia conoscenza della fauna carcinologica della Papuasias. delle Molucche e dell' Australia. *Annali del Museo Civico di Genova, serie 2*, 20 (40): 230–282.
- Patoka J, Blaha M, Kouba A (2015) *Cherax (Astaconephrops) gherardii*, a new crayfish (Decapoda: Parastacidae) from West Papua, Indonesia. *Zootaxa* 3964 (5): 526–536. <https://doi.org/10.11646/zootaxa.3964.5.2>
- Patoka J, Bláha M, Kouba A (2017) *Cherax acherontis* (Decapoda: Parastacidae), the first cave crayfish from the Southern Hemisphere (Papua Province, Indonesia). *Zootaxa* 4363 (1): 137–144. <https://doi.org/10.11646/zootaxa.4363.1.7>
- Posada D (2008) jModelTest: Phylogenetic model averaging. *Molecular Biology and Evolution* 25: 1253–1256. <https://doi.org/10.1093/molbev/msn083>
- Ronquist F, Huelsenbeck JP (2003) MRBAYES 3: Bayesian phylogenetic inference under mixed models. *Bioinformatics* 19: 1572–1574. <https://doi.org/10.1093/bioinformatics/btg180>
- Roux J (1911) Nouvelles especes de Decapodes d'eau douce provenant de Papouasie. *Notes Leyden Museum* 33: 81–106. [figs 1–5]
- Stamatakis A, Hoover P, Rougemont J (2008) A rapid bootstrap algorithm for the RAxML web servers. *Systematic Biology* 57: 758–771. <https://doi.org/10.1080/10635150802429642>
- Swofford DL (2002) PAUP* (version 4.0). Phylogenetic analysis using parsimony (*and other methods). Sinauer Associates, Sunderland, Mass.

Morphological re-description and molecular identification of Tabanidae (Diptera) in East Africa

Claire M. Mugasa^{1,2}, Jandouwe Villinger¹, Joseph Gitau¹, Nelly Ndungu^{1,3},
Marc Ciosi^{1,4}, Daniel Masiga¹

1 International Centre of Insect Physiology and Ecology (ICIPE), Nairobi, Kenya **2** School of Biosecurity Biotechnical Laboratory Sciences, College of Veterinary Medicine, Animal Resources and Biosecurity (COVAB), Makerere University, Kampala, Uganda **3** Social Insects Research Group, Department of Zoology and Entomology, University of Pretoria, Hatfield, 0028 Pretoria, South Africa **4** Institute of Molecular Cell and Systems Biology, University of Glasgow, Glasgow, UK

Corresponding author: Daniel Masiga (dmasiga@icipe.org)

Academic editor: T. Dikow | Received 19 October 2017 | Accepted 9 April 2018 | Published 26 June 2018

<http://zoobank.org/AB4EED07-0C95-4020-B4BB-E6EEE5AC8D02>

Citation: Mugasa CM, Villinger J, Gitau J, Ndungu N, Ciosi M, Masiga D (2018) Morphological re-description and molecular identification of Tabanidae (Diptera) in East Africa. ZooKeys 769: 117–144. <https://doi.org/10.3897/zookeys.769.21144>

Abstract

Biting flies of the family Tabanidae are important vectors of human and animal diseases across continents. However, records of Africa tabanids are fragmentary and mostly cursory. To improve identification, documentation and description of Tabanidae in East Africa, a baseline survey for the identification and description of Tabanidae in three eastern African countries was conducted. Tabanids from various locations in Uganda (Wakiso District), Tanzania (Tarangire National Park) and Kenya (Shimba Hills National Reserve, Muhaka, Nguruman) were collected. In Uganda, octenol baited F-traps were used to target tabanids, while NG2G traps baited with cow urine and acetone were employed in Kenya and Tanzania. The tabanids were identified using morphological and molecular methods. Morphologically, five genera (*Ancala*, *Tabanus*, *Atylotus*, *Chrysops* and *Haematopota*) and fourteen species of the Tabanidae were identified. Among the 14 species identified, six belonged to the genus *Tabanus* of which two (*T. donaldsoni* and *T. guineensis*) had not been described before in East Africa. The greatest diversity of tabanid species were collected from the Shimba Hills National Reserve, while collections from Uganda (around the shores of Lake Victoria) had the fewest number of species. However, the *Ancala* genus was found in Uganda, but not in Kenya or Tanzania. Maximum likelihood phylogenies of mitochondrial cytochrome c oxidase 1 (*COI*) genes sequenced in this study show definite concordance with morphological species identifications, except for *Atylotus*. This survey will be critical to building a complete checklist of Tabanidae prevalent in the region, expanding knowledge of these important vectors of human and animal diseases.

Keywords

Tabanids, biting flies, morphology, cytochrome c oxidase 1, *COI*, Kenya, Uganda, Tanzania

Introduction

Biting flies of the family Tabanidae (Order Diptera) are of both medical and veterinary importance because the females of most species are blood feeders that can transmit various pathogens to hosts as they feed on animals and humans (Foil 1989, Waage 1949). Pathogens transmitted by Tabanidae include bacteria, protozoa, helminths and viruses (Foil 1989). Moreover, because of their stout mouthparts, tabanids inflict painful bites while feeding, which affects livestock production as the animals are distracted from feeding, resulting in reduced growth rates, weight gain, reduced milk production, and reduced drought resistance, among others. The bite site may also predispose the animal to secondary infections, resulting in loss of hide quality (Yagi 1968).

Because different tabanid genera have been implicated as vectors of various pathogens, their accurate identification is important for disease ecology and management. The role of tabanids in the transmission of arboviruses such as Bovine Leukaemia Virus (BLV) has been documented (Monti et al. 2007). The potential for mechanical transmission of pathogens was explored by Buxton et al. (1985) and Foil et al. (1988). Buxton and colleagues investigated the ability of tabanids to transmit BLV in an experimental set-up. Using capillary action, infected blood was applied to the mouthparts of *Chrysops* spp. and *Tabanus atratus* Fabricius, 1775, which were removed to create inoculum that infected two sheep (Buxton et al. 1985). Similarly, experiments by Foil et al. (1988) demonstrated BVL transmissibility of groups of 50 and 100 horseflies (*Tabanus fuscicostatus*) from a cow with an infectious viral titre between 10^3 and 10^4 doses per ml. Likewise, the role of genus *Tabanus* in the horizontal transmission (transfer from one host to another) of BLV has been reported (Manet et al. 1989). Further, there are reports on the mechanical transmission of *Trypanosoma congolense* (Desquesnes and Dia 2003) and *Trypanosoma vivax* (Desquesnes and Dia 2004) by tabanids of different genera, including *Atylotus*. Indeed, tabanids are the principal vectors of *T. vivax* outside the sub-Saharan Africa tsetse fly belt (Gardiner and Wilson 1987). The genus *Chrysops* is reported to vector *Francisella tularensis* bacteria that cause tularemia in temperate regions, while in the tropics this genus is known to transmit the filarial nematode, *Loa loa*, in many sub-Saharan countries, including Uganda (Duke 1955). Therefore, effective control of diverse vectored diseases can be aided by accurate identification of tabanids in East Africa, which is crucial for monitoring their potential for invasion into naïve ecosystems and for vector control strategies.

To date, identification of tabanids is based on morphological keys and literature that was published over half a century ago (Oldroyd 1954). At present, the description of the tabanid fauna of eastern Africa is fragmented and sparsely documented without final valid checklists. The lack of concrete surveys and documentation of East African tabanids since 1954 constrains investigations of their ecology, zoogeography, vector-host interactions and importance as disease vectors.

Given the limited information on the taxonomy of these flies, their precise identification and classification is currently virtually impossible. This hurdle can be better overcome with the use of molecular DNA barcoding approaches (Hebert et al. 2003; Ratnasingham and Hebert 2007). Indeed, DNA barcoding based on the mitochondrial cytochrome c oxidase subunit 1 (*COI*) gene sequences has been used to discover new or previously unknown biodiversities due to its ability to differentiate diverse arthropod species including insect pests such as tussock moths, Lepidoptera: Lymantriidae (Ball and Armstrong 2005), mayflies (Ephemeroptera) (Ball et al. 2005) and spiders (Barret and Hebert 2005). More recently, Morita et al. (2016) successfully revised the phylogenetic framework of *Tabanidae* by employing four sets of genes including the mitochondrial *COI* on a data set of 110 horsefly species.

This study was undertaken to describe, identify and document a baseline *COI* barcode record of tabanid species occurring at diverse locations in Kenya, Uganda and Tanzania using morphological identifications to support a baseline *COI* barcode record.

Methods

Fly collection sites

In Uganda, flies were trapped in the Lake Victoria basin, specifically in Wakiso District from various sites (Table 1 and Fig. 1), between March and May 2013. Collection efforts were concentrated primarily around the swampy areas of the shores of Lake Victoria scattered with short shrubs, except for a few sites as indicated in Table 1.

In Kenya, flies were collected in four sites in the Shimba Hills National Reserve (Buffalo Ridge, Marere Circuit) and the environs in Zunguluka and Muhaka in August 2012. The Buffalo Ridge and Marere Circuit are in designated conservation areas where human activity is limited. Flies were also collected in two sites (Sampu and Mukinyo) in the Nguruman conservation area of southern Kenya in August 2012. The area is characterised by short grasslands interspersed with trees. In Tanzania, flies were collected from two sites (Sangaiwe and Poachers Hide) in the Tarangire National Park in August 2013.

Trapping and preservation of flies

In Uganda, the F-traps (Kuzoe and Schofield 2005) baited with 1,8-octenol were deployed in the various sites selected depending on proximity to grazing land and swampy area or close to running water for 3 to 5 days depending on the fly density. In Kenya and Tanzania, tabanids trapped corresponded to incidental trapping as part of a tsetse fly trapping campaign using NG2G traps baited with less than 3 weeks old cow urine and acetone (Brightwell et al. 1987). All flies from Kenya and Tanzania were stored in 95% ethanol and transported to *icipe* at room temperature, while flies collected from Uganda were stored in 70% ethanol in a cool box.

Table 1. Fly collection sites and their respective GPS coordinates.

| Country | Site name | Latitude | Longitude | Elevation (m) | Exact Collection sites |
|----------|----------------|----------------|-----------------|---------------|---------------------------|
| Uganda | Bubebere | 0°5'1.968"N | 32°25'39.4392"E | 1136 | Swamp at Lake shore |
| | Jahazi | 0°5'37.212"N | 32°26'20.9256"E | 1140 | Swamp at Lake shore |
| | Kisubi Beach | 0°7'9.984"N | 32°26'58.5672"E | 1137 | Swamp at Lake shore |
| | Nabinonya | 0°4'13.084"N | 32°28'46.9416"E | 1135 | Swamp at Lake shore |
| | Katalemwa | 0°13'59.52"N | 32°26'30.2928"E | 1154 | Away from open water |
| | Sanda | 0°13'0.516"N | 32°26'30.0552"E | 1157 | Away from open water |
| | Sissa | 0°11'43.692"N | 32°26'35.7756"E | 1144 | Away from open water |
| | Kawuku | 0°9'17.064"N | 32°26'44.8008"E | 1175 | Away from open water |
| | Bussi | 0°9'59.904"N | 32°25'38.2044"E | 1172 | Away from open water |
| Kenya | Sampu | 1°53'23.1108"S | 36°4'26.2452"E | 663 | Conservation/tourist area |
| | Mukinyo | 1°50'2.778"S | 36°4'59.3508"E | 672 | Conservation/tourist area |
| | Marere Circuit | 4°13'36.1164"S | 39°24'46.116"E | 390 | Conservation/tourist area |
| | Zunguluka | 4°20'11.9472"S | 39°15'52.1892"E | 137 | Conservation/tourist area |
| | Buffalo Ridge | 4°14'29.9724"S | 39°26'18.0348"E | 367 | Conservation/tourist area |
| | Muhaka | 4°19'51.1284"S | 39°31'16.8492"E | 663 | Conservation/tourist area |
| Tanzania | Sangaiwe | 3°56'29.76"S | 35°52'45.768"E | 1000 | National Park |
| | Poachers' Hide | 3°52'57.792"S | 35°56'1.428"E | 999 | National Park |

Morphological re-description of flies

Flies were pinned and placed in entomological boxes for morphological identification and labelled with area and date of collection. Entomological boxes were kept in the Bi-systematic Support Unit (BSU) in *icipe*. Subsequently, the flies were examined under a light microscope at a magnification of X10; for finer details, a higher magnification of X40 was used. The morphological keys used were those documented by Oldroyd (1952, 1954, 1957). After morphological identification, images of selected specimens were taken using a Nikon D90 camera for the gross specimen and Leica EZ4D to capture finer details. Images of the gross specimen are presented as Figs 2–4 as well as Suppl. material 2: Figures S1–S13.

Molecular characterisation of flies

From each group of morphologically identical specimens, a tibia was isolated from at least one fly in each group (with similar morphological features) and placed in separate plate-wells with 30 µl of 70% ethanol each. Two hundred and nine tissue samples were submitted for DNA extraction and *COI* barcode sequencing to the Canadian Centre for DNA Barcoding, University of Guelph, out of which 84 sequences could be generated (Suppl. material 1). An image of the dorsal and ventral side of the whole fly was also submitted for each tissue sample. For assessment of taxonomic relation-

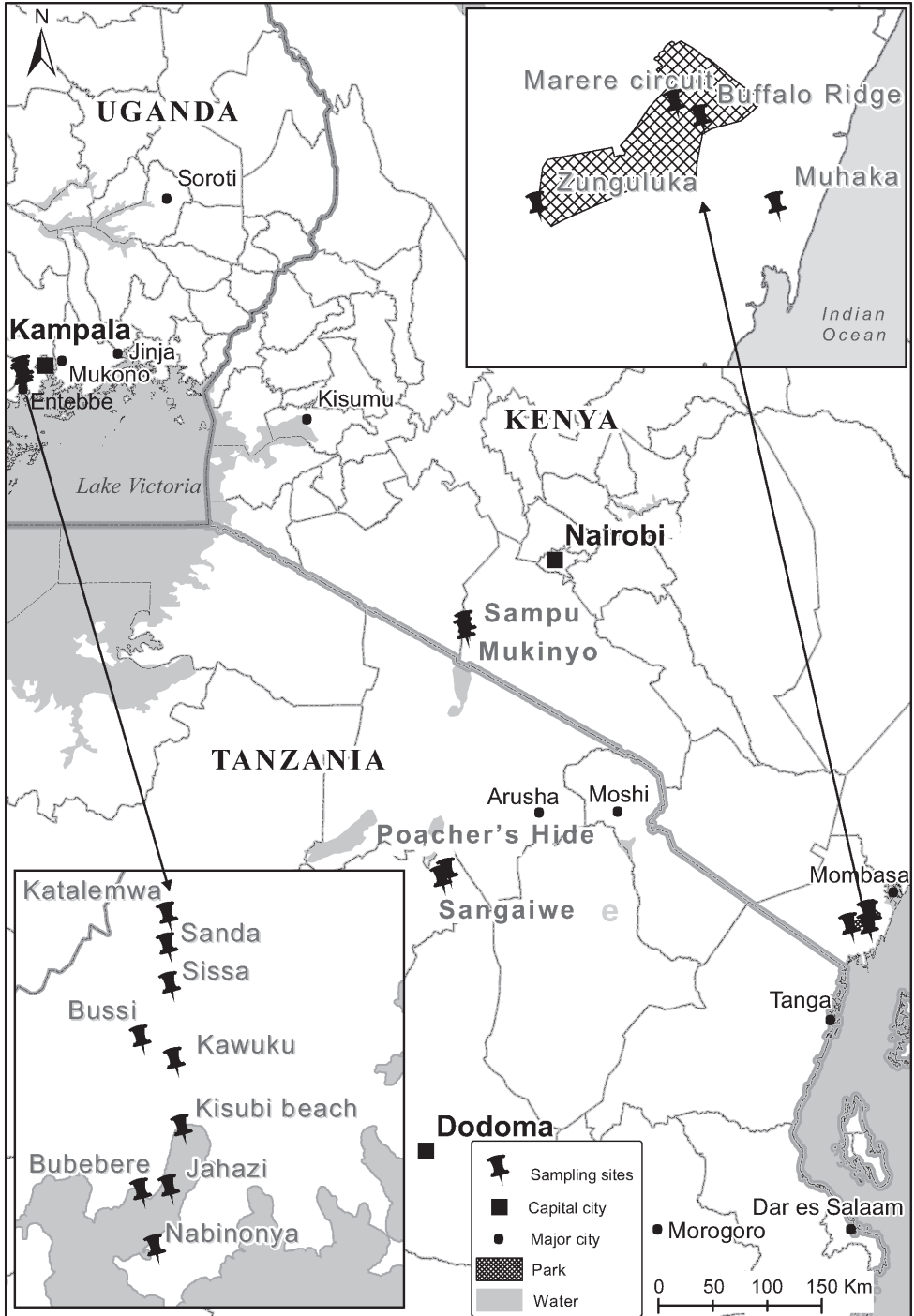


Figure 1. Fly collection sites in East Africa. In Uganda, collection sites were concentrated around the Lake Victoria basin close to swamps; in Kenya, there were two study regions one being more inland while the other was closer to the coast; in Tanzania flies were collected more inland.

ships, the *COI* mitochondrial gene was targeted to generate a DNA fragment of about 648-bp (Ratnasingham and Hebert 2007). The verified barcode sequences associated with specimen metadata and pictures in the Barcode of Life Database (BOLD) were submitted to GenBank (accessions KX946496–KX946580).

Phylogenetic analysis

We used MAFFT (Kato and Standley 2013) within Geneious v8.1.4 (available from <http://www.geneious.com>), software created by Biomatters (Kearse et al. 2012), to align all sequences alongside related tabanid sequences identified by querying against the GenBank nr database (<http://www.ncbi.nlm.nih.gov/>) using the Nucleotide Basic Local Alignment Search Tool (BLASTn) (Altschul et al. 1990), with *Rhagio tringarius* (GenBank accession KT105420) as an outgroup. Using PhyML v. 3.0 (Guindon et al. 2010), we inferred a maximum likelihood phylogeny from this alignment. The phylogeny employed the Akaike Information Criterion for automatic model selection and tree topologies were estimated using nearest neighbor interchange (NNI) improvements over 1000 bootstrap replicates. A midpoint rooted phylogenetic tree was then generated from the phylogeny using FigTree v1.4.2 (Drummond and Rambaut 2007).

Results

From Uganda, 995 female tabanids were collected, while approximately 2300 female tabanids were collected in both Kenya and Tanzania. Male flies were collected in negligible numbers and were thus not included in the study. The tabanids collected were grouped based on both morphology and *COI* barcode sequence phylogenies (Fig. 2) into five genera (*Tabanus*, *Ancala*, *Atylotus*, *Haematopota* and *Chrysops*) comprising 12 species as shown in Table 2.

Molecular sequences of collected flies

Clusters within the maximum likelihood phylogeny of *COI* sequences (Fig. 2) corresponded closely with species' identifications derived from morphological characters (below), except in the case of *T. thoracinus*, which formed two distinct clades designated as *T. thoracinus* A and *T. thoracinus* B (Fig. 2). DNA barcoding separated samples according to the species and the site of collection. The tree separates into two main branches representing the subfamilies Chrysopinae and Tabaninae; the latter further branches into the *Haematopota* species, *Tabanus*, *Ancala* and *Atylotus* species along with *Hippocentrum*, and *Hybomitra* reference sequences.

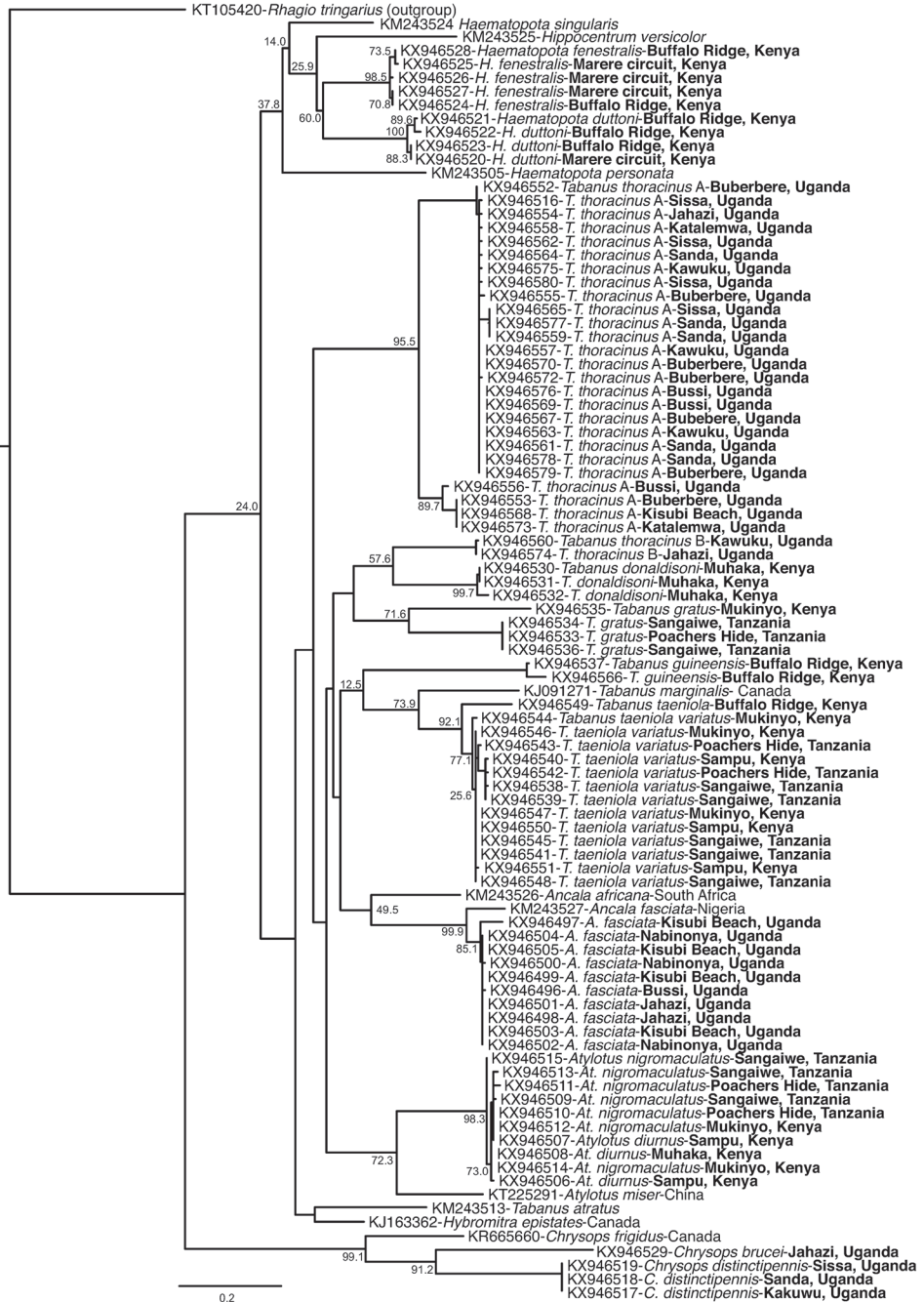


Figure 2. Maximum likelihood phylogenetic tree of *Tabanidae* COI sequences. Sequences from samples collected in Kenya, Tanzania and Uganda alongside reference sequences obtained from GenBank. GenBank accessions, tabanid species and sampling locations (where available) are shown. Study sequences are indicated with sampling sites in bold. The branch length scale bar indicates nucleotide substitutions per site. Bootstrap values at the major nodes are of percent agreement among 1000 replicates.

Table 2. Samples of each morphological identification that were submitted for sequencing from each locality per country.

| Country | Site of collection | Genus | Species | No. Submitted | No. Sequenced |
|-----------------|---------------------------|----------------------|-----------------------------|---------------|---------------|
| Kenya | Buffalo Ridge | <i>Haematopota</i> | <i>H. duttoni</i> | 5 | 3 |
| | | | <i>H. fenestralis</i> | 4 | 2 |
| | | <i>Tabanus</i> | <i>T. taeniola</i> | 1 | 1 |
| | | | <i>T. guineensis</i> | 2 | 2 |
| | Mukinyo | <i>Tabanus</i> | <i>T. taeniola variatus</i> | 3 | 3 |
| | | | <i>T. gratus</i> | 1 | 1 |
| | Marere Circuit | <i>Haematopota</i> | <i>H. fenestralis</i> | 3 | 3 |
| | | | <i>H. duttoni</i> | 1 | 1 |
| | Zunguluka | <i>Haematopota</i> | <i>H. fenestralis</i> | 4 | 0 |
| | Sampu | <i>Tabanus</i> | <i>T. taeniola variatus</i> | 3 | 3 |
| | | <i>Atylotus</i> | <i>At. diurnus</i> | 2 | 2 |
| | Muhaka | <i>Tabanus</i> | <i>T. donaldsoni</i> | 3 | 3 |
| <i>Atylotus</i> | | <i>At. diurnus</i> | 3 | 1 | |
| Tanzania | Sangaiwe | <i>Tabanus</i> | <i>T. taeniola variatus</i> | 5 | 5 |
| | | | <i>T. gratus</i> | 5 | 2 |
| | | <i>Atylotus</i> | <i>At. nigromaculatus</i> | 8 | 3 |
| | Poacher's Hide | <i>Tabanus</i> | <i>T. gratus</i> | 1 | 1 |
| | | | <i>T. taeniola variatus</i> | 2 | 2 |
| <i>Atylotus</i> | <i>At. nigromaculatus</i> | 2 | 2 | | |
| Uganda | Mabamba | <i>Tabanus</i> | <i>T. thoracinus</i> | 23 | 1 |
| | | <i>Chrysops</i> | <i>C. brucei</i> | 1 | 0 |
| | | <i>Ancala</i> | <i>A. fasciata</i> | 2 | 0 |
| | Bussi | <i>Tabanus</i> | <i>T. thoracinus</i> | 12 | 4 |
| | Bubebere | <i>Tabanus</i> | <i>T. thoracinus</i> | 37 | 6 |
| | Bugogo | <i>Tabanus</i> | <i>T. thoracinus</i> | 1 | 0 |
| | Mikka | <i>Tabanus</i> | <i>T. thoracinus</i> | 2 | 0 |
| | Elubbe | <i>Tabanus</i> | <i>T. thoracinus</i> | 3 | 0 |
| | Nabinonya | <i>Ancala</i> | <i>A. fasciata</i> | 2 | 2 |
| | Kawuku | <i>Chrysops</i> | <i>C. distinctipennis</i> | 1 | 1 |
| | | <i>Tabanus</i> | <i>T. thoracinus</i> | 11 | 5 |
| | Katalemwa | <i>Tabanus</i> | <i>T. thoracinus</i> | 7 | 3 |
| | Sissa | <i>Tabanus</i> | <i>T. thoracinus</i> | 16 | 4 |
| | Sanda | <i>Chrysops</i> | <i>C. distinctipennis</i> | 1 | 1 |
| | | <i>Tabanus</i> | <i>T. thoracinus</i> | 6 | 5 |
| | Kisubi | <i>Ancala</i> | <i>A. fasciata</i> | 4 | 4 |
| | | <i>Tabanus</i> | <i>T. thoracinus</i> | 9 | 1 |
| Jahazi | <i>Ancala</i> | <i>A. fasciata</i> | 4 | 3 | |
| | <i>Chrysops</i> | <i>C. brucei</i> | 1 | 1 | |
| | <i>Tabanus</i> | <i>T. thoracinus</i> | 4 | 1 | |
| Total | 209 | 85 | | | |

Morphological description of tabanids collected

Images of the tabanids collected during this study and morphologically described at the genus and species level are presented in Figures 3 and 4 as well as in Suppl. material 2: Figure S1–S13.

We identified tabanid species based on their morphology and in reference to literature of Oldroyd (1952, 1954, 1957) as well as Morita (2008).

Genus *Ancala*

Ancala fasciata Fabricius, 1775

Fig. 3A

Location. Shores of Lake Victoria, Uganda

Description. Head. Head as wide as thorax (Suppl. material 2: Figure S1A). Eyes shiny green (in freshly collected specimen), turn black after preservation in ethanol. Eyes separated by narrow brown frons with brown and black short hair. Callus (cs) brown, wide basally and tapering posteriorly to form a spindle-shaped upper callus, reaching midway frons. Scar-like callus at posterior end of frons (Suppl. material 2: Figure S1B). Antennae brown, first antennal segment (scape) is yellowish golden-brown with predominantly white hair and few black hairs that appear as a thorn-like anterior projection as on second segment. Third segment (flagellum) brown, relatively wide, with small white hair and four dark brown annulations. Second segment of the palpus is yellowish white with white recumbent hair, interspersed with few black hairs. Palpus with black tip and black labellum (Suppl. material 2: Figure S1C).

Thorax. Thorax brown with brownish-black patterns and black and golden-brown hair, with light brown median stripe that runs down to posterior end of the mesonotum. Median sublateral stripes (st) light brown; may be obscured and only reach half way of mesonotum. Scutellum yellowish and brown shades (brown with yellow postero-lateral border) with white and black hair. Prominent white hair tuft (hf) below postalar callus at base of wing (Suppl. material 2: Figure S1D). Halteres whitish yellow with a yellow stalk. Wing with typical basicosta and costa covered with short black hair with a longitudinal hairless groove. Wing with brown longitudinal cross band that runs up to discal cell and does not reach hind margin. The discal cell (dc) brown (Suppl. material 2: Figure S1A). Fore tibia differs in the species, “swollen” and black with black hair (Fig. 4A; Suppl. material 2: Figure S1E). Fore femur is brown with black and white hair, tarsus black with black hair. Hind tibia brown with a darker shade distally and lighter basally. Distally hair predominantly black with few white hair, proximal more white hair. Hind femur brownish yellow or golden yellow with white hair, tarsus dark brown with black hair. Middle leg same as hind leg.

Abdomen. Abdomen yellow with yellow and black hair. Seventh segment pointed (Suppl. material 2: Figure S1A). Ventral surface yellow with yellow hair except on last segment with white and black hair.

Genus *Tabanus*

Tabanus donaldsoni Carter, 1912

Fig. 3C

Location. Muhaka, Kenya.

Description. Head. Head wider than thorax. Eyes dark green in freshly collected insects (Fig. 4C, Suppl. material 2: Figure S3A), but turn black after storage and separated by brown narrow frons with black and white hair. Callus brown; lower callus round-oval and projects upward in form of thick line (Suppl. material 2: Figure S3B). Antennae golden brown (typical of the genus *Tabanus*). Scape with white hair at base with black hair anteriorly. Small pedicel with short white hair all over and black hair only at anterior border. Palpus (lp) yellowish white with white and black hair; labellum golden brown (Suppl. material 2: Figure S3C).

Thorax. Thorax blackish brown with white and black hair. Median stripe not seen, sub-lateral stripes light brown and indistinct (only seen up to middle of thorax). Halteres yellowish brown. Wing clear and R4 on the wing has prominent appendix (px). Tufts of white hair (hf) near postalar callus indistinct (Fig. 4C, Suppl. material 2: Figure S3D). Fore tibia and fore femure yellowish brown, fore tibia covered with white and black hair, fore femur with only white hair. Fore tarsus light brown with black and white hair. Hind and middle legs similar to forelegs (Suppl. material 2: Figure S3E).

Abdomen. Golden-brown dorsal and ventral surfaces of abdomen without patterns but have black and white recumbent hair (Suppl. material 2: Figure S3A).

Tabanus gratus Loew, 1858

Fig. 3F

Location. Tarangire National Park, Tanzania.

This fly is darker brown, smaller and slenderer than *T. taeniola* Palisot de Beauvois (1807). However, the colour of *T. gratus* Loew (1858) collected from Nguruman, Kenya is lighter brown with golden stripes on abdomen.

Description. Head. Head wider than thorax with slightly concave posterior vertex (Suppl. material 2: Figure S6A). Eyes black with green and black bands when fresh that disappear after the sample dries up. Eyes separated by dark brown frons with black hair. Basal callus dark brown, large and as wide as frons, extending upwards in slender projection connecting with smaller upper tear-drop shaped callus. On each side of upper callus a thick comma-shaped black shade. Long white parafacial hair (Suppl. material 2: Figure S6B). Scape large, light brown with white hair except at tip of the segment with black hair. Pedicel small and brown, more or less covered (obscured) between scape and flagellum, black hair at anterior end. Third segment orange brown with few black hairs. Second palpal segment whitish grey with black and white hair. Labellum brownish grey.

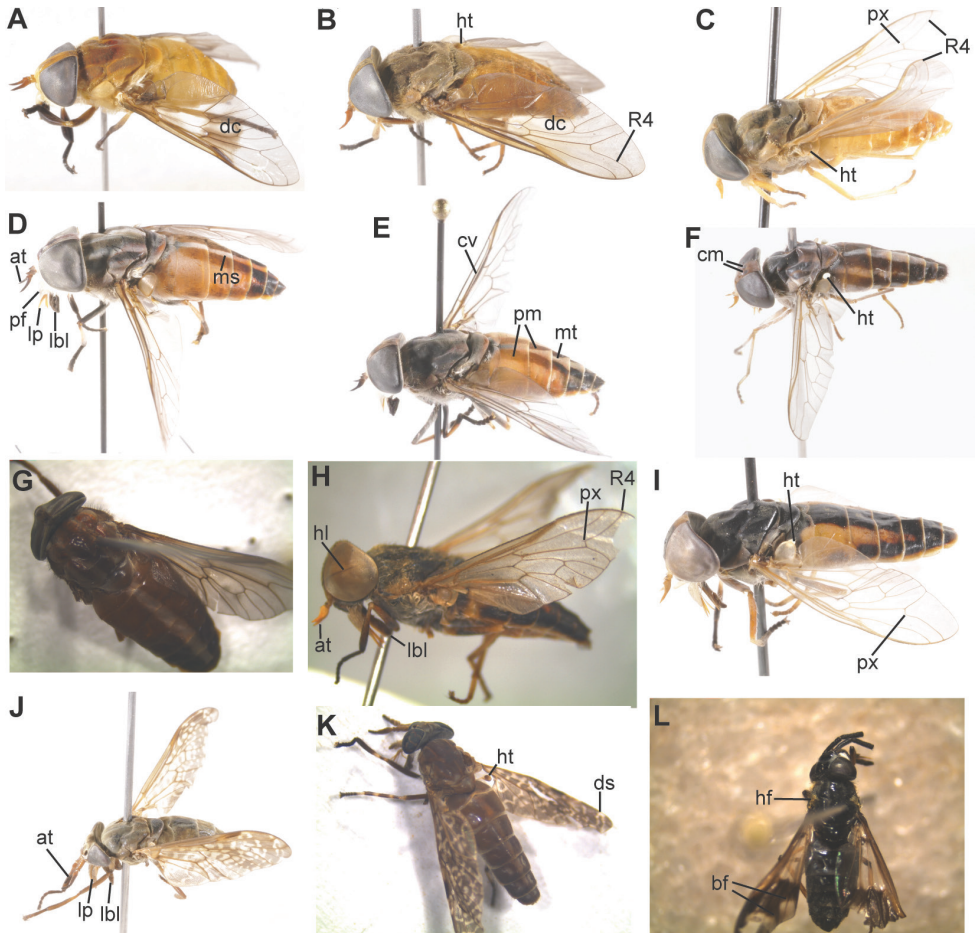


Figure 3. Whole tabanid flies. **A** *Ancala fasciata*, discal cell (dc) **B** *Tabanus thoracinus*, discal cell (dc), haltare (ht) **C** *Tabanus donaldsoni*, distinct R4 appendix (px) **D** *Tabanus taeniola*, median stripe (ms), parafacial hair (pf), antennae (at), labellum (lbl), palpus (lp) **E** *Tabanus taeniola variatus*, medial triangles (mt), peri-median bands (pm) **F** *Tabanus gratus*, haltares (ht), comma shaped shades (cm) **G** *Tabanus guineensis* **H** *Atylotus nigromaculatus*, eyes with thin black horizontal line (hl) **I** *Atylotus diurnus*, haltares (ht), wing with indistinct appendix (px) **J** *Haematopota duttoni* **K** *Haematopota fenestralis*, double white streak (ds) **L** *Chrysops distinctipennis*, hair tufts (hf), bifurcating band (bf).

Thorax. Thorax black with black and brown hair; brown median stripe traverses thorax and lateral margins of the scutellum. Sub-lateral stripes greyish brown with golden brown hair. Lateral margins of thorax greyish white. Hair tufts only seen ventrally at the base of wing. White halteres (Suppl. material 2: Figure S6A). Brown fore tibia covered with short white and black hair except anteriorly dark brown covered with black hair. Fore femur brown with black hair and long white hair. Fore tarsus black with black hair. Hind tibia light brown with white and black hair. Hind femur light brown with long white hair. Tarsus yellowish brown with black and white hair.

Middle legs same as hind legs. Wing clear and R4 has no appendix (Suppl. material 2: Figure S6C).

Abdomen. Abdomen brown, slender and tapers to the posterior end with black and brown hair, has white median and two lateral stripes pale brownish orange grey, with orange brown part at posterior end of each segment. Stripes have whitish hair. Median stripe narrow in first two segments but widens on the third, widest on the fourth segment before it tapering down to last segment. Lateral stripes wide on first and second segments but gradually narrow as they converge slightly at posterior end of abdomen. Lateral abdominal margins ashy grey (Suppl. material 2: Figure S6A). Ventral abdominal surface brown with white hair.

***Tabanus guineensis* Wiedemann, 1824**

Fig. 3G

Location. Shimba Hills, Kenya

Generally, the body is brown and slender (Suppl. material 2: Figure S7A).

Description. Head. Head black, as wide as thorax. Black eyes separated by black frons. Bi-partite callus dark brown joined by wide constricted neck and occupies more than half of frons (Suppl. material 2: Figure S7B). Antennae slender, golden-orange with black hair. Scape has prominent black anterior projection, as does pedicel. Projection on flagellum not prominent and annulations appear blackish. Second palpi white with black hair. Labellum greyish black.

Thorax. Brown thorax with two inconspicuous lateral greyish stripes. Thorax covered with recumbent black and white hair. Lateral thoracic margins grey with white hair. Scutellum brown with lighter shade posteriorly with brownish white hair especially at lateral margin. Yellowish brown hair tufts at postalar callus. Halteres light brown. Wing clear with brown pigment at the anterior margin; R4 has a short but visible appendix (Suppl. material 2: Figure S7C). Fore and hind tibia and femur brown with black hair.

Abdomen. Elongate with more or less parallel sides. Anterior abdominal segments light brown and become darker brown posteriorly with black and white hair. Abdomen bisected by a whitish median stripe with white hair. Last segment flat and rectangular (Suppl. material 2: Figure S7A).

***Tabanus taeniola* Palisot de Beauvois, 1807**

Fig. 3D

Location. Tarangire, Nguruman, Shimba Hills, Kenya

Description. Head. Head wider than thorax with long white parafacial hair (Suppl. material 2: Figure S4A). Eyes dark green in freshly collected specimen without any band; on preservation in ethanol, green colour is lost and eyes remain black. Palps with

white hair; labellum black (Suppl. material 2: Figure S4B). Antennae brown and black (typical of genus *Tabanus*). Scape and pedicel orange-brown with black hair. Flagellum orange-brown at base and darkens towards dark brown to black annulations (Suppl. material 2: Figure S4B). Eyes separated by narrow pale brown frons with black and brown hair with brown bell-shaped callus that does not taper posteriorly (Suppl. material 2: Figure S4C).

Description. Thorax. Thorax greyish black with black and whitish hair and median whitish stripe almost reaching posterior end of thorax. Sub-lateral stripes (st) ashy grey, distinctly visible with white hair and continue to posterior mesonotum. Scutellum brown with indistinct hair. Hair tufts at postalar area whitish to golden brown. Halteres yellowish white (Suppl. material 2: Figure S4C). The distal 1/3 of fore tibia blackish brown with black hair, proximal 2/3 light brown/yellow. Fore femur greyish black with black and long silver-white hair and black tibia with black hair. Hind tibia (Suppl. material 2: Figure S4D) yellowish brown with black and white hair and hind femur greyish black with white hair; tarsus light brown with black hair. Middle leg similar to hind leg.

Abdomen. Abdomen orange brown and black, tapers posteriorly such that last segment appears pointed. Abdomen with two peri-median longitudinal orange rectangular bands that progressively darken to dark brown then to black on fifth and sixth segment. Peri-median longitudinal bands enclosing lighter coloured median stripe starts anteriorly as white, becomes orange then finally darkens to light brown on sixth segment. Seventh segment completely black (Suppl. material 2: Figure S4A). Ventro-medially, fine black recumbent hair that gives abdomen dark brown appearance.

Tabanus taeniola variatus Oldroyd, 1954

Fig. 3E

Location. Tarangire National Park, Tanzania

Description. Head. Head wide, posterior vertex slightly concave (Suppl. material 2: Figure S5A). Eyes black without bands, separated by greyish frons with white hair and black hair posteriorly. Bell-shaped callus; dark brown basal callus joined to upper callus by narrow constriction (Suppl. material 2: Figure S5B). Distinct white parafacial hair as seen in *T. taeniola* described by Oldroyd (1954) (Suppl. material 2: Figure S4A), but with a different callus shape, where upper callus ends flat (not tapering), thus a different subspecies (*T. taeniola variatus*). Antennae with two shades of brown; scape is light brown with white hair at base and black hair at anterior. Anterior-most point of scapes has brownish orange tinge. Pedicel also light brown, small, appears engulfed between scape and flagellum segment with black hair anteriorly that appear as thorn-like projection. Flagellum light brown at base up to projection, but darkens anteriorly to dark brown; annulations black, similar to *T. taeniola* (Suppl. material 2: Figure S5A). Second segment of palpus dull white with white hair ventrally, dorsally few black hairs mixed among the white. Labellum black with black hair as described in *T. taeniola*.

Thorax. Thorax greyish brown with long whitish grey hair mixed with black hair. Median stripe distinctly whitish grey reaching posterior thorax. Sublateral stripes greyish white and less distinct, but nevertheless reach the posterior thorax. Dark brown scutellum with recumbent grey hair, especially at margins. Tufts of white hair at postalar callus wing base. Halteres whitish to golden yellow (Suppl. material 2: Figure S5B). Wing clear and R4 without appendix (Suppl. material 2: Figure S5C). Middle leg same as hind leg. Distal third (1/3) of fore tibia of foreleg is black with black hair; the rest of tibia light brown with white hair interspersed with few black hair (Suppl. material 2: Figure S5D). Brownish yellow hind tibia with white hair interspersed with few black hair, hind femur ashy grey with long white hair. Tarsus light brown with black hair (Suppl. material 2: Figure S5E) and each leg has two tarsal claws.

Abdomen. Abdomen golden brown with black and white hair, with dorso-medial black band on first two segments, broad on first segment and narrower on second. Band does not completely traverse second segment. Segments with distinct triangular pattern medially light brown anteriorly and fades into greyish brown posteriorly. Triangular patterns have black hair mixed with white hair. Abdomen with black hair laterally; medial abdomen greyish brown with white and black hair. Ventrally brown surface with whitish hair except for last two black segments (Suppl. material 2: Figure S5A).

***Tabanus thoracinus* Palisot de Beauvois, 1806**

Fig. 3B

Location. Shores of Lake Victoria, Uganda

Two genetic variants, that could not be distinguished on the basis of the morphological keys identified in the present study.

Description. Head. Head wider than the thorax (Suppl. material 2: Figure S2A) with yellowish white parafacial hair (pf). Eyes dark green (when freshly collected, before drying) without a band, separated by brown narrow frons with black and white hair. Antennae golden-brown (typical of *Tabanus*). Scape with white hair at base and black hair anteriorly, thus appearing to have a black tip (Suppl. material 2: Figure S2B). Small pedicel with short white hair all over and black hair only at anterior border. Callus (cs) brown; basal callus round-oval and projects upward tapering to form a thick black line (Suppl. material 2: Figure S2C). Palps yellowish white with white and black hair; labellum brown (Suppl. material 2: Figure S2B).

Thorax. Thorax blackish brown with white and black hair and invisible median stripe, sub-lateral stripes indistinct light brown only to middle of thorax. Wing clear and R4 does not have appendix (Suppl. material 2: Figure S2A). Fore tibia and fore femur yellowish brown; fore tibia covered with white and black hair, fore femur with white hair (Suppl. material 2: Figure S2D). Fore tarsus light brown with black and white hair. Hind and middle legs similar to forelegs. Halteres yellowish brown. Indistinct tufts of white hair near postalar callus.

Abdomen. Dorsal and ventral surfaces of abdomen orange-brown without patterns, have black and white recumbent hair. Ventral surface may have black hair concentrated on second last segment that appears as dark patch (Suppl. material 2: Figure S2A).

Genus *Atylotus*

Atylotus nigromaculatus Ricardo, 1900

Fig. 3H

Location. Tarangire National Park, Tanzania; Nguruman, Kenya.

Generally, slender body covered with dense golden-brown hair (Suppl. material 2: Figure S8A).

Description. Head. Head wide, posterior vertex slightly concave. Eyes pale golden brown with thin black horizontal line or band. Eyes separated by narrow golden-brown frons on posterior quarter and black anteriorly. Callus in two well-separated lower and upper parts shiny black and vaguely round (Suppl. material 2: Figure S8B). Antenna golden brown; Scapes with white hair and black hair anteriorly as does the pedicel. Pedicel less distinct as it closely adheres to much larger flagellum. Second palp segment white with white and black hair but only white hair seen ventrally; brown labellum (Suppl. material 2: Figure S8B).

Thorax. Black thorax with indistinct stripes and golden-brown hair (Suppl. material 2: Figure S8C). Indistinct hair tufts at postalar callus. Halteres yellowish white and clear wing; R4 with small appendix (Fig. 4D; Suppl. material 2: Figure S8A). Fore tibia black distally and light brown towards femur with black and white hair. Fore femur brown with grey patch at proximal end with white hair all over. Fore tarsus black with black hair (Suppl. material 2: Figure S8D). Hind tibia light brown with black and white hair, while hind femur light brown and proximally blackish grey with white hair all over the femur. Hind tarsus light brown with black and white hair (Suppl. material 2: Figure S8E); middle leg similar to hind leg.

Abdomen. Brown abdomen, slender and slightly tapers posteriorly. Broad black median band that longitudinally dissects abdomen; band with black recumbent hair (Fig. 4D). Brown patches with brown recumbent hair on either side of the band on first to fourth segment. Fifth to seventh segments black. Lateral abdominal margins black (Suppl. material 2: Figure S8C). Ventral surface of abdomen brown with white hair and dark grey margins.

Note. *Atylotus nigromaculatus* is the only species in genus *Atylotus* described by Oldroyd (1954) whose eyes have no band. The morphological features described in this study are similar to features described by Taioe et al. (2017) of specimen collected from South Africa.

***Atylotus diurnus* Walker, 1850**

Fig. 3I

Location. Muhaka, Shimba Hills, Nguruman, all in Kenya.

Generally, the body is slender and not as hairy as in *At. nigromaculatus* described above.

Description. Head. Head wider than thorax and eyes pale black without band (Suppl. material 2: Figure S9A). Eyes separated by narrow frons brown on posterior quarter and black anteriorly with black and golden-brown hair. Basal callus brownish black and upper callus black. Two small calli vaguely rounded and well separated (Suppl. material 2: Figure S9B). Antenna yellowish orange; scape light yellow with white hair at base and black hair at anterior end as does the pedicel. Pedicel small with projection and is less distinct as it closely adheres to the much larger flagellum. Flagellum orange with blunt projection with small black hair. Second palp segment white with white and black hair; labellum dark brown (Suppl. material 2: Figure S9A).

Thorax. Thorax greyish black without visible median stripe, but lateral stripes black and indistinct, halteres white (Suppl. material 2: Figure S9A). Clear wing and R4 with short appendix (Suppl. material 2: Figure S9C). Legs as described in *At. nigromaculatus*.

Abdomen. Abdomen with thick black band running medially to last segment with black and few white hair; light brown part that is broader anteriorly but narrows posteriorly such that the sixth and seventh segments are completely black. Brown parts of abdomen with black and white hair, black part with mostly black hair and few white hairs. Lateral margins of abdomen black (Suppl. material 2: Figure S9A).

Note. *Atylotus diurnus* is the only species described by Oldroyd (1952) whose wing has an appendix on the R4 of the wing. Though the other morphological features described here are different from those described by Oldroyd (1952), they are similar to those described by Taioe et al. (2017), thus confirming that the specimen are indeed *Atylotus diurnus*.

Genus *Haematopota****Haematopota duttoni* Newstead, Dutton & Todd, 1907**

Fig. 3J

Location. Shimba Hills, Kenya.

Description. Head. Head wider than thorax with vertex at the posterior distinctly concave (Suppl. material 2: Figure S10A). Black eyes with brightly coloured zig-zag bands that fade on preservation. Eyes separated by wide frons; anterior third (1/3) of frons brown with brown and black hair, posteriorly blackish grey with whitish grey hair. Frontal callus shiny brown, wider than long, spanning entire width of frons. Pair of round dark brown purplish velvety spots above frontal callus at either side towards lateral margins of frons. Below frontal callus velvety dark brownish black sub callus.

Below vertex of frons medially small black round velvety spot (Suppl. material 2: Figure S10B). Antennae typical of genus *Haematopota*; three segments dark brown with black and few short white hairs. Scape long and slightly wide, pedicel globular with anterior spike-like projection. Flagellum long and slender with three black annulations that have fine black hair. Second palpal segment elongate, light brown with white and black hair. Labellum dark brown (Suppl. material 2: Figure S10C).

Thorax. Thorax greyish brown with black and white hair. Median and sub lateral stripes whitish and run down to the posterior end of thorax. Fore tibia laterally flattened and dark brown with black and (few) white hair. Fore femur dark brown with black hair. Hind tibia dark brown with black and white hair; hind femur dark brown with black hair. Middle legs resemble hind legs. Tarsi of all legs dark brown with black hair. Wing is brown and mottled characteristic of genus, with typical basicosta with sharp projection and costa covered with short black hair without longitudinal groove. Wing with brown patterns (descriptive of species *H. duttoni*) and right-angled thick white line (shaped as “7”) running from vein A1 towards wing margin. Wing vein R4 with long appendix (Fig. 4E, Suppl. material 2: Figure S10D). Halteres yellowish white centrally and progressively darken to light brown and then to darker brown at margin. Stalk of halteres yellowish white.

Abdomen. Abdomen dark brownish black without patterns and with black and white hair and lateral margins almost parallel to each other. Ventrally, abdomen ashy grey with black hair. Median part dark brown with fine white hair (Suppl. material 2: Figure S10A).

***Haematopota fenestralis* Oldroyd, 1952**

Fig. 3K

Location. Shimba Hills, Zunguluka, Kenya,

Flies in this species are smaller than *H. duttoni* Newstead, Dutton & Todd (1907) described above.

Description. Head. Head black, broader than long (Suppl. material 2: Figure S11A). Eyes black with colourful bands and separated by wide, more or less square greyish black frons. Frons with short black hair and few white hairs. Frontal callus black and glossy, broad but shorter than and not as convex as in previously described species. Sub callus brownish black and velvety, continuous with frontal callus. Small oval pale black spot medially above frontal callus close to vertex. Antennae brownish grey (tan) with three segments typical of *Haematopota*; scape long and narrower than in *H. duttoni* with black hair, second is globular with anterior thorn-like projection with black hair, flagellum narrow and brown towards base, black annulations with black hair. Second segment of palpus grey with black and white hair, labellum brownish black (Fig 4F; Suppl. material 2: Figure S11B).

Thorax. Thorax greyish brown with clear thin brown medial stripe extending to posterior end of mesonotum, and brown sublateral stripes, slightly wider than median

stripe but only reach half way mesonotum. Posterior mesonotum ashy grey, scutellum greyish brown. Halteres yellowish white medially but progressively darken into brown at periphery. Stalks of halteres yellowish white. Fore tibia slightly swollen (wide) anteriorly with yellowish transverse band towards proximal end with white hair. Fore femur dark brown with dark brown hair and few white hairs. Fore tarsus dark brown with dark brown hair. Hind tibia with two transverse bands, proximally and medially; hind femur dark brown with black and white long hair; hind tibia dark brown with black hair and white bands with white hair. Middle leg looks like hind leg. No hair tufts at postalar tufts. Wing with brown and mottled patterns descriptive of genus. Thick double white streak running across wing apex from anterior, as indicated in black oval in Suppl. material 2: Figure S11C.

Abdomen. Narrow abdomen tapers slightly posteriorly (Suppl. material 2: Figure S11A). Dark brown and even darker on segments 4 to 7 with black and white hair. Ventral abdominal surface ashy grey with white hair; thick shiny brown patch with fine black hair medially on all segments.

Genus *Chrysops*

Generally, members of this genus are fragile black flies smaller than all the previously described genera. Members have a characteristic black band that transverses the wing from anterior to posterior margin (Fig. 3L).

Chrysops distinctipennis Austen, 1906

Fig. 3L

Location. Wakiso, Uganda

Description. Head. Head as wide as thorax with black eyes separated by greyish black frons. Frons widens slightly towards antennae with black and long white standing hair (Suppl. material 2: Figure S13A). Callus black and glossy. Basal callus wider than long and rectangular shaped; upper callus with three black ocelli arranged in triangular pattern (two lateral and one median ocellus). Antennae black, long and slender with black hair. Scape and pedicel equal in length and longer than in *C. brucei* (Suppl. material 2: Figure S13B); flagellum has 4 annulations. Second segment of palpus brownish black, slender with black hair; black labellum.

Thorax. Thorax black with black and white hair, no evident stripes. Tufts of golden yellow hair at postalar callus and at notopleural and humeral lobes (Suppl. material 2: Figure S3B). Halteres black with black stalk. Legs brown with black hair; fore tibia darker brown shade and black distally; tarsus of fore leg black with black hair; tarsi of middle and hind legs brown with black hair. Femurs of all legs black proximally and distally. Clear wing with longitudinal dark brown band that bifurcates into two smaller bands that reach posterior wing margin (Suppl. material 2: Figure S13C).

Abdomen. Abdomen black with black hair and parallel lateral sides; posterior border of each segment distinctly grey. Seventh segment rather rounded (Suppl. material 2: Figure S13C). Ventral surface black with long fine whitish hair.

***Chrysops brucei* Austen, 1907**

Fig. 4G

Location. Wakiso, Uganda

Description. Head. Head as wide as thorax with black eyes separated by dark brown frons. Frons widened slightly towards antennae and has black and brown long-standing hair. Callus black and glossy. Lower callus wider than long and oval shaped; upper callus with three ocelli arranged in triangular pattern (two lateral and one median ocellus) (Suppl. material 2: Figure S12A). Antennae black with long black hair. Scape and pedicel almost of equal length although scapes slightly longer. Flagellum equally slender with indistinctly marked annulations. Second segment of the palpus brown, slender with black hair; labellum black (Fig. 4G; Suppl. material 2: Figure S12B).

Thorax. Black thorax with black and brown hair; sub-lateral stripes brown and reach posterior border of mesonotum. Basicosta of wing black with prominent thorn-like projection, while the costa is slender and long without longitudinal groove. Clear wing with longitudinal dark brown band that does not reach posterior margin. Fore leg dark brown with dark brown hair (Suppl. material 2: Figure S12B). Black halteres and stalk.

Abdomen. Abdomen black with black and white hair and parallel lateral sides that taper slightly at fifth segment. Each segment ashy grey at posterior margin with predominantly white hair. Indistinct greyish median stripe. Seventh segment rounded; ventral abdominal surface black with long fine whitish hair.

Discussion

The aim of this study was to identify, re-describe and document tabanids in East Africa using morphological features and molecular tools and therefore contribute to understanding the diversity of this important group of disease vectors. It is evident that a highly diverse tabanid fauna is prevalent in the areas where the study was carried out.

The specimens in the genus *Atylotus* were initially assigned species names based on their morphological features and were found to differ from those that had been described by Oldroyd (1954). These differences may be accounted for by differences in sampling sites in Ethiopia (Oldroyd 1954) versus Tanzania (Tarangire National Park) and Kenya (Nguruman, southern Kenya) in the current study. These observations may be due to cryptic speciation as was suggested by Schutz et al. (1989). This observation followed a population-genetic study of adult female *Tabanus lineola lineola* Fairchild from New Jersey and Louisiana and determined the coastal and inland “varieties” *T.*



Figure 4. Key morphological features of sampled tabanid species. **A** *Ancala fasciata* **B** *Tabanus donaldsoni* green eyes (in fresh sample) **C** *Tabanus donaldsoni*, wing with distinct R4 appendix (px), indistinct hair tuft (hf) **D** *Atylotus nigromaculatus*, wing with short, clear appendix on R4 **E** *Haematopota duttoni*, mottled wing with a right angled white thick line (in black circle) between vein A1 and the wing margin, the R4 has a long appendix **F** *Haematopota fenestralis*, shiny black callus on frons, eyes have bright coloured bands **G** *Chrysops brucei*, lateral view of head showing the antenna, black mouth parts and brown legs (partial).

lineola binellus Philip and *T. lineola lineola* Fairchild based on four easily measured morphological characters. In that study, Schutz et al. (1989) found that nine individuals in the study population were genetically distinct from all other specimens and probably represented a third cryptic species. In the current study, the two different *Atylotus* species (*At. nigromaculatus* and *At. diurnus*) clustered together irrespective of their distribution and morphology. These species that were collected in different areas in Kenya (Sampu, Muhaka, Mukinyo) and Tanzania (Sangaiwe, and Poachers Hide)

could not be differentiated based on their *COI* barcode sequences, which were nonetheless different from *At. miser* previously sampled in China (Wang et al. 2016). Furthermore, *COI* barcoding in the current study showed that *T. gratus* from Nguruman in Kenya differed from *T. gratus* collected from Tanzania. Morphological differences were also observed where *T. gratus* from Kenya showed a lighter brown abdomen when compared to those from Tanzania.

In addition, *COI* barcoding was able to differentiate *T. taeniola* sensu stricto from its subspecies *T. taeniola variatus*; the later showed some morphological differences (shape of the callus and the patterns on the dorsal surface of the abdomen) and formed a cluster distinct from *T. taeniola*. These observed differences may be due to the sampling locations of the specimen. Similarly, in India, a total of 46 specimens belonging to seven species in four genera in two subfamilies were analysed in a recent study using DNA barcoding; all morphologically identifiable species were successfully discriminated. The study further demonstrated the presence of cryptic species in *Chrysops dispar* and was also able to discriminate closely related species in a “*Tabanus striatus* species complex” that had no stable taxonomic distinguishing characters (Benerjee et al. 2015). Differences in morphological features and DNA barcodes were used as a basis to consider new haplomorphs of deerflies and horseflies that were identified in the study conducted in Canada. Among the specimens, each tabanid species was found to possess distinct sets of *COI* haplotypes which discriminated well among species (Cywinska et al. 2010). Therefore, the authors suggested that *Chrysops montanus* be provisionally differentiated into two haplotypes namely *Ch. montanus* haplomorph 1 and *Ch. montanus* haplomorph 2, each defined by their molecular sequences and by newly discovered differences in structural features near the ocelli. Cryptic species have also been described in other insect species including biting midges in Sweden, where two cryptic species were created within each of the species of *Culicoides obsoletus* and *C. newsteadi* (Diptera: Ceratopogonidae) following the demonstration of a relatively deep intraspecific divergence (Ander et al. 2013). This may be the case with two *T. thoracinus* B sequences obtained in this study, which were morphologically indistinguishable from those in the distinct *T. thoracinus* A clade, but clustered closer to *T. donaldsoni*. Our results demonstrate that morphologically identical *T. thoracinus* could correspond to different species, thus the need to revise the taxonomy of tabanids.

Given the continuous ecosystem with the movement of pastoralists and their livestock across borders, as well as wild fauna, the presence of diverse species of tabanids across the East African region is indicative of the risk for disease transmission. Further study of tabanids in the region is warranted. A better coverage of the tabanids in different ecosystems, including the conservation areas and farming communities, will allow better understanding of the risk of transmission of diseases vectored by these flies in both wild and domestic animals. Such information will also be useful for the ecologist and epidemiologist as expounded by Valentini et al. (2008). The conservation areas of Shimba Hills in Kenya were found to have a more varied range of tabanids despite the fact that the tabanid flies were not the main target of the collection but rather the tsetse fly. Traps routinely used for tsetse flies (NG2G and biconical) (Egri et al. 2013; All-

sopp 1984) were used in Kenya and Tanzania and this may have led to non-exhaustive sampling. The varied range may be attributed to by the higher number of tabanids that were collected in the Shimba Hills compared to numbers collected in other study areas. Further surveys should use traps better optimised for tabanids including canopy traps that have been documented to efficiently trap tabanids (Muirhead-Thomson 1991) and have been further improved by addition of carbondioxide (CO₂) or chemical attractants, e.g. ammonia, phenol, octenol or acetone (Hribar et al. 1992; Mihok et al. 2006; Mihok and Lange 2012). To further enhance the catch of male tabanids, there have been suggestions to supplement the canopy trap with a liquid trap that enhances catches 2.4–8.2 times more tabanids than the canopy trap alone (Egri et al. 2013). The Nzi trap is another option that is used in Africa to capture tabanids; it is simple, economic and efficient (Mihok 2002); it was shown to trap statistically more tabanids than other conventional traps (including NG2G, a triangular, one-winged trap) and equivalent to the canopy trap (Mihok 2002).

Attempts to document Tabanidae in conservation areas in East Africa have been minimal. Nonetheless, tabanids of the Afrotropical region of southern Africa have been recently re-described, including discussion on their biology, immature stages, economic importance, and classification with a resultant identification key of Afrotropical Tabanidae (Chainey 2017). Studies exploring tabanid flies in Muhale Mountains National Park in Tanzania have similarly shown a sizable number of species (17) that fed on chimpanzees (Sasaki and Nishida 1999; Sasaki 2005). One of the species in Muhale (*T. gratus*) was also found in Tarangire National Park in the current study; all the other species were different. The difference may be due to the different techniques used (NG2G trap in Tarangire versus Nzi trap in Muhale) but may also be attributed to the differences in the climate and vegetation cover of the two sites in Tanzania that were a forested mountain and a thickly and mixed woodland. Inevitably, there is need to understand the influence of climate on the prevalence of vectors thus be able to forecast vector-borne disease outbreaks in a given ecosystem (Gubler 2008).

There are new technologies that can be used to enhance the understanding of relationships between the environment and vector as well as risk of emerging vector-borne diseases. These tools continuously capture and analyse a wide range of environmental data including weather, land cover and use, water and atmospheric conditions (Ostfeld et al. 2005) that can be applied in research on vector-borne diseases (Beck et al. 2000). Using new statistical methods, spatial patterns in this data can reveal relationships between the vector and vector-borne pathogen (cause) and disease (effect) (Hay et al. 2000, 2007).

In East Africa, inter-organismic relationship studies using DNA barcoding have been done to identify the source(s) of blood meal for tsetse flies (genus *Glossina*) and reported diverse source of blood meal including wild mammals (buffalo, giraffe, warthog, elephant and spotted hyena), livestock (cattle). These approaches have similarly been used to identify the diverse blood meal hosts of mosquitoes (Lutomiah et al. 2014; Omondi et al. 2015). The authors of these studies note that these results are useful in designing effective vector control strategies based on their host preferences in

the various intervention areas. Among others, these studies strongly suggest that DNA barcoding is a promising tool for diversity studies, phylogeographic analyses as well as evolutionary studies of arthropods specifically as vectors, and thus could provide a globally important tool for controlling pests. However, to efficiently use these novel tools, there is a need for sustained capacity building in public health as well as in environmental/climatic studies and to understand how the two disciplines can be merged in vector-borne disease research (Fish 2002).

Conclusion

This is the first study that describes in detail the morphology of diverse tabanids from various locations in Kenya, Tanzania and Uganda. The list of tabanids presented in this paper is largely incomplete given the limited study sites and duration of sampling. Thus, further investigation is required to comprehend the whole fauna of tabanid flies and their habitat. Wider surveys that integrate climatic factors, pathogens carried by the tabanids, blood meal sources for the flies, as well as the effect of human activity on their distribution are necessary if the diversity, prevalence and role of tabanids in disease transmission are to be better understood. This will, in turn, enable the instigation of more efficient control measures against these neglected vectors. The findings from the hand-full of sampling sites indicate a need to further investigate neglected insects on a larger scale to establish a concrete tabanid checklist in East Africa.

Acknowledgements

We thank the Coordinating Office for Control of Trypanosomiasis in Uganda (COC-TU), Kenya Wildlife Service, and Tanzania National Parks Authority for facilitating the collections. We are grateful to Canadian Centre for DNA Barcoding, University of Guelph for the sequence analysis of the samples used in this study. We are also thankful to members of the Bio-systematics Unit (BSU) in *icipe*-Nairobi for technical assistance rendered. This work was supported by Training Health Researchers into Vocational Excellence in East Africa (THRiVE), grant number 087540 funded by the Wellcome Trust, with additional support from the Wellcome Trust (grant 093692) to the University of Glasgow, and *icipe* institutional funding from the UK's Department for International Development (DFID), the Swedish International Development Cooperation Agency (SIDA), the Swiss Agency for Development and Cooperation (SDC), and the Kenyan Government. The funding bodies did not play a role in the design of this study, the collection, analyses and interpretation of data, the writing of the manuscript, or decision to submit the manuscript for publication. The contents of this study are solely the responsibility of the authors and do not necessarily represent the official views of the supporting offices.

References

- Allsopp R (1984) Control of tsetse flies (Diptera: Glossinidae) using insecticides: a review and future prospects. *Bulletin of Entomology Research* 74: 1–3. <https://doi.org/10.1017/S0007485300009895>
- Altschul SE, Gish W, Miller W, Myers EW, Lipman DJ (1990) Basic local alignment search tool. *Journal of Molecular Biology* 215:403–410. [https://doi.org/10.1016/S0022-2836\(05\)80360-2](https://doi.org/10.1016/S0022-2836(05)80360-2)
- Ander M, Troell K, Chirico J (2013) Barcoding of biting midges in the genus *Culicoides*: a tool for species determination. *Medical and Veterinary Entomology* 27: 323–331. <https://doi.org/10.1111/j.1365-2915.2012.01050.x>
- Ball SL, Hebert PDN, Burian SK, Webb JM (2005) Biological identifications of mayflies (*Ephemeroptera*) using DNA barcodes. *Journal of North American Benthological Society* 24: 508–524. <https://doi.org/10.1899/04-142.1>
- Barret RDH, Hebert PDN (2005) Identifying spiders through DNA barcodes. *Canadian Journal of Zoology* 83: 481–491. <https://doi.org/10.1139/z05-024>
- Beck LR, Lobitz BM, Wood BL (2000) Remote sensing and human health: new sensors and new opportunities. *Emerging Infectious Diseases* 6: 217–227. <https://doi.org/10.3201/eid0603.000301>
- Brightwell R, Dransfield RD, Kyorku C, Golder TK, Tarimo SA, Mungai D (1987) A new trap for *Glossina pallidipes*. *Tropical Pest Management* 33: 151–189. <https://doi.org/10.1080/09670878709371136>
- Buxton BA, Hinkle NC, Schultz RD (1985) Role of insects in the transmission of bovine leukosis virus: potential for transmission by stable flies, horn flies, and tabanids. *American Journal of Veterinary Research*, 46: 123–126.
- Chainey J (2017) Horse-flies, deer-flies and clegs (Tabanidae). In: Kirk-Sprogs AH, Sinclair BJ (Eds) *Manual of Afrotropical Diptera, Nematoceros Diptera and lower Brachycera*. South African National Biodiversity Institute, Pretoria, 893–913.
- Cywinska A, Hannan MA, Kevan PG, Roughley RE, Iranpour M, Hunter FF (2010) Evaluation of DNA barcoding and identification of new haplomorphs in Canadian deerflies and horseflies. *Medical and Veterinary Entomology* 24: 382–410. <https://doi.org/10.1111/j.1365-2915.2010.00896.x>
- Desquesnes M, Dia ML (2003) Mechanical transmission of *Trypanosoma congolense* in cattle by the African tabanid *Atylotus agrestis*. *Experimental Parasitology* 105: 226–231. <https://doi.org/10.1016/j.exppara.2003.12.014>
- Desquesnes M, Dia ML (2004) Mechanical transmission of *Trypanosoma vivax* in cattle by the African tabanid *Atylotus fuscipes*. *Veterinary Parasitology* 119: 9–19. <https://doi.org/10.1016/j.vetpar.2003.10.015>
- Drummond AJ, Rambaut A (2007) BEAST: Bayesian evolutionary analysis by sampling trees. *BMC Evolutionary Biology* 7: 214. <https://doi.org/10.1186/1471-2148-7-214>
- Duke BOL (1955) Symposium on loiasis. IV The development of *Loa* in flies of the genus *Chrysops* and the probable significance of the different species in the transmission of loiasis. *Transactions of the Royal Society of Tropical Medicine and Hygiene* 49: 115–121.

- Egri Á, Blahó M, Száz D, Kriska G, Majer J, Herceg T, Gyurkovszky M, Farkas R, Horváth G (2013) A horizontally polarizing liquid trap enhances the tabanid-capturing efficiency of the classic canopy trap. *Bulletin of Entomological Research* 103: 665–674. <https://doi.org/10.1017/S0007485313000357>
- Fish D (2002) Interdisciplinary focus Vector Borne Zoonotic Diseases. *Vector-Borne and Zoonotic Diseases* 2: 1. <https://doi.org/10.1089/153036602760260715>
- Foil LD, Seger CL, French DD, Issel CJ, McManus JM, Ohrberg CL, Ramsey RT (1988) Mechanical transmission of bovine leukemia virus by horse flies (Diptera: Tabanidae). *Journal of Medical Entomology* 25: 374–376. <https://doi.org/10.1093/jmedent/25.5.374>
- Gardiner PR, Wilson AJ (1987) *Trypanosoma* (Duttonella) *vivax*. *Parasitology Today* 3: 49–52. [https://doi.org/10.1016/0169-4758\(87\)90213-4](https://doi.org/10.1016/0169-4758(87)90213-4)
- Gubler DJ (2008) The global threat of emergent/re-emergent vector-borne diseases. *Vector-Borne Diseases: Understanding the environmental, human health, and ecological connections*; Institute of Medicine. The National Academies Press, Washington, D.C., 43–64
- Guindon S, Dufayard JF, Lefort V, Anisimova M, Hordijk W, Gascuel O (2010) New Algorithms and Methods to Estimate Maximum-Likelihood Phylogenies: Assessing the Performance of PhyML 3.0. *Systematic Biology* 59: 307–321. <https://doi.org/10.1093/sysbio/syq010>
- Hay SI, Randolph SE, Rogers DJ (2000) Remote sensing and geographical information systems in epidemiology. *Advances in Parasitology*, Academic Press, London, UK.
- Hay SI, Graham AJ, Rogers DJ (2007) Global mapping of infectious diseases: Methods, examples and emerging applications. *Advances in Parasitology*, Academic Press, London, UK.
- Hribar LJ, LePrince DJ, Foil LD (1992) Ammonia as an attractant for adult *Hybomitra lasiophthalma* (Diptera: Tabanidae). *Journal of Medical Entomology* 29: 346–348. <https://doi.org/10.1093/jmedent/29.2.346>
- Katoh K, Standley DM (2013) MAFFT Multiple Sequence Alignment Software Version 7: Improvements in Performance and Usability. *Molecular Biology and Evolution* 30: 772–778. <https://doi.org/10.1093/molbev/mst010>
- Kearse M, Moir R, Wilson A, Stones-Havas S, Cheung M, Sturrock S, Buxton S, Cooper A, Markowitz S, Duran C, Thierer T, Ashton B, Meintjes P, Drummond A (2012) Geneious Basic: An integrated and extendable desktop software platform for the organization and analysis of sequence data. *Bioinformatics* 28: 1647–1649. <https://doi.org/10.1093/bioinformatics/bts199>
- Kent RJ (2009) Molecular methods for arthropod blood meal identification and applications to ecological and vector-borne disease studies. *Molecular Ecology Resources* 9: 4–18. <https://doi.org/10.1111/j.1755-0998.2008.02469.x>
- Kuzoe FAS, Schofield CJ (2005) Strategic review of traps and targets for tsetse and African trypanosomiasis control <http://www.who.int/tdr/publications/tsetsetraps.html>.
- Lutumiah J, Omondi D, Masiga D, Mutai C, Mireji PO, Ongus J, Linthicum KJ, Sang R (2014) Blood meal analysis and virus detection in blood-fed mosquitoes collected during the 2006–2007 Rift Valley fever outbreak in Kenya. *Vector-Borne and Zoonotic Diseases* 14: 656–664. <https://doi.org/10.1089/vbz.2013.1564>
- Manet G, Guilbert X, Roux A, Vuillaume A, Parodi AL (1989) Natural mode of horizontal transmission of bovine leukemia virus (BLV): the potential role of tabanids (*Tabanus*

- spp.). *Veterinary Immunology and Immunopathology* 22: 255–263. [https://doi.org/10.1016/0165-2427\(89\)90012-3](https://doi.org/10.1016/0165-2427(89)90012-3)
- Mihok S (2002) The development of a multipurpose trap (the Nzi) for tsetse and other biting flies. *Bulletin of Entomological Research* 92: 385–403.
- Mihok S, Carlson DA, Krafusur ES, Foil LD (2006) Performance of the Nzi and other traps for biting flies in North America. *Bulletin of Entomological Research* 96: 367–397. <https://doi.org/10.1079/BER2002186>
- Morita SI, Bayless KM, Yeates DK, Wiegmann B M (2016) Molecular phylogeny of the horse flies: a framework for renewing tabanid taxonomy. *Systematic Entomology* 41: 56–72. <https://doi.org/10.1111/syen.12145>
- Muturi CN, Ouma JO, Malele II, Ngure RM, Rutto JJ, Mithöfer KM, et al. (2011) Tracking the feeding patterns of tsetse flies (*Glossina* genus) by analysis of blood meals using mitochondrial cytochromes genes. *PLoS ONE* 6(2): e17284. <https://doi.org/10.1371/journal.pone.0017284>
- Monti GE, Frankena K, De Jong MCM (2007) Evaluation of natural transmission of bovine leukaemia virus within dairy herds of Argentina. *Epidemiology and Infection* 135: 228–237. <https://doi.org/10.1017/S0950268806006637>
- Mihok S, Lange K (2012) Synergism between ammonia and phenols for *Hybomitra* tabanids in northern and temperate Canada. *Medical and Veterinary Entomology* 26: 282–290. <https://doi.org/10.1111/j.1365-2915.2011.00999.x>
- Muirhead-Thomson RC (1991) *Trap Responses of Flying Insects: The Influence of Trap Design on Capture Efficiency*. Academic Press, Harcourt Brace Jovanovich Publishers, London, New York.
- Oldroyd H (1952) The horseflies (Diptera: Tabanidae) of the Ethiopian Region. Volume I. *Haematopota* and *Hippocentrum*. British Museum (Natural History), London, 226 pp.
- Oldroyd H (1954) The horseflies (Diptera: Tabanidae) of the Ethiopian Region. Volume II. *Tabanus* and related genera. British Museum (Natural History), London, 341 pp.
- Oldroyd H (1957) The horseflies (Diptera: Tabanidae) of the Ethiopian Region. Volume III. Subfamilies *Chrysopsinae*, *Scepsidinae* and *Pangoniinae* and a revised classification. British Museum (Natural History), London, 489 pp.
- Omondi D, Masiga DK, Ajamma YU, Fielding BC, Njoroge L, Villinger J (2015) Unraveling host-vector-arbovirus interactions by two-gene high resolution melting mosquito blood-meal analysis in a Kenyan wildlife-livestock interface. *PLoS ONE* 10: e0134375. <https://doi.org/10.1371/journal.pone.0134375>
- Ostfeld RS, Glass GE, Keesing F (2005) Spatial epidemiology: an emerging (or re-emerging) discipline. *Trends in Ecological Evolution* 20: 328–336. <https://doi.org/10.1016/j.tree.2005.03.009>
- Ratnasingham S, Hebert PDN (2007) BOLD: The Barcode of Life Data System. *Molecular Ecology Notes* 7: 355–364. <https://doi.org/10.1111/j.1471-8286.2007.01678.x>
- Schutz SJ, Gaugler RR, Vrijenhoek RC (1989) Genetic and morphometric discrimination of coastal and inland *Tabanus lineola* (Diptera: Tabanidae). *Annual Entomological Society of America* 82: 220–224. <https://doi.org/10.1093/aesa/82.2.220>
- Sasaki H (2005) Tabanid flies (Diptera: *Tabanidae*) of the Mahale Mountains National Park, Tanzania, East Africa. *Journal of Rakuno Gakuen University* 30: 93–98.

- Sasaki H, Nishida T (1999) Notes on the flies associated with wild chimpanzees at Ma hale Mountains National Park, Tanzania, East Africa. *Medical Entomology and Zoology* 50: 151–155. <https://doi.org/10.7601/mez.50.151>
- Taioe MO, Motloang YM, Namangala B, Chota A, Molefe NI, Musinguzi S, Suganuma K, Hayes P, Tsilo TJ, Chainey J, Inoue N, Thekiso, OMM (2017) Characterization of tabanid flies (Diptera: *Tabanidae*) in South Africa and Zambia and detection of protozoan parasites they are harbouring. *Parasitology* 144: 1162–1178. <https://doi.org/10.1017/S0031182017000440>
- Valentini A, Pompanon F, Taberlet P (2008) DNA barcoding for ecologists. *Trends in Ecology and Evolution* 24: 110–117. <https://doi.org/10.1016/j.tree.2008.09.011>
- Walker F (1850) Diptera. Part I. In: Saunders WW (Ed.) 1. *Insecta Saundersiana: Or Characters of Undescribed Insects in the Collection of William Wilson Saunders, Esq., F.R.S., F.L.S., &c.*, Van Voorst, London, 6–17.
- Wang K, Li X, Ding S, Wang N, Mao M, Wang M, Yang D (2016) The complete mitochondrial genome of the *Atylotus miser* (Diptera: Tabanomorpha: Tabanidae), with mitochondrial genome phylogeny of lower Brachycera (Orthorrhapha) 586: 184–96. <https://doi.org/10.1016/j.gene.2016.04.013>
- Waugh J (2007) DNA barcoding in animal species: progress, potential and pitfalls. *BioEssays* 29: 188–197. <https://doi.org/10.1002/bies.20529>

Supplementary material I

Tabanidae collected (n) from Uganda, Kenya and Tanzania

Authors: Claire M. Mugasa, Jandouwe Villinger, Joseph Gitau, Nelly Ndungu, Marc Ciosi, Daniel Masiga

Copyright notice: This dataset is made available under the Open Database License (<http://opendatacommons.org/licenses/odbl/1.0/>). The Open Database License (ODbL) is a license agreement intended to allow users to freely share, modify, and use this Dataset while maintaining this same freedom for others, provided that the original source and author(s) are credited.

Link: <https://doi.org/10.3897/zookeys.769.21144.suppl1>

Supplementary material 2**Supplementary figures S1–S13**

Authors: Claire M. Mugasa, Jandouwe Villinger, Joseph Gitau, Nelly Ndungu, Marc Ciosi, Daniel Masiga

Copyright notice: This dataset is made available under the Open Database License (<http://opendatacommons.org/licenses/odbl/1.0/>). The Open Database License (ODbL) is a license agreement intended to allow users to freely share, modify, and use this Dataset while maintaining this same freedom for others, provided that the original source and author(s) are credited.

Link: <https://doi.org/10.3897/zookeys.769.21144.suppl2>

Species of the subgenus *Empis* (*Xanthempis*) from South Korea (Diptera, Empididae)

Jiale Zhou¹, Igor Shamshev², Yongjung Kwon³, Ding Yang¹

1 Department of Entomology, College of Plant Protection, China Agricultural University, Beijing 100193, China **2** Zoological Institute, Russian Academy of Sciences, Universitetskaya nab. 1, St. Petersburg, 199034, Russia **3** School of Applied Biosciences, College of Agriculture & Life Sciences, Kyungpook National University, Daegu 702-701, South Korea

Corresponding author: Ding Yang (dyangcau@126.com); (yangding@cau.edu.cn)

Academic editor: M. Ivković | Received 19 February 2018 | Accepted 21 May 2018 | Published 26 June 2018

<http://zoobank.org/A4E64AF7-9E14-4B8A-92AE-FB93AC54EF90>

Citation: Zhou J, Shamshev I, Kwon Y, Yang D (2018) Species of the subgenus *Empis* (*Xanthempis*) from South Korea (Diptera, Empididae). ZooKeys 769: 145–155. <https://doi.org/10.3897/zookeys.769.24545>

Abstract

The subgenus *Empis* (*Xanthempis*) is newly recorded from South Korea with the following two species: *E. (X.) sesquata* (Ito, 1961) and *E. (X.) subhi* **sp. n.** A key to the known species of *Xanthempis* from Eastern Asia is presented. The distribution of *Xanthempis* in eastern Asia is briefly discussed.

Keywords

Diptera, Empididae, new species, South Korea, *Xanthempis*

Introduction

Xanthempis Bezzi, 1909 is a small subgenus of the genus *Empis* Linnaeus, 1758 with 52 known species, which are distributed only in the Palaearctic region (Yang et al. 2007, Shamshev and Kustov 2008, Daugeron 2009, Kustov 2011, Daugeron and Lefebvre 2015). The subgenus is characterized by a relatively large size (4–8 mm), yellow coloration of the body, posterior elongation of the head, relatively small eyes separated by a wide frons in both sexes, long antennal scape, strong reduction of the body chaetotaxy, and some other features (Chvála 1996, Shamshev and Kustov 2008). The Palaearctic species were studied by Chvála (1994, 1996), Daugeron (1997, 2000, 2009), Sham-

shev (1998), Shamshev and Kustov (2008) and Daugeron and Lefebvre (2015). Shamshev (1998) compiled a key to all species of the subgenus. Later, Shamshev and Kustov (2008) keyed the species of *Xanthempis* found from the Caucasus, including a species described from Iran, and Daugeron (2009) provided a key to Pyrenean species. The swarming and mating behaviors of *Xanthempis* species were reported by Plant (1994) and Preston-Mafham (1999).

In the present paper, two species are added to the fauna of South Korea, one of which is described as new to science. A key to the known species of the subgenus *Xanthempis* from eastern Asia is presented, mainly based on Shamshev (1998).

Materials and methods

Specimens used for our study are deposited in the Insect Collection of Kyungpook National University, Daegu, South Korea. Terminalia preparations of males were made by macerating the apical portion of the abdomen in cold 10% NaOH for 12–15 hours. After examination, the preparations were transferred to fresh glycerine and stored in microvial pinned below the dry-pinned specimen, and the descriptions are based on dry-pinned material. Morphological terminology for adult structures mainly follows McAlpine (1981), and the structures of the male genitalia follow Cumming and Wood (2009). Photographs were taken with a Digital Microscope VHX-1000 series at China Agricultural University and then stacked by Helicon Focus 6.0. The following abbreviations are used:

| | | | |
|------------|-----------------------|-------------|-----------------------|
| acr | acrostichal seta(e), | ppn | postpronotal seta(e), |
| d | dorsal seta(e), | prsc | prescutellar seta(e), |
| dc | dorsocentral seta(e), | pa | postalar seta(e), |
| npl | notopleural seta(e), | sa | supraalar seta(e), |
| oc | ocellar seta(e), | sc | scutellar seta(e). |

Taxonomy

Key to species (males) of subgenus *Xanthempis* from Eastern Asia

- 1 Mesoscutum entirely yellow *Empis (Xanthempis) kovalevi* Shamshev
- Mesoscutum with brownish to blackish longitudinal vittae and sometimes also with spots **2**
- 2 Mesoscutum with broad median vitta running also over scutellum and postnotum and with elongate blackish spot between postpronotal lobe and suture *Empis (Xanthempis) sesquata* (Ito)
- Mesoscutum only with median vitta **3**

- 3 Occiput with large rhomboid spot dorsally
 *Empis* (*Xanthempis*) *stercorea* Linnaeus
- Occiput with drop-like to wedge-shaped spot dorsally (including ocellar tubercle) 4
- 4 Mesoscutal vitta disappearing before prescutellar depression 5
- Mesoscutal vitta running to base of scutellum 6
- 5 Mesoscutum (dorsal view) shiny, median vitta distinctly bordered; epandrial lamella broad (lateral view); hypandrium with small pointed apical prominence bearing 2 minute hair-like setae .. *Empis* (*Xanthempis*) *japonica* Frey
- Mesoscutum (dorsal view) faintly greyish pollinose, rather subshiny; epandrial lamella narrow (lateral view); hypandrium with large apical prominence bearing 2 spinules *Empis* (*Xanthempis*) *richteri* Shamshev
- 6 Mesoscutal vitta very narrow, in front of suture occupying about 1/4 of space between rows of dc setae; phallus with dorsal projection on subapical part (lateral view) *Empis* (*Xanthempis*) *subi* sp. n.
- Mesoscutal vitta broader, in front of suture occupying at least 1/3 of space between rows of dc setae; phallus smoothly curved on subapical part (lateral view) 7
- 7 Hypandrium with large subtriangular apical prominence (ventral view)
 *Empis* (*Xanthempis*) *zlobini* Shamshev
- Hypandrium with straight margin apically
 *Empis* (*Xanthempis*) *belousovi* Shamshev

Empis (*Xanthempis*) *sesquata* (Ito)

Figs 1–6

Xanthempis sesquata Ito, 1961: 127, Abb. 6, 7. Type locality: Karyôsan (Aki) [now Hiroshima Prefecture], Japan (Honsyû).

Diagnosis. Mesoscutum with broad black median longitudinal vitta running also over scutellum and postnotum and elongate blackish spot between postpronotal lobe and suture. Occiput with contrastingly black, wedge-shaped spot including ocellar tubercle. Prothoracic spiracle yellow.

Description. Male (Fig. 1). *Body* length 6.0–6.1 mm, wing length 8.5–8.6 mm. Head (Fig. 4) largely brownish yellow or yellow, faintly pale greyish pollinose; frons and face dark yellow, occiput with narrow contrastingly black, wedge-shaped spot including ocellar tubercle. Eyes dichoptic, ommatidia equally small. Frons broad, parallel-sided, with minute dark setulae laterally. Occiput (Fig. 6) with short sparse black setae arranged in two almost regular transverse rows on upper part and some pale setae behind mouth-opening. Ocellar tubercle with two short proclinate oc and some minute setulae. Antennal scape and pedicel brownish, postpedicel and stylus black; scape

long, approx. five times longer than wide, with some black setulae; pedicel very short, subglobular, with cirlet of black subapical setulae; postpedicel very long, narrow, subconical, approx. eight times longer than wide; stylus very short, nearly 0.3 times as long as postpedicel. Proboscis long, labrum approx. two times longer than head height; palpus yellow, with scattered blackish setulae.

Thorax largely yellow, faintly pale greyish pollinose, with greatly reduced, only black setation; mesoscutum (Fig. 3) with broad, black, distinct, median longitudinal vitta running also over scutellum and postnotum, as well as with elongate, blackish, less distinct spot between postpronotal lobe and suture on each side; antepnotum with dark spot dorsally. Prothoracic spiracle yellow. Prosternum bare. Proepisternum with 2–3 hair-like setulae on lower part. Antepnotum with several spinule-like setulae on each side. Postpronotal lobe with one short inclinate ppn and additional shorter seta anteriorly. Mesonotum with one short thin presutural sa, one long npl, one short pa (sometimes with 1–2 additional setulae), four sc (apicals short, laterals minute); acr absent; dc uniserial, 6–7 in row, situated outside black median vitta, hair-like, minute (except 1–2 prsc). Laterotergite with several black setulae of different lengths. Legs yellowish to brownish yellow, only tarsomere 5 dark brown; lacking prominent bristles (except circllets of short subapical setae on tibiae). Wing nearly hyaline; brownish yellow stigma long, narrow; veins dark brown; basal costal bristle black, very short. Calypter yellowish, blackish fringed. Halter yellow.

Abdomen extensively yellow but tergites broadly brownish dorsally forming uniform vitta, subshiny; with scattered, mostly yellowish to brownish yellow setulae longer and darker on sternite 8 posteriorly. Hypopygium (Fig. 5) large, almost entirely yellow, only cerci narrowly brownish apically. Cercus rather large, with deep excision, dorsal arm long, broad, somewhat concave apically (lateral view), ventral arm short, finger-like; covered with dark minute setulae and bearing a moderately long seta on ventral arm. Epandrial lobe rather trapezoid, with upper posterior corner broadly rounded and lower posterior corner narrowly elongated; covered with dark setae longer along upper margin and on posterior corner. Hypandrium subtriangular viewed ventrally, with two black closely set spinules apically. Phallus strongly curved, attenuated on about middle part, with dorsal projection on subapical part (lateral view), long beak-like apical opening.

Female (described for the first time, Fig. 2). Body length 7.2–7.9 mm, wing length 8.2–8.5 mm. Very similar to male, but mesonotum with somewhat long setae; scutal lateral spots less distinct and sometimes absent. Cercus long, slender, brown, clothed in minute setulae.

Material examined. South Korea: one male, Hongcheon-gun GW, Yeongnae-ri Duchon-myeon, Mt. Baegu (37°50'39.14"N, 128°0'49.90"E), 25.V.2013, Yongjung Kwon; one male, Gangweon Prv., Mt. Obongsan (38°0'6.08"N, 127°48'22.36"E), 17.V.1981, Yongjung Kwon; one female, same locality, 19.V.1981; one female, Gangweon Prv., Mt. Seolagsan (37°50'39.14"N, 128°0'49.90"E), 19.V.1981, Yongjung Kwon.

Distribution. Palaearctic: Japan (Hiroshima), South Korea.

1

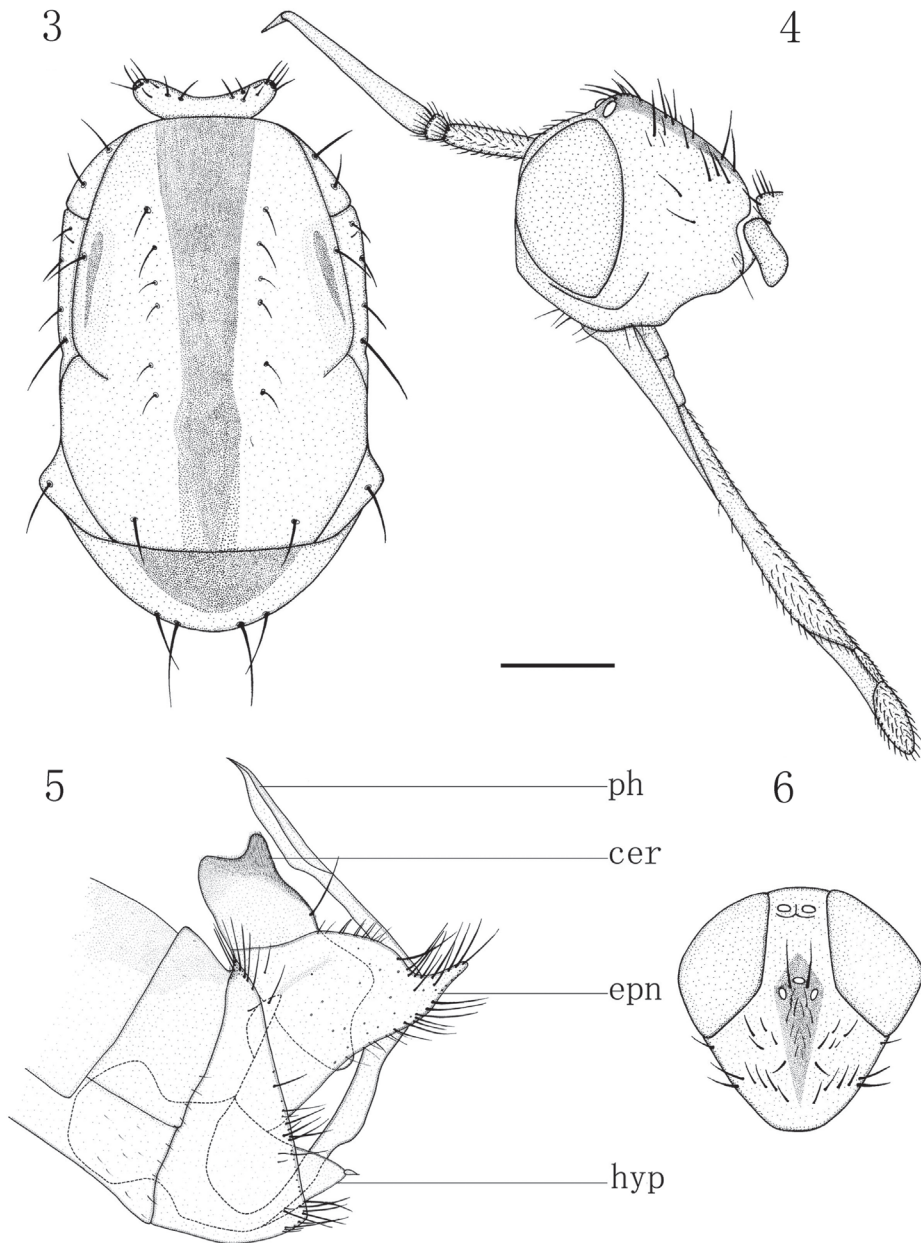


2



Figures 1–2. *Empis* (*Xanthempis*) *sesquata* (Ito), habitus, lateral view. **1** Male **2** Female. Scale bar: 1 mm.

Remarks. The species has been known for a long time only from the holotype male described by Ito (1961) from Honsyû Island (Hiroshima Prefecture) of Japan. Here we record *E. sesquata* from South Korea for the first time, where this species was collected



Figures 3–6. *Empis (Xanthempis) sesquata* (Ito), male. **3** Thorax, dorsal view **4** Head, lateral view **5** Genitalia, lateral view **6** Head, dorsal view. Scale bar: 1 mm. Abbreviations: ph = phallus, cer = cercus, epn = epandrium, hyp = hypandrium.

from a mountain area of Gangweon Province on dates ranging from the middle of May till the end of June. *Empis sesquata* can be readily distinguished from other species of *Xanthempis* known from the eastern Asia by its distinctive scutal pattern.

***Empis (Xanthempis) subii* sp. n.**

<http://zoobank.org/6442F43B-1CA9-4E5B-B296-1219403C3888>

Figs 7–12

Diagnosis. Mesoscutum with very narrow black median vitta running to base of scutellum. Occiput with narrow drop-like brown spot including ocellar tubercle. Prothoracic spiracle brown.

Description. Male (Fig. 7). Body length 6.0–6.1 mm, wing length 8.2–8.8 mm. Head (Fig. 10) yellow, faintly pale greyish pollinose; occiput with narrow brown drop-like spot including ocellar tubercle. Eyes dichoptic, ommatidia equally small. Frons broad, parallel-sided, with minute dark setulae laterally. Occiput (Fig. 12) with short sparse black setae on upper part and some pale setae behind mouth-opening. Ocellar tubercle with two short proclinate oc and some minute setulae. Antennal scape and pedicel brown, postpedicel and stylus black; scape long, 4.3 times longer than wide, with some black setulae; pedicel very short, subglobular, with circle of black subapical setulae; postpedicel very long, narrow, subconical, nearly 9.5 times longer than wide; stylus very short, 0.2 times as long as postpedicel. Proboscis long, labrum 2.5–3.0 times longer than head height; palpus yellow, with scattered blackish setulae.

Thorax almost entirely yellow, faintly pale greyish pollinose, with greatly reduced, only black setation; mesoscutum (Fig. 9) with very narrow black median vitta running to base of scutellum; antepronotum with brownish spot dorsally, upper border of anepisternum brown, postnotum with small indistinct brownish spot dorsally. Prothoracic spiracle brown. Prosternum bare. Proepisternum with 2–3 hair-like minute setulae on lower part. Antepronotum with several spinule-like setulae on each side. Postpronotal lobe with one moderately long inclinate ppn and 1–2 additional setulae anteriorly. Mesonotum with one moderately long presutural sa, one longest npl, one moderately long pa, four sc (apicals long, laterals short); acr absent; dc uniserial, 7–9 in row, situated far outside black median vitta, hair-like, very short (except 2–3 longer prsc); additionally, notopleuron with several setulae anteriorly. Laterotergite with numerous black setulae of different lengths. Legs yellowish, but tarsi brownish yellow to brownish; lacking prominent bristles (except circllets of short subapical setae on tibiae). Wing nearly hyaline; brownish yellow stigma long, narrow; veins dark brown; basal costal bristle black, short. Calypter yellowish, blackish fringed. Halter yellow.

Abdomen extensively yellow, but tergites broadly brownish dorsally forming uniform vitta (except tergite 8), subshiny; mostly yellowish to brownish yellow setulae longer laterally, segment 8 with black setae posteriorly. Hypopygium (Fig. 11) large, almost entirely yellow, only cerci narrowly brownish apically. Cercus rather large, with deep excision; dorsal arm long, broad, somewhat concave apically (in lateral view), ventral arm short finger-like; covered with dark minute setulae and bearing one moderately long seta on ventral arm. Epandrial lobe rather trapezoid, with upper posterior corner broadly rounded and lower posterior corner narrowly elongated; covered with dark short setae somewhat long along upper margin and on posterior corner. Hypandrium subtriangular in ventral view, with two black closely

7

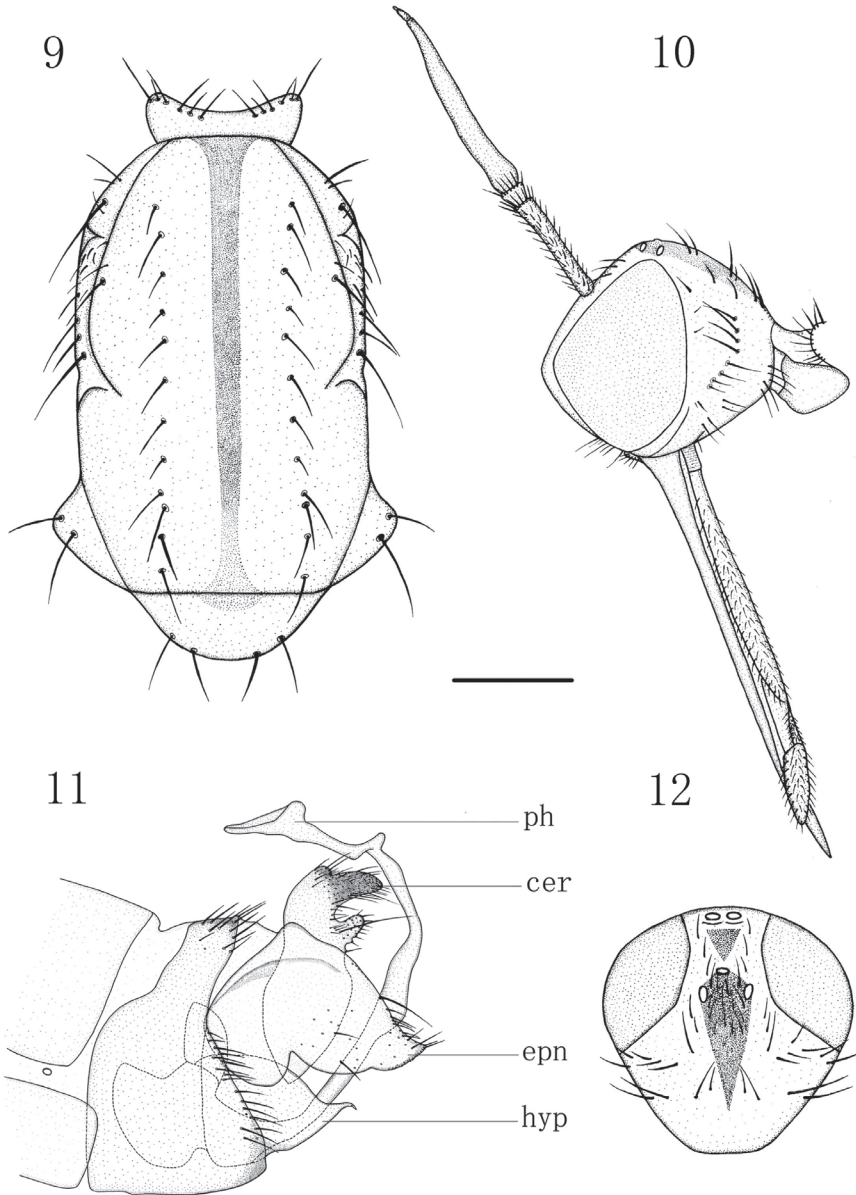


8



Figures 7–8. *Empis (Xanthempis) subhi* sp. n., habitus, lateral view. **7** Male **8** Female. Scale bar: 1 mm.

set spinules apically. Phallus strongly curved, somewhat broad near base, otherwise of more or less uniform thickness, with small dorsal tubercle closer to short beak-like apical opening.



Figures 9–12. *Empis (Xanthempis) subi* sp. n., male. **9** Thorax, dorsal view **10** Head, lateral view **11** Genitalia, lateral view **12** Head, dorsal view. Scale bar: 1 mm. Abbreviations: ph = phallus, cer = cercus, epn = epandrium, hyp = hypandrium.

Female (Fig. 2). Body length 7.1–7.2 mm, wing length 7.9–8.3 mm. Very similar to male, but postpedicel somewhat short, 8.4 times longer than wide in single specimen examined; abdominal tergites with narrower brown dorsal area. Cercus long, slender, brown, clothed in minute setulae.

Type material. Holotype, male, Korea, Gangweon Pr., Mt. Seolagsan (37°50'39.14"N, 128°0'49.90"E), 29.VI.1984, Yongjung Kwon. Paratypes, one male (dissected), two females, same data as holotype.

Distribution. Palaearctic: South Korea.

Remarks. In the scutal pattern, the new species is similar to *E. belousovi* Shamshev, 1998 and *E. zlobini* Shamshev, 1998 known from the Russia Far East (including Sakhalin Island) and to *E. japonica* Frey, 1955 known from Hokkaido and Kuril Islands (Kunashir) (Shamshev 1998). *Empis subi* sp. n. can be distinguished from these species as it has been given in the key.

Etymology. The species is named in honor of Prof. Sang Jae Suh, Daegu in order to express our sincere thanks to him during the course of this study.

Discussion

At the present the subgenus *Xanthempis* is known exclusively from the Palaearctic region with 53 described species. There are eight species known in Eastern Asia, including the Russian Far East, Mongolia, the Korean Peninsula, and Japan. The subgenus *Xanthempis* is recorded from South Korea for the first time with the following two species: *E. (X.) sesquata* (Ito) and *E. (X.) subi* sp. n. *Empis sesquata* is found in both the Korean Peninsula and Japan. The new species is similar to *E. belousovi* Shamshev, 1998 and *E. zlobini* Shamshev, 1998 from Russian Far East (including Sakhalin Island), and to *E. japonica* Frey, 1955 known from Hokkaido and Kuril Islands (Kunashir) (Shamshev 1998). *Empis kovalevi* Shamshev and *E. richteri* Shamshev are distributed on the Asian continent, and *E. stercorea* Linnaeus widely spreads in the Palaearctic region. *Xanthempis* has not been reported from China yet; however, some species of the subgenus may occur in northeast China. Further collections and investigations of *Xanthempis* from these areas may provide additional data on the fauna and distribution of this subgenus in Asia.

Acknowledgements

We are grateful to Prof. Sang Jae Suh (Daegu) for his kind help during the study. The research was funded by the National Natural Science Foundation of China (No. 31772497). Igor Shamshev is thankful to Prof. Ding Yang for providing the possibility to visit China Agricultural University and to Ms Jiale Zhou for her hospitality; his study was partly performed within the frame of the Russian State Research Project no. AAAA-A17-117030310210-3.

References

- Chvála M (1994) The Empidoidea (Diptera) of Fennoscandia and Denmark. III Genus *Empis*. Fauna Entomologica Scandinavica 29: 1–192.
- Chvála M (1996) Classification and phylogeny of European *Empis* subgenus *Xanthempis* Bezzi (Diptera, Empididae). *Studia Dipterologica* 3(1): 3–18.
- Cumming JM, Wood DM (2009) Adult morphology and terminology. In: Brown BV, Borkent A, Cumming JM, Wood DM, Woodley NE, Zumbado MA (Eds) *Manual of Central American Diptera*, Vol. 1. NRC Research Press, Ottawa, 9–50.
- Daugeron C (1997) Découverte du sous-genre *Xanthempis* Bezzi en Afrique du Nord et description de trois espèces nouvelles (Diptera: Empididae). *Annales de la Société Entomologique de France* 33(2): 155–164.
- Daugeron C (2000) The subgenus *Xanthempis*: new species and taxonomical data (Diptera: Empididae). *Annales de la Société Entomologique de France* (NS) 36(4): 371–388.
- Daugeron C (2009) Two new species of *Xanthempis* Bezzi (Diptera, Empididae, Empidinae) endemic to the Pyrenees. *Zootaxa* 2087: 59–64.
- Daugeron C, Lefebvre V (2015) Descriptions of two new species of Empidinae Schiner, 1862 (Diptera: Empididae) from the Mercantour National Park, France. *Zoosystema* 37(4): 605–610. <https://doi.org/10.5252/z2015n4a6>
- McAlpine JF (1981) Morphology and terminology – adults. In: McAlpine JF, Peterson BV, Shewell GE, Teskey HJ, Vockeroth JR, Wood DM (Coords) *Manual of Nearctic Diptera* (Vol. 1). Agriculture Canada Monograph 27: 9–63.
- Ito S (1961) Neue Empididen aus Japan (1) mit der Beschreibung der unbeschriebenen weibchen. Entomological Laboratory, College of Agriculture, University of Osaka, Sakai No. 6: 123–128.
- Kustov SY (2011) A new species of the dance-fly subgenus *Xanthempis* Bezzi, 1909 of the genus *Empis* Linnaeus, 1758 (Diptera: Empididae) from the Caucasus. *Caucasian Entomological Bulletin* 7: 109–111.
- Plant AR (1994) Epigamic swarming behaviour of *Rhamphomyia* (*Megacyttarus*) *crassirostris*, *Hilara lundbecki* and *Empis* (*Xanthempis*) *scutellata* (Empididae). *Dipterists Digest* 1: 72–77.
- Preston-Mafham KG (1999) Courtship and mating in *Empis* (*Xanthempis*) *trigramma* Meig., *E. tessellata* F. and *E. (Polyblepharis) opaca* F. (Diptera: Empididae) and the possible implications of ‘cheating’ behaviour. *Journal of Zoology* 247(2): 239–246.
- Shamshev IV (1998) Revision of the genus *Empis* Linnaeus (Diptera : Empididae) from Russia and neighbouring lands. 1. Subgenus *Xanthempis* Bezzi. *International Journal of Dipterological Research* 9(2): 127–170.
- Shamshev IV, Kustov SY (2008) New and little-known species of the dance-fly subgenus *Xanthempis* Bezzi, genus *Empis* L. (Diptera, Empididae), from the Caucasus. *Entomological review* 88: 1115–1126. <https://doi.org/10.1134/S0013873808090108>
- Yang D, Zhang KY, Yao G, Zhang JH (2007) *World catalog of Empididae* (Insecta: Diptera). China Agricultural University Press, Beijing, 599 pp.

